School of Civil and Mechanical Engineering

Investigation on bacterial biopolymers and biominerals for soil stabilization

Asha Latha Ramachandran

This thesis is presented for the Degree of

Doctor of Philosophy

of

Curtin University

June 2021

Author's declaration

To the best of my knowledge and belief, this thesis contains no material previously published by any other person except where due acknowledgement has been made.

This thesis contains no material which has been accepted for the award of any other degree or diploma in any university.

Asha Ramachandran

Date: 16th June 2021

Investigation on bacterial biopolymers and biominerals for soil stabilization

Abstract

Soil stabilization has become inevitable in current day geotechnical engineering practices due to rapid industrialization and infrastructure development. In Australia, chemical stabilization using lime, cement, gypsum, and fly ash is commonly employed to stabilize soil against erosion, liquefaction, and the vast road networks. However, high greenhouse gas emissions, leaching of chemicals into the groundwater, and its effect on natural lifeforms pose a serious concern regarding its environmental impact. Therefore, a sustainable solution is essential for a country like Australia with the highest roads per capita and significant generation of mine tailings.

Inspired by several natural formations in Australia, such as beach rocks, stromatolites and corals, bio-based stabilizers such as biomineralization and biopolymerization emerge as a potential solution to the problem. Biomineralization by carbonate precipitation, known as Microbially induced calcite precipitation (MICP), is a well-researched area. It can improve soil properties such as stiffness, resistance to water absorption and strength. However, the generation of ammonia gas as a byproduct of the process is a growing concern. In comparison, the role of biopolymers has remained relatively unexplored and yet have the potential to overcome limitations of MICP, including high alkalinity and ammonia generation.

Our study on the beach rock samples collected from Lucky Bay, Esperance, Australia, revealed that biomineralization is strongly associated with biopolymer formation, and a synergy between the two was noticed. This study reports the mechanisms behind the formation of beach rock sediments at Lucky Bay, Esperance in Western Australia. The observation of ferruginous, aluminosilicate and carbonate cements along with bacterial biopolymers were reported, and mineralogical, morphological and nanomechanical characterization of the beach rock was carried out.

Like biomineralization, the biopolymer can be deposited within the soil through bacterial metabolism, or manufactured biopolymers can be mixed with soil to achieve stabilization. This thesis is the first attempt to reveal the basic mechanism of stabilizing sand using manufactured bacterial biopolymer xanthan gum by conducting investigations spanning from microscopic to macroscopic scales. Disintegration upon

exposure to moisture is a major concern while dealing with manufactured biopolymers such as Xanthan gum. Although Xanthan gum was able to bind the sand, exposure to moisture considerably affected its strength. The addition of varying dosage of clay significantly improved the performance by reinforcing the polymer. The study revealed the potential of bacterial polymerization as a means of sustainable soil stabilization through a detailed experimental investigation spanning from macroscale to microscale.

Biopolymeric stabilization is a rapid, single-step process. Moreover, in this process release of toxic ammonia of MICP is avoided. However, biopolymers are susceptible to moisture to the extent that quite a few of the manufactured biopolymers, including Xanthan gum, are soluble in water. Further, this thesis explores a synergy between biopolymer and biominerals under laboratory conditions to stabilize road base samples. The results revealed that synergizing biopolymer with MICP surface treatment helped significantly reducing the amount of ammonia released during the MICP process to achieve a target strength. The durability of the samples stabilized with xanthan gum alone improved with MICP treatment establishing the synergy between biopolymers and biominerals.

Further, the in-situ synthesis of insoluble bacterial biopolymer dextran was carried out in laboratory conditions. The nano and macro mechanical properties of dextran produced by bacterial culture *Leuconostoc mesenteroids* were quantified using advanced characterization techniques such as nanoindentation and Atomic Force Microscopy. This study has demonstrated novel methods for testing in situ polymers and opened the channels for their applications in numerous subsurface and surface applications.

The thesis was a novel attempt to explore the fundamental mechanism of biopolymer stabilization from varying length scales. The study revealed that the performance of biopolymer could be further improved by reinforcing it with a varying dosage of clay. Further, the study was successful in establishing the synergy between biopolymers and MICP. The study was also successful in the in-situ synthesis of insoluble bacterial biopolymer dextran and quantification of its nano and micromechanical properties for soil stabilization applications.

Acknowledgements

First and foremost, I would like to thank my supervisor Professor Abhijit Mukherjee for the privilege of working in his laboratory and for the unique opportunity he gave me to explore my research interests in bio-based stabilizers. I am truly thankful for his contribution to this project and all the commentaries and guidance provided to my research throughout the PhD journey.

I would also like to express my gratitude to my co-supervisor, Dr Navdeep Dhami, for her guidance. I would like to thank her for her expertise in biotechnology and academic writing. Your positive feedback was fundamental to keep my enthusiasm throughout my research work.

I would like to express my gratitude to the Civil Engineering department of Curtin University for granting me this opportunity to pursue my PhD. I would also like to thank the Head of the Department, Associate Professor Andrew Whyte, my thesis chairperson Assoc. Prof Prabir Sarker and Dr Ranjan Sarukkalige for their support. I would also like to thank the office staff members Frankie, Cheryl, and Evelyn, for their help and support with administrative matters.

I thank Professor D.N Singh for being a constant source of inspiration during my PhD research journey and will be a source of inspiration throughout my life. Dr Thomas Becker, thank you for helping me out with the AFM experiments and Ms Elaine Miller for her expertise in SEM. I would also like to extend my heartfelt gratitude to the Technical Operations Coordinator of the Civil Engineering department Mr Mark Whittaker for his help and support. Thanks to the lab technician's Dr Arne, Darren and others, for helping me out in the civil labs.

Thanks to my colleagues Pelin, Hannah, Subhra, Elaheh, Jay, Nimrat, Sakshi, Aparna, Yikuan, Sukrit for being my support system in Australia. Thank you for your valuable friendship and helpful discussions over the years.

I cannot thank my parents enough for being extremely understanding and patient during my journey—also, thanks to my brother and sister for always being there. Finally, thanks to Nazreen, Saimy, Dinah, Jacob and Vignesh for their love and encouragement.

This thesis is dedicated to my parents.

Mom and dad, your hard work and persistence have always been my greatest motivation!

Attributes

The contributions of the following co-authors are hereby acknowledged for their contribution to various extent as per the list below.

Chapter 3 is published as 'Ramachandran, A.L., et al., *Understanding and creating biocementing beachrocks via biostimulation of indigenous microbial communities.* Applied Microbiology and Biotechnology, 2020: p. 1-19.'
https://doi.org/10.1007/s00253-020-10474-6

Chapter 4 is published as Ramachandran, A. L., A. A. Dubey, N. K. Dhami and A. Mukherjee (2021). "*Multiscale Study of Soil Stabilization Using Bacterial Biopolymers."* Journal of Geotechnical and Geoenvironmental Engineering 147(8): 04021074.

Chapter 2, 5 and 6 are manuscripts under various stages of review.

List of co-authors:

Miss. Asha Latha Ramachandran (AR)

Miss. Pelin Polat (PP)

Mr. Anant Aishwarya Dubey (AD)

Mr. Mohamed Ghalib (MG)

Dr. Navdeep Kaur Dhami (ND)

Professor Abhijit Mukherjee (AM)

Contribution:

Chapter 2: State-of-the-art review on bio-based soil stabilizers

Co-Author list	Concept and Design	Data acquisition and Methods	Data Conditioning and Manipulation	Interpretation and Discussion	Write-up
AR	×	×	×	×	×
I acknowledge the contribution stated above are accurate to the best of my knowledge					

Co-Author list	Concept and Design	Data acquisition and Methods	Data Conditioning and Manipulation	Interpretation and Discussion	Write-up
ND	×			×	×
I acknowledge the contribution stated above are accurate to the best of my knowledge					

Co-Author list	Concept and Design	Data acquisition and Methods	Data Conditioning and Manipulation	Interpretation and Discussion	Write-up
AM	×			×	×
I acknowledge the contribution stated above are accurate to the best of my knowledge					

168

169 **Chapter 3: Understanding and creating biocementing beachrocks via**
170 **biostimulation of indigenous microbial communities**

Co-Author list	Concept and Design	Data acquisition and Methods	Data Conditioning and Manipulation	Interpretation and Discussion	Write-up
AR	×	×	×	×	×
I acknowledge the contribution stated above are accurate to the best of my knowledge					

Co-Author list	Concept and Design	Data acquisition and Methods	Data Conditioning and Manipulation	Interpretation and Discussion	Write-up
PP	×	×	×	×	
I acknowledge the contribution stated above are accurate to the best of my knowledge					

Co-Author list	Concept and Design	Data acquisition and Methods	Data Conditioning and Manipulation	Interpretation and Discussion	Write-up
ND	×			×	×
I acknowledge the contribution stated above are accurate to the best of my knowledge					

Co-Author list	Concept and Design	Data acquisition and Methods	Data Conditioning and Manipulation	Interpretation and Discussion	Write-up
AM	×			×	×
I acknowledge the contribution stated above are accurate to the best of my knowledge					

171

172 **Chapter 4: Multi-Scale Study of Soil Stabilization Using Bacterial Biopolymers**

Co-Author list	Concept and Design	Data acquisition and Methods	Data Conditioning and Manipulation	Interpretation and Discussion	Write-up
AR	×	×	×	×	×
I acknowledge the contribution stated above are accurate to the best of my knowledge					
Co-Author list	Concept and Design	Data acquisition and Methods	Data Conditioning and Manipulation	Interpretation and Discussion	Write-up
AD		×			
I acknowledge the contribution stated above are accurate to the best of my knowledge					
Co-Author list	Concept and Design	Data acquisition and Methods	Data Conditioning and Manipulation	Interpretation and Discussion	Write-up
ND	×			×	×
I acknowledge the contribution stated above are accurate to the best of my knowledge					
Co-Author list	Concept and Design	Data acquisition and Methods	Data Conditioning and Manipulation	Interpretation and Discussion	Write-up
AM	×		×	×	×
I acknowledge the contribution stated above are accurate to the best of my knowledge					

Chapter 5: Multi-functional Performance of Biopolymers and Biocement in Aggregation of Sandy Soil and Road Bases

Co-Author list	Concept and Design	Data acquisition and Methods	Data Conditioning and Manipulation	Interpretation and Discussion	Write-up
AR	×	×	×	×	×
I acknowledge the contribution stated above are accurate to the best of my knowledge					
Co-Author list	Concept and Design	Data acquisition and Methods	Data Conditioning and Manipulation	Interpretation and Discussion	Write-up
ND	×			×	×
I acknowledge the contribution stated above are accurate to the best of my knowledge					
Co-Author list	Concept and Design	Data acquisition and Methods	Data Conditioning and Manipulation	Interpretation and Discussion	Write-up
MG		×			
I acknowledge the contribution stated above are accurate to the best of my knowledge					
Co-Author list	Concept and Design	Data acquisition and Methods	Data Conditioning and Manipulation	Interpretation and Discussion	Write-up
AM	×		×	×	×
I acknowledge the contribution stated above are accurate to the best of my knowledge					

Chapter 6: Nanoscale to macroscale characterization of in – situ bacterial biopolymers for applications in soil stabilization

Co-Author list	Concept and Design	Data acquisition and Methods	Data Conditioning and Manipulation	Interpretation and Discussion	Write-up
AR	×	×	×	×	×
I acknowledge the contribution stated above are accurate to the best of my knowledge					
Co-Author list	Concept and Design	Data acquisition and Methods	Data Conditioning and Manipulation	Interpretation and Discussion	Write-up
ND	×			×	×
I acknowledge the contribution stated above are accurate to the best of my knowledge					
Co-Author list	Concept and Design	Data acquisition and Methods	Data Conditioning and Manipulation	Interpretation and Discussion	Write-up
AM	×		×	×	×
I acknowledge the contribution stated above are accurate to the best of my knowledge					

179

180 **Table of contents**

181

182 **Chapter 1: Introduction 1**

183 1.1 Motivation 1

184 1.2 Problem statement and research objective 2

185 1.3 Thesis outline 2

186 1.4 References 4

187 **Chapter 2: State of the art review on bio-based soil stabilizers 7**

188 2.1 Abstract 7

189 2.2 Introduction 7

190 2.3 Significance of bio-based stabilizers 9

191 2.4 Bio-based stabilizers in nature 10

192 2.5 Evolution of biopolymers for soil stabilization 12

193 2.5.1 Polymers for soil stabilization 12

194 2.5.2 Limitations of polymers 13

195 2.5.3 Emergence of biopolymers 13

196 2.6 Microbially Induced Polymers (MIP) 14

197 2.6.1 MIP: What are they? 14

198 2.6.2 MIP Pathways 14

199 2.6.3 MIP for soil stabilization applications 15

200 2.6.4 Advantages and limitations of MIP 20

201 2.7 Emerging techniques for characterizing microbial polymers 22

202 2.7.1 Atomic Force Microscopy (AFM) 22

203 2.7.2 Nanoindentation 27

204 2.7.3 Penetration testing 31

205 2.7.4 Benefits of testing at various length scales 33

206 2.8 Challenges 34

207 2.9 Concluding remarks 35

208 2.10 Future recommendations 35

209 2.11 Acknowledgements 42

210 2.12 Reference 42

Chapter 3: Understanding and creating biocementing beachrocks via biostimulation of indigenous microbial communities 57

3.1 Abstract 57
3.2 Introduction 57
3.3 Materials and Methods 61
3.3.1 Site description 61
3.3.2 Sample collection and details 62
3.4 Characterisation of natural beachrocks 63
3.4.1 Chemical analysis of leachate, seawater, and sediments 63
3.4.2 Morphological characterisation 63
3.4.3 Mineralogical characterisation 63
3.4.4 Nanomechanical characterisation via Nanoindentation 65
3.4.5 Microbial diversity characterisation of native beachrocks 65
3.5 Enrichment of beachrock associated microbial communities and characterisation of biogenically induced minerals under laboratory conditions 65
3.5.1 Microbial enrichment and mineralisation 65
3.5.2 Microbial characterisation 66
3.6 Results 67
3.6.1 Characterisation of natural beachrock 67
3.6.2 Lab synthesized beachrock biocement 77
3.7 Discussion 83
3.7.1 Formation of beachrock sediments in nature 83
3.7.2 Formation of beachrock cements in the lab 87
3.8 Conclusions 90
3.9 Acknowledgements 91
3.10 References 91

Chapter 4: Multi-Scale Study of Soil Stabilization Using Bacterial Biopolymers 97

4.1 Abstract 97
4.2 Introduction 97
4.3 Experimental investigation 100
4.4 Materials and methods 100

4.4.1 Materials 100
4.4.2 Preparation of cylinder specimens 102
4.5 Testing methods 104
4.5.1 Unconfined compressive strength (UCS) 104
4.5.2 Digital Image correlation 104
4.5.3 Water absorption test 104
4.5.4 Scanning Electron Microscopy (SEM) 104
4.5.5 Nanoindentation and PeakForce-QNM 105
4.6 Results and discussion 106
4.6.1 Compaction characteristics 106
4.6.2 Performance of commercial biopolymer stabilized samples at macro-scale 108
4.6.3 Micrographic analysis 118
4.6.4 Micro-mechanical properties of clay-reinforced biopolymer 121
4.7 Conclusions and Recommendations 127
4.8 Data availability statement 128
4.9 Acknowledgements 128
4.10 References 128
Chapter 5: Multi-functional Performance of Biopolymers and Biocement in Aggregation of Sandy Soil and Road Bases 136
5.1 Abstract 136
5.2 Introduction 136
5.3 Experimental investigation 139
5.4 Materials and methods 140
5.4.1 Materials 140
5.4.2 Sample preparation 142
5.4.3 Sample designation and description 143
5.5 Testing methods 143
5.5.1 Unconfined compressive strength (UCS) 143
5.5.2 Digital Image correlation 144
5.5.3 Water absorption test 144
5.5.4 Scanning Electron Microscopy (SEM) 144
5.5.5 Quantitative EDS mapping 144

5.5.6 Ammonia generation of samples with MICP 145
5.6 Results and discussion 145
5.6.1 Compaction characteristics 145
5.6.2 Stress-strain behaviour 146
5.6.2 Mechanical properties with varying MICP 152
5.6.3 Damage progression and failure modes 153
5.6.4 Water absorption 158
5.6.5 Micrographic analysis 161
5.6.6 Ammonia generation 163
5.7 Conclusions 165
5.8 Data availability statement 167
5.9 Acknowledgements 167
5.10 References 167
Chapter 6: Nanoscale to macroscale characterization of in – situ bacterial biopolymers for applications in soil stabilization 172
6.1 Abstract 172
6.2 Introduction 172
6.3 Materials and methods 175
6.3.1 Microorganism and growth medium 175
6.3.2 Soil specimen preparation 175
6.3.3 Dextran production 177
6.3.4 Dextran purification 177
6.3.5 Scanning Electron Microscopy (SEM) 178
6.3.6 Nanoindentation 178
6.3.7 Peakforce QNM 179
6.3.8 Needle penetration 179
6.4 Results and discussion 181
6.4.1 Bacterial growth and biopolymer production 181
6.4.2 Scanning Electron Microscopy (SEM) 184
6.4.3 Nano-indentation 185
6.4.4 Peakforce QNM 188
6.4.5 Needle penetration 190
6.4.6 Microscopic investigation of stabilised soils 192

6.4.7 Discussion 193
6.5 Conclusion 197
6.6. Reference 198
Chapter 7: Conclusions 205
7.1 Introduction 205
7.2 Recommendation for future research 208
7.3 References 208

List of Figures

Fig 2. 1 a) Formation of beach rocks on Lucky Bay, Esperance, Western Australia. b) Beach rocks composed of iron and calcium biominerals [14]. Fig.1 c) and d) Cave speleothems collected from Lake Cave [28]. 11
Fig 2. 2 MICP in nature occurs utilizing indigenous bacteria and naturally occurring nutrients, at micromolar concentrations [36] 12
Fig 2. 3 a) and b) Dry MIP bridging the sand particles c) and d) MIP in the hydrated state [93] 16
Fig 2. 4 Unconfined compressive strength of biopolymer-treated soils at a dry condition a) Coarse soil b) Fine soil [66]. 17
Fig 2. 5 SEM micrograph of MIP generated in-situ (unpublished data) 19
Fig 2. 6 Advantages and limitations of bio-based stabilizers 22
Fig 2. 7 AFM instrument at Curtin University 23
Fig 2. 8 Schematic of an AFM [132] 24
Fig 2. 9 Surface imaging of MIP stabilized clays using a) Nanoindentation b) Atomic Force Microscopy 27
Fig 2. 10 General view of the Maruto modified Eijkelkamp (right) penetrometers and their parts [142]- 1) presser, (2) chuck, (3) penetration, (4) load scale, (5) load indication ring, (6) UCS–NPR correlation chart given by the manufacturer, (7) removable cap, (8) penetration needle produced according to the Japan Civil Engineering Society's guideline, (9) indicator ring, (10) penetrometer tube, (11) spring, (12) end cap, (13) scale, (14) extension rod, and (15) needle block. 32

Fig 3. 1 Beach rock sediments collected from different locations in Lucky Bay, Esperance 2 (a, b) sample BR-1 and sample BR-2 at intermediate stage 3 (c, d) sample BR-3 and sample BR-4 at terminal stage 4 (e, f) e: seawater; f: brown water displaying iron leaching and in the highlighted section is 5 slimy layer on sand surface indicative of microbial activity. 61
Fig 3. 2 Scanning electron micrographs of beach rock formations from a-d) intermediate 7 samples BR-1 and intermediate sample BR-2 e-h) terminal sample BR-3 and BR-4. Natural 8 cements (NC) in between sand grains, microbial borings (MB), mineralised bacterial cell 9 (MBC), possible microbial footprints (PMF) recorded in certain locations. Mineralised Ca 10 rods and Fe globules were also seen. 70

Fig 3. 3 Energy dispersive X ray spectrum of a,b) intermediate sample BR-1, BR-2 c,d) 12 terminal sample BR-3, BR-4..... 71
Fig 3. 4 a) Fourier transform infrared spectrum of beach rock samples: intermediate sample BR-14 1 and BR-2 and terminal sample BR-3, BR-4 indicating the presence of different minerals 15 including quartz (Q), kaolinite (K), hematite (H), goethite (H), aragonite (A), feldspar (F)..... 72
Fig 3. 5 a) X ray diffraction analysis of different beach rock samples i, ii) intermediate BR-1 17 and BR-2 iii, iv) terminal BR-3 and terminal BR-4 indicating the presence of different 18 minerals including quartz (Q), orthoclase (O), kaolinite (K), hematite (H), goethite (Ge), 19 aragonite (A), calcite (C), Nontronite (N), feldspar (F). b) TIMA analysis of (a) intermediate BR-1 and BR-2 (b) terminal BR-3 and BR-4..... 73
Fig 3. 6 Microstructures for nanoindentation through optical microscope fitted with 22 nanoindenter for: (a, b) intermediate BR-1 (c, d) intermediate BR-2 (e, f) terminal BR-3 and 23 (g, h) terminal BR-4 76
Fig 3. 7 Effect of biogenic and abiogenic enrichments on (a) absorbance (b) pH and (c) 25 amount of precipitation. Enr1 = enrichment under glucose; Enr2 = enrichment under lactate; 26 Enr3 = mix of glucose and lactate; C= control. Values are mean ± SD (n=3)..... 79
Fig 3. 8 Bacterial population composition at phylum level in natural and laboratory enriched 28 conditions (based upon 16S rRNA gene sequencing presented as a fraction from the total 29 population) wherein Enr1 = enrichment under glucose; Enr2 = enrichment under lactate; Enr3 30 = mix of glucose and lactate and NBR = Native beachrock 81
Fig 3. 9 (a-d) Scanning electron micrographs of bacterial cells and biogenically precipitated 32 crystals under in vitro conditions. Bacterial cells acting as nucleation sites were recorded. 33 Heterogeneous mixture of acicular crystals as in aragonite, lettuce crystals as in vaterite, 34 rhombohedral crystals as in calcite and semirounded nanoglobules as in ferruginous cements 35 were clearly recorded..... 82
Fig 3. 10 (a, b) Energy dispersive X ray spectrum and (c) X ray diffraction analysis of biogenically precipitated crystals under in vitro conditions depicting the presence of calcium and iron rich minerals in the form of calcite, vaterite, hematite and magnetite 83

Fig 4. 1 Schematic of the present experimental investigation 100
Fig 4. 2 Particle size distribution of the manufactured sand 101
Fig 4. 3 Compaction curves of the samples 107
Fig 4. 4 The variation of γd and OMC with varying clay content 108
Fig 4. 5 Stress-strain behaviour of biopolymer stabilized samples with varying clay content 109
Fig 4. 6 UCS and secant modulus of the biopolymer stabilized samples with varying clay content 110
Fig 4. 7 Stress-strain characteristics of samples with varying biopolymer dosage cured at 60^{o}C 111
Fig 4. 8 UCS and secant moduli samples with varying biopolymer dosage cured at 60^{o}C 111
Fig 4. 9 Stress-strain characteristics of samples with varying biopolymer dosage cured at ambient temperature 112
Fig 4. 10 UCS and secant moduli samples with varying biopolymer dosage cured at ambient temperature 112
Fig 4. 11 Failure modes of the biopolymer stabilized samples 114
Fig 4. 12 Vertical strain in the samples prior to failure obtained by DIC analysis 114
Fig 4. 13 Water absorption of the stabilized samples with time 116
Fig 4. 14 SBC0 sample failure due to local absorption of water 116
Fig 4. 15 Samples with clay-reinforced biopolymer after water absorption test 117
Fig 4. 16 Stress-strain behaviour of the biopolymer stabilized sample after exposure to moisture 117
Fig 4. 17 UCS of the stabilized sample after exposure to moisture 118
Fig 4. 18 Secant modulus of the stabilized samples after exposure to moisture 118
Fig 4. 19 SEM micrographs of biopolymer stabilized sand samples (SBC0) 120
Fig 4. 20 SEM micrographs of clay reinforced biopolymer sheets 120
Fig 4. 21 Schematic representation of mechanism of stabilization by biopolymers 121
Fig 4. 22 SEM micrographs of the hydrated samples 121
Fig 4. 23 Load-displacement response of the sample during nanoindentation 123
Fig 4. 24 Elastic modulus and hardness as a function of the penetration depth 123
Fig 4. 25 Variation in modulus and hardness of the clay reinforced biopolymer sample 124

Fig 4. 26 The AFM tip scanning the sample surface 126
Fig 4. 27 Surface topography and modulus mapping of the clay reinforced biopolymer sample surface a) and b) prior to moisture exposure; c) and d) after exposure to moisture. 127

Fig 5. 1 Schematic of experimental investigation and test matrix 140
Fig 5. 2 Particle size distribution of manufactured sand and road base material 140
Fig 5. 3 Stress-strain behaviour of samples with MICP treatment cycles 147
Fig 5. 4 Stress-strain behaviour of samples with various treatments 148
Fig 5. 5 Stress-strain behaviour of clay-biopolymer samples with MICP treatment cycles 149
Fig 5. 6 Stress-strain behaviour and of road base material 149
Fig 5. 7 Stress-strain of biopolymer stabilized samples with MICP treatment 151
Fig 5. 8 Mechanical properties of the stabilized road base material 151
Fig 5. 9 E_{50} of $C_{10}B_0M_x$ and $C_{10}B_{0.5}M_x$ samples with varying M_c 152
Fig 5. 10 q_u of $C_{10}B_0M_x$ and $C_{10}B_{0.5}M_x$ samples with varying M_c 153
Fig 5. 11 Failure patterns of the samples 154
Fig 5. 12 DIC analysis on $C_{10}B_{0.5}M_{12}$ samples 155
Fig 5. 13 DIC analysis on road base samples 157
Fig 5. 14 Water absorption of $C_{10}B_{0.5}M_c$ samples 159
Fig 5. 15 Condition of samples with and without MICP layer after water absorption 159
Fig 5. 16 w_r of $C_{10}B_{0.5}M_c$ samples with varying M_c 160
Fig 5. 17 Water absorption of road base samples 160
Fig 5. 18 SEM micrographs of $C_{10}B_{0.5}M_0$ sample 162
Fig 5. 19 SEM micrographs showing the surface layer of calcite 162
Fig 5. 20 EDS mapping of sample a), b) and c) sample $C_{10}B_{0.5}M_0$ and d), e) and f) sample $C_{10}B_{0.5}M_{14.3}$ 163
Fig 5. 21 Relation between q_u and a_r of the stabilized samples 165

Fig 6. 1 Particle size distribution of the manufactured sand 176
Fig 6. 2 Petri dish sample prepared for needle penetration testing after completion of in-situ biopolymer treatment (Sample SBC10). 181

Fig 6. 3 Bacterial growth in media with different sucrose concentrations..... 183
Fig 6. 4 Variation of pH with sucrose concentration 183
Fig 6. 5 Biopolymer yield with varying sucrose concentration 184
Fig 6. 6 SEM micrographs of bacterial biopolymer on glass-slides 185
Fig 6. 7 Biopolymer sample embedded in resin for nanoindentation testing b) image of a typical indent on the sample..... 187
Fig 6. 8 a) Elastic modulus and hardness as a function of the penetration depth b) Variation in modulus of dry and hydrated biopolymer sample..... 187
Fig 6. 9 Survey scanning results on the polished sample after indentation 187
Fig 6. 10 a) Modulus mapping on 180x180 micro m^2 area using nanoindentation b) variation in modulus across horizontal direction 188
Fig 6. 11 Surface topography obtained from a) nanoindentation 500x500 μm^2b) PF-QNM on 20x20 μm^2..... 189
Fig 6. 12 AFM modulus mapping results 190
Fig 6. 13 a) Modulus contour map and b) modulus distribution across the horizontal and vertical section..... 190
Fig 6. 14 Needle penetration of in-situ biopolymer..... 191
Fig 6. 15 Needle penetration results on petri dish samples treated with Xanthan gum 191
Fig 6. 16 Correlation between the slope of the needle penetration curve and UCS of Xanthan gum treated samples 192
Fig 6. 17 SEM of in-situ biopolymers between sand grains 193
Fig 6. 18 SEM of in-situ biopolymer-clay matrix..... 193

List of Tables

Table 2. 1 Summary of some polymers used for soil stabilization 37
Table 2. 2 Commercially available MIP and their composition 38
Table 2. 3 Summary of some biopolymers used for soil stabilization 39
Table 2. 4 Summary of advanced characterization techniques 41

Table 3. 1 Designation of the collected samples, details, and analysis techniques.... 62
Table 3. 2 Detailed media composition of the enrichment media under laboratory conditions 66
Table 3. 3 Leachate and seawater analysis (elemental concentrations in mg/L) 67
Table 3. 4 Elemental analysis of trace metals in beach rock sediments (mg/kg)..... 68
Table 3. 5 Mechanical properties of different rock samples obtained through nanoindentation 76

Table 4. 1 Particle size distribution and chemical composition of clay 101
Table 4. 2 Designation for samples stabilized with commercial biopolymer 103
Table 4. 3 Designation for samples stabilized with varying biopolymer content and cured at varying temperatures. 103
Table 4. 4 Details of sample polishing for the nanoindentation test. 105

Table 5. 1 Particle size distribution and chemical composition of clay 140
Table 5. 2 Atterberg's limit for the road base material 141
Table 5. 3 Details of bacterial media and cementation media used for MICP..... 141
Table 5. 4 Description and designation of the samples..... 143
Table 5. 5 Details of sample polishing for quantitative EDS mapping..... 144
Table 5. 6 Results of compacted samples 146
Table 5. 7 Estimate of ammonia generation..... 164

Table 6. 1 Particle size distribution and chemical composition of the clay 176
Table 6. 2 Media for the growth of bacteria and biopolymer production 177
Table 6. 3 Steps involved in polishing for nanoindentation..... 178

507 Table 6. 4 Sample designation for Needle penetration testing..... 181
508

509 **Glossary of terms**

MICP	Microbially Induced Calcium carbonate Precipitation
MIP	Microbially Induced Polymer
DEM	Discrete Element Method
UCS	Unconfined Compressive Strength
AFM	Atomic Force Microscopy
LMC	Low Magnesium Calcite
HMC	high magnesium calcite
ICP-MS	inductively coupled plasma mass spectrometry
FESEM	field emission scanning electron microscope
EDS	energy dispersive x-ray spectroscopy
XRD	X-ray diffractometry
TIMA	TESCAN Integrated Mineral Analyser
FTIR	Fourier-Transform Infrared Spectroscopy
OD	Optical Density
NCBI	National Centre for Biotechnology Information
OTUs	Operational Taxonomic Units
ANOVA	Analysis of Variance
MB	Microbial Borings
PMF	Possible Microbial Footprints
FC	Ferruginous Cements
EPS	Extra Polymeric Substances
DIC	Digital Image Correlation
SEM	Scanning Electron Microscopy
PeakForce-QNM	Peak Force Quantitative Nanomechanical Mapping
CSM	Continuous Stiffness Measurement
DMT	Derjaguin-Muller-Toporov
OMC	Optimum Moisture Content
γd	Maximum Dry Density
qu	Compressive strength
PBS	Phosphate buffered saline
ar	Ammonia released
NPR	Needle Penetration Resistance
MRS	De Man, Rogosa and Sharpe

510

Chapter 1: Introduction

1.1 Motivation

The practice of soil stabilization has become inevitable in present-day engineering projects owing to the rapid pace of industrial and infrastructure development. Due to the growing scarcity of naturally available soil suitable for construction, there is a huge demand for chemical stabilizers such as cement, lime, and fly ash for soil stabilization applications [1]. Especially in Australia, soil deposits susceptible to erosion [2], clayey soils prone to desiccation [3], shrinkage [4], and tailings generated by the mining industry [5] require stabilization. To address these issues, the most used stabilizers in Australia are cement, lime, and fly ash [2, 6].

The negative impact on the environment caused by the usage of chemical stabilizers can no longer be ignored [7]. The research revealed the production of 3.6 billion tonnes of cement per year, which is expected to cross 5 billion tonnes by 2030 [8]. It has been reported that 5% of global carbon dioxide emissions from industrial process and fossil-fuel combustion during the year 2013 were due to the calcination of carbonate rocks during cement production [9, 10]. To sum up, the production of 1 kg of cement leads to the generation of 0.9 kilograms of carbon dioxide [11, 12]. Moreover, the use of chemical stabilizers poses various threats to the native flora and fauna by altering the soil and groundwater pH and affecting natural drainage [6]. Hence, there is a growing concern regarding the use of chemical stabilizers and an urgent need to explore the potential of sustainable alternatives for soil stabilization.

Australian landscape comprising of natural formations such as beach rocks, stromatolites and microbialites are examples of notable low energy cementation occurring under ambient conditions [13-15]. The most common form of cementation occurring in the above-mentioned formations is known as biomineralization. It is a process by which living organisms, mainly bacteria, produce inorganic minerals as a part of their basic metabolic activities [16]. Extensive research was carried out in soil stabilization by exploiting the technique of microbially induced calcium carbonate precipitation (MICP), which is a special case of biomineralization leading to the precipitation of calcium carbonate mineral [17-19]. In most cases, biomineralization occurs in conjunction with biopolymer production [20, 21]. The potential of biopolymers in soil stabilization has

often gained less attention in comparison to MICP. The overall objective of the thesis is to investigate the effect of bacterial biopolymers and biominerals on soil stabilization.

1.2 Problem statement and research objective

With the emergence of bio-based stabilizers in Geotechnical Engineering, understanding the fundamentals of the stabilization process is of paramount importance. To gain an understanding of the mechanism of bio-based stabilization, characterisation of the locally occurring natural formation such as beach rocks can be highly beneficial. Also, investigation spanning from macro to micro scale is essential to elucidate the mechanism of stabilization. Previous research has mainly focussed on biomineralization as a sustainable soil stabilization technique. However, the potential of biopolymers is yet to be explored in detail. This thesis is a novel attempt to investigate the underlying mechanism of bacterial biopolymer formation from varying length scales. An attempt has been made to synergise bacterial biopolymer formation with biomineralization to emulate the natural accretion process. Keeping this in view, the research objectives were formulated as follows.

- Understanding the mechanism of cementation in the natural geological formation such as beach rock from Esperance, Western Australia.
- Investigate the role of ex-situ bacterial biopolymers in the aggregation of soil
- Investigate the synergistic effect of bacterial biopolymers and biominerals on stabilization of soil
- Investigate the potential of in-situ bacterial biopolymer formation on stabilization of soil

1.3 Thesis outline

The thesis is presented as a hybrid version comprising of five manuscripts out of which one is published (Chapter 3) and chapter 4 is accepted for publication. Chapter 2, 5 and6 are under various stages of review in journals. The overall objective of the thesis is to investigate the effect of bacterial biopolymers and biominerals on soil stabilization. A summary of each chapter and its context are discussed below.

Chapter 1: Introduction

This chapter consists of discussion on overall motivation for carrying out the work and describes the thesis outline.

Chapter 2: State of the art review on bio-based soil stabilizers

It describes the emergence of bio-based stabilizers in the field of geotechnical engineering with a focus on biopolymers. The state-of-the-art techniques used for the characterisation of these stabilizers were also highlighted. Key gaps in the existing literature were identified, leading to the formulation of research objectives.

Chapter 3: Understanding and creating biocementing beachrocks via biostimulation of indigenous microbial communities

This paper is published in the journal as '*Ramachandran, A.L., et al., Understanding and creating biocementing beachrocks via biostimulation of indigenous microbial communities. Applied Microbiology and Biotechnology, 2020: p. 1-19.' https://doi.org/10.1007/s00253-020-10474-6*. It reports the mechanisms behind the formation of beachrock sediments at Lucky Bay, Esperance in Western Australia. The observation of ferruginous, aluminosilicate and carbonate cements along with bacterial biopolymers were reported. The mineralogical, morphological, and nano-mechanical characterisation of the bio cement was carried out. This study pointed out the role of bacterial biopolymer in the aggregation of soils leading to the investigation of its potential in soil stabilization.

Chapter 4: Multi-Scale Study of Soil Stabilization Using Bacterial Biopolymers

Chapter 4 is published as as *Ramachandran, A. L., A. A. Dubey, N. K. Dhami and A. Mukherjee (2021). "Multiscale Study of Soil Stabilization Using Bacterial Biopolymers." Journal of Geotechnical and Geoenvironmental Engineering 147(8): 04021074.*This is a novel attempt to reveal the basic mechanism behind the stabilization of sand-clay mixtures using bacterial biopolymer (xanthan gum) by conducting investigations spanning from microscopic to macroscopic scales. The stabilized samples were characterised for strength and water absorption. The mechanism of stabilization has been revealed through advanced microscopic investigations using scanning electron microscopy (SEM), nanoindentation and atomic force microscopy (AFM). The study reveals the potential of bacterial polymerisation as a means of sustainable soil stabilization. This chapter has been submitted to the journal for publication.

Chapter 5 Multi-functional Performance of Biopolymers and Biocement in Aggregation of Sandy Soil and Road Bases

The manuscript explores the synergistic effect of combined biopolymer (xanthan gum) and MICP. The soil of varying grain size distribution spanning from sand to clay has been aggregated using both the biopolymer and further treated with MICP. The performance of the stabilized samples was evaluated in terms of compressive strength, water absorption and microscopic analysis. The unconfined compressive strength tests and micrographic analysis through scanning electron microscope and energy dispersive X-ray spectroscopy results revealed that the synergistic effect of biopolymer and MICP resulted in superior compressive strength. Water absorption test indicated that xanthan gum was susceptible to water attack and incorporation of MICP helped in addressing the concern. Likewise, the addition of biopolymers reduces the release of ammonia into the atmosphere. The present study was successful in overcoming the individual limitations of biopolymer and MICP by combining the two techniques. This manuscript has been submitted to a journal for publication.

Chapter 6: Nanoscale to macroscale characterization of in – situ bacterial biopolymers for applications in soil stabilization

This chapter is currently under review in Frontiers in Materials, section Polymeric and Composite Materials as *"Nanoscale to macroscale characterization of in – situ bacterial biopolymers for applications in soil stabilization "*Limited information is available on the mechanical properties and effect of in-situ bacterial biopolymers on soil stabilization. Hence, an attempt was made in the present manuscript to quantify the nano and macro mechanical properties of in-situ bacterial biopolymer dextran produced by the bacteria *Leuconostoc mesenteroids*. The mechanism of stabilization has been revealed through advanced microscopic investigations using scanning electron microscopy, needle penetration testing, nanoindentation and atomic force microscopy. The study is the first of its kind in exploring the mechanical properties of biopolymers from macro to micro-scale. The study reveals the potential of bacterial polymerisation as a means of sustainable soil stabilization.

1.4 References

1. Jayanthi, P. and D. Singh, *Utilization of Sustainable Materials for Soil Stabilization: State-of-the-Art.* Advances in Civil Engineering Materials, 2016. 5(1): p. 46-79.

2. Indraratna, B., et al., *Predicting the erosion rate of chemically treated soil using a process simulation apparatus for internal crack erosion.* Journal of Geotechnical and Geoenvironmental Engineering, 2008. 134(6): p. 837-844.
3. Premkumar, S., et al., *Experimental study on contact erosion failure in pavement embankment with dispersive clay.* Journal of Materials in Civil Engineering, 2016. 28(4): p. 04015179.
4. Kirby, J., et al., *Field swelling, shrinking, and water content change in a heavy clay soil.* Soil Research, 2003. 41(5): p. 963-978.
5. Santini, T.C. and N.C. Banning, *Alkaline tailings as novel soil forming substrates: Reframing perspectives on mining and refining wastes.* Hydrometallurgy, 2016. 164: p. 38-47.
6. Vinod, J.S., B. Indraratna, and M.A. Mahamud, *Stabilisation of an erodible soil using a chemical admixture.* Proceedings of the Institution of Civil Engineers-Ground Improvement, 2010. 163(1): p. 43-51.
7. Xi, F., et al., *Substantial global carbon uptake by cement carbonation.* Nature Geoscience, 2016. 9: p. 880.
8. Imbabi, M.S., C. Carrigan, and S. McKenna, *Trends and developments in green cement and concrete technology.* International Journal of Sustainable Built Environment, 2012. 1(2): p. 194-216.
9. Pade, C. and M. Guimaraes, *The CO2 uptake of concrete in a 100 year perspective.* Cement and Concrete Research, 2007. 37(9): p. 1348-1356.
10. Gao, T., et al., *Analysis on differences of carbon dioxide emission from cement production and their major determinants.* Journal of Cleaner Production, 2015. 103: p. 160-170.
11. Mohammadinia, A., et al., *Stabilization of demolition materials for pavement base/subbase applications using fly ash and slag geopolymers.* Journal of Materials in Civil Engineering, 2016. 28(7): p. 04016033.
12. Ali, M.B., R. Saidur, and M.S. Hossain, *A review on emission analysis in cement industries.* Renewable and Sustainable Energy Reviews, 2011. 15(5): p. 2252-2261.
13. Suosaari, E.P., et al., *New multi-scale perspectives on the stromatolites of Shark Bay, Western Australia.* Scientific Reports, 2016. 6(1): p. 20557.

14. Proemse, B.C., et al., *Stromatolites on the rise in peat-bound karstic wetlands.* Scientific Reports, 2017. 7(1): p. 15384.
15. Dhami, N.K., M.S. Reddy, and A. Mukherjee, *Biomineralization of calcium carbonate polymorphs by the bacterial strains isolated from calcareous sites.* J. Microbiol. Biotechnol, 2013. 23(5): p. 707-714.
16. Anbu, P., et al., *Formations of calcium carbonate minerals by bacteria and its multiple applications.* SpringerPlus, 2016. 5(1): p. 250.
17. Porter, H., N.K. Dhami, and A. Mukherjee, *Sustainable road bases with microbial precipitation.* Proceedings of the Institution of Civil Engineers-Construction Materials, 2018. 171(3): p. 95-108.
18. DeJong, J.T., et al., *Bio-mediated soil improvement.* Ecological Engineering, 2010. 36(2): p. 197-210
19. DeJong, J.T., M.B. Fritzges, and K. Nüsslein, *Microbially induced cementation to control sand response to undrained shear.* Journal of Geotechnical and Geoenvironmental Engineering, 2006. 132(11): p. 1381-1392.
20. Decho, A.W., *Overview of biopolymer-induced mineralization: What goes on in biofilms?* Ecological Engineering, 2010. 36(2): p. 137-144.
21. Azulay, D.N., et al., *Biopolymers from a Bacterial Extracellular Matrix Affect the Morphology and Structure of Calcium Carbonate Crystals.* Crystal Growth & Design, 2018. 18(9): p. 5582-5591.

Chapter 2: State of the art review on bio-based soil stabilizers

2.1 Abstract

In recent years, several environmental challenges, such as global warming and climate change, have risen to the forefront of human focus and attention. In this context, the contribution of cement manufacturing to global carbon dioxide emissions can no longer be ignored. Geotechnical engineering practises such as soil stabilization, grouting and construction of pavement consumes a large amount of cement. However, the present socio-economic developments demand environmentally friendly stabilizers which meet the requirement for adequate engineering performance. With bio-geotechnology emerging as a sub-discipline of geotechnical engineering, numerous laboratory and field-scale experiments has been already conducted on bio-based stabilizers with a focus on biomineralization. However, the potential of biopolymer for soil stabilization application has received less notice in comparison to biomineralization. This comprehensive review will address the limitations of traditional stabilizers leading to the development of sustainable alternatives with a prime focus on biopolymers. The evolution of biopolymers and advanced characterizing tools used for studying the interactions between biopolymers and soils are also reviewed. Finally, the existing challenges in their large-scale implementation, as well as the direction of future research, are also presented.

Keywords: Sustainable stabilizers, bio-mineralization, biopolymers, advanced characterization techniques

2.2 Introduction

Highly erodible and dispersive soils are common in many parts of the world, especially Australia, wherein soil loss by erosion exceeds several billion tonnes per year [1, 2]. In addition to this, the damage due to expansive soils every year is estimated to be $1 billion in the USA, £150 million in the UK, and several billion pounds across the globe [3]. Moreover, the construction of pavement structures on soft and expansive subgrade leads to a substantial increase in the cost of highway projects [4]. Another key issue to be addressed in Australia is the management of large quantities of tailings generated by the mining industry [5]. Mine tailings, if not disposed of appropriately, could cause serious environmental issues and are susceptible to liquefaction which results in a rapid and dramatic loss of soil strength [6]. Scientific techniques of soil stabilization have relied on

719 the exploitation of cementitious materials like cement, hydraulic lime, bitumen, and
720 asphalt, to address issues such as high erodibility, low strength, and containment of mine
721 tailings [7]. In Australia, chemical stabilization using lime, cement, gypsum, and fly ash
722 is commonly employed for the stabilization of soil against erosion, liquefaction, and the
723 construction of road base [1, 8, 9]. Out of all the chemical stabilizers, cement has been
724 used extensively for the stabilization of soft soils and pavement materials. However,
725 cracking of the stabilized pavements caused due to shrinkage issues related to chemical
726 stabilizers is a dominant mode of pavement distress [1]. The use of chemical stabilizers
727 poses various threats to the native flora and fauna by altering the soil and groundwater
728 pH and affecting natural drainage [1]. Research reveals that we produce around 3.6 billion
729 metric tonnes of cement per year, which is expected to rise to more than 5 billion metric
730 tonnes by 2030 [10]. The fact that global emissions of CO_2 due to fossil fuel combustion
731 and cement production have continued to grow by 2.5% per year over the past decade is
732 highly alarming, and novel ways to create low energy alternative materials are required
733 [11]. With this background, the aim of the current study is to explore the potential, status
734 and challenges for the alternative class of newly emerged sustainable technology of
735 biocementation.

736 Several natural formations such as beach rocks, caves, microbialites and corals are a
737 classic example of the cementation of loose granular material leading to its aggregation
738 [12, 13]. The leading process that governs the cementation of these durable constructions
739 in nature is known as biocementation, the process by which living organisms form
740 inorganic solids and polymers as part of their basic metabolic activities. The two major
741 drivers of this process are microbially induced calcium carbonate precipitation (MICP)
742 and microbially induced polymer (MIP) production. Tremendous research has been
743 conducted on applications of biocementation via MICP while MIP is still in its infancy,
744 although, in nature, this mechanism is found widely. Beach rocks and microbial mats are
745 two such prime examples wherein the immense role of MIP has been recorded in a few
746 locations, including Australia [14]. The basic process of formation of biopolymer varies
747 within bacterial species and nutrient conditions and thus cannot be generalized [15]. The
748 potential of these MIP in soil applications has been recently recorded and will be
749 discussed in the next section in detail. The role of advanced instrumentation techniques
750 in the investigation of bio-based stabilizers is also mentioned. To sum up, this review

provides a fresh perspective on the possible role of MIP in geotechnical engineering, including examples of their application and a discussion of salient issues.

2.3 Significance of bio-based stabilizers

Global urbanization has led to an increase in demand for cement-based materials amounting to a whopping 76.2 billion tons from 1930 to 2013 [16]. A cement consumption of 600kg per capita has been reported in countries with per capita GDPs above the US $25,000 [17]. The production of cement across Australia in 2014-15 by three leading manufacturers was 9.1 million tonnes [18]. The cement manufacturing industry is highly energy-intensive, consuming about 12-15% of the total industrial energy use [19]. Cement production contributes 5-8% of global carbon dioxide emissions [10, 16, 18, 20-23]. The cumulative carbon dioxide emissions from 1930-2013 are estimated to be 38.2 Gt [16, 22]. To sum up, 1 kg of cement produced releases 0.9 kg of carbon dioxide, which equates to 3.24 billion tonnes of CO_2 per year [10, 19, 24, 25]. More than 55% of the emissions from cement manufacture result from heating of limestone, 32% are due to the burning of fossil fuels; the remaining 13% is due to electricity used to grind the material [18]. Data shows that global emissions in 2016 were around 1.5 $GtCO_2$, which is equivalent to about 4% of emissions from fossil fuels [23]. Geotechnical engineering discipline heavily relies on cement-based stabilizers for numerous applications such as grouting, soil stabilization, stabilization of mine tailings and construction of road base. The excessive heat of hydration generated due to the application of cement-based stabilizers in the soil leading to cracking is another issue of concern [26].

Moreover, the volumetric heaving due to the formation of ettringite in cement or lime stabilized soils containing sulphate is a common problem [26]. European countries have introduced ‘Green Deal’ which aims to make Europe climate neutral by 2020, thereby affecting the cement industry through higher energy and carbon emission prices (global Cement Magazine, July-August 2020). The application of alternate sustainable stabilizers can minimise the utilization of cement-based stabilizers. Significant progress has been achieved in sustainable cementitious materials by blending Portland cement clinker with increasing levels of supplementary cementitious materials (such as calcined clays and limestone) [27]. However, the scope of the present review is limited to bio-based stabilizers.

2.4 Bio-based stabilizers in nature

Biomineralization due to the metabolic activity of microorganisms is an essential process driving the formation of numerous geological structures in nature [28]. It has been reported that a significant portion of the insoluble carbonate present on the Earth's surface is of biogenic origin [29]. Microorganisms play an active role in the creation of sustainable natural formations such as beach rocks, cave speleothems and microbial mats with minimal embodied energy in an environmentally benign manner [30]. Our study reports the formation of beachrock sediments (Fig 2.1a) at Lucky Bay in Western Australia by the natural accretionary processes and activities of bacterial communities [14]. Ferruginous, aluminosilicate and carbonate cements (as seen in Fig 2.1 b) along with extensive extracellular polymeric substances were observed in the beach rocks. In addition to this, geological formations such as caves provide insight into carbonate deposits formed over a geological timescale [28, 31]. These rock-like deposits are commonly known as speleothems and vary in shape and size. The Leeuwin-Naturaliste ridge in the Margaret River region of Southwest Western Australia is home to several such deposits. Stromatolites generally defined as sedimentary structures that are produced by microbial communities through trapping and binding of sediment, and/or precipitation of carbonate in marine environments [32]. A recent study conducted on stromatolite formation in Hamelin Pool, Western Australia, has revealed that coccoid cyanobacteria predominate in mat communities forming lithified discrete stromatolite formation [33].

In nature, the formation of polymers by bacteria is commonplace, as it serves as a protective structure for the cells by increasing the resistance to environmental stresses. The role of MIP in microbial calcification is well documented [29, 34]. Cyanobacteria is one of the major producers of polymers resulting in carbonate precipitation [34, 35]. Since MIP contains various functional groups, they significantly influence bacterial adhesion leading to precipitation [29]. Moreover, MIP also enhances the cohesion of loose sediments by holding them together [35]. Therefore, it can be concluded that bio-based stabilizers in natural formation are environmentally benign, consume low energy for their formation and possess a low carbon footprint, as shown in Fig.2.1 and 2.2.

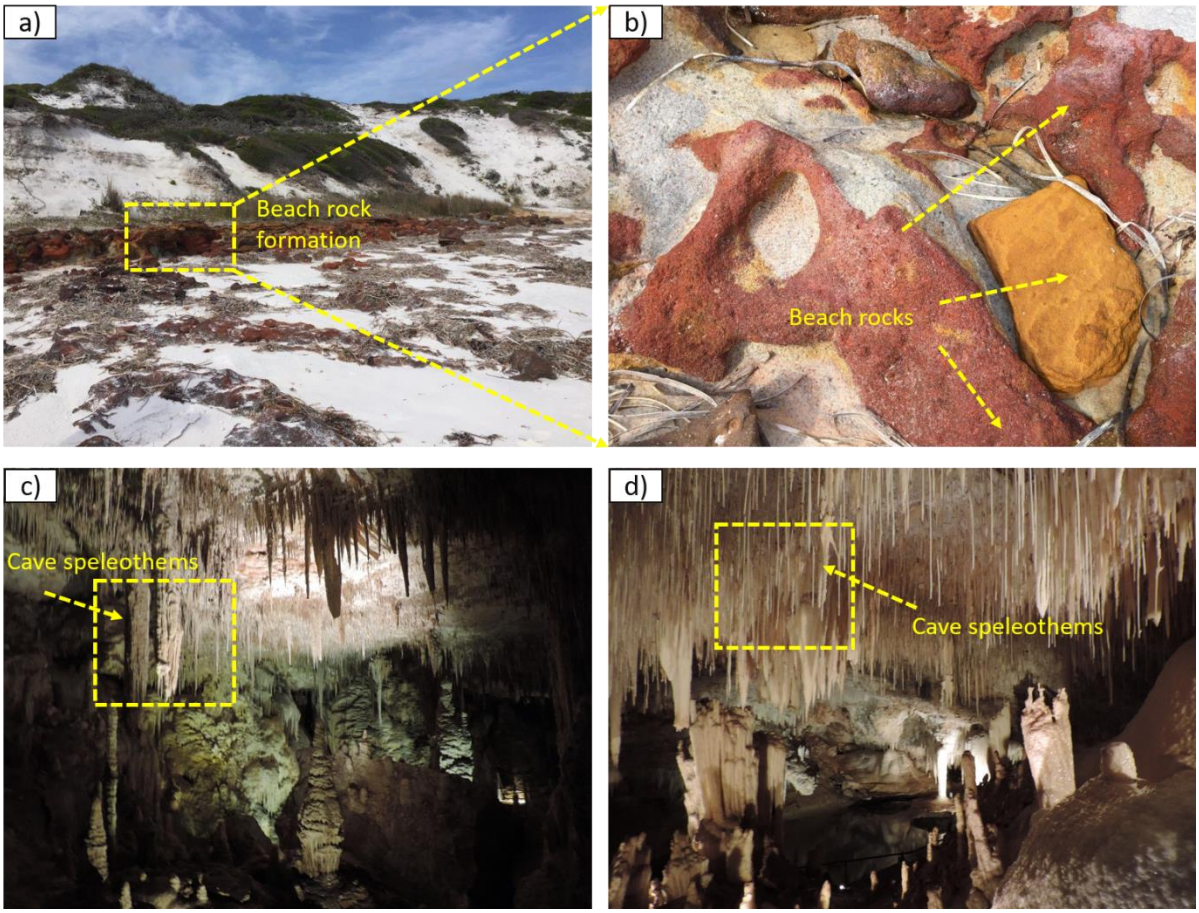

Fig 2. 1 a) Formation of beach rocks on Lucky Bay, Esperance, Western Australia. b) Beach rocks composed of iron and calcium biominerals [14]. Fig.1 c) and d) Cave speleothems collected from Lake Cave [28].

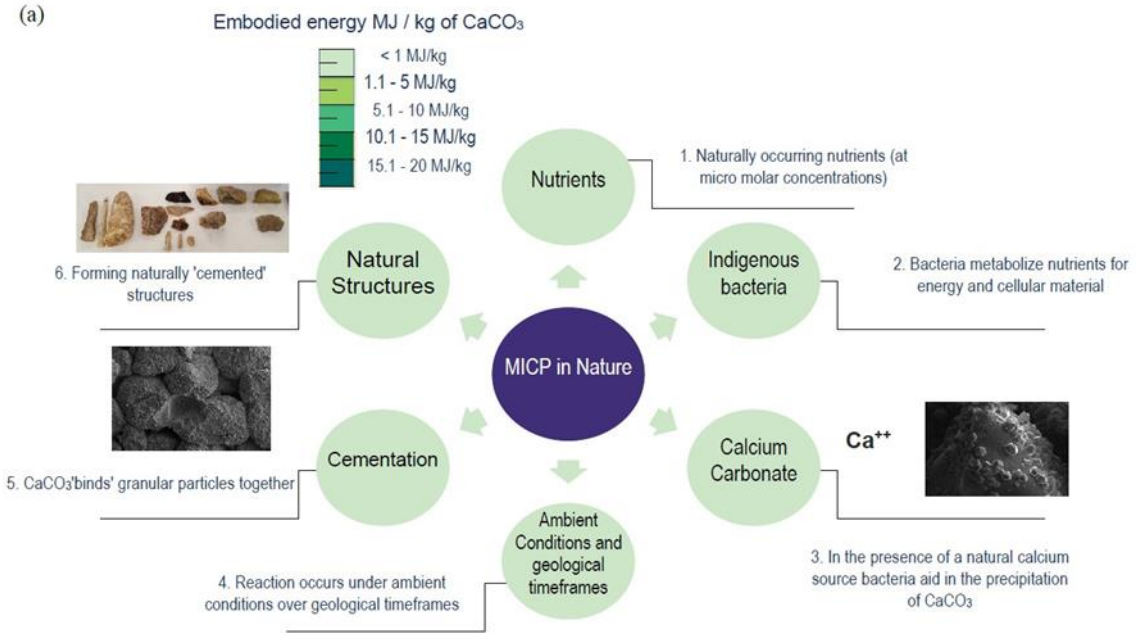

Fig 2. 2 MICP in nature occurs utilizing indigenous bacteria and naturally occurring nutrients at micromolar concentrations [36]

2.5 Evolution of biopolymers for soil stabilization

This section briefly reviews the use of polymers in geotechnical engineering applications, emphasising its advantages and limitations. An introduction to biopolymers is then presented to enable the readers to comprehend the benefits of its usage in soil stabilization.

2.5.1 Polymers for soil stabilization

The use of polymers in soil stabilization dates to the 1960s in the studies of Fungaroli and Prager [37], wherein they investigated the potential of acrylic polymers for stabilization of low plasticity soils. The pH of the polymers generally lies between 9-10, which is much lower in comparison to lime and cement-treated soils [38, 39]. Polymers such as polyacrylamide [40-45], lignosulphates [46-48], methyl methacrylate [49, 50], polyacrylate [51], polypropylene polymer [52], acrylic resin [53] and Polyvinyl alcohol [54] were used to stabilize both fine-grained and granular soils.

When lime proved ineffective in stabilizing high plasticity clays, polymers and lignosulphates were successfully employed to increase the Unconfined Compressive Strength (UCS) of the untreated samples [39, 47, 55]. Their use in soil bentonite vertical cut off walls for hydraulic containment application was also beneficial due to the low hydraulic conductivity when in contact with aggressive inorganic solutions [55, 56]. Furthermore, as an added benefit, the use of polymer-based additives results in a far lower carbon footprint than cement-based additives [44]. Soil stabilization method comprising of injecting polyurethane prepolymer was patented [57]. The advantage of using polyvinyl alcohol over traditional stabilizers on fine sandy loam soil was that it did not hamper plant growth or nitrogen uptake [58]. Polymers were initially employed to increase the resistance of sand to wind and water erosion [41, 59-63]. The advantages of using polymers in soil stabilization are that they display ductile behaviour during deformation, which is highly desirable for the design of pavements [38]. The key findings of soils stabilized with polymers are listed in Table 2.1.

2.5.2 Limitations of polymers

When used with coarse grains soils, volume expansion of the polymer due to contact with water can be a concern [64]. The polymer-stabilized specimens displayed significant strength loss after the wet-dry cycles, both in compression and flexure [65, 66]. This demonstrated that the volumetric expansion of polymer when in contact with water can affect the engineering properties of the stabilized soil. The amount of polymer dosage must be limited in these conditions to avoid volume expansion [55]. The direct mixing of viscous polymers into the soil can also have practical difficulties. Contamination of the groundwater and soil by leaching chemicals added in high dosage is also an issue of concern [7]. A barrier to the acceptance of nontraditional stabilization additives is the lack of standardized test procedures for evaluating product potential [47]. For polymer-stabilized soils, it was observed that higher strength was achieved in the vicinity of the point of injection [65]. Even though PAM was used widely in soil stabilization applications in the past, studies have shown that the residual monomers produce toxicity, which impacts the nervous system, brain, and damage DNA increase cancer risk [66]. The limitations of traditional stabilizers, including polymers, have urged researchers to explore alternative stabilizers with low environmental impact.

2.5.3 Emergence of biopolymers

The present socio-economic developments demand environmentally friendly stabilizers, which meet the requirement for sufficient engineering performance. This has led to the rise of biopolymers as they are formed by natural processes and offer the benefits of being environmentally benign and having a low carbon footprint. In general, the biopolymer can be termed as any polymer obtained from natural sources and sometimes used interchangeably with polymers produced by microorganisms. To be precise, we use the term biopolymers in general for polymers of natural origin and MIP for the polymers produced by microorganisms. The role of biopolymers in the stabilization of soils are not new. For example, ancient civilizations were known to use natural bitumen, straw, and sticky rice binders [67]. Biopolymers are of natural origin and are considered sustainable construction material. In specific applications, biopolymers offer distinct advantages in performance and cost over their synthetic counterparts [68]. However, we will limit the

review of literature in the forthcoming section to biopolymer of microbial origin termed as MIP.

2.6 Microbially Induced Polymers (MIP)

This section presents a review of major MIP and highlight their advantages over synthetic polymers and identify their overall contribution to soil stabilization. The general advantages and limitations are also discussed, leading to a few field-scale applications.

2.6.1 MIP: What are they?

MIP consists of monomeric units and is classified as polynucleotides (RNA and DNA), polypeptides (composed of amino acids), and polysaccharides [63]. Among them, polysaccharides are the most widely used biopolymers in various applications, including soil stabilization. Many biopolymers of microbial origin have developed and shown promise for soil applications, including xanthan, chitosan, sodium alginate, dextran, levan and gellan gum. MIP has shown promise as one of the most effective organic agents for promoting soil aggregate stability. The common MIP and their composition are given in Table 2.2.

2.6.2 MIP Pathways

Majority of the biopolymers are synthesized intracellularly and exported to the extracellular environment as macromolecules [70]. However, dextrans and levans are biopolymers whose synthesis and polymerization occur outside the cells by the action of secreted enzymes that convert the substrate into the polymer in the extracellular environment [70]. Although the composition and amount of biopolymer produced by a bacterium are genetically determined traits, they are highly influenced by media components and cultivation. The production of most bacterial biopolymers occurs under aerobic conditions. However, for optimal production of some biopolymers such as xanthan gum, maximal aeration is required [76]. Sugars are the most commonly used carbon sources for the production of bacterial biopolymers. Traditional methods to improve biopolymer yield include strain selection and optimization of conditions. However, genetic modification of the gene expression can be used to increase the biopolymer yield as well [77]. The detailed discussion of MIP pathways is beyond the scope of this article.

2.6.3 MIP for soil stabilization applications

In recent times, MIP has emerged as a sustainable stabilizer for various geotechnical engineering applications. The standard methods of their application to soil have been via 1) passive mixing by adding biopolymers already produced by microorganisms 2) actively mixing live bacteria with nutrients into the soil 3) injection of biopolymers already extracted from microorganisms in the soil.

2.6.3.1 Ex-situ applications

Xanthan gum was the first industrially produced MIP and extensively used for soil stabilization applications. Xanthan gum, produced by the bacterium *Xanthomonas campestris* was initially used in silty soils for a potential application of construction of impervious barriers [78]. Xanthan gum was effective in stabilizing various soils such as mine tailings [79-82], road base material [83], red mud waste [84], sand [85-92], bentonite and kaolinite [85, 93-96], other clays [97], silts [78], organic peat [98] and earthen construction material [89]. It has been reported that xanthan gum monomers can directly bond clayey particles through cation bridging and hydrogen bonding between the carboxyl group and the hydroxyl group of the biopolymer and clay particles [80, 94, 96, 99]. The low moisture, they behave like glassy brittle materials, while at higher levels of moisture, they are plastic [100]. Data also suggests that well-graded soils are likely to be improved by biopolymers due to greater inter-particle contacts. Particle size distribution is a key factor in the impact of biopolymers on shear behaviour [100]. For non-ionic polymers, hydrogen bonding is the dominant method of adsorption, while anionic polymers interact with the positively charged edge of kaolinite via electrostatic attraction [96]. Our recent study on xanthan gum stabilized soils reveals the basic mechanism of stabilizing sand using bacterial biopolymer by conducting investigations spanning from microscopic to macroscopic scales (unpublished study). Fig. 3 a) and b) shows the Scanning Electron Microscopy (SEM) micrograph of dried xanthan gum bridging the sand particles leading to bonding between the particles. The MIP in the hydrated state is shown in Fig.3 c) and d). The considerable difference in the structure of the MIP can be observed in the dry and hydrated state. Soil stabilization by other biopolymers such as sodium alginate [85, 101, 102], chitosan [103], Agar and modified starch [91], casein and sodium caseinate [104], β-3, 3/1, 6-glucan [92] were also investigated.

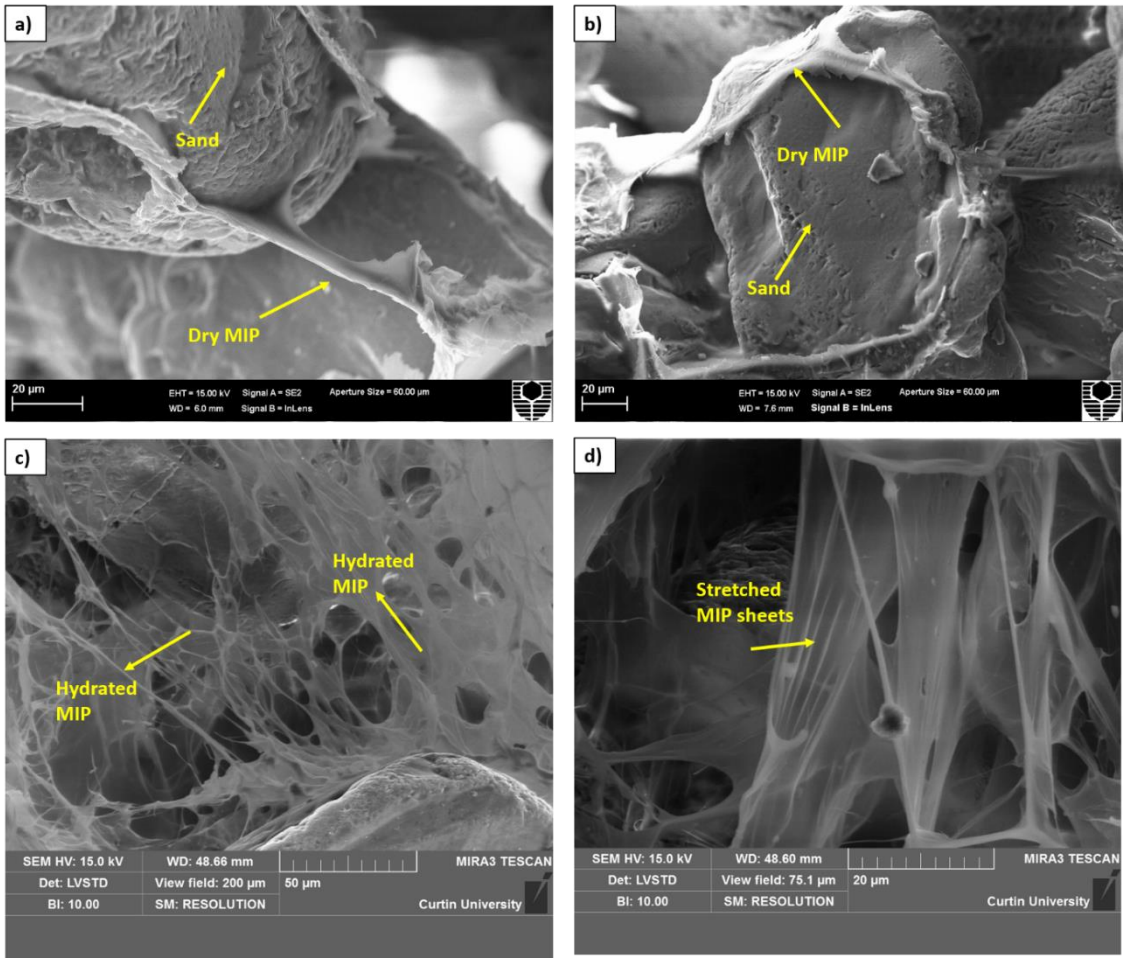

Fig 2. 3 a) and b) Dry MIP bridging the sand particles c) and d) MIP in the hydrated state [93]

2.6.3.1.1 Effect of biopolymers on geotechnical properties of soil

Unconfined compressive strength

Biopolymers generally increased the UCS of soils with superior performance in the presence of clay. For example, the study revealed that the UCS of mine tailings stabilized with 0.5% xanthan gum was 150% greater than untreated mine tailings [80]. For road base material, 2% xanthan gum treatment increased the UCS twice as that of the untreated sample with three days of curing [83]. The UCS value reached 4.19 MPa with 1% xanthan gum and 28 days of curing [83]. The addition of sodium alginate biopolymer to clayey soil resulted in a 69% increase in compressive strength [101]. The compressive strength of biopolymer xanthan gum treated sand increased with biopolymer dosage and curing time [87]. 2% guar gum improved the compressive strength of sand-clay mixture by 30% and 35% after 7 days and 28 days, respectively as compared to 10% cement-treated

sample [89]. Also, 2% xanthan gum treated samples displayed 50% higher strength than cement stabilized samples after 7 days of curing of sand-clay mixture [89]. Gellan gum treated sand had a compressive strength ranging from 130.2kPa to 434.6kPa with a dosage of 0.5-2% [90]. For the clay with 0.5% xanthan gum biopolymer, compressive strength values were measured to be 383, 471, 613, and 669 kPa at 0, 7, 28, and 56 days, respectively [97]. An increase in strength up to 50% was achieved by using 1% xanthan gum biopolymer in stabilizing sand [78]. The UCS of various biopolymer treated soils are shown in Fig. 2.4.

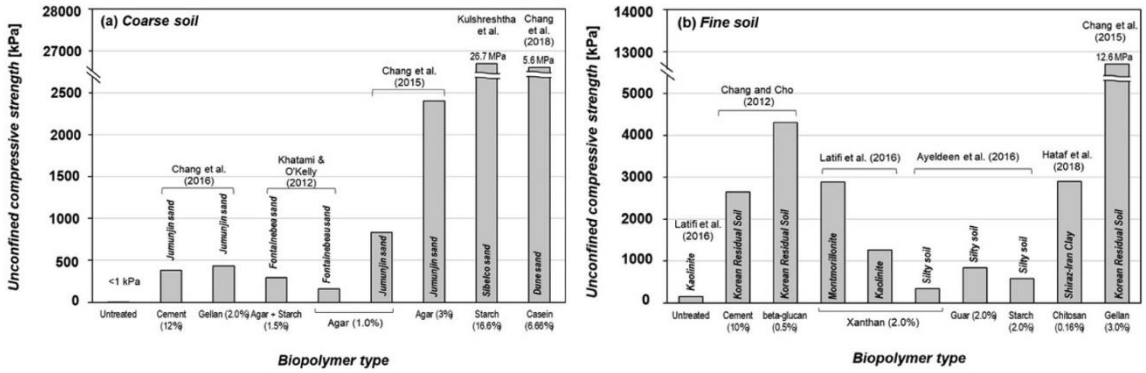

Fig 2. 4 Unconfined compressive strength of biopolymer-treated soils at a dry condition a) Coarse soil b) Fine soil [66].

Shear strength

The undrained shear strength of mine tailings increased from 1.6 to 22.3 kPa with 0 -2% of guar gum and from 1.6 kPa to 5 kPa with 0-3% dosage of xanthan gum [79]. The cohesion of mine tailings increased from 241.6kPa to 514.4 kPa with an increase in xanthan gum dosage from 0-0.5% [80]. Increase in direct shear strength and friction angle (23-46%) occurred in 3% and (73-90%) 5% xanthan gum stabilized sand [86]. Another study reported that the cohesion of sand increased from 0-240kPa with biopolymer treatment [91]. However, the friction angle decreased from 32.3-17.6^{o} [91]. Gellan gum increased the shear strength of clays, even at high water content, as observed by vane shear testing [93]. The study showed that guar gum is an excellent stabilizer for mitigating the dispersion and dusting behaviour of red mud waste [84].

Tensile strength

Moreover, the tensile strength of 2% xanthan gum treated soil exceeds cement-treated soil by 38% after 28 days of curing [89]. The surface strength of mine tailings increased from 212.8N to 340.6 N with a xanthan gum dosage of 1.6% [81]. With guar gum, the

increase was from 212.8 N to 428 N [81]. Further, biopolymers also promote the growth of natural vegetation [67].

Permeability

Xanthan gum treatment reduced the permeability of sands by 3-4 orders of magnitude [87]. The permeability of sands reduced to 1 $X10^{-8}$ cm/s from 2.1$X10^{-4}$ cm/s with gellan gum treatment [90]. The hydraulic conductivity of sands reduced by 10 and 100 times when treated with 1% sodium alginate and xanthan gum, respectively [78]. For example, the test results showed that the coefficient of permeability (k) of samples decreased sharply from 6.5 × 10−7 cm=s (clay only) to 1.2 × 10−7 cm=s by adding 1.0% xanthan gum [97].

2.6.3.1.2 Mechanism of stabilization

Gellan gum: In general, gellan gum forms uniform hydrocolloids, which transform into firm hydrogels via the virtue of thermo-gelation upon cooling. The hydrogels have extremely high water retention capacity [93]. Hydrated biopolymers interact with clay particles and coagulate them, while electrically neutral sand particles have no direct interaction with biopolymers. For clay, the strengthening depends on the gellan gum-to clay ratio by mass [93]. The study revealed that the gellan gum–clay matrix of kaolinite clay is optimized at around 4%, regardless of the soil composition and soil water content [93].

Xanthan gum: Interparticle aggregation is the main phenomenon leading to stabilization of clays at low xanthan gum to clay ratios [95]. Generally, xanthan gum biopolymers at lower concentrations (up to 1%) prevented interaction with clay particles by filling the pores [97]. However, a larger amount of xanthan gum biopolymer (more than 1%) displaces more particles of clay, thereby increasing the pore fluid viscosity and inducing a ductile material [97]. The reaction mechanism between clay and xanthan gum biopolymer is due to van der Waals forces and the hydrogen bonding. The hydrogen bonds are built between the hydrogen and the hydroxyl of clay and those of the groups D-glucuronic, D-mannose, and pyruvate of the xanthan gum molecule [97].

2.6.3.2 In-situ applications of biopolymers

The in-situ biopolymer can be generated by the addition of microorganisms accompanied by a medium, which initiates the formation of biopolymer within the soil. The biopolymer produced by bacterial culture such as by *Alcaligenes faecalis, Alcaligenes* eutrophus and

Alcaligenes viscolactis [78], *Microbacterium arborescens* [78], *Rhizobium tropici* [105, 106], *Enterobacter aerogenes* and *Pseudomonas fluorescens* [107] and *Leuconostoc mesenteroids* [73, 108]. Fig.2 shows in-situ production of biopolymer by bacterial cells on a glass substrate.

Investigations into soil properties that affect biopolymer – soil particle binding characteristics could result in the identification of specific geochemical attributes that lead to increased soil strengthening, thereby enhancing engineering practices related to erosion, dust abatement or foundation support. The geotechnical properties improved by in-situ biopolymers are strength and stiffness [78, 105, 106], ductility [73], hydraulic conductivity [73, 78, 107] and cohesion leading to erosion resistance [108].

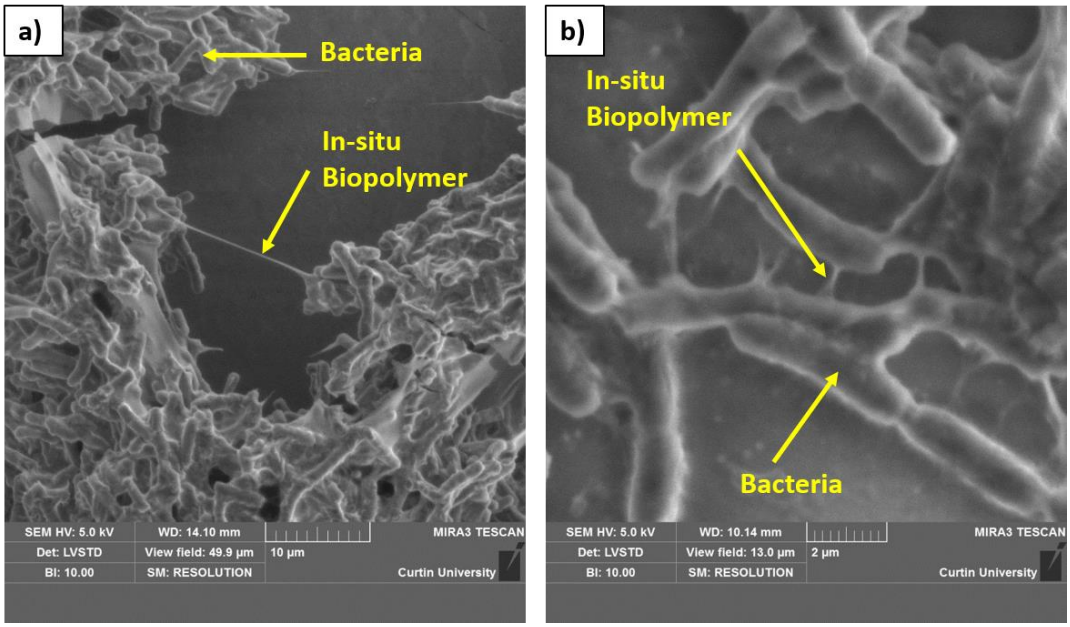

Fig 2. 5 SEM micrograph of MIP generated in-situ (unpublished data)

2.6.3.2.1 Laboratory studies

The results of the study revealed that the in-situ microbial biopolymer formation by bacteria *Leuconostoc mesenteroides* increased the critical shear stress and surface erosion resistance, which the researchers attributed to the increased cohesion by grain-coating biopolymer slimes and the reduced seepage flows due to pore clogging [108]. A similar studied reported that the permeability of the sand was reduced by more than one order of magnitude by the production of insoluble biopolymer, dextran, produced by *L. mesenteroides* [109]. Moreover, the electrical resistivity of in situ biopolymers treated

sand increased by more than 100%, which was caused by the occupation of the pore spaces by dextran leading to a subsequent decrease in the porosity [73].

2.6.4 Advantages and limitations of MIP

The ex-situ application of MIP has several advantages over other biological approaches, such as no requirement for microbial or nutrient injections, a shorter treatment time, and compatibility with clayey soils [105]. In addition to this, as MIP is omnipresent in natural formations and most of the commercially available varieties are known to be harmless, hence they are a sustainable, eco-friendly construction material [67]. The pH of the clayey soil reached a value of 8.2 with 4% sodium alginate from an initial value of 8.2 [102]. The pH of silt reached a value of 7.7 from 7.5 with 6% alginate content [102]. The pH is much lower than cement and lime treated soils. The use of MIP to improve the engineering properties of a variety of geologic materials is a promising technique that exhibits both cost and environmental benefits [106]. Flexibility in production and application as well as biodegradability offer certain unique advantages and some disadvantages over synthetic polymers [106]. For example, MIP offers the potential advantage of being amenable to both ex-situ and in situ production [106].

For the successful application of MIP in geotechnical engineering applications, the limitations of the technology must be addressed. The main constraint to their commercial products is the cost associated with substrate and downstream processing [70]. In addition to this, there are few technical issues that must be overcome for practical applications. The key issue is the gradual reduction in the strength of MIP when exposed to moisture [90, 110]. During the process of drying, as MIP-treated soils lose moisture via dehydration, their strength increases significantly. It has been reported that the interaction between MIP and water weakens the bond between the biopolymers and soils and greatly reduces the corresponding strength of the material [110, 111]. In addition to this, the overall workability (mixing and application methods) of the biopolymer-soil mixtures is limited by the high viscosity of the biopolymer-soils [67]. Therefore, the current practised must be modified to incorporate the rheology of the biopolymers and biopolymer-soil mixtures.

Another major issue limiting its application is the upscaling issue associated with biopolymer stabilizer. Biopolymer technology has not yet reached full-fledged field-scale testing. The major drawback limiting its application is the susceptibility to the presence of water. To achieve field-scale implementation, it is essential that the durability of biopolymer treated soils should be tested in large scale test conditions. Researchers have made progress in this area with commercially available biopolymers such as xanthan gum [67]. Biopolymer application in the field should be carried out with caution as most of the biopolymers are hydrophilic, leading to swelling and clogging. However, most of the studies are confined to laboratory conditions. Moreover, the potential of in-situ insoluble biopolymers needs to be explored as well.

2.6.5 Synergistic system: MIP and MICP

Along with minerals, the presence of MIP has also been reported in natural formations such as stromatolites, beach rocks and microbial mats [112-115]. Inspired by natural formations, soil stabilization via carbonate precipitation is a well-researched area that mainly focuses on MICP [116-119]. Bio mediated soil improvement refers to a chemical reaction mediated by biological activity whose by-products alter the engineering properties of the soil [116, 120-123]. Biological activities provide an ability to control and manage the timing, rate, and spatial distribution of the chemical reaction [116, 124]. It has been reported to increase the strength [125-127], stiffness [118], durability and hydraulic conductivity [85] of mainly sandy soils. Recent studies demonstrate the ability of MICP in stabilizing fine-grained soils as well [126].

The natural formation is a classic example of synergy between the two bio-based stabilizers, MICP and MIP. The frugal energy consumption and environmental compatibility associated with their formation sparks interest among researchers in the exploitation of this synergy for engineered systems. Therefore, it is the author's apprehension that the individual limits of the two technologies can be overcome by synergising MIP with MICP. Fig 2.6 sums up the benefit of synergizing the two bio-based stabilizers. A similar coloured box shows the complementation nature of both technologies. For example, MICP has high efficiency in sandy soils, while MIP is more effective in stabilizing clays. Hence, synergising the technologies widens in application to sand-clay mixtures as well.

MIP		MICP	
Advantages	**Limitations**	**Limitations**	**Advantages**
Supports vegetation growth	High susceptibility to moisture	Might not support vegetation due to high pH	Low susceptibility to moisture
Neutral pH	Low efficiency with sand	Alkaline pH	High efficiency with sand
No ammonia gas released during production		Ammonia released during production	
High efficiency with clay		Low efficiency with clay	
High ductility		Brittle nature	

Fig 2. 6 Advantages and limitations of bio-based stabilizers

2.7 Emerging techniques for characterizing microbial polymers

This section reviews the role of advanced instrumentation techniques used for measuring the performance of bio-based stabilizers. The key highlights of the discussion include penetration testing at varying scales from macro to nanometer.

2.7.1 Atomic Force Microscopy (AFM)

AFM technique is widely used for the investigation of the microstructure of materials through surface imaging [128, 129]. Depending on the mode of operation and stiffness of the material under examination, AFM can be employed to study surface topography, phase separation and mechanical properties such as adhesion and stiffness of the sample [130]. Moreover, AFM is an ideal tool for measuring intermolecular forces at the nanoscale level [131]. The force sensitivity in nanonewton and nanometre-scale resolution of the displacement sensitivity are advantages of using AFM technique [131]. It is ideal for measuring nanoscale and microscale forces within a composite material, such as biopolymer stabilized clays [132]. Further, the technique does not rely on optical transparency and resolution is not limited by the wavelength of light [133]. Fig 2.7 shows the AFM facility at Curtin University.

Fig 2. 7 AFM instrument at Curtin University

2.7.1.1 Sample preparation

The most important factor in any microscopic technique is sample preparation [134]. The AFM eliminates the need for extensive sample preparation, such as in SEM and nanoindentation techniques. The surface topography of the sample needs to be as smooth as possible to avoid any sudden changes causing oscillation of the cantilever [134]. Regarding imaging of biopolymer, SEM does not allow observation of the biopolymer in its hydrated state due to the extensive sample preparation required. The complete and real biopolymer structure can be visualized by the atomic force microscope, which does not require any preparation method [134]. There are also advanced technologies adopted for sample preparation, for instance, the focussed ion beam (FIB) technology. The focussed ion beam (FIB) technology in sample surface preparation for PeakForce QNM test was also reported [135].

2.7.1.2 Configuration and operation

The primary component of an AFM is the microscope, which includes the sample stage, scanner, high-resolution probe/tip, and detector [130]. The schematic of an AFM can be seen in Fig 2.8. The basic working principle of AFM is that a sharp tip probes the surface of a sample while continuously collecting information about the sample. The cantilever

tip which is located at the free end of a cantilever, is usually only several microns in length (100 − 200 μm) [130]. Further, the vertical displacement and lateral distortion in the cantilever is measured and mapped as the tip probes the specimen surface [130, 131]. Recording the deflection of cantilever as a function of sample position generates a force map or image of the surface [136]. Imaging can be carried out in either contact mode (CM) or non-contact mode (NCM). The applied force in NCM is much lower than the CM [125]. The tapping mode can generate both topographical and phase contrast images [123]. Height images provide information with respect to the topography as the probing tip is raster scanned across the sample surface. For imaging, the AFM is generally used with a silicon nitride probing tip (diameter on the order of 10 nm) in tapping mode [128]. In tapping mode, a piezoelectric element is used to vertically oscillate the cantilever at certain amplitudes and intermittently make low force contact with the surface. This is the preferred mode for soft, adhesive, or fragile substances [128]. The AFM tapping mode imaging technique is a versatile and powerful tool for scanning the surfaces of soft materials because it was developed to minimize sample deformation and avoid the surface and/or tip damage found in contact mode AFM [132].

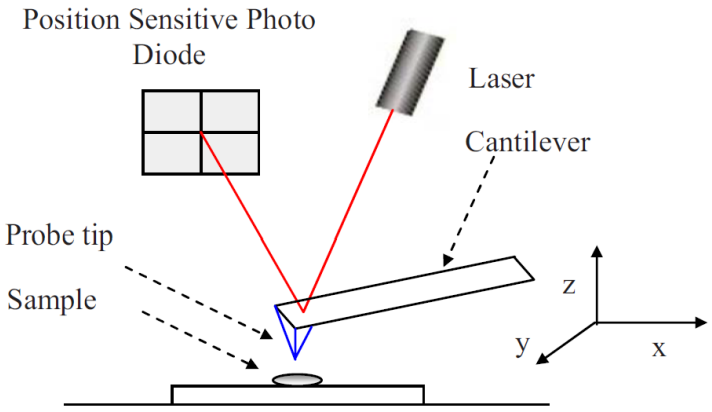

Fig 2. 8 Schematic of an AFM [132]

2.7.1.3 Nanomechanical mapping

The AFM probe consisting of a tip and the cantilever is used to scan the surface of the specimen by applying a sinusoid wave with a normal frequency range of 0.5-2 kH [137]. Further, a force curve is collected at every pixel, and the peak value of each force curve is considered as the feedback signal of the image. Therefore, the detailed interaction

between tip and specimen can be obtained at each pixel. The Young's modulus of the material was calculated according to the Derjaguin-Muller-Toropov (DMT) model [137], using the following equations:

$$F_{interaction} = \frac{4}{3} E^* \sqrt{R(d - d_0)^3} + F_{adh}$$

Where E*is the reduced elastic modulus, R is the curvature radius of the tip, d is the displacement of the scanning tube, d_0 is the deformation of the cantilever, so d-d_0 is the deformation of the specimen. The Young's modulus of the material can be obtained from the following equation:

$$E^* = \left[\frac{[(1 - \nu_s^2)}{E_s} + \frac{1 - \nu_{tip}^2}{E_{tip}} \right]^{-1}$$

Where, v_s and v_{tip} are the Poisson ratios of the specimen and the tip E_s and E_{tip} and are the elastic modulus of the specimen and the tip, respectively.

As for the measuring system, Nanoscope software is used, and the test system under the path of Mechanical Properties/Quantitative Nanomechanical Mapping/Peakforce QNM in the air is chosen. A standard is used to calibrate the deflection coefficient of the probe, as well as the curvature radius of the tip and the spring constant of the cantilever within the system [137]. For mapping, the nanomechanical properties, the imaging scan rate, as well as the driving frequency of the cantilever must be maintained. The raw AFM topography images are further processed using a first-order plane fitting routine using the Bruker Nanoscope Analysis 1.50 software [138].

2.7.1.4 Adhesion studies

While performing adhesion studies, the cantilever is brought into contact with a liquid droplet, and a nanoscopic capillary bridge is formed between the tip and the sample surface. The force required to pull off the cantilever completely from the sample surface (adhesion, F_{ad}) is the force against all electrostatic attractions (F_{el}), capillary forces (F_{cap}), van der Waals forces (F_{vdW}) and chemical interactions (F_{chem}) between the tip and the sample [138]. The adhesion (F_{ad}), therefore, provides information about the tip-sample

interactions, which are strongly related to the chemical composition of both the sample and tip.

2.7.1.5 Results and interpretation

The surface image of the sample obtained using AFM may or may not be representative of bulk constituents [133]. It should be noted that the area imaged may not be representative of the overall surface characteristics since the samples are usually inhomogeneous at several scales [133]. Further, serval factors affect the quality of results obtained using an AFM. Some of them include experimental/instrumental factors, including contamination of the cantilever or probe tip, changes in setpoint and incorrectly set gains in the feedback loop that can result in dramatic changes in the image. Anomalies such as apparent phase inversion and changes in the resolution are often the result of these factors [133].

2.7.1.6 Applications in geotechnical engineering

In the area of civil engineering, the use of AFM is relatively new. The PF-QNM technique is immensely powerful to characterize the mechanical properties of micro-and nanostructures in cement-based materials. It does not have strict requirements for the test environment, and it does not damage the surface of the material [137]. High-resolution images can be obtained very easily, and they can be analysed statistically.AFM was mainly used to map the modulus variation in a mortar sample [139].

The lack of sample preparation required for AFM also makes it very popular for sensitive substances such as clay and biopolymers. Fig 2.9 shows the scale variation between nanoindentation and AFM imaging. The clay particles embedded in the biopolymer is clearly visible in the latter, making it an ideal tool to study such materials. While the values obtained from nanoindentation are useful in estimating the property of the composite, the PeakForce-QNM reveals the variation in properties at a much finer scale, enabling the study of microscopic changes in the composite. In a recent study, PeakForce-QNM revealed the map of elastic modulus of the composite at 1μm resolution and helped in understanding the micro-mechanism behind the reduction in strength of the sample after exposure to moisture (unpublished study). This quality is highly desirable to

investigate biopolymer stabilized soils as they are prone to moisture disintegration. The clay particles which were held fixed by the biopolymer became loose owing to the weakening of the biopolymer network on exposure to moisture. This micromechanical phenomenon resulted in the reduction in strength of the stabilized samples at a macro scale.

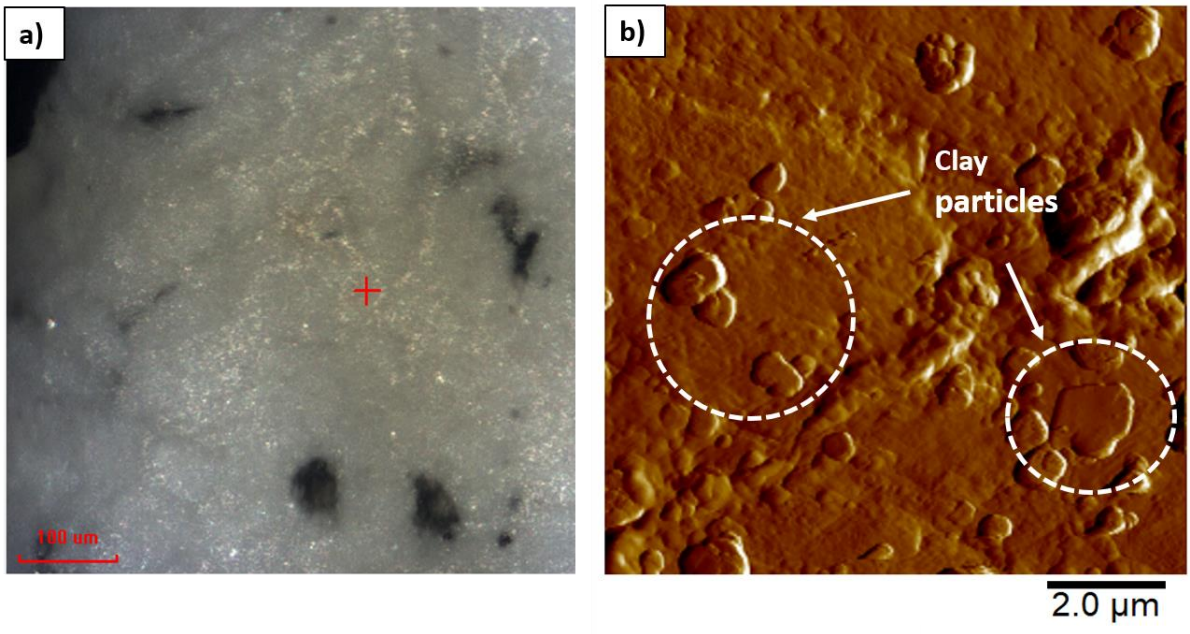

Fig 2. 9 Surface imaging of MIP stabilized clays using a) Nanoindentation b) Atomic Force Microscopy

PeakForce-QNM mode in AFM can be to study the nanomechanical properties of the biopolymer at a high resolution. This mode offers the mapping of elastic properties of the sample with a lateral resolution of a nanometer. The PeakForce-QNM is suitable to determine the nanomechanical properties of soft materials such as MIP as they operate at low forces and, consequently, smaller deformations. This method has been employed to study the nanomechanical properties of soft materials such as MIP.

2.7.2 Nanoindentation

In nanoindentation technique, a small specimen of unknown properties is indented with a probe made of known material properties [139]. The length scales are distinct from mechanical experiments with AFM, which uses a much smaller tip [128]. The load and displacement response measured during the withdrawal of the probe from the specimen is used to extract the elastic modulus and hardness of the indented specimen [139].

2.7.2.1 Sample preparation

The biggest challenge and critical step in preparing samples for nanoindentation are to polish the sample to provide a smooth and flat surface while minimizing the sample disturbance [140]. Moreover, the average indentation depth, which is more than three times the average surface roughness of the sample, must be maintained to avoid the effects of roughness [140]. Given that the measurements are nanometre length scales, the roughness of the specimen surfaces can adversely affect the precision of the measured indentation depth, thereby affecting the accuracy nanomechanical properties [139]. Therefore, it is essential to prepare specimens with the lowest possible surface roughness. To ensure a smooth surface, the test specimens are generally polished with three different grades of sandpaper (600–1,200 grit), starting from the most abrasive grade to the least abrasive grade [139]. The specimens were then polished with a series of colloidal solutions of 1.00, 0.30, and 0.05 μm alumina suspensions to ultimately achieve a 0.05 μm level of smoothness [139]. During these polishing steps, water is continuously used to wash the chafed particles to prevent unintended scratches on the specimen surfaces [139].

2.7.2.2 Configuration and operation

The specimen is securely placed at the central zone of the stage inside the environmental chamber of the nanoindenter prior to testing. It is then viewed through an optical microscope to select the areas of interest. The number of selected indentation points should be high enough to make the analysis statistically representative and conclusive [139]. Further, sufficient lateral spacing should be maintained between consecutive indentations to avoid the influence of neighbouring indentations [139]. The Berkovich probe fitted with the nanoindenter is generally used to indent the sample. The Berkovich probe is a three-sided, pyramidal probe with an included angle of 142.35° plane to edge, a half-angle of 65.35°, an aspect ratio of 1:8, and an average radius of curvature equal to150 nm [139].

2.7.2.3 Results and interpretation

To obtain the elastic modulus of the sample, the load indentation measurements corresponding to the elastic recovery of the specimen material is fitted with analytical

models [139, 141]. Generally, Oliver and Pharr method is used to analyse the load-displacement data obtained from the test [141].

2.7.2.4 AFM based nanoindentation

The AFM indentation tests were analysed using the same approach that is typically used for conventional indentation tests to determine the mechanical properties of the asphalt materials being considered. In this analysis, the force-distance curves must be transformed into force-indentation curves. However, the indentation depth in the AFM is computed using Eq. (2) based on the cantilever deflection and piezo-driver displacement, which is different from the conventional indentation tests [132]. To calculate the elastic modulus from the force-indentation curves, Sneddon's modification of the Hertzian model for the indentation of a flat, soft sample by a stiff tip was employed.

$$\delta = z - d$$

d- cantilever deflection

z-piezo-driver displacement

delta-indentation depth

2.7.2.5 Applications in geotechnical engineering

Such experiments were initially conducted on asphalt materials for obtaining linear viscoelastic properties [137]. Details on nanoindentation can be found elsewhere [135, 138]. It has been widely used in civil engineering for mapping of material properties across the aggregate-matrix interfaces [133], asphalt concrete [123, 139, 140], determining micromechanical properties of bitumen [141, 142], porous asphalt concrete [143], to study the ITZ of concrete [144] and mortars using RAC at microscale [145] cement paste and rocks [146]. The requirement of small specimens, as well as mapping of mechanical properties of the material at a microscale, are the advantages associated with the technique. Further, this technique can be effectively used to characterize the fundamental properties of different phases in heterogeneous mixtures such a concrete, rocks, and asphalt [133]. The enhanced precision of material properties by using small-

volume specimens can improve the accuracy of materials characterization as well as modelling [133]. Studies have reported that small-scale properties of aggregates, bitumen, and matrices using small-volume specimens were more accurate and reliable in comparison to standardized test methods [133].

Nanoindentation can be a useful tool to probe the micromechanical properties of soil stabilized with bio-based materials. In a recent employing MICP for stabilization of Road base material, nanoindentation testing was conducted to estimate the relative bond strengths between the binder and the sand. Of special interest in this investigation were the mechanical properties of cement bonding, MICP bonding and a combined MICP–cement bonding system [147]. The experimental investigation revealed that in cement-stabilized samples, MICP improved the strength by reinforcing the bridging structures between grains and the bridge/sand grain interface [147]. Nanoindentation testing was also carried out on dry clay reinforced biopolymer sample (Xanthan gum) to quantify the micromechanical properties of the stabilizer (unpublished study). The average hardness and elastic modulus of the clay reinforced biopolymer sample obtained from nanoindentation testing are 0.078 ±0.03 GPa and 5.02 ±1.3 GPa, respectively.

2.7.2.6 Limitations

For anisotropic cement-based materials, however, the nanoindentation technique still presents some problems; the nanoindentation apparatus, for instance, cannot give a real-time image of the indenting process; this leads to deviations in the indentation and pre-set positions. Moreover, the measured specimen cannot be used again due to the surface damage caused by the nanoindentation procedure. Besides, the incidence of the single-point indentation usually ranges between1-3 μm if a sample is tested by grid lattice technique; the chosen grid dimension and distance are often greater than 10 μm, so it is uncertain whether the indentation point can fully represent the grid where it is located.[131]. The nanoindentation experiments are conducted in an exceedingly small volume of material, opening up many possibilities for future research in assessing mastic properties in an asphalt concrete sample [123]. However, a limitation of the conventional nanoindentation technique is that the properties cannot be measured at a specific location or asphalt phase within the sample [136]. These challenges include high heterogeneity at

multiple length scales, physicochemical interactions, and viscoelastic behaviour entering at small length scales that are difficult to access using traditional methods. These challenges motivate the primary advantages of using nanoindentation over any macroscale techniques, which focus on bulk, composite behaviour [128].

2.7.3 Penetration testing

Penetration test has been a promising technique for characterizing the surface strength of a crusted surface. It requires less sample preparation and can be employed in both field and laboratory. It can also be used when sampling is not allowed due to various reasons [142].

2.7.3.1 Configuration

The most used needle penetrometer is the SH-70 penetrometer manufactured by Maruto Corporation, Ltd, Tokyo, Japan [142]. The equipment is housed in a lightweight portable device and consists primarily of a 0.84 mm diameter needle, which can be pushed slowly into the sample [142]. The penetration force is recorded as a function of the penetration depth. The general view of the commonly used needle penetrometers is shown in Fig. 8.

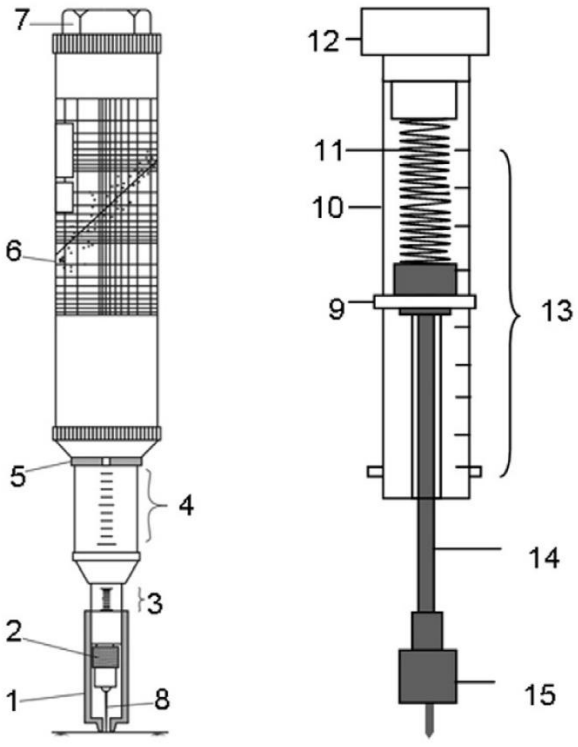

Fig 2. 10 General view of the Maruto modified Eijkelkamp (right) penetrometers and their parts [142]- 1) presser, (2) chuck, (3) penetration, (4) load scale, (5) load indication ring, (6) UCS–NPR correlation chart given by the manufacturer, (7) removable cap, (8) penetration needle produced according to the Japan Civil Engineering Society's guideline, (9) indicator ring, (10) penetrometer tube, (11) spring, (12) end cap, (13) scale, (14) extension rod, and (15) needle block.

2.7.3.2 Results and interpretation

The needle penetration resistance (NPRM) is obtained by dividing the penetration load, i.e., 100 N or, the maximum load at a penetration depth of 10mm, by the penetration depth, i.e., the penetration depth at a penetration load of 100 N or, respectively 10mm [142]. UCS of the sample can be estimated from NPRM readings using the correlation introduced by the SH-70 manufacturer using the equation given below [142].

$$\log UCS = 0.978 \log(NPR_M) + 2.621$$

Where UCS is expressed in kPa and NPR_M in N/mm.

A modified version of the penetrometer, which is a name of equipment manufactured by Eijkelkamp, the Netherlands, is used instead of the Maruto penetrometer. The standard Eijkelkamp cone has been replaced by a short needle made of hardened steel. Needles with a diameter of 1 or 1.4 mm and with a flat or a conical tip are available. It should be noted that their conical part (if any) is less than 1.3 mm long while the shaft of the Maruto needle increases slowly from 0 to 0.84 mm diameter over about 10 mm [142].

2.7.3.3 Application in geotechnical engineering

Numerous researchers have conducted experimental and numerical investigation on surface stabilized soils treated with biopolymers [143, 144]. The flat-ended penetrometer method applied load to a known area covering several soil grains and can be easily adapted for field use [143]. The most common NP model is the SH-70 penetrometer manufactured by Maruto Corporation Ltd., Tokyo, Japan that is a lightweight, portable device, which consists primarily of a 0.84 mm diameter needle [142]. The needle penetration resistance (NPR) is obtained by dividing the penetration load by the penetration depth, and UCS values can be estimated from NPR values using various empirical correlations. Correlations exist between NPR values and Elastic Modulus, UCS, Tensile strength, Cohesion, Friction angle, P and S wave velocities [142]. The

stiffness of the sample is dependent on the penetration depth [142]. Therefore, fixing the upper load level or the amount of the allowable penetration depth is important while correlating NPR values with the geo-mechanical properties of the soil [142]. Many penetrometer testings on the same sample is essential to obtain a fair strength estimation. During penetration, very high compressive and shear stresses develop under the needle and stress normal to the needle shaft increase [142].

2.7.4 Benefits of testing at various length scales

Advanced characterization techniques have provided powerful tools for characterizations of many materials at micro-and nanoscales worldwide. They have empowered many researchers to reveal how the composition, structure, and properties of materials at a nanoscale influence their performance at a macro scale, which consequently enables to modify the materials at multiple scales. By developing a clearer understanding of the micromechanical behaviour of the stabilized soils and linking their behaviour to chemical composition and macroscopic properties, one can engineer stabilizers that will result in improved mechanical properties and eventually longer-lasting and better-performing [130]. Combined, nanoindentation and AFM can be used to establish links between the binder microstructure and bulk behaviour, which can ultimately serve as improved inputs to developing multiscale models for the complex behaviour of biopolymer modified soils. Generally, the fundamental properties of any stabilizer are affected by the material properties at the nanoscale. To improve the performance of biopolymer stabilized soils, it is imperative to understand the nanoscale properties. Atomic force microscopy (AFM) is used to determine local mechanical properties along with high-resolution imaging, and it is just gaining importance in the study of nanostructure of cementitious materials [145]. AFM has been successfully implemented for different soft materials; however, it provides qualitative information and proportional values for the elastic modulus of the sample [145]. Whereas nanoindentation has proved to be a reliable technique to determine local mechanical properties quantitatively, however the lack of high-resolution imaging of the sample poses a serious concern for heterogeneous materials. In general, the results of nanoindentation are consistent with the results of PeakForce QNM, but small differences still exist. Based on the observation by PeakForce QNM, it is proposed that cement paste was likely to be a granular material in which the sub-micron scale grains or basic

nanoscale units packed together [135]. It was suggested that the different grains packing at two different investigated length scales might be the reason for different modulus results measured by PeakForce QNM and nanoindentation, and the greater distribution range of elastic modulus measured by PeakForce QNM may be attributed to the change of packing density of nanoscale grains during the sample preparation procedure. After all, the indentation depth in PeakForce QNM is far smaller than that in nanoindentation [135].

2.8 Challenges

Hence, to sum up, the significant potential of this technology for future soil stabilization applications is highly promising. However, the upscaling issue associated with any bio-based stabilizer remains a challenge due to various reasons. A field-scale study involving the surficial application of MICP was completed at a mine site located in the province of Saskatchewan, Canada [147]. The testing also revealed that the MIP treated soil surfaces exhibited a higher surface stiffness and less surface erosion as compared to untreated surfaces [67]. Another example is the slope surface stabilization of an embankment at a national highway construction site in Seosan, Korea [67]. The site was observed for a period of one year after construction to determine the erosion response of the exposed biopolymer-soil surface under real climate conditions, and it was found that the higher biopolymer concentrations imparted a higher resistance. MIP stabilized soil has been attempted to be used in the construction of a river levee structure along the Nakdong river near Andong, Korea [67]. Long-term observations over a year period and revealed that the MIP treated soils had a beneficial effect on the growth of vegetation in the soils, especially for the naturally occurring vegetation [67]. However, biopolymer technology hasn’t yet reached full-fledged field-scale testing. The major drawback limiting its application is the susceptibility to the presence of water. To achieve field-scale implementation, it is essential that the durability of biopolymer treated soils should be tested in large scale test conditions. Researchers have made progress in this area with commercially available biopolymers such as xanthan gum [67]. However, the potential of in-situ insoluble biopolymers needs to be explored as well.

Not many field-scale tests are carried out using MIP. MIP stabilized soils were used in the stabilization of soil for pavement application in the target site in Korea (KAIST, Daejeon, Korea).

2.9 Concluding remarks

The current socio-economic developments demand environmentally friendly stabilizers, which meet the requirement for adequate engineering performance. This has led to the emergence of bio-based as they are formed by natural processes and offer the benefits of being environmentally benign and having a low carbon footprint. The recent advances in the field of bio-geotechnology with a focus on MIP for soil stabilization application are discussed in this review paper. The emergence of MIP as a sustainable stabilizer has been well recorded. MIP applications can be useful in areas such as stabilization of unpaved roads, slopes, dust suppression and stabilization of mine tailings. Their benefits include being environmentally benign, having a low carbon footprint and can be employed to obtain both permanent and temporary solutions. MIP stabilized soils do not hamper the growth of native flora and fauna by altering the soil chemistry. In addition to this, MIP offers the flexibility of in-situ as well as ex-situ method of application. Moreover, the role of state-of-the-art characterization techniques such as nanoindentation and AFM in elucidating the stabilization mechanism cannot be ignored. Hence, to sum up, the significant potential of this technology for future soil stabilization applications is highly promising.

To sum up, studies have demonstrated that biopolymer treated soils improve the strength of soils which is maximized in the presence of clay. Further, they increase resistance to erosion, reduce permeability and promote the growth of local flora and fauna. Further research is essential to understand the behaviour of various biopolymers with different soils. The research should be directed towards producing biopolymers that are less prone to moisture ingress. Workability issues with the mixing of biopolymer with soils can also be overcome by using in-situ biopolymer producing bacteria in the soil. Further research is required to optimise the process and understand its best application.

2.10 Future recommendations

MIP technology offers immense benefits in soil stabilisation but must overcome a few hurdles before successful commercial applications. More studies need to be conducted on unpinning the fundamental processes involved in the formation of biopolymers under natural conditions to gain more knowledge about the underlying mechanisms. Moreover,

the utilisation of native bacteria via biostimulation needs to be investigated further. It can be noticed that most of the research in MIP is focussed on the utilization of utilisation of laboratory-grade high purity chemicals to produce polymers. Efforts must be taken in the economisation of the technology, including screening of alternative sources as industrial by-products and cheaper carbon substrates.

Another issue of concern during the application of this technology is the sensitivity and degradation of biopolymers under saturated conditions, which considerably affect their performance. It is desirable to identify methods to mitigate this issue. The underlying mechanism behind the reduction in strength is due to the interaction between the water molecules and MIP. One possible approach to alleviate this problem is the use of crosslinking, which is a method of increasing the number of inter-particle bonds between two chemical compounds. The reinforcement of biopolymers with clay is effective in our studies leading to a reduction of water absorption and providing an overall increase in the strength in both wet and dry conditions. However, it will be essential to investigate further the effect of cross-linking on the overall workability of the MIP soil mixtures, and more research should be conducted in this area.

As cementitious materials, there are several properties of MIP that are not fully understood. These include properties as hydrophilicity, behaviour in soils and water, high water-holding capability, effects on the permeability of soils, impact on the plasticity and overall water-related behaviour of clayey soils. Additional testing is required to overcome these boundaries. Advanced techniques such as nano-indentation and AFM are necessary to study the interaction of MIP with clayey soils to unpin the mechanisms at the micro-level. As such, further tests on the water-soil related effects of MIP are also needed. Moreover, field-scale testing must be encouraged to gauge the performance of this technology in actual field conditions. Training of professionals as well as the development of codes and database for experimental investigation using MIP will be highly beneficial.

Table 2. 1 Summary of some polymers used for soil stabilization

Reference	Soil	Polymer used and dosage	Soil parameter improved			
			UCS (MPa)	Cohesion (kPa)	Angle of friction(^{o})	California Bearing Ratio (%)
[37]	subgrade soil	Polymer E, R and s (0.5%, 1% and 2%)	1-4	-	-	-
[157]	Low plasticity silt	Lignin 2-12%	0.2-0.7	-	-	15-35% (94% compaction) 15-40 (96% compaction)
[38]	Subgrade soil	Superabsorbent polymer (0.5% and 1%)	-	50-130	14-22	-
[158]	Kaolinite, illite and montmorillonite	Polymer (0.1%)	-	210-350	14-49	-
[46]	Clay	Polymer (2-5% optimum)	3-7 dry 1-2 wet	-	-	-
[65]	Limestone quarry fines	Acrylic polymer (2.27 mL/kg- 11.35 mL/kg)	0.3- 2.5			
	Clay	Acrylic resin (5%, 8% and 10%) and cement 8%	2.0-3.5	-	-	-
[52, 159]	Clay	Acrylic resin R790 and R83 Dosage (5, 8, 10%) and cement 8%, 12%	1.8-3	-	-	-
[160]	Sand	epoxy resin Epoxy/water ratio (0.5, 1, 1.5 2%)	1-10	50-497	18-23	-

[161]	Sand	Organic polymer stabilizer (1%, 2%, 3%, 4%) and polypropylene fiber	0.023-0.536	9.87-50.44	21.08-34.01	-

Table 2. 2 Commercially available MIP and their composition

Reference	**MIP**	**Composition**	**Microorganism**	**Main characteristics**
[68]	Xanthan gum	Glucose, Mannose, Glucoronic acid, Acetate, Pyruvate	*Xanthomonas campestri*	1. Highly viscous and pseudoplastic rheology 2. Commonly used in drilling muds and soil treatment
[69]	Gellan gum	Glucose, Rhamnose, Glucoronic acid, Acetate, Glycerate	*Sphingomonas*	1. Temperature-dependent viscosity variation (thermogelation) 2. Irreversible gel formation once cooled below 40°C
[70]	Alginate	Mannuronic, guluronic acid, Acetate	*Azotobater and Pseudomonas*	1.Hydrocolloid 2.Gellling capacity 3.Film-forming
[70]	Levan	Fructose	*Aerobacter, Erwinia*	1.Low viscosity 2.High water solubility 3.Biological activity 4. Adhesive strength 5.Film-forming capacity
[68, 71]	Scleroglucan	Glucose, galactose, Acetate, Pyruvate, Succinate, 3-hydroxybutyrate	*Sclerotium rolfsii*	1.Significant use in horizontal well drilling 2.Improving the water retention of soils
[68, 72]	Welan Gum	Glucose, Rhamnose, Mannose	*Alcaligenes*	1.Excellent thermal stability 2.retention of viscosity at elevated temperatures
[73, 74]	Dextran	Glucose	*Leuconostoc*	1.Flexible biopolymer 2.Lowers permeability in aqueous medium 3.Emulsifier
[75]	Pullulan	Maltotriose	*Aureobasidium*	

Table 2. 3 Summary of some biopolymers used for soil stabilization

Reference	**Soil**	**Biopolymer used and dosage**	**Soil parameter improved**			
			UCS (MPa)	Cohesion (kPa)	Angle of friction(^{o})	CBR (%)
[95]	Fine-grained soil	Sodium alginate (0-6%)	0.4-0.8	-	-	-
[94]	Soil	Sodium alginate and fiber	2.23 -4.44	-	-	-
[86]	Sodium bentonite and kaolinite	Xanthan gum (0.5%, 1%, 1.5%, 2 % and 2.5%)	0.5-3	200-600	20-26	
[75]	Road base	Xanthan gum (1, 1.5, 2%)	1.1-4.9	-	-	-
[82]	Sand, kaolin.	Gellan gum (0.2-5%)	-	18.5-127.3	18.7-43.4	-
[108]	sand	Gellan gum (0.5, 1 2%)	0.1-0.5	-	-	-
[97]	Sand	Casein and sodium caseinate (0. 5, 1, 2, 3 and 5%)	0.4-1.6	100-140	35-45	20-85
[96]	Clay soil	Chitosan (0.02-0.16%)	0.5-2.5	15.7-30.3	20.3-22.3	-
[84]	Sand	Agar and modified starch (0.3-1.2%)	0.15-0.3	62-240	17.6-32.3	-

[72]	Mine tailings	Xanthan gum (0, 0.3 and 0.5%)	1-2.2.3	425.1-514.4	36.7-41.4	
[85]	Residual soil and sand	β-3, 3/1,6-glucan polymer (2.46-4.92g/kg)	2.17-4.310	-	-	-
[78]	Sand	Xanthan gum (1-5%)	-	-	20-54	-
[90]	Organic peat	Xanthan gum (0.5, 1, 1.5, 2 and 2.5%)	0.015-0.1	15-40	25-29	-
[73,89]	Clay	Xanthan gum (0, 0.5, 1, 1.5, 2 and 3%)	0.382 – 0.852	71.89- 103.90	28.06-43.20	-
[79,101]	sand	Xanthan gum (0, 0.5, 1 and 1.5%)	1.13 - 2.71	32-91	28-33	-
[89, 91]	Collapsible soil	Xanthan gum and guar gum (0.25, 0.5, 1, 2, 3 and 4%)	-	11.7-161.5	35.53-38.44	-
[92, 167]	Sand	Xanthan gum (0.1% and 0.5%)	-	3.7-298.4	33.2-50.4	-
[83, 92]	Sand	Gellan gum (0.5, 1, 1.5, 2 and 5%)				

[168]	Sand, clay	Gellan and agar gum (1%, 3%)	1.050-4.66	-	-	-
[81,102]	Earthen construction materials	Guar gum and xanthan gum (0.5-3%)	1.0-4.75	-	-	-

Table 2. 4 Summary of advanced characterization techniques

Reference	**Techniques**	**Mechanical Parameters obtained**	**Advantages and limitations**
[135, 137, 138]	Peak force QNM	Young's modulus; Adhesion force; Energy dissipation; Maximum deformation	Higher resolution and faster mapping than nanoindentation; mainly used for small area test; limited modulus test range; Test results may be easily affected by the sample surface
[135, 146]	Nanoindentation	Young's modulus; Hardness; Indentation load; Indentation depth	Measure in a large area; multiphase interaction in heterogeneous materials; Large spacing restricts more precise measurement.
[142]	Penetration testing	Penetration, load at penetration	Used as an index test, accuracy is low, can be used to predict UCS

2.11 Acknowledgements

The authors would like to acknowledge the contribution of Curtin International Postgraduate Research Scholarship (CIPRS) in supporting this research. Part of this research was undertaken using the instrumentation FESEM (Field Emission Scanning Electron Microscope) and Tescan Mira3 VP-FESEM at the John de Laeter Centre, Curtin University. We also acknowledge the use of equipment, scientific and technical assistance of the Curtin University Electron Microscope Facility, which has been partially funded by the University, State and Commonwealth Governments.

2.12 Reference

1. Vinod, J.S., B. Indraratna, and M.A. Mahamud, *Stabilisation of an erodible soil using a chemical admixture.* Proceedings of the Institution of Civil Engineers-Ground Improvement, 2010. **163**(1): p. 43-51.

2. Foster, M., R. Fell, and M. Spannagle, *The statistics of embankment dam failures and accidents.* Canadian Geotechnical Journal, 2000. **37**(5): p. 1000-1024.

3. Firoozi, A.A., et al., *Fundamentals of soil stabilization.* International Journal of Geo-Engineering, 2017. **8**(1): p. 26.

4. Premkumar, S., et al., *Experimental study on contact erosion failure in pavement embankment with dispersive clay.* Journal of Materials in Civil Engineering, 2016. **28**(4): p. 04015179.

5. Santini, T.C. and N.C. Banning, *Alkaline tailings as novel soil forming substrates: reframing perspectives on mining and refining wastes.* Hydrometallurgy, 2016. **164**: p. 38-47.

6. Rankine, K., N. Sivakugan, and R. Cowling, *Emplaced geotechnical characteristics of hydraulic fills in a number of Australian mines.* Geotechnical & Geological Engineering, 2006. **24**(1): p. 1-14.

7. Kuntikana, G. and D. Singh, *Contemporary issues related to utilization of industrial byproducts.* Advances in Civil Engineering Materials, 2017. **6**(1): p. 444-479.

8. Indraratna, B., et al., *Predicting the erosion rate of chemically treated soil using a process simulation apparatus for internal crack erosion.* Journal of Geotechnical and Geoenvironmental Engineering, 2008. **134**(6): p. 837-844.

9. Gnanendran, C. and D.K. Paul, *Fatigue characterization of lightly cementitiously stabilized granular base materials using flexural testing.* Journal of Materials in Civil Engineering, 2016. **28**(9): p. 04016086.

10. Imbabi, M.S., C. Carrigan, and S. McKenna, *Trends and developments in green cement and concrete technology.* International Journal of Sustainable Built Environment, 2012. **1**(2): p. 194-216.

11. Friedlingstein, P., et al., *Persistent growth of CO 2 emissions and implications for reaching climate targets.* Nature geoscience, 2014. **7**(10): p. 709-715.

12. Castanier, S., G. Le Métayer-Levrel, and J.-P. Perthuisot, *Ca-carbonates precipitation and limestone genesis—the microbiogeologist point of view.* Sedimentary geology, 1999. **126**(1-4): p. 9-23.

13. Dhami, N.K., M.S. Reddy, and A. Mukherjee, *Biomineralization of calcium carbonate polymorphs by the bacterial strains isolated from calcareous sites.* J. Microbiol. Biotechnol, 2013. **23**(5): p. 707-714.

14. Ramachandran, A.L., et al., *Understanding and creating biocementing beachrocks via biostimulation of indigenous microbial communities.* Applied Microbiology and Biotechnology, 2020. **104**(8): p. 3655-3673.

15. Wingender, J., T.R. Neu, and H.-C. Flemming, *What are bacterial extracellular polymeric substances?*, in *Microbial extracellular polymeric substances*. 1999, Springer. p. 1-19.

16. Xi, F., et al., *Substantial global carbon uptake by cement carbonation.* Nature Geoscience, 2016. **9**(12): p. 880-883.

17. Davidson, E., *Defining the trend: Cement consumption versus gross domestic product.* Glob. Cem. Mag, 2014: p. 8-14.

18. Emissions, B.Z., *Zero carbon industry plan: rethinking cement*. 2016: Beyond Zero Emissions.

19. Ali, M.B., R. Saidur, and M.S. Hossain, *A review on emission analysis in cement industries.* Renewable and Sustainable Energy Reviews, 2011. **15**(5): p. 2252-2261.

20. Pade, C. and M. Guimaraes, *The CO2 uptake of concrete in a 100 year perspective.* Cement and concrete research, 2007. **37**(9): p. 1348-1356.

21. Gao, T., et al., *Analysis on differences of carbon dioxide emission from cement production and their major determinants.* Journal of Cleaner Production, 2015. **103**: p. 160-170.

22. Miller, S.A., et al., *Carbon dioxide reduction potential in the global cement industry by 2050.* Cement and concrete research, 2018. **114**: p. 115-124.

23. Andrew, R.M., *Global CO 2 emissions from cement production.* Earth System Science Data, 2018. **10**(1): p. 195-217.

24. Turner, L.K. and F.G. Collins, *Carbon dioxide equivalent (CO2-e) emissions: A comparison between geopolymer and OPC cement concrete.* Construction and Building Materials, 2013. **43**: p. 125-130.

25. Mohammadinia, A., et al., *Stabilization of demolition materials for pavement base/subbase applications using fly ash and slag geopolymers.* Journal of Materials in Civil Engineering, 2016. **28**(7): p. 04016033.

26. Jayanthi, P.N. and D. Singh, *Utilization of sustainable materials for soil stabilization: state-of-the-art.* Advances in Civil Engineering Materials, 2016. **5**(1): p. 46-79.

27. Scrivener, K.L., *Options for the future of cement.* Indian Concr. J, 2014. **88**(7): p. 11-21.

28. Dhami, N.K., A. Mukherjee, and E.L. Watkin, *Microbial diversity and mineralogical-mechanical properties of calcitic cave speleothems in natural and in vitro biomineralization conditions.* Frontiers in microbiology, 2018. **9**: p. 40.

29. Zhu, T. and M. Dittrich, *Carbonate precipitation through microbial activities in natural environment, and their potential in biotechnology: a review.* Frontiers in bioengineering and biotechnology, 2016. **4**: p. 4.

30. Dhami, N.K., M.E.C. Quirin, and A. Mukherjee, *Carbonate biomineralization and heavy metal remediation by calcifying fungi isolated from karstic caves.* Ecological Engineering, 2017. **103**: p. 106-117.

31. Rusznyák, A., et al., *Calcite biomineralization by bacterial isolates from the recently discovered pristine karstic Herrenberg cave.* Applied and environmental microbiology, 2012. **78**(4): p. 1157-1167.

32. Lepot, K., et al., *Microbially influenced formation of 2,724-million-year-old stromatolites.* Nature Geoscience, 2008. **1**(2): p. 118-121.

33. Suosaari, E., et al., *New multi-scale perspectives on the stromatolites of Shark Bay, Western Australia.* Scientific reports, 2016. **6**(1): p. 1-13.

34. Dittrich, M. and S. Sibler, *Calcium carbonate precipitation by cyanobacterial polysaccharides.* Geological Society, London, Special Publications, 2010. **336**(1): p. 51-63.

35. Tourney, J. and B.T. Ngwenya, *The role of bacterial extracellular polymeric substances in geomicrobiology.* Chemical Geology, 2014. **386**: p. 115-132.

36. Porter, H.E., *Stabilisation of Geomaterials using Microbially Induced Calcium Carbonate Precipitation*. 2018, Curtin University.

37. Fungaroli, A.A. and S.R. Prager, *Evaluation of Some Acrylic Polymers as Soil Stabilizers.* Product R&D, 1969. **8**(4): p. 450-453.

38. Iyengar, S.R., et al., *Pavement Subgrade Stabilization Using Polymers: Characterization and Performance.* Journal of Materials in Civil Engineering, 2013. **25**(4): p. 472-483.

39. Wu, H., et al., *Experimental Study on Moisture Susceptibility of Subgrade Soil with Superabsorbent Polymers.* Journal of Materials in Civil Engineering, 2019. **31**(7): p. 04019120.

40. Miller, W.P., R.L. Willis, and G.J. Levy, *Aggregate stabilization in kaolinitic soils by low rates of anionic polyacrylamide.* Soil Use and Management, 1998. **14**(2): p. 101-105.

41. Orts, W.J., et al., *Use of Synthetic Polymers and Biopolymers for Soil Stabilization in Agricultural, Construction, and Military Applications.* Journal of Materials in Civil Engineering, 2007. **19**(1): p. 58-66.

42. Chen, Z., et al., *Effects of polyacrylamide on soil erosion and nutrient losses from substrate material in steep rocky slope stabilization projects.* Science of The Total Environment, 2016. **554-555**: p. 26-33.

43. Georgees, R.N., R.A. Hassan, and R.P. Evans, *A potential use of a hydrophilic polymeric material to enhance durability properties of pavement materials.* Construction and Building Materials, 2017. **148**: p. 686-695.

44. Georgees, R.N., et al., *Resilient Response Characterization of Pavement Foundation Materials Using a Polyacrylamide-Based Stabilizer.* Journal of Materials in Civil Engineering, 2018. **30**(1): p. 04017252.

45. Soltani-Jigheh, H., M. Bagheri, and A.R. Amani-Ghadim, *Use of hydrophilic polymeric stabilizer to improve strength and durability of fine-grained soils.* Cold Regions Science and Technology, 2019. **157**: p. 187-195.

46. Santoni, R.L., J.S. Tingle, and S.L. Webster, *Stabilization of silty sand with nontraditional additives.* Transportation research record, 2002. **1787**(1): p. 61-70.

47. Tingle, J.S. and R.L. Santoni, *Stabilization of clay soils with nontraditional additives.* Transportation Research Record, 2003. **1819**(1): p. 72-84.

48. Alazigha, D.P., et al., *Mechanisms of stabilization of expansive soil with lignosulfonate admixture.* Transportation Geotechnics, 2018. **14**: p. 81-92.

49. Anagnostopoulos, C.A., *Cement–clay grouts modified with acrylic resin or methyl methacrylate ester: Physical and mechanical properties.* Construction and Building Materials, 2007. **21**(2): p. 252-257.

50. Anagnostopoulos, C.A., *Laboratory study of an injected granular soil with polymer grouts.* Tunnelling and Underground Space Technology, 2005. **20**(6): p. 525-533.

51. De Varennes, A., C. Cunha-Queda, and A. Ramos, *Polyacrylate polymers as immobilizing agents to aid phytostabilization of two mine soils.* Soil use and management, 2009. **25**(2): p. 133-140.

52. Azzam, W.R., *Utilization of polymer stabilization for improvement of clay microstructures.* Applied clay science, 2014. **93**: p. 94-101.

53. Estabragh, A.R., et al., *Strength of a clay soil and soil–cement mixture with resin.* Proceedings of the Institution of Civil Engineers-Ground Improvement, 2013. **166**(2): p. 108-114.

54. Mirzababaei, M., A. Arulrajah, and M. Ouston, *Polymers for stabilization of soft clay soils.* Procedia engineering, 2017. **189**: p. 25-32.

55. Yazdandoust, F. and S.S. Yasrobi, *Effect of cyclic wetting and drying on swelling behavior of polymer-stabilized expansive clays.* Applied Clay Science, 2010. **50**(4): p. 461-468.

56. Scalia IV, J., et al., *Long-term hydraulic conductivity of a bentonite-polymer composite permeated with aggressive inorganic solutions.* Journal of Geotechnical and Geoenvironmental Engineering, 2014. **140**(3): p. 04013025.

57. Endo, S., et al., *Soil stabilization method*. 1973, Google Patents.

58. Stefanson, R., *Soil stabilization by polyvinyl alcohol and its effects on the growth of wheat.* Soil Research, 1974. **12**(1): p. 59-62.

59. Siddiqi, R.A. and J.C. Moore, *Polymer stabilization of sandy soils for erosion control.* Transportation Research Record, 1981(827).

60. Lahalih, S.M. and G. Hovakeemian, *Development of novel polymeric soil stabilizers.* Industrial & engineering chemistry research, 1988. **27**(10): p. 1806-1810.

61. Weaver, M., *Starch-g-Poly (Methyl Acrylate) Latexes for Stabilizing Soil to Water Erosion: Extending the Range of Polymer Add-On.* Starch-Stärke, 1989. **41**(3): p. 106-110.

62. Ben-Hur, M., *Using synthetic polymers as soil conditioners to control runoff and soil loss in arid and semi-arid regions—a review.* Soil Research, 2006. **44**(3): p. 191-204.

63. Liu, J., et al., *Effect of polyurethane on the stability of sand–clay mixtures.* Bulletin of Engineering Geology and the Environment, 2012. **71**(3): p. 537-544.

64. Onyejekwe, S. and G.S. Ghataora, *Stabilization of quarry fines using a polymeric additive and Portland cement.* Journal of Materials in Civil Engineering, 2016. **28**(1): p. 04015070.

65. Krizek, R.J. and T. Perez, *Chemical grouting in soils permeated by water.* Journal of Geotechnical Engineering, 1985. **111**(7): p. 898-915.

66. Chang, I., et al., *Review on biopolymer-based soil treatment (BPST) technology in geotechnical engineering practices.* Transportation Geotechnics, 2020. **24**: p. 100385.

67. Cho, G.-C. and I. Chang. *Cementless Soil Stabilizer–Biopolymer*. in *Proceedings of the 2018 World Congress on Advances in Civil, Environmental, & Materials Research (ACEM18) Songdo Convensia, Incheon, Korea*. 2018.

68. Plank, J., *Applications of biopolymers in construction engineering.* Biopolymers Online: Biology• Chemistry• Biotechnology• Applications, 2005. **10**.

69. Giavasis, I., L.M. Harvey, and B. McNeil, *Gellan gum.* Critical reviews in biotechnology, 2000. **20**(3): p. 177-211.

70. Freitas, F., V.D. Alves, and M.A. Reis, *Advances in bacterial exopolysaccharides: from production to biotechnological applications.* Trends in biotechnology, 2011. **29**(8): p. 388-398.

71. Schmid, J., V. Meyer, and V. Sieber, *Scleroglucan: biosynthesis, production and application of a versatile hydrocolloid.* Applied microbiology and biotechnology, 2011. **91**(4): p. 937-947.

72. Topakas, E., C. Vafiadi, and P. Christakopoulos, *Microbial production, characterization and applications of feruloyl esterases.* Process Biochemistry, 2007. **42**(4): p. 497-509.

73. Ta, H.X., et al., *Effects of bacterial dextran on soil geophysical properties.* Environmental Geotechnics, 2017. **5**(2): p. 114-122.

74. Naessens, M., et al., *Leuconostoc dextransucrase and dextran: production, properties and applications.* Journal of Chemical Technology & Biotechnology: International Research in Process, Environmental & Clean Technology, 2005. **80**(8): p. 845-860.

75. Srikanth, S., et al., *Statistical optimization of molasses based exopolysaccharide and biomass production by Aureobasidium pullulans MTCC 2195.* Biocatalysis and Agricultural Biotechnology, 2014. **3**(3): p. 7-12.

76. Rehm, B.H., *Alginate production: precursor biosynthesis, polymerization and secretion*, in *Alginates: biology and applications*. 2009, Springer. p. 55-71.

77. Yang, S.-T., *Bioprocessing for value-added products from renewable resources: new technologies and applications*. 2011: Elsevier.

78. Martin, G., T. Yen, and S. Karimi. *Application of biopolymer technology in silty soil matrices to form impervious barriers*. in *7th Australia New Zealand conference on geomechanics: geomechanics in a changing world: conference proceedings*. 1996. Institution of Engineers, Australia.

79. Chen, R., L. Zhang, and M. Budhu, *Biopolymer stabilization of mine tailings.* Journal of geotechnical and geoenvironmental engineering, 2013. **139**(10): p. 1802-1807.

80. Chen, R., et al., *Experimental investigation on biopolymer strengthening of mine tailings.* Journal of Geotechnical and Geoenvironmental Engineering, 2016. **142**(12): p. 06016017.

81. Chen, R., I. Lee, and L. Zhang, *Biopolymer stabilization of mine tailings for dust control.* Journal of Geotechnical and Geoenvironmental Engineering, 2015. **141**(2): p. 04014100.

82. Chen, R., et al., *Improving dust resistance of mine tailings using green biopolymer.* Environmental Geotechnics, 2019: p. 1-10.

83. Lee, S., et al., *Xanthan Gum Biopolymer as Soil-Stabilization Binder for Road Construction Using Local Soil in Sri Lanka.* Journal of Materials in Civil Engineering, 2019. **31**(11): p. 06019012.

84. Reddy, N., B. Rao, and K.R. Reddy, *Biopolymer amendment for mitigating dispersive characteristics of red mud waste.* Géotechnique Letters, 2018. **8**(3): p. 201-207.

85. Bouazza, A., W.P. Gates, and P.G. Ranjith, *Hydraulic conductivity of biopolymer-treated silty sand.* Géotechnique, 2009. **59**(1): p. 71-72.

86. Cabalar, A.F. and H. Canakci, *Direct shear tests on sand treated with xanthan gum.* Proceedings of the Institution of Civil Engineers-Ground Improvement, 2011. **164**(2): p. 57-64.

87. Cabalar, A., M. Wiszniewski, and Z. Skutnik, *Effects of xanthan gum biopolymer on the permeability, odometer, unconfined compressive and triaxial shear behavior of a sand.* Soil Mechanics and Foundation Engineering, 2017. **54**(5): p. 356-361.

88. Etemadi, O., et al., *Stabilization of metals in subsurface by biopolymers: laboratory drainage flow studies.* Soil and Sediment Contamination, 2003. **12**(5): p. 647-661.

89. Muguda, S., et al., *Mechanical properties of biopolymer-stabilised soil-based construction materials.* Géotechnique letters, 2017. **7**(4): p. 309-314.

90. Chang, I., J. Im, and G.-C. Cho, *Geotechnical engineering behaviors of gellan gum biopolymer treated sand.* Canadian Geotechnical Journal, 2016. **53**(10): p. 1658-1670.

91. Khatami, H.R. and B.C. O'Kelly, *Improving mechanical properties of sand using biopolymers.* Journal of Geotechnical and Geoenvironmental Engineering, 2013. **139**(8): p. 1402-1406.

92. Chang, I. and G.-C. Cho, *Strengthening of Korean residual soil with β-1, 3/1, 6-glucan biopolymer.* Construction and Building Materials, 2012. **30**: p. 30-35.

93. Chang, I. and G.-C. Cho, *Shear strength behavior and parameters of microbial gellan gum-treated soils: from sand to clay.* Acta Geotechnica, 2019. **14**(2): p. 361-375.

94. Latifi, N., et al., *Improvement of problematic soils with biopolymer—an environmentally friendly soil stabilizer.* Journal of Materials in Civil Engineering, 2017. **29**(2): p. 04016204.

95. Chang, I., et al., *Soil consistency and interparticle characteristics of xanthan gum biopolymer–containing soils with pore-fluid variation.* Canadian Geotechnical Journal, 2019. **56**(8): p. 1206-1213.

96. Kang, X., et al., *Physicochemical and mechanical properties of polymer-amended kaolinite and fly ash–kaolinite mixtures.* Journal of Materials in Civil Engineering, 2019. **31**(6): p. 04019064.

97. Cabalar, A.F., M.H. Awraheem, and M.M. Khalaf, *Geotechnical properties of a low-plasticity clay with biopolymer.* Journal of Materials in Civil Engineering, 2018. **30**(8): p. 04018170.

98. Latifi, N., et al., *Xanthan gum biopolymer: an eco-friendly additive for stabilization of tropical organic peat.* Environmental Earth Sciences, 2016. **75**(9): p. 825.

99. Ayeldeen, M., et al., *Enhancing mechanical behaviors of collapsible soil using two biopolymers.* Journal of Rock Mechanics and Geotechnical Engineering, 2017. **9**(2): p. 329-339.

100. Chen, C., L. Wu, and M. Harbottle, *Exploring the effect of biopolymers in near-surface soils using xanthan gum–modified sand under shear.* Canadian Geotechnical Journal, 2020. **57**(8): p. 1109-1118.

101. Galán-Marín, C., C. Rivera-Gómez, and J. Petric, *Clay-based composite stabilized with natural polymer and fibre.* Construction and Building Materials, 2010. **24**(8): p. 1462-1468.

102. Arab, M.G., et al., *Resilient Behavior of Sodium Alginate–Treated Cohesive Soils for Pavement Applications.* Journal of Materials in Civil Engineering, 2019. **31**(1): p. 04018361.

103. Hataf, N., P. Ghadir, and N. Ranjbar, *Investigation of soil stabilization using chitosan biopolymer.* Journal of Cleaner Production, 2018. **170**: p. 1493-1500.

104. Fatehi, H., et al., *A novel study on using protein based biopolymers in soil strengthening.* Construction and Building Materials, 2018. **167**: p. 813-821.

105. Cole, D.M., D.B. Ringelberg, and C.M. Reynolds, *Small-scale mechanical properties of biopolymers.* Journal of Geotechnical and Geoenvironmental engineering, 2012. **138**(9): p. 1063-1074.

106. Ringelberg, D., et al., *Compressive strength of soils amended with a bacterial succinoglycan: effects of soluble salts and organic matter.* Canadian geotechnical journal, 2014. **51**(7): p. 747-757.

107. Proto, C., J. DeJong, and D. Nelson, *Biomediated permeability reduction of saturated sands.* Journal of Geotechnical and Geoenvironmental Engineering, 2016. **142**(12): p. 04016073.

108. Ham, S.-M., et al., *Improvement of surface erosion resistance of sand by microbial biopolymer formation.* Journal of Geotechnical and Geoenvironmental Engineering, 2018. **144**(7): p. 06018004.

109. Noh, D.H., et al., *P and S wave responses of bacterial biopolymer formation in unconsolidated porous media.* Journal of Geophysical Research: Biogeosciences, 2016. **121**(4): p. 1158-1177.

110. Chang, I., et al., *Strength durability of gellan gum biopolymer-treated Korean sand with cyclic wetting and drying.* Construction and Building Materials, 2017. **143**: p. 210-221.

111. Yakimets, I., et al., *Effect of water content on the structural reorganization and elastic properties of biopolymer films: a comparative study.* Biomacromolecules, 2007. **8**(5): p. 1710-1722.

112. Dhami, N.K., et al., *Bacterial community dynamics and biocement formation during stimulation and augmentation: implications for soil consolidation.* Frontiers in microbiology, 2017. **8**: p. 1267.

113. Chan, C.S., et al., *Microbial polysaccharides template assembly of nanocrystal fibers.* Science, 2004. **303**(5664): p. 1656-1658.

114. Foster, J.S., et al., *Molecular and morphological characterization of cyanobacterial diversity in the stromatolites of Highborne Cay, Bahamas.* The ISME journal, 2009. **3**(5): p. 573-587.

115. DeJong, J.T., M.B. Fritzges, and K. Nüsslein, *Microbially induced cementation to control sand response to undrained shear.* Journal of geotechnical and geoenvironmental engineering, 2006. **132**(11): p. 1381-1392.

116. DeJong, J.T., et al., *Bio-mediated soil improvement.* Ecological Engineering, 2010. **36**(2): p. 197-210.

117. Gomez, M.G., et al., *Large-scale comparison of bioaugmentation and biostimulation approaches for biocementation of sands.* Journal of Geotechnical and Geoenvironmental Engineering, 2017. **143**(5): p. 04016124.

118. Achal, V. and A. Mukherjee, *A review of microbial precipitation for sustainable construction.* Construction and Building Materials, 2015. **93**: p. 1224-1235.

119. DeJong, J., et al. *Biogeochemical processes and geotechnical applications: progress, opportunities and challenges*. in *Bio-and Chemo-Mechanical Processes in Geotechnical Engineering: Géotechnique Symposium in Print 2013*. 2014. Ice Publishing.

120. Terzis, D. and L. Laloui, *A decade of progress and turning points in the understanding of bio-improved soils: A review.* Geomechanics for Energy and the Environment, 2019. **19**: p. 100116.

121. Terzis, D., R. Bernier-Latmani, and L. Laloui, *Fabric characteristics and mechanical response of bio-improved sand to various treatment conditions.* Géotechnique Letters, 2016. **6**(1): p. 50-57.

122. Achal, V., A. Mukherjee, and M.S. Reddy, *Microbial concrete: way to enhance the durability of building structures.* Journal of materials in civil engineering, 2011. **23**(6): p. 730-734.

123. Mujah, D., M.A. Shahin, and L. Cheng, *State-of-the-art review of biocementation by microbially induced calcite precipitation (MICP) for soil stabilization.* Geomicrobiology Journal, 2017. **34**(6): p. 524-537.

124. Venuleo, S., et al., *Microbially induced calcite precipitation effect on soil thermal conductivity.* Géotechnique Letters, 2016. **6**(1): p. 39-44.

125. Tagliaferri, F., et al., *Observing strain localisation processes in bio-cemented sand using x-ray imaging.* Granular Matter, 2011. **13**(3): p. 247-250.

126. Xiao, Y., et al., *Unconfined compressive and splitting tensile strength of basalt fiber–reinforced biocemented sand.* Journal of geotechnical and geoenvironmental engineering, 2019. **145**(9): p. 04019048.

127. Wang, Y., et al., *Microscale visualization of microbial-induced calcium carbonate precipitation processes.* Journal of Geotechnical and Geoenvironmental Engineering, 2019. **145**(9): p. 04019045.

128. Veytskin, Y., C. Bobko, and C. Castorena, *Nanoindentation and atomic force microscopy investigations of asphalt binder and mastic.* Journal of Materials in Civil Engineering, 2016. **28**(6): p. 04016019.

129. AbuQtaish, L., et al., *AFM-based approach to study blending between RAP and virgin asphalt binders.* Journal of Materials in Civil Engineering, 2018. **30**(3): p. 04017300.

130. Allen, R.G., D.N. Little, and A. Bhasin, *Structural characterization of micromechanical properties in asphalt using atomic force microscopy.* Journal of Materials in Civil Engineering, 2012. **24**(10): p. 1317-1327.

131. Tarefder, R.A. and A.M. Zaman, *Nanoscale evaluation of moisture damage in polymer modified asphalts.* Journal of Materials in Civil Engineering, 2010. **22**(7): p. 714-725.

132. Nazzal, M.D., et al., *Multiscale evaluation of the composite asphalt binder in high–reclaimed asphalt pavement mixtures.* Journal of Materials in Civil Engineering, 2014. **26**(7): p. 04014019.

133. Pauli, A., et al., *Morphology of asphalts, asphalt fractions and model wax-doped asphalts studied by atomic force microscopy.* International Journal of Pavement Engineering, 2011. **12**(4): p. 291-309.

134. Loeber, L., et al., *New direct observations of asphalts and asphalt binders by scanning electron microscopy and atomic force microscopy.* Journal of microscopy, 1996. **182**(1): p. 32-39.

135. Luo, Z., et al., *Research progress in advanced nanomechanical characterization of cement-based materials.* Cement and Concrete Composites, 2018. **94**: p. 277-295.

136. Burnham, N.A., et al., *Probing the surface forces of monolayer films with an atomic-force microscope.* Physical review letters, 1990. **64**(16): p. 1931.

137. Ren, M., et al., *Mechanical Properties of Micro-regions in Cement-based Material based on the PeakForce QNM Mode of AFM.* Journal of Wuhan University of Technology-Mater. Sci. Ed., 2019. **34**(4): p. 893-899.

138. Dorakumbura, B.N., T. Becker, and S.W. Lewis, *Nanomechanical mapping of latent fingermarks: A preliminary investigation into the changes in surface interactions and topography over time.* Forensic Science International, 2016. **267**: p. 16-24.

139. Karki, P., et al., *Nanomechanical Properties of Constituent Phases in Bituminous Mixtures.* Journal of Materials in Civil Engineering, 2016. **28**(10): p. 04016090.

140. Xiao, J., et al., *Properties of interfacial transition zones in recycled aggregate concrete tested by nanoindentation.* Cement and Concrete Composites, 2013. **37**: p. 276-292.

141. Oliver, W.C. and G.M. Pharr, *An improved technique for determining hardness and elastic modulus using load and displacement sensing indentation experiments.* Journal of materials research, 1992. **7**(6): p. 1564-1583.

142. Ngan-Tillard, D., et al., *Application of the needle penetration test to a calcarenite, Maastricht, the Netherlands.* Engineering geology, 2011. **123**(3): p. 214-224.

143. Chen, R., et al., *Experimental and numerical investigation into surface strength of mine tailings after biopolymer stabilization.* Acta Geotechnica, 2016. **11**(5): p. 1075-1085.

144. Danjo, T. and S. Kawasaki, *A study of the formation mechanism of beachrock in Okinawa, Japan: Toward Making Artificial Rock.* Int. J. of Geomate, 2013. **5**(1): p. 633-638.

145. Mondal, P., S.P. Shah, and L.D. Marks, *Nanoscale characterization of cementitious materials.* ACI Materials Journal, 2008. **105**(2): p. 174.

146. Oliver, W.C. and G.M. Pharr, *Measurement of hardness and elastic modulus by instrumented indentation: Advances in understanding and refinements to methodology.* Journal of materials research, 2004. **19**(1): p. 3-20.

147. Gomez, M.G., et al., *Field-scale bio-cementation tests to improve sands.* Proceedings of the Institution of Civil Engineers-Ground Improvement, 2015. **168**(3): p. 206-216.

148. Zhang, T., G. Cai, and S. Liu, *Application of lignin-stabilized silty soil in highway subgrade: A macroscale laboratory study.* Journal of Materials in Civil Engineering, 2018. **30**(4): p. 04018034.

149. Rauch, A.F., et al., *Measured effects of liquid soil stabilizers on engineering properties of clay.* Transportation Research Record, 2002. **1787**(1): p. 33-41.

150. Estabragh, A., I. Beytolahpour, and A. Javadi, *Effect of resin on the strength of soil-cement mixture.* Journal of Materials in Civil Engineering, 2011. **23**(7): p. 969-976.

151. Anagnostopoulos, C. and T. Papaliangas, *Experimental investigation of epoxy resin and sand mixes.* Journal of geotechnical and geoenvironmental engineering, 2012. **138**(7): p. 841-849.

152. Liu, J., et al., *Strength properties of sand reinforced with a mixture of organic polymer stabilizer and polypropylene fiber.* Journal of Materials in Civil Engineering, 2018. **30**(12): p. 04018330.

153. Chang, I., et al., *Soil strengthening using thermo-gelation biopolymers.* Construction and Building Materials, 2015. **77**: p. 430-438.

Chapter 3: Understanding and creating biocementing beachrocks via biostimulation of indigenous microbial communities

3.1 Abstract

Bacterially induced precipitation of minerals leading to cementation of natural geological formations has been well recorded in a variety of environments. A range of microbial pathways and geochemical processes has been found to influence the cementation processes, but detailed formation mechanisms and biogeochemical relationships are still not clear. There has been a growing demand for the application of bacterially driven biocementation in several geotechnical engineering applications recently. Here we aimed to unpin the mechanisms behind the formation of actively mineralising beachrock sediments at Lucky Bay in Western Australia to understand the natural accretionary processes and potential of indigenous bacterial communities in biocementation. We observed ferruginous, aluminosilicate and carbonate cements along with extensive extra polymeric substances, borings with possible microbial activities in certain sections of native beachrock sediments. Cement precipitation under calcium and iron-rich microenvironments sourced from seawater and iron creek seems to be driven by both biogenic and abiogenic processes in nature. Native microbial communities with the dominance of genus *Halococcus* and *Marinobacter* were recorded. Enrichment of native bacterial communities under seawater media conditions was conducted, which lead to successful biomineralisation of calcitic and ferruginous cements under in vitro conditions although the community composition changed significantly. Nanomechanical properties of natural and laboratory synthesised cement crystals showed that engineered biocement is highly promising. The results of this study clearly demonstrate biological influence in the formation of natural cements and hint significant potential of biostimulation, which can be harnessed for different engineering applications, including coastal erosion.

Keywords: Beachrocks, Biodiversity, Biocement, Calcium carbonate minerals, Ferruginous minerals, Nanomechanical characterisation

3.2 Introduction

Microbial metabolic activities and physicochemical processes leading to precipitation of minerals in different natural environments have been recorded to influence the formation of several geological structures [1]. Inspired by the natural capability of

biophysicochemical processes to coprecipitate metal ions and cement loose sands, research in biomineralization has taken a great leap in the last few decades [2, 3]. A couple of the advancements include improving the mechanical properties and bearing capacity of the soil, Bio-clogging, slope stabilization application, mitigation of soil liquefaction and dust suppression [1,2]. Increasing concerns about the hazardous effects of conventional cementation agents on the environment have made biocementation processes more attractive as they are natural, self-healing and highly sustainable [3-5]. Successful biocementation applications are significantly influenced by the metabolic activities and pathways of bacterial communities [1, 5]. Most lab-scale and a few field-scale demonstrations have focused on augmentation of pure strains from culture collections whose efficacy under field applications is a challenge due to which upscaling of these processes are still at infancy stages [6, 7]. A deeper understanding of biophysicochemical processes in natural cementation and the role of microbial communities is imperative to develop more links between perspectives of microbiologists, mineralogists, geologists, and engineers.

Beachrock formations are one such example wherein biogeochemical processes lead to cementation of coastal sands in short time scales of a few years; compared to other sedimentary rocks taking hundreds of years [8-11]. Inorganic and physical chemistry driving the precipitation of these sediments has been well documented in several studies, but the active role of microbes has been recorded recently by a few researchers [10]. In these accretionary formations, cements have been found to deposit layer by layer over a period via the interactions of chemical and biological agents as they occur in environments with nutrients (from industrial/ natural sources) and cementation reagents (from seawater) [12, 13]. As far as the formation mechanisms are concerned, there have been a few reports unpinning the processes which indicate that the formation is either due to direct precipitation from meteoric or marine water [14-16] or due to evaporation and degassing of CO_2 [17, 18]. The deposits are found in the tidal and intertidal zone of sandy beaches in tropical and subtropical regions [19]. In most of the studies, beachrock formations have been recorded to comprise calcium carbonate cements predominantly [10, 12, 13, 17, 20] but recently a few have also reported the precipitation of iron compounds in coastal environments [12]. Several studies have analysed the mineralogy and geochemistry of beachrock sediments. The main components of beachrocks and surrounding material in the previous studies of

Arrieta, Iturregui [12] and Khan, Danjo [19] were calcium carbonate or silica wherein the mineralogical composition was seen to vary from $CaCO_3$ polymorphs including aragonite, low magnesium calcite (LMC), high magnesium calcite (HMC), iron oxides/hydroxides, silica dioxide to aluminium oxide. A few studies documented that the iron oxides also exist in different forms varying from poorly ordered minerals as ferrihydrate and as crystalline forms as goethite, lepidocrocite, hematite and magnetite [21]. Further investigation is required for a deeper understanding of mineralogical dynamics involved in the formation of these sediments.

The seminal role of microbes in natural cementation processes has been demonstrated in different natural formations like caves, corals, microbialites [1, 22]. A variety of microbial metabolic pathways that influence and lead to precipitation of microbially induced biominerals including calcium carbonate, silicate and iron oxides have also been found to be associated with those structures [1, 23, 24]. The presence of aragonite crystals has been recorded in new beachrock cements mostly via abiotic physicochemical processes, but recently biological influence has also been recorded in their formation by McCutcheon, Nothdurft [10]. These cements have been found to be encapsulated in microbial extracellular polymeric substances [13, 25] and their formation is suggested via localised higher calcium concentration. Although biological influence has been recorded not much has been reported about the diversity of the microbial communities in these formations and truly little has been done to investigate the biocementation potential of these indigenous populations. Along with this, their associations with mineralogy remain largely unexplored which have been recorded in a few studies in geological formations as stromatolites, caves before [22, 26, 27]. The biostimulation potential of indigenous communities from soils under high nutrient conditions has been found successful in a few previous studies [4, 7]. But not much has been explored about the potential of beachrock associated communities for biomineralisation under simulated seawater conditions [4, 22, 28]. Further investigation in this area will improve the fundamental understanding and widen the scope of biocementation technology for applications in areas like erosion mitigation while utilising native cultures effects [29].

Along with the biophysicochemical processes involved in the formation of natural cements, there has also been a wide interest in exploring the mechanical properties of these minerals. To truly explore the potential of biocement for engineering applications,

further insights into the mechanical properties of natural as well synthesised biominerals are mandatory. The mineral composition has been reported to play an important role in determining the overall structure and strength of such cements [22, 30, 2018, 31]. Recently, nanoindentation has emerged as a potential tool for testing small amounts of materials at (sub) micrometre scale [32]. This technique has been successfully utilised in a few studies for investigating the mechanical properties of polyphasic materials [30, 33]. This technique has offered the advantage of accuracy and reliability by utilising a minimal amount of the material as getting access to such natural materials for bulk tests is a significant issue [34, 35]. Fortunately, a few results are available for different rock minerals [33, 36]. Utilising the same technique for analysing the nanomechanical properties of these cements can shed more light about the performance of various minerals and phases within a material along with a more comprehensive analysis of micro-mineralo-mechanical characterisation [37]. The comparison between natural and engineered biocement will not only elucidate more about the differences between these two formation processes but also highlight the prospects of synthesised biominerals.

The formation of beachrocks has been recorded in many places in the world, and fortunately, a few in Australia [8-10]. Lucky Bay at Esperance Western Australia is one such site wherein ferruginous beachrock formations have been recorded (Fig 3.1). Multiple stages of beachrock formations are seen along the shoreline. This gave us the chance to have a comprehensive analysis of these naturally cementing structures for their micro-morpho-mineralo and mechanical properties in their native state giving the comprehensive cementation picture. Most studies till date have focussed on these aspects separately. In the second phase, we aimed to elucidate the potential of native communities in biocement formation under near natural seawater conditions. This study also addresses the significant variations between microbial signatures, mineralogy and their corresponding effects on the nanomechanical properties of biocement. In brief, the objectives include

(1) Microbial-morphological-mineralogical characterisation of natural beachrock sediments (2) Effect of mineralogy on nanomechanical properties of accreted cements (3) Biomineralisation potential of biostimulated native communities under seawater

3.3 Materials and Methods

3.3.1 Site description

Beachrock samples were collected during April 2016 from different locations of Lucky Bay, Esperance situated on the south coast of Western Australia in the Cape Le Grand National Park. The beachrock samples were collected under low tide conditions and have been highlighted in Fig 3.1.

Fig 3. 1 Beach rock sediments collected from different locations in Lucky Bay, Esperance 2 (a, b) sample BR-1 and sample BR-2 at intermediate stage 3 (c, d) sample BR-3 and sample BR-4 at terminal stage 4 (e, f) e: seawater; f: brown water displaying iron leaching and in the highlighted section is 5 slimy layer on sand surface indicative of microbial activity.

3.3.2 Sample collection and details

The beachrock existed in various forms ranging from loosely aggregated deposits to hard rock formations. We collected around 10 grams of beachrock sample at different stages of aggregation using sterile forceps, spatula, and chisel. Sampling locations were selected based upon the level of cementation as loosely aggregated and completely consolidated. We classified them as intermediate and terminal stage samples (Table 3.1). All the samples were cleaned, and the weathered surface removed (Fig 3.1).

Interestingly, there existed a freshwater source flowing into the sea in the locality of beachrock formations. Water samples from this creek were also collected along with seawater sample around the terminal stage beachrock (Table 3.1). The water source displayed brown colour at specific locations, which pointed towards high organic matter and iron content in the water source (Fig 3.1). The existence of a slimy layer on the surface of the sand at specific locations in the proximity of rock formation indicated biological activity. The presence of a weed bank consisting of old seaweed also suggests that organic matter is abundant in the vicinity of the beachrock formation. Slimy brown mats were also seen on the surface of the creek. The brown colour could be an indicator of iron leaching from the proximal areas as there had been iron mining industries in the proximity a few years back. All the specimens were collected aseptically, transported under refrigeration to the laboratory, and stored at -20°C until use. The samples were separated into three sections to correlate mineralogical-morphological, nanomechanical and microbial properties. The specific labelling of the samples was as per the codes mentioned in Table 3.1.

Table 3. 1 Designation of the collected samples, details, and analysis techniques.

Sample	Description	Code
Sediment 1	Intermediate, away from shore	BR-1
Sediment 2	Intermediate, near shore	BR-2
Sediment 3	Terminal, away from shore	BR-3
Sediment 4	Terminal, near shore	BR-4
Water 1	Leachate water	BR-W1
Water 2	Sea water	BR-W2

3.4 Characterisation of natural beachrocks

3.4.1 Chemical analysis of leachate, seawater, and sediments

Water samples for chemical analysis were filtered through a 0.2 µm filter (Whatman) and kept on ice during procurement to the laboratory and stored at 4°C before the experiments. The analysis included pH, conductivity, and metal analysis of ferrous, chloride, nitrate, sulfate, calcium via inductively coupled plasma mass spectrometry (ICP-MS). Concentrations of minor and trace elements in collected beachrock sediments were also recorded via ICP-MS following standard procedures (Table 3.2 and 3.3). All the measurements were carried out in triplicates for each sample.

3.4.2 Morphological characterisation

In order to determine the micro-morphology and elemental composition of different beachrock sediments, the samples were analysed via scanning electron microscopy and energy dispersive X ray spectroscopy using Zeiss Evo 40XVP microscope equipped with an Oxford Instruments INCA x-sight energy dispersive spectrometer for elemental analysis as well as Zeiss Neon 40 EsB dual beam field emission scanning electron microscope (FESEM) (Zeiss, Abingdon, UK). Initially, the whole fragments of beachrock sediments were cut into around 5 mm sections and fixed using 4 % glutaraldehyde followed by dehydration through an ethanol dehydration series (25 %, 50 %, 75 %, 100 %). The samples were mounted onto stainless steel stubs using carbon tape. The sections were then subjected to sputter coating with platinum (thickness of approximately 5 nm) using a SCD005 sputter coater (Leica microsystems, Liechtenstein, Germany) to avoid surface charging. This was followed by SEM imaging at an accelerating voltage of 15 kV and a working distance of 10 mm via backscatter mode. In another set, thin sections from different samples were cut, mounted in resin, and polished. These samples were analysed for SEM and energy dispersive x-ray spectroscopy (EDS) via spot analysis at points across the sample using W-filament Zeiss ECO 40 XVP. Data acquisition and analysis were made using AZtec software (Oxford Instruments, High Wycombe, UK).

3.4.3 Mineralogical characterisation

3.4.3.1 X-ray diffractometry (XRD)

To gain insights into mineralogy of beachrock samples, around 1 gram of each dry sample was crushed and powdered using a ball mill grinder. X-ray patterns of the samples were recorded at room temperature using Bruker D8 Advance Powder

Diffractometer (Bruker AXS, Karlsruhe, Germany) operating at Cu Kα radiation source (λ=1.54 Å) run at 40 kV/40 mA with a LynxEye detector (Bruker AXS, Karlsruhe, Germany). The scanning range was from 7.5^{o} – 90^{o} at a step size of 0.015^{o} and a rate of 0.7 s/step. Mineral identification and processing of data (determination of background, smoothing, and peak localisation) were conducted in HighScore, a PANalytical software (version 3.0e Plus® software at https://www.malvernpanalytical.com), with an integrated International Centre for Diffraction Data (ICDD) and Inorganic Crystal Structure Database (ICSD) mineral database (www.icdd.com).

3.4.3.2 TESCAN Integrated Mineral Analyser (TIMA)

TIMA aids in providing particle-by-particle quantitative mineralogical data on complex inorganic samples. It is sometimes difficult to identify mineral phases through XRD under different conditions as low concentrations or overlapping peaks, poorly crystalline nature of materials with high amorphous content, or high and low-temperature variants, and TIMA analysis is quite helpful in such environments. The principle TIMA is similar to other SEM-EDS techniques, which combine ultra-fast data acquisition (up to 100,000 mineral grains analysed per hour via the collection of approximately 60000 x-ray counts per second) with software resulting in mineralogical information of single particles.

The resin-impregnated and polished samples from SEM-EDS were analysed using the TIMA SEM-EDS system at John de Laeter Centre, Curtin University, Australia (Manufacturer Tescan, Brno, Czech Republic) as per the protocols developed in Dhami, Mukherjee [22]. TIMA comprised of a SEM with four silicon drift EDS detectors arranged at approximately 90^{o} intervals around the chamber. The conditions used for the current analysis were beam energy 25000 eV, current 6.32 nA, beam intensity 19.56, working distance 15 mm, SEM type TIMA3FE GMU with Pulse Tor 30 detector model at 7.009 µm pixel. Further, the spectroscopic data was matched with the mineral definition files to identify the mineral phases.

3.4.3.3 Fourier-transform infrared spectroscopy (FTIR)

The major and minor minerals of dried beachrocks were also qualitatively determined via FT-IR technique using Nicolet iS50 FTIR-ATR (attenuated total reflectance) (Thermo fisher scientific, Walthum, Massachusetts, USA). The infrared spectrum was collected using a Nicolet iS50 FTIR fitted with a dedicated single-bounce diamond ATR purged with dry nitrogen, and no additional preparation of the samples is required for

this technique. Sixty-four background and sixty-four sample scans were co-averaged and ratioed to produce a transmission spectrum. A spectral resolution of 4 wavenumbers, with 2 levels of post zero-filling, Norton-Beer strong apodization, and Mertz phase correction was used. The spectra were taken in the mid-region of 4000-400 cm^{-1}.

3.4.4 Nanomechanical characterisation via Nanoindentation

To gain a deeper understanding of the mechanical properties at the microscopic level, nanoindentation testing at different regions and cements in beachrock formation were undertaken. Nanoindentation was undertaken using a G200 Agilent Technologies (California, USA) Nanoindenter using a Berkovich shaped diamond tip. For this, polished and resin embedded samples were taken. Locations for nanoindentation were manually selected using the 40X optical microscope fitted to the nanoindenter. Selected locations for nanoindentation were on the grain, on the bridge/cement between grains, on the grain/bridge interface and on the epoxy resin as a control. The detailed protocol for indentation analysis was from Porter, Dhami [37].

3.4.5 Microbial diversity characterisation of native beachrocks

This part has been reported in the section on in vitro synthesis of biocement under laboratory conditions.

3.5 Enrichment of beachrock associated microbial communities and characterisation of biogenically induced minerals under laboratory conditions

3.5.1 Microbial enrichment and mineralisation

To investigate the role of microbes in beachrock formation, simulation under lab conditions with supplemental organics (glucose, lactate) was carried out. The media compositions and labelling has been described in Table 3.3. One-gram beachrock sample from intermediate stage 2 stored aseptically was inoculated into flasks containing 100 ml autoclaved artificial seawater media of Berges, Franklin [39] containing 2mM $CaCl_2$ supplemented with different organics as glucose (10mM) and lactate (10mM) along with 2.5% $FeSO_4$ and 1% $FeCl_3$ to reflect the iron-rich environment. Higher growth was observed with lactate which was selected for further studies. For abiogenic control, the beachrock sample was subjected to autoclaving prior to inoculation into the flasks containing sterile media to remove any microbial associations. Dry autoclaving may have impacted the mineralogy but as the aim of this experiment was to differentiate

biotic vs abiotic mineralisation, we assumed little effect of the mineral change on crystal precipitations. All the flasks were then incubated at 30°C in an orbital shaker at 50 rpm under dark for five days (low rpm were to ensure the least loss of surface deposits from rock samples which could interfere with the precipitates) as per Rusznyak, Akob [38] after conducting an initial screening study at different temperatures between 20-35°C (although mineral sediments do interfere with the measurement of optical density precautions were taken to minimise their effect by careful sampling). This was followed by the second set of enrichment wherein the grown cultures were subcultured for another ten days in the same media and monitored for growth via optical density (OD_{600} nm) and pH as well as precipitate formation. This was then followed by characterisation of the mineral precipitates in each set. For this, 10 ml of the culture was filtered using Whatman No. 1 filter paper, and the precipitated crystals were harvested as per Zamarreno, Inkpen [2]. These precipitates were washed with sterile distilled water, dried at room temperature for 48 hours and analysed for morphological, chemical and nanomechanical properties with SEM, EDS, XRD and nanoindentation as described previously. Though the conditions for in vitro precipitation experiments were quite different from actual conditions including physical temperature variations, humidity, minimal nutrients, but the aim of the experiment was to investigate mineralisation potential of heterotrophic communities associated with the sediments in shorter time spans.

Table 3. 2 Detailed media composition of the enrichment media under laboratory conditions

No	Media composition	Label
1	ASW (25ml) + Glucose (10mM) + $FeSO_4$ (2.5%) + $FeCl_2$ (1%) + $CaCl_2$ (2mM)	Enr 1
2	ASW (25ml) + Lactate (10mM) + $FeSO_4$ (2.5%) + $FeCl_2$ (1%) + $CaCl_2$ (2mM)	Enr 2
3	ASW (25ml) + Glucose (5mM) + Lactate (5mM) + $FeSO_4$ (2.5%) + $FeCl_2$ (1%) + $CaCl_2$ (mM)	Enr 3

3.5.2 Microbial characterisation

To investigate the diversity of microbial communities associated with native beachrocks and under enriched laboratory conditions, genomic DNA was extracted from all samples in triplicates. In case of native beachrocks, around 1g sediment was suspended in sterile

phosphate buffer saline and vortexed at high speed followed by sonication in an ultrasonic water bath to detach the surface cells. The cell suspension was then harvested by microfiltration, and biomass was further washed in PBS as per Dhami, Mukherjee [22]. In the case of enrichment samples, 1 ml bacterial culture broth was taken at the end of enrichment and centrifuged at 13,000 X *g* (4° C) for ten minutes. DNA extraction from both native and enriched cultures, along with their sequencing studies, was done following the protocols from Dhami, Mukherjee [22]. The obtained sequences were submitted to the National Centre for Biotechnology Information (NCBI) (BioProject ID PRJNA562124 with submission ID SUB6207293). The results are provided as a percentage of sequencing reads for the identified operational taxonomic units (OTUs) in each sample. All experiments were conducted in triplicate as biological replicates. The data were analysed by Analysis of Variance (ANOVA), and the means were compared with Tukey's test. All analyses were performed using Graph Pad Prism® software version 6.0. (GraphPad Software, San Diego, USA).

3.6 Results

3.6.1 Characterisation of natural beachrock

3.6.1.1 Chemical analysis of leachate and seawater

The metal concentrations in leachate and seawater are shown in Table 3.4 and 3.5. It was recorded that the concentration of ferrous ions was very high in the leachate. The calcium content in the seawater was in a similar range reported in some previous studies, but the concentration of iron in leachate was much higher than the seawater [41-43]. Similarly, other salts as chlorides and sulfates were much higher in the seawater compared to the iron-rich leachate water.

In the case of sediments collected from different locations, noticeable differences were seen in their iron and calcium contents along with other elements. Intermediate sediments collected near the creek source had much higher iron as well as calcium content compared to the one collected closer to shore. The terminal samples displayed higher concentration of iron compared to the intermediate stage samples indicating the entrapment of iron over time.

Table 3. 3 Leachate and seawater analysis (elemental concentrations in mg/L)

	Leachate	Sea water
pH	6.9	7.1
DO	20.8	22.7

Ferrous iron	40.8	5.3
Chloride	17.3	4328
Sulfate	2.8	1823
Nitrate	8.3	10.2
Calcium	23.3	456

Table 3. 4 Elemental analysis of trace metals in beach rock sediments (mg/kg)

Element	Sodium	Magnesium	Aluminium	Sulfur	Potassium	Calcium	Manganese	Iron
BR-Intermediate 1	4562	1643	87234	187	27653	497	18.3	9782
BR-Intermediate 2	7823	1421	92083	232	32013	11342	14.2	253
BR-Terminal 1	7040	2130	81800	414	61900	635	21.5	39900
BR-Terminal 2	6387	1729	53456	245	15789	27723	29.3	12456

3.6.1.2 Morphological, mineralogical, and mechanical properties

The beachrocks comprised of fine sand grains glued together by isopachous cements at point contacts between the grains (Fig 3.2 a, e, g). The cements were noticed both on the fringes as well as within intergranular spaces. The samples at different locations displayed different morphologies and cementing. The terminal beachrock sample BR-3 showed more cementation compared to the intermediate sticky sample BR-1 and had much lesser pore spaces compared to the softer counterparts (Fig 3.2 a, e). This cementation was seen mostly at the meniscus points in softer beachrock samples while it was seen extensively in terminal ones. Some polymeric layers were also noticeable on the surface in certain sections (Fig 3.2 a). In certain areas, borings and degradations/ dissolutions were recorded, which could be due to the transitions in different states (Fig 3.2 b, f). Microbial imprints were recorded in a few sections indicating their associations in the formation or dissolution of these structures (Fig 3.2 b, d, f, h). In the case of both BR-2 and BR-4 samples, clear acicular and needle-shaped crystals were found. The non-homogenous crystals indicated iron minerals while acicular crystals represented more of Ca in the form of aragonite as reported in the earlier studies in beachrocks (Fig 3.2 d, h) [44]. A closer section of the cements revealed that the needle-like crystals ranged from 10 to 100 µm in size (Fig 3.2d, h). Along with these needles were seen discontinuous ferruginous globular round crystals (Fig 3.2 h). These cements displayed conjunction of carbonate and iron-rich composites as per the morphologies displayed, but overall, the

carbonaceous cements were dominating in samples collected near shore compared to ferruginous ones. Similar morphologies have also been linked to weathering processes or action of leaching waters on iron-rich materials [11]. In many areas, the crystalline nature of the cements indicated abiotic mineral formation, but closer sections revealed extensive EPS, microbial borings (MB) and possible microbial imprints (PMF) in some sections hinting the role of microbial communities (Fig 3.2 d, f, h).

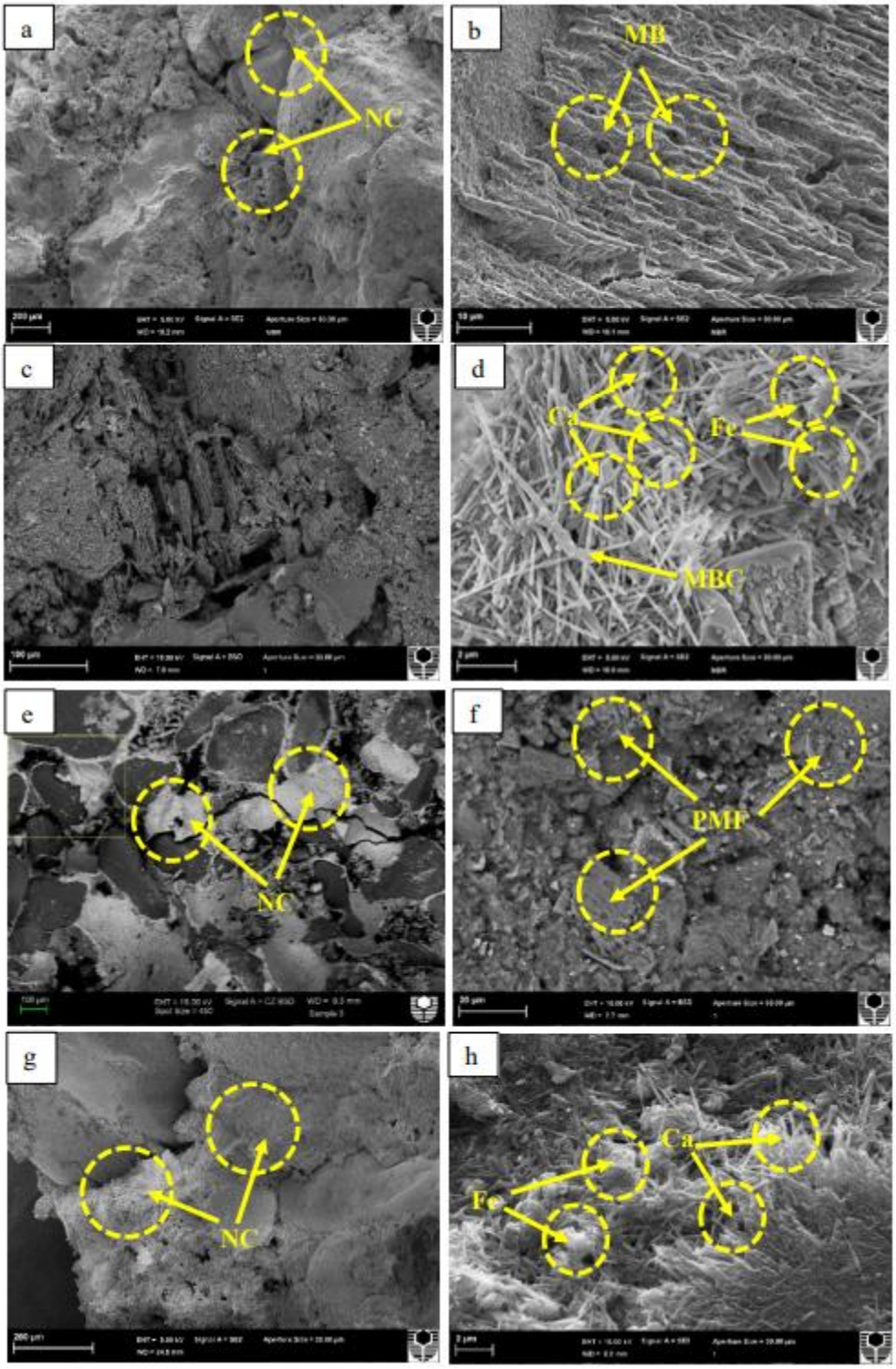

Fig 3. 2 Scanning electron micrographs of beach rock formations from a-d) intermediate 7 samples BR-1 and intermediate sample BR-2 e-h) terminal sample BR-3 and BR-4. Natural 8 cements (NC) in between sand grains, microbial borings (MB), mineralised bacterial cell 9 (MBC), possible microbial footprints (PMF) recorded in certain locations. Mineralised Ca 10 rods and Fe globules were also seen.

Energy dispersive X ray spectrum (EDS) analysis was then carried out to determine the composition of different cements observed in the SEM images of different samples. Sand mixed with iron and aluminium was recorded in beachrock samples BR-1 and BR-3 collected away from the shore while both iron and calcium was recorded in the EDS spectrum of BR-2 and BR-4 which were collected nearby (Fig 3.3 a-d). It was noticeable that intermediate sample BR-2 displayed higher calcium content compared to iron which was predominant in the terminal stage sample BR-4 (Fig 3.3 b, d). In the terminal sample BR-3 collected near the iron creek, no Ca and only Fe was recorded showing its prevalence (Fig 3.3c). In the elemental spectrum maps, Ca was seen more near the grains while Fe displayed more prevalence in the cavities. The intensities of these elements varied slightly. Along with these major elements, the other elements were O, C, Si, Mg, Si, Al, P with traces of Cl, Na and S. Ferruginous cements (FC) were probably related to iron oxides and silicates possibly as aluminosilicates while Ca have been from the carbonaceous cement as aragonite or calcite. The presence of Na and Cl could be due to sodium chloride from seawater. The minor elements as C, Al, Si, Cl, Na indicated the presence of clay minerals, silicates with iron-enriched cements covering carbonaceous cements.

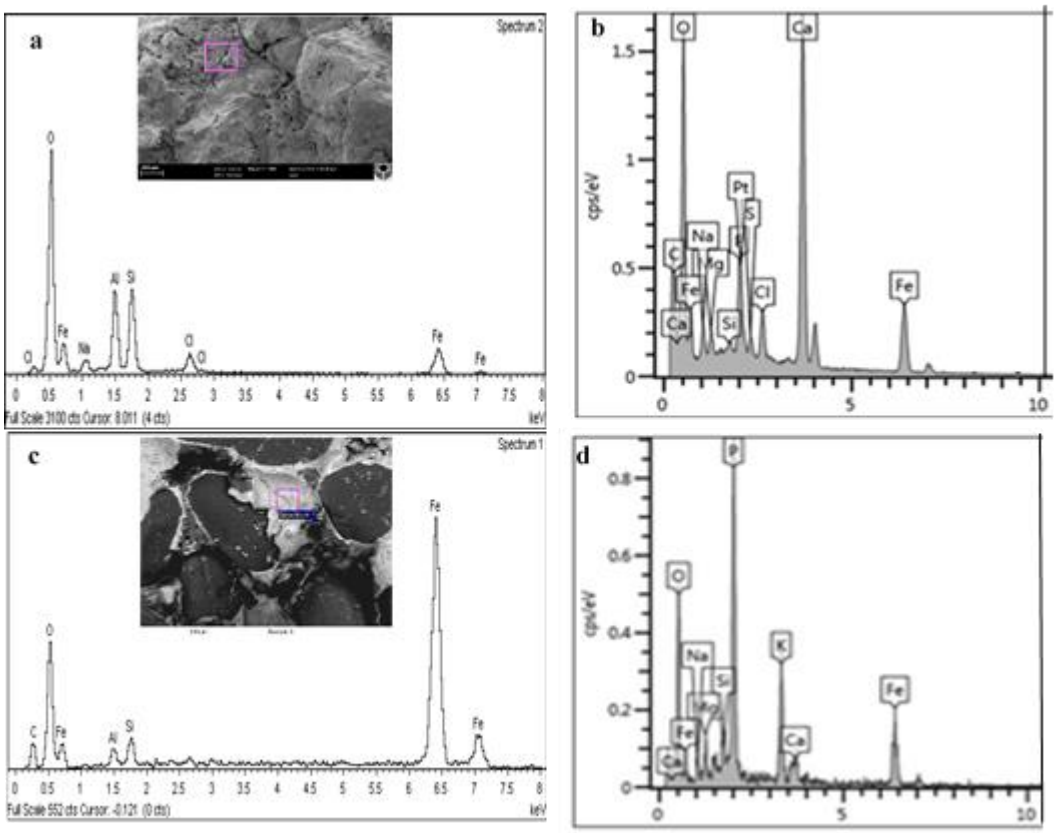

Fig 3. 3 Energy dispersive X ray spectrum of a,b) intermediate sample BR-1, BR-2 c,d) 12 terminal sample BR-3, BR-4

The absorption frequencies of the peaks in spectra of each sample have been demonstrated in Fig 3.4 a) via FT-IR analysis. By comparing these frequencies with the literature, there was further support for the presence of quartz, kaolinite, hematite, magnetite and aragonite in the current samples [13]. Sample BR-1 had dominance of hematite along with quartz and aluminosilicates minerals while the terminal creek sample BR-3 had a predominance of Iron in the form of hematite, goethite and nontronite along with other minerals which are supportive of the EDS analysis. In the other intermediate and terminal samples BR-2 and BR-4 collected near the shore, the presence of aragonite was again recorded along with goethite and magnetite. Quartz is a ubiquitous and abundant constituent in all the samples. It is seen widely in several sediments as well as sedimentary and igneous rocks. Similar peaks have been reported by several other studies [13].

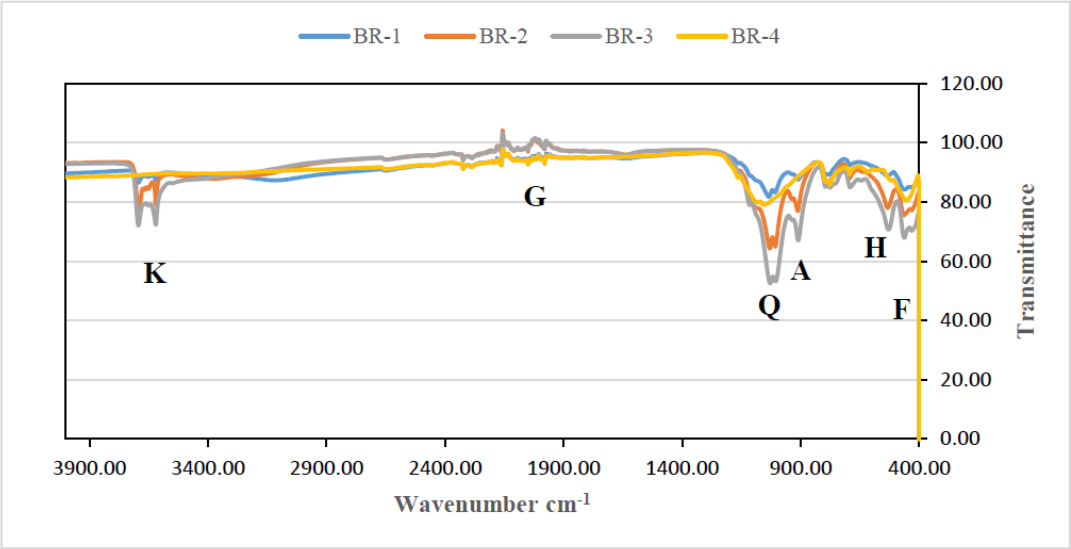

Fig 3. 4 a) Fourier transform infrared spectrum of beach rock samples: intermediate sample BR-14 1 and BR-2 and terminal sample BR-3, BR-4 indicating the presence of different minerals 15 including quartz (Q), kaolinite (K), hematite (H), goethite (H), aragonite (A), feldspar (F)

The mineralogy was further investigated by XRD analysis (Fig 3.5 a). In this case also the XRD analysis of samples far shore BR-1 and BR-3 displayed the presence of quartz, kaolinite, orthoclase, hematite, magnetite, while nearshore samples BR-2 and BR-4 exhibited the presence of quartz, orthoclase, kaolinite, goethite, hematite, and aragonite/calcite. These results agreed with the previous analysis of FT-IR, though, in XRD, the prevalence of goethite and magnetite was recorded. Although both FT-IR and XRD have been used conventionally to provide clear assignment of oxide phases as well as the measurement of the degree of crystallinity of materials, all techniques have their own advantages and disadvantages with the crystalline phases, textural relationships between minerals and chemical compositions [45, 46]. The discrepancies might also be due to the immense variations in specific sections of the samples analysed.

1965

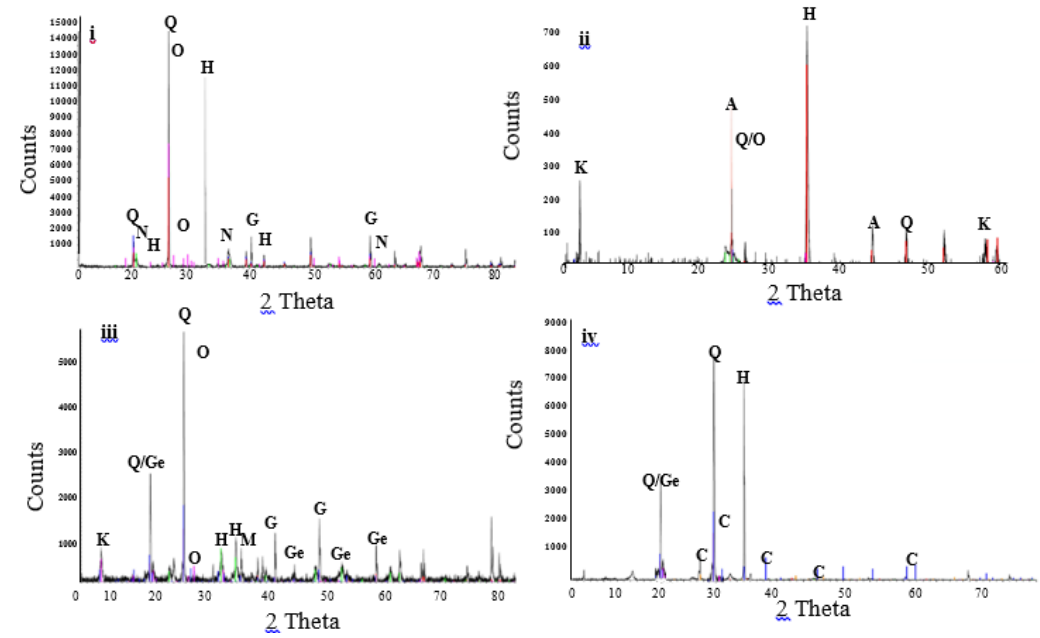

1966

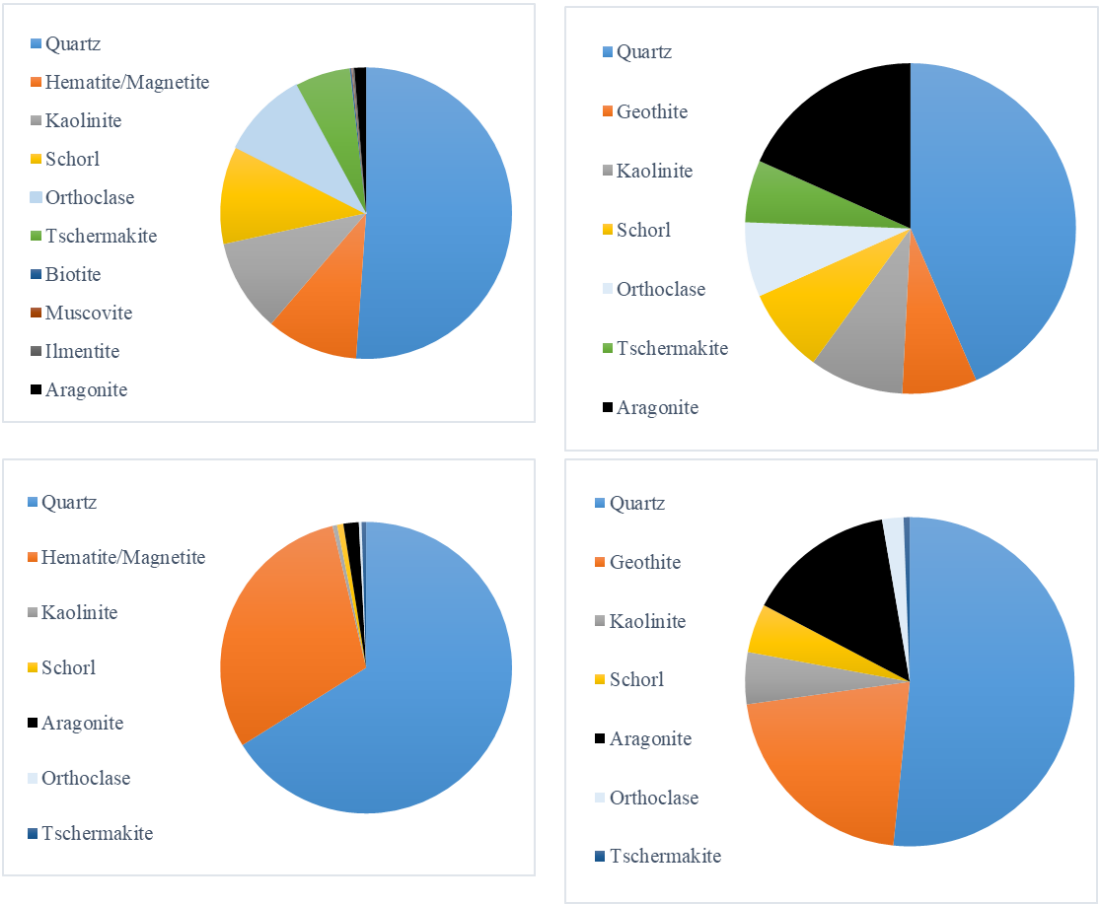

1967 *Fig 3. 5 a) X ray diffraction analysis of different beach rock samples i, ii) intermediate*
1968 *BR-1 17 and BR-2 iii, iv) terminal BR-3 and terminal BR-4 indicating the presence of*
1969 *different 18 minerals including quartz (Q), orthoclase (O), kaolinite (K), hematite (H),*

goethite (Ge), 19 aragonite (A), calcite (C), Nontronite (N), feldspar (F). b) TIMA analysis of (a) intermediate BR-1 and BR-2 (b) terminal BR-3 and BR-4

Further analysis of the mineralogy via TIMA analysis in intermediate and terminal samples has been demonstrated in Fig 3.5 b). In this case, the samples showed a significant increase in iron mineral content in terminal samples. The minerals, in this case, were quartz, hematite/magnetite, kaolinite, schorl, orthoclase and tschermakite along with minor minerals. In the case of BR-3 and BR-4 samples, TIMA analysis demonstrated the presence of ferruginous as well as carbonate cements. In this case, the composition of intermediate and terminal samples showed significant differences as the concentration of iron hydroxides/oxyhydroxides was much higher in terminal samples compared to the intermediate ones. Also, in this case, the prevalence of iron hydroxides over oxides was noted compared to the BR-1 and BR-2 samples, which is indicative of the on-going iron hydration processes. Calcium carbonate in the form of aragonite was highly prevalent in both intermediate and terminal samples near the shore which was also recorded in the micrographic and elemental analysis indicating the ongoing calcium carbonate precipitation/dissolution cycle. Similar observations have been recorded in previous studies [10, 12, 47].

3.6.1.3 Nanomechanical properties of beachrocks

The mineral constituents, cements and interphase areas were carefully chosen and indented after polishing avoiding any interference of the resin matrix, but there is still a possibility of indenting the interfacial zone where a thin veneer of resin is left on the particle. Fig 3.6 represents the indented areas on grains of varying morphologies and sizes, cements formed in between as well as grain – bridge interfaces in both intermediate as well as terminal samples BR-1 to BR-4. Indentation sites were selected to cover at least 50 % of the image area. Through load indentation analysis, hardness and elastic modulus of different samples were calculated as shown in Table 3.5. It was quite evident that different components within the same sample had significant variations in the properties with grains depicting as the hardest component followed by cements and weaker interfacial zones although considerable variations were noticed across the cross-sections in all regions. All the nanomechanical values were validated through their close agreement with previously available data [30, 35, 48]. Fortunately, properties of some of the pure minerals and oxides have been investigated including calcite, aragonite,

vaterite, hematite, magnetite, goethite, clay minerals etc. in a few earlier studies [22, 30, 33, 34, 49] although information regarding the nanomechanical properties of natural beachrocks is unavailable hitherto. In a comparison of samples from different sites, BR-2 and BR-4 with mixed ferruginous and carbonate cements were found to have higher modulus and hardness compared to BR-1 and BR-3 with predominantly ferruginous cements. In the case of grains and bridge-grain interface behaviour also, a similar trend in the modulus and hardness properties was recorded. In our previous studies, we recorded a modulus of 64.50 ± 2.7 GPa and a hardness of 3.92 ± 0.43 GPa for pure calcium carbonate calcite crystals precipitated using bacterial isolate *Sporosarcina pasteurii* (ATCC 11859) which was similar in case of biocement formed in road bases [37]. The modulus and hardness for complex ferruginous oxides including magnetite, hematite and goethite have been recorded to be 52 GPa with the hardness of 5.3 GPa; 65 GPa at the hardness of 2.7 GPa and 50 GPa at a hardness of 1.1 GPa [49]. In this case, the modulus and hardness for terminal ferruginous cemented BR-2 sample were found out to be 74.7 ± 7.8 with a hardness of 2.7 ± 0.38 GPa while in case of carbonate-ferruginous cement BR-4, it was recorded to be 93.7 ± 6.27 GPa with a hardness of 4.6 ± 0.31 GPa. Although these values were found to be higher compared to previous studies, these variations could be due to complexities of minerals in natural formations. The Mohr's hardness of calcite is 3, Geothite lies between 5-5.5, Hematite and Magnetite are 6.5. In the study, the modulus and hardness for terminal ferruginous cemented BR-2 sample were found out to be 74.7 ± 7.8 with a hardness of 2.7 ± 0.38 GPa while in case of carbonate-ferruginous cement BR-4, it was recorded to be 93.7 ± 6.27 GPa with a hardness of 4.6 ± 0.31 GPa. The theory of conventional plasticity stated that the mechanical properties of a material are independent of its length scale. However, natural minerals are usually far from the idealization. In the case of a macroscale indentation (such a Vickers test), the sample inhomogeneity is averaged out, and a mean hardness value is obtained due to the large indent size. However, microscale indentation (nano-indentation) is an ideal tool to characterize segregation and banding, to identify constituents, and to characterize surface hardness/microstructure [30, 32]. Thus, macro tests yield an average material hardness, while micro- and nanoscale tests indicate variations in different parts of the sample microstructure [32].

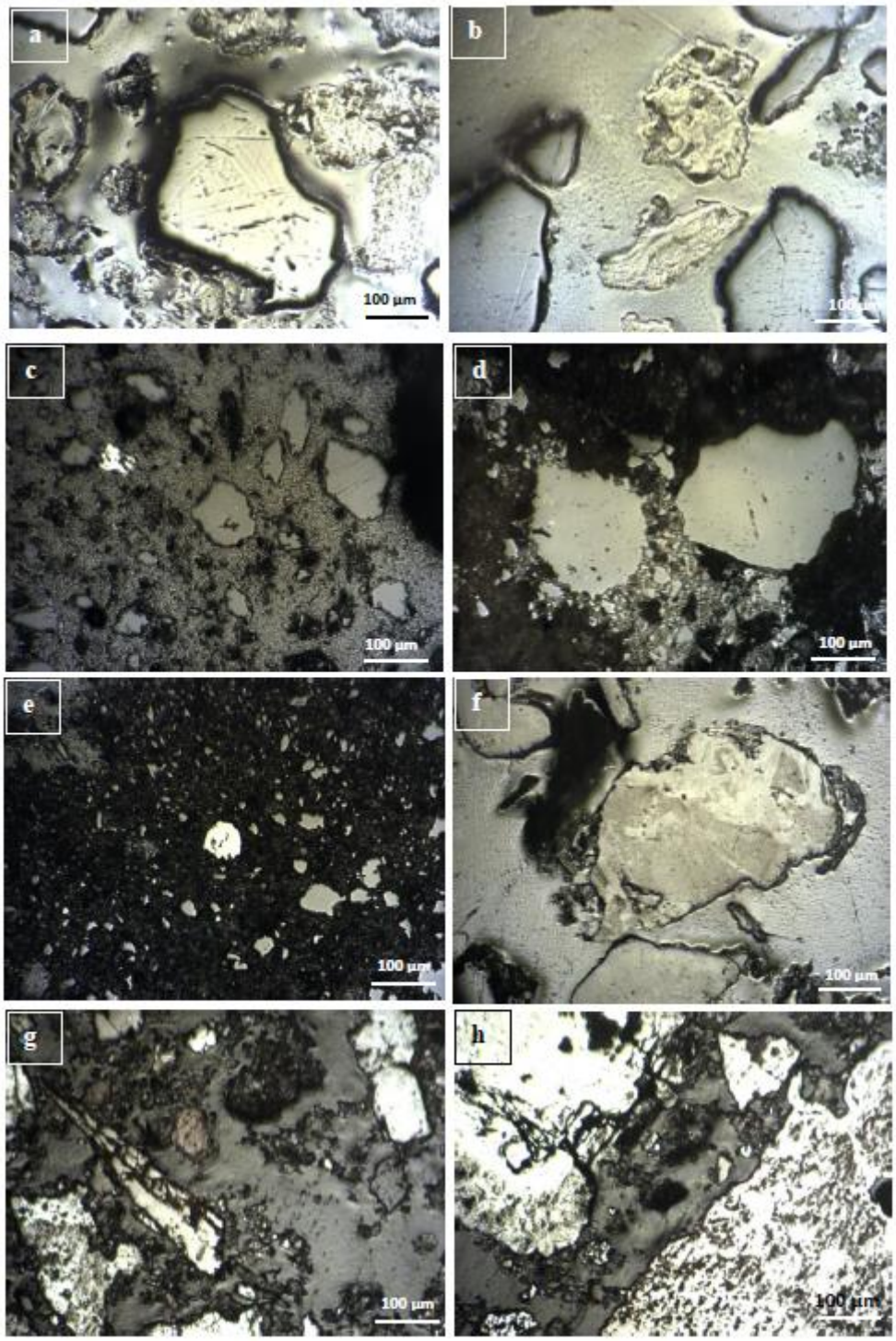

Fig 3. 6 Microstructures for nanoindentation through optical microscope fitted with 22 nanoindenter for: (a, b) intermediate BR-1 (c, d) intermediate BR-2 (e, f) terminal BR-3 and 23 (g, h) terminal BR-4

Table 3. 5 Mechanical properties of different rock samples obtained through nanoindentation

Sample	Location	Modulus (GPa)	Std. Error	Hardness (GPa)	Std. Error
BR-1	Grain	90.7	9.6	12.2	3.4
	Cement	43.5	3.6	1.9	0.34
	Bridge-grain interface	26.8	2.7	1.76	0.54
BR-3	Grain	136.8	12.9	14.8	3.8
	Cement	74.7	7.8	2.7	0.38
	Bridge-grain interface	34.3	5.9	1.92	0.63
BR-2	Grain	119.3	8.6	12.8	2.18
	Cement	65.1	5.57	1.85	0.62
	Bridge-grain interface	36.7	2.76	1.13	0.35
BR-4	Grain	168	9.2	17.8	2.47
	Cement	93.7	6.27	4.6	0.31
	Bridge-grain interface	48.4	2.97	3.8	0.11
Resin		6.02	0.8	0.08	0.02
Quartz		105	5	13	1
Feldspar		85	5	9	1
Aragonite		67	9.6	4.9	0.31
Pure magnetite		223	12	6.3	0.9
Pure hematite		237	14	8.2	1.2
Pure geothite		187	13	6.7	1.1
Complex magnetite		52	4.5	5.3	0.8
Complex hematite		65	5.3	2.7	0.6
Complex geothite		50	4.7	1.1	0.8

3.6.2 Lab synthesized beachrock biocement

3.6.2.1 Role of microbial processes in biocementation

The next phase of the study was to investigate the role of microbial processes in mineralisation and precipitation of beachrocks. Formation of iron and calcium compound minerals via biogenic processes have been reported to be driven by microbial processes in a few earlier studies [1, 12, 21, 22, 44]. In order to gain further insights into the role of associated microbes during mineralisation processes, mimicking the real conditions in laboratory are imperative (including temperature cycles, light/dark cycles, humidity, nutrients, chemicals) but highly challenging given the time scales and conditions. So, in the current study, we only attempted to investigate the mineralisation

potential of surface-associated microbial communities keeping in mind that this does not represent the actual process but do shed light on the role of microbial influence.

To confirm the association and role of beachrock associated communities, at the first stage, their growth and pH was monitored under minimal nutrient conditions with additional carbon for accelerated growth. Significant differences in absorbance and pH changes were noted in different enrichment and control sets (Fig 3.7). In biogenically induced sets, highest biomass growth was recorded in set 1 with supplemented glucose followed by lactate and mix of both initially. No turbidity was recorded in any of the control sets confirming successful biogenic enrichments. Even in the case of the pH, there was a noticeable increase in the biogenically induced sets indicating active microbial metabolism. There were slight variations in pH in abiogenic sets too. The amount of precipitation in biogenic and abiogenic sets under different enrichment conditions was recorded after ten days by taking the weight of precipitates after filtration. In this case, also, the precipitation was found to be significantly higher in all biogenically enriched sets compared to the abiogenic controls indicating the potential of biological activity in catalysing mineralisation. Amounts of precipitation amongst different enrichment media case were again highest in Enr1. In the current study, extremely low mineral precipitation was observed in the control experiments.

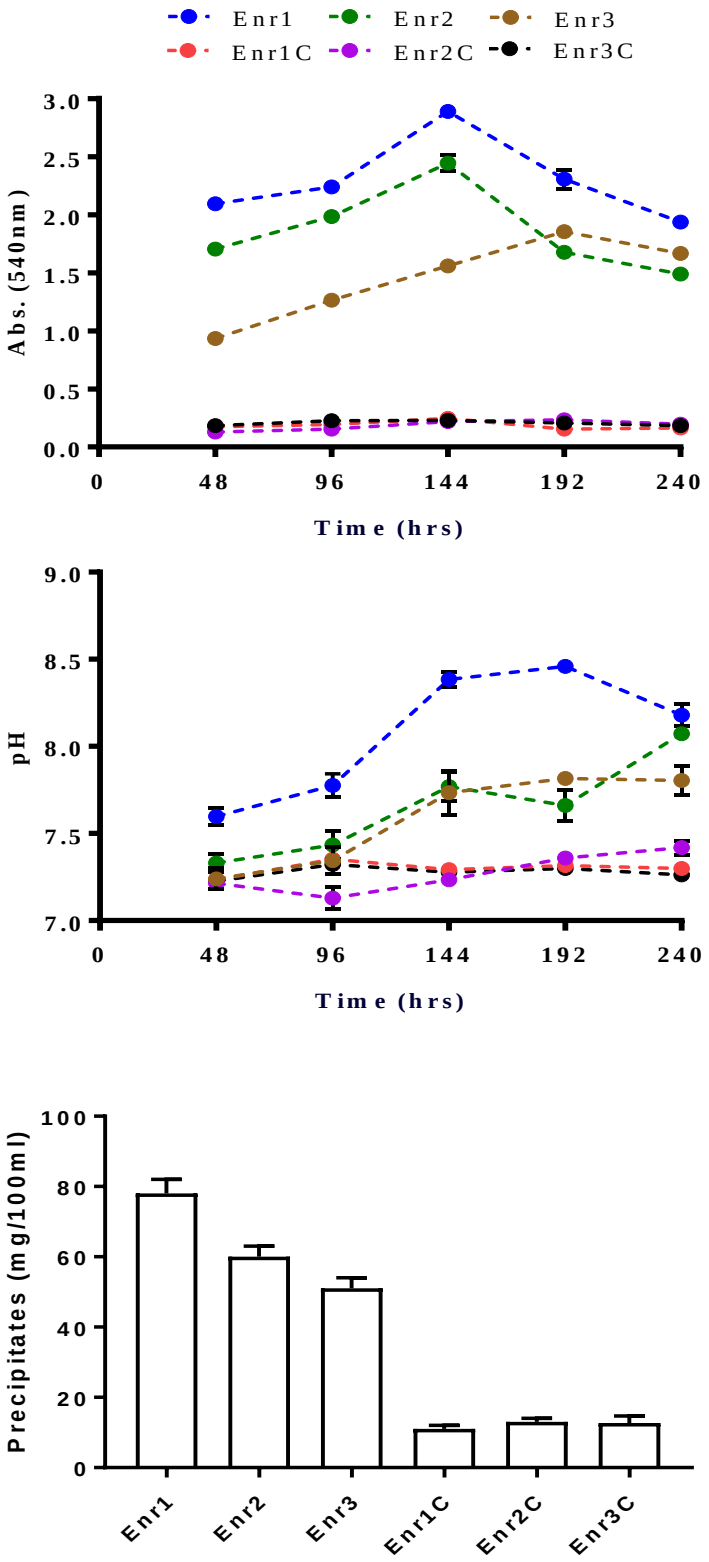

2070

2071 *Fig 3. 7 Effect of biogenic and abiogenic enrichments on (a) absorbance (b) pH and*

2072 *(c) 25 amount of precipitation. Enr1 = enrichment under glucose; Enr2 = enrichment*

under lactate; 26 Enr3 = mix of glucose and lactate; C= control. Values are mean ± SD (n=3)

3.6.2.2 Analysis of microbial diversity

To further confirm the presence and association of microbial communities in native and enriched beachrocks, their community structure was analysed and identified to relate their role in potential role in iron and calcium mineralisation processes. The sequences were submitted to NCBI and were grouped into OTUs (accession number PRJNA562124). The classification was against the Greengene database that provides the community resolution up to genus/ species level. It was recorded that the microbial diversity decreased significantly under laboratory enrichment conditions compared to native conditions highlighting the selection and dominance of these communities under various environments.

Fig 3.8 represents the relative abundance of microbial communities at phylum level. Tremendous variations in the bacterial compositions in native and different enrichments routes were recorded. In the case of native beachrocks, the dominant phylum was recorded to be *Proteobacteria* and *Actinobacteria* followed by *Euryarchaeota*. The most predominant genus under natural conditions were *Halococcus* (*Euryarchaeota*), *Marinobacter* (*Gammaproteobacteria*) and unidentified cultures from *Rhodobacteracea* (*Alphaproteobacteria*), *Halobacteraceae* (*Euryarchaeota*), *Acidimicrobiales* (*Actinobacteria*), *Rhodothermales* (*Bacteroidetes*) and *Sinobacteraceae* (*Proteobacteria*). While under laboratory conditions, the community structure was quickly overtaken by *Proteobacteria* under all enrichments showing the influence of environmental conditions including pH, oxygen, temperature and carbon sources which affect not only the biomass concentration but also the structure of these communities. The most predominant genus under enriched conditions was recorded to be *Marinomonas* (from Order *Oceanospirillales* of *Gammaproteobacteria*).

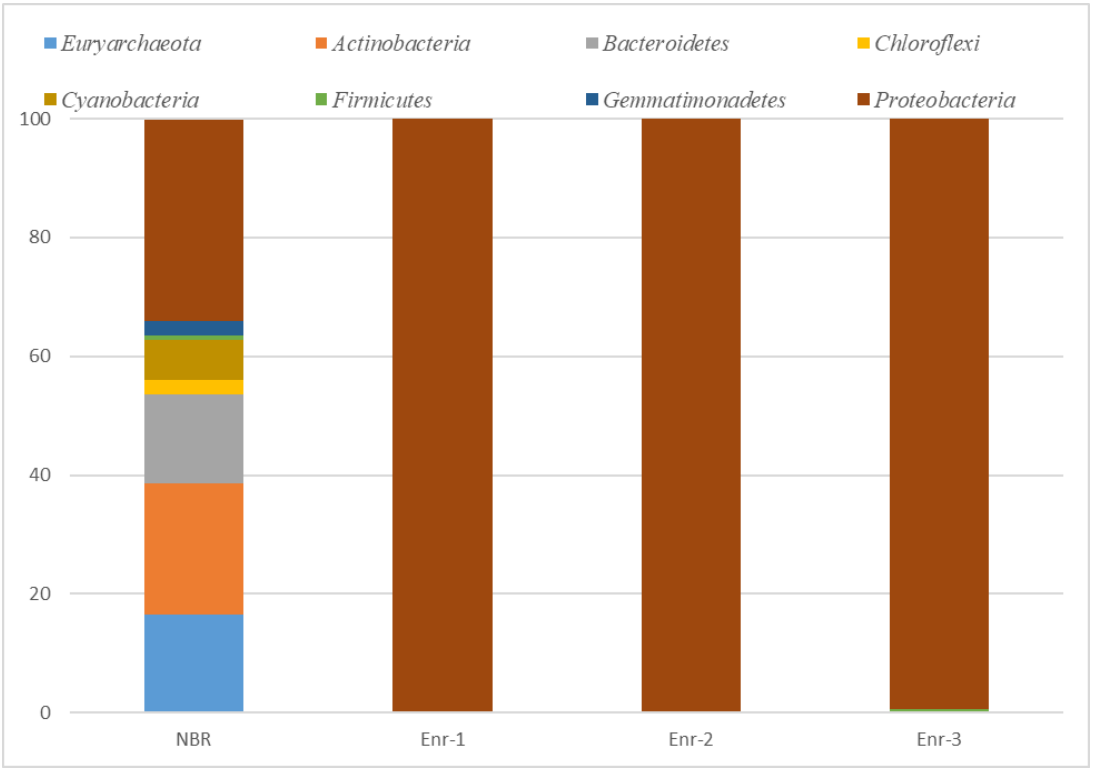

Fig 3. 8 Bacterial population composition at phylum level in natural and laboratory enriched 28 conditions (based upon 16S rRNA gene sequencing presented as a fraction from the total 29 population) wherein Enr1 = enrichment under glucose; Enr2 = enrichment under lactate; Enr3 30 = mix of glucose and lactate and NBR = Native beachrock

3.6.2.3 Micrographical, mineralogical and nanomechanical analysis of laboratory synthesised biominerals

The morphology and mineralogy of these biologically induced minerals was further analysed for morphographic and mineralogical details through SEM, EDS and XRD analysis. In the case of SEM, a mixture of round, spherical, globular and needle-shaped crystals were recorded (Fig 3.9a-d). A heterogeneous mixture of acicular crystals as in aragonite, lettuce crystals as in vaterite, rhombohedral crystals as in calcite and semirounded nanoglobules as in ferruginous cements were clearly recorded as seen in several previous studies [12, 24, 44] (Fig 3.9a-c). The crystals were seen clearly associated with bacterial cells indicating that they act as nucleation sites, leading to their entrapment and formation (Fig 3.9a - c). In general, a mixture of spherical, lettuce, round, circular, needle-shaped, of sizes varying from 2-30 µm was recorded (Fig 3.9d).

EDS and XRD analysis further confirmed indicated the presence of Fe and Ca in the form of hematite, magnetite, calcite and vaterite which were significantly different from the native beachrocks polymorphs probably due to the differences in physical and chemical environments (Fig 3.10a-c). In this case, also nanoindentation analysis was carried out on the precipitated crystals, and it was found that the modulus, in this case, varied from 31 ± 8.4 to 57 ± 6.4 GPa while the hardness of the crystals varied from 1.9 ± 0.18 to 3.32 ± 0.27 GPa.

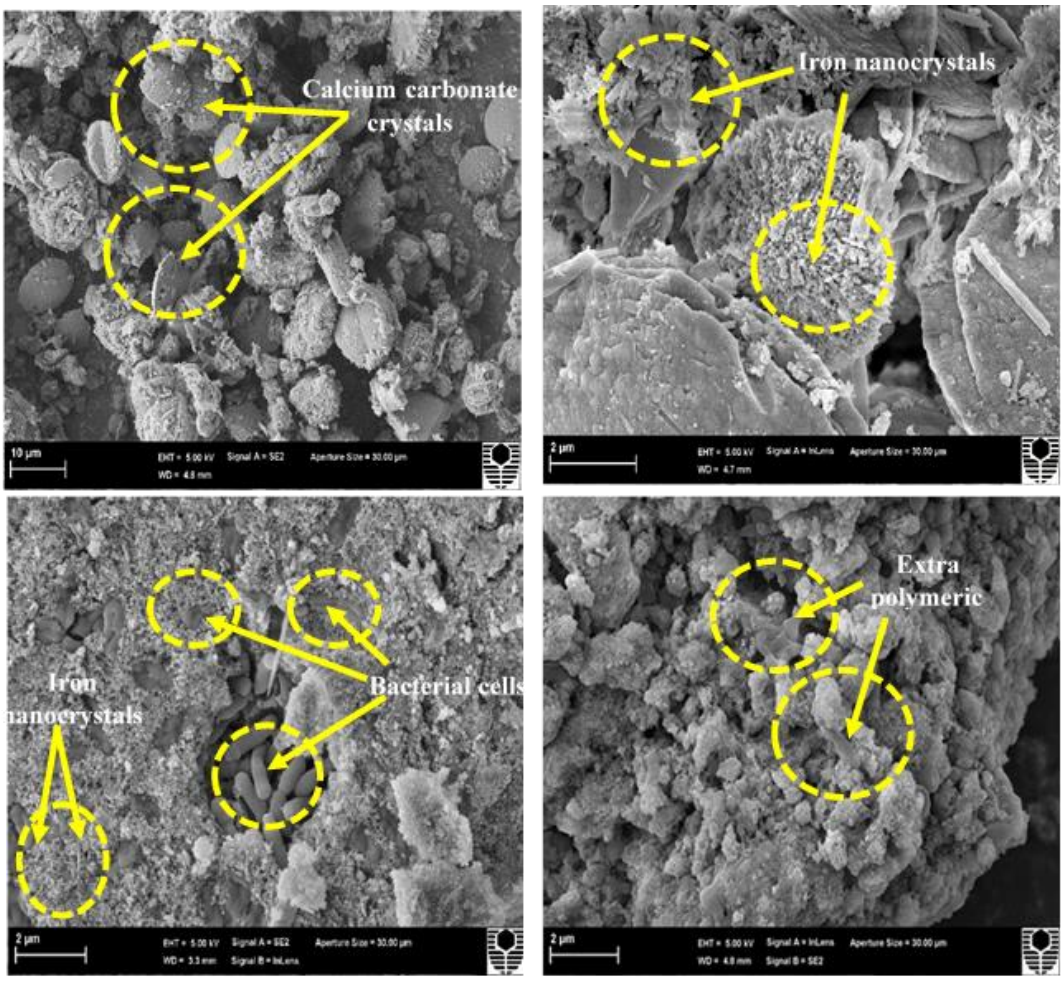

Fig 3. 9 (a-d) Scanning electron micrographs of bacterial cells and biogenically precipitated 32 crystals under in vitro conditions. Bacterial cells acting as nucleation sites were recorded. 33 Heterogeneous mixture of acicular crystals as in aragonite, lettuce crystals as in vaterite, 34 rhombohedral crystals as in calcite and semirounded nanoglobules as in ferruginous cements 35 were clearly recorded

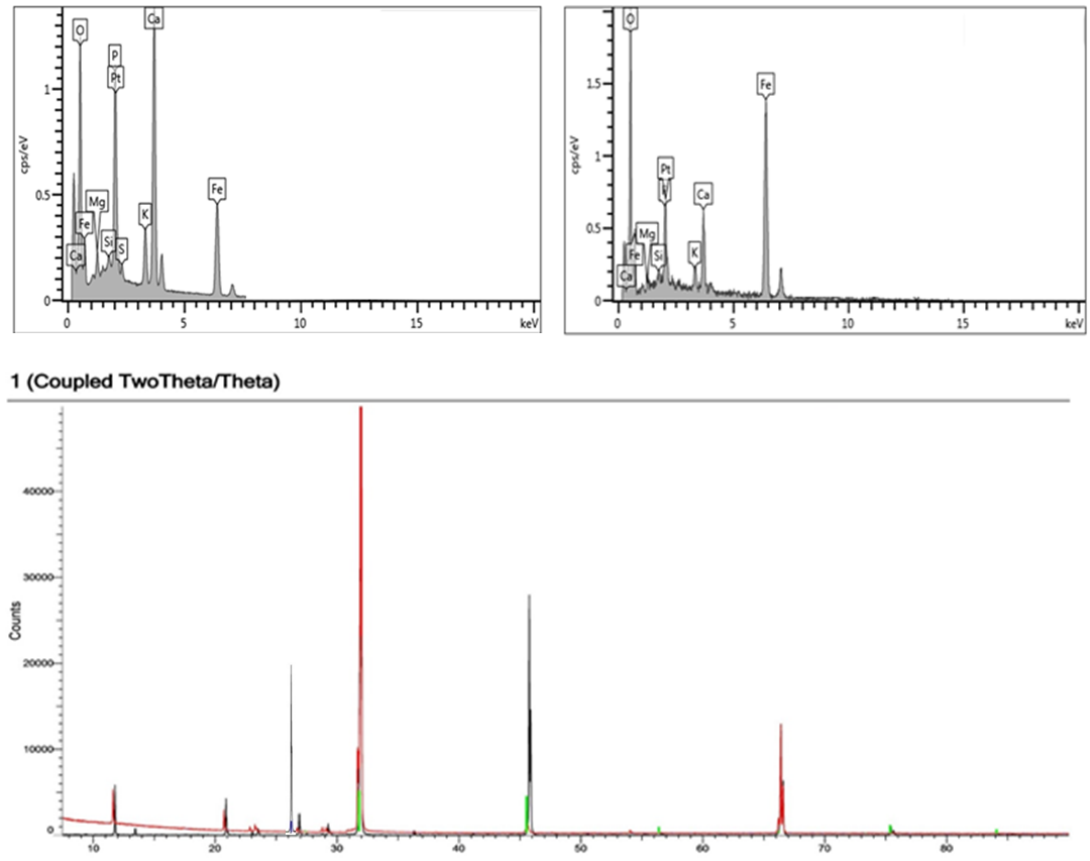

Fig 3. 10 (a, b) Energy dispersive X ray spectrum and (c) X ray diffraction analysis of biogenically precipitated crystals under in vitro conditions depicting the presence of calcium and iron rich minerals in the form of calcite, vaterite, hematite and magnetite

3.7 Discussion

3.7.1 Formation of beachrock sediments in nature

Elemental, micrographical, mineralogical and nanomechanical analysis of the beachrock sediments collected at different locations of the seashore was conducted to understand a comprehensive picture of the biogeochemical processes and their effects on the formation of cements produced in nature. The overall analysis indicated the effect of biogeochemical environments on the formation of different natural structures. Ferruginous, calcium carbonate and aluminosilicate cements were the chief cements in the current study. The properties and constituents of different beachrock sediments demonstrated significant differences depending upon the proximity of the sediments to the seashore and creek. Microbial imprints and extra polymeric substances were recorded in a few places in the sediments, indicating the feasibility of microbial roles and associations in their synthesis/dissolution processes.

In the case of chemical analysis, a range of elements chiefly silica, aluminium, magnesium, calcium, and iron were recorded along with several others in minute quantities. Amongst them, aside from siliceous nature of the beachrocks significant differences in the concentration of different elements were recorded especially in case of iron and calcium (in the leachate as well as sediments) at different locations. These differences in case of iron can be accounted to the proximity of these sediments to iron-rich creek comprising products from industrial/mining activities in the adjacent area. The precipitation of iron-rich minerals in sediments could correspond to local dissolution processes, infiltration of iron-bearing solutions through pore spaces and re-precipitation under reduced conditions. The dissolved metals also migrate through the pore spaces to basic areas due to hydrated weak basic conditions of seawater giving rise to the formation of iron minerals. In the earlier studies of Aramendia, Gomez-Nubla [50], iron-rich wastes trapped in beachrock units constantly exposed to the outdoor conditions created local moisture films which generate reducing environment and make iron to be mainly in the reduced form (Fe^{2+}) which is most soluble in water. Even in case of calcium, variations in the intertidal zones and onshore locations might be the cause for differences in their content at varying locations. Complete prevalence of ferruginous precipitates on the surface of calcium-rich bedrock in near creek samples might be due to much higher iron minerals in that environment with lesser seawater exposure.

Owing to the heterogeneity in the distribution of different kinds of cements and crystals in beachrock sediments, detecting different kinds of cements was an arduous task. A general view revealed isopachous cements standing out from the grains and filling the cavities/pores between sand grains (Fig 3.2). The cementation characteristics concord with iron-based ferruginous cements predominantly in near creek samples and needle-shaped possibly aragonitic cements were widespread in the nearshore samples [44, 51]. The ferruginous cements have been found to appear in two forms accompanying carbonate cements as discontinuous non-homogenous layers and as uniform continuous cement [12, 52] and that is how they observed in the current samples. Depending upon the Fe oxidation state (Fe^{2+}/Fe^{3+}), oxides of iron exhibit different structures with hematite (α-Fe_2O_3) being the most stable one [53]. It is believed that hematite mineral phase in the form of hexagonal platelets also undergoes hydrolysis or dissolution leading to the formation of needle-like sub crystals of goethite [54] but just by micrographic

inspection this analysis was hard to determine and needed further verification. The structural polymorphism in case of carbonate cements as calcitic or aragonitic is indicative of different diagenetic stages [55] with more aragonite shaped crystals being indicative of active/ on-going precipitation events. For instance, the presence of calcite has been related to the prolonged exposition of marine, denser aragonite cement to meteoric weathering process. The prevalence of calcium carbonate in the form of less stable aragonite has also been recently related to microbial and EPS roles which we will verify in the next section [10]. Closer views of the sediments revealed certain areas with partial dissolution indicative of vadose conditions for current sediments. Interestingly in a few sections of different samples, microbial imprints, borings, and extra polymeric substances (EPS) layers were also recorded. These signatures were highly indicative of the active role of microbes in precipitation and dissolution of different cements. Fig 3. 2b and 2F suggested that microbial borings are actively occurring near the surface. Dissolution by acid production is a classic example of this process [1]. Both heterotrophic and phototrophic bacterial communities have been reported to influence calcium carbonate precipitation equilibrium via altering the saturation index and affecting the pH due to their metabolic activities. In this case, also, EPS and microbial communities seem to play a highly active role in precipitation and dissolution processes.

Mineralogical and elemental studies via different tools as XRD, TIMA, FTIR and EDS confirmed the presence of ferruginous, aluminosilicate and carbonate-rich cements (Fig. 3.3-3.5). This compositions of nearshore and near creek samples confirmed the effect of physicochemical environment on mineralogy. The mineralogy observed in this study via different techniques is characteristically attributed to marine vadose environments. These findings suggest the role of weathering processes and action of leaching waters on the surface of bedrocks, causing the removal of soluble constituents and precipitation as insoluble minerals depending upon the physicochemical environments. Presence of high amounts of iron from the creek from industrial activities leads to the formation of ferruginous cements on the surface of carbonate cements via partial dissolution and drainage processes in the meteoric environments and vadose zones. Precipitation of calcium carbonate has been studied widely in several geological formations, including the current one. As the mineralogy of different carbonate polymorphs as calcite, aragonite, vaterite is dependent on a range of physicochemical factors including pH, temperature, saturation index, dissolved organic carbon concentration, Ca^{2+}/CO_3^{2-} ratio

along with microbial associations, a clear causative parameter is hard to point out [24, 56]. The mechanism for the precipitation of calcium carbonate cements seems to be influenced by both abiogenic and biogenic processes in this case. In the case of ferruginous cements, different mineral forms were recorded, which depend upon the Fe oxidation state (Fe^{2+}/Fe^{3+}). Prevalence of hematite cements in beachrocks near creek and goethitic based oxyhydroxides from the seashore indicate the effect of hydration, oxidation, and reduction environments on determining the mineralogical state of these minerals. Magnetite formation has been related to a reduction of hematite by SO_2 [54] while the oxyhydroxide goethite has been reported to form under hydration conditions in basic seawater area [12, 57]. The other forms of ferruginous cement can also form through weathering activities of hematite. As iron-rich wastes get trapped in beachrock units and are continuously exposed to outdoor conditions, the local environments and contact with water determine their fate as seen via variations of carbonate polymorphs and ferruginous minerals in this case. Several aqueous as well as atmospheric processes seem to be triggered by redox chemical reactions and hydrolysis cycles. Meteoric-vadose diagenetic events influence the formation of ferruginous and carbonaceous cements [12]. Overall, early diagenetic cementation of carbonate and ferruginous minerals is recorded in the beachrock sediments, and microbial metabolic activities seem to have some influence in these formation and dissolution processes.

Mineralogy was also found to affect the nanomechanical properties of different sediments as higher strengths were recorded with older beachrock sediments compared to the younger ones with higher hematite and aragonitic signatures (Fig 3.6). Mixed oxides of iron have been recorded to have lower nanomechanical properties compared to carbonates in the previous literature which might support the outcome of a current study indicating a direct influence of mineralogy on the nanomechanical behaviour of different materials. The variations in the modulus and hardness properties within different carbonate polymorphs have been previously rationalised based on structural differences, packing and orientations of Ca^{2+} and CO_3^{2-} [30]. Similar variations have also been recorded for iron oxides and hydroxides supporting the current findings as within the same sections of the cements and grains, considerable variations were recorded [49]. Although clear connections between mineralogy and nanomechanical behaviour in complex natural systems are hard to be inferred, trends could be clearly recorded as terminal samples, and mixed carbonate/ferruginous samples displayed higher

nanomechanical behaviour compared to early-stage sediments and ferruginous cement samples.

Further investigations in different sections and depths within the samples should be carried out to obtain more reliable data. More multidisciplinary studies need to be carried out on multi-phase materials to underpin the relationships between elemental, mineralogical and microbial roles using non-destructive advanced tools for analysis including X ray fluorescence, Raman spectroscopy, and functional genomics. Although in some of the earlier studies with carbonate polymorphs, the effect of Ca^{2+} and CO_3^{2-} packing on mechanical properties in different carbonate polymorphs has been clearly demonstrated but very little has been explored for iron minerals [35, 48, 58]. This is the first study wherein we tried to investigate these nanomechanical properties; however, much needs to be explored yet.

3.7.2 Formation of beachrock cements in the lab

To further investigate the role of indigenous microbial communities for in vitro synthesis of biominerals and cementation, their mineralisation potential under low nutrient artificial seawater media conditions was recorded. Growth, pH, and calcium precipitation studies clearly recorded metabolic activity by indigenous microbial communities associated with native beachrock sediments in biogenic sets (Fig 3.7). Successful biomineral production of both ferruginous and calcium carbonate minerals was recorded in biogenic sets while little precipitation occurred in the abiogenic sets (wherein microbial imprints were removed via autoclaving) confirming the role of bio-geochemical processes in formation of biocement.

The mineralisation of carbonate and ferruginous minerals by indigenous communities was further confirmed by micrographic and mineralogical studies (Fig 3. 9, 3.10). Microbial cells and EPS acting as the sites for nucleation of iron nanocrystals as hematite/magnetite and calcium carbonate in the form of vaterite and calcite was recorded (Fig 3.9, 3.10). There were slight variations in the carbonate polymorphs recorded in the natural samples and lab samples which can be related to the differences in physicochemical environments in both states. Despite extensive studies on bacterial carbonatogenesis, little is known about the cause(s) of polymorph selection though there have been a few hypotheses. The causative agents have been found to be: specific proteins in biological polymeric materials, characteristics of EPS, amount of dissolved

inorganic carbon, the composition of bacterial culture medium, mineralogy of the substrate, bacterial communities associated [51, 56, 59, 60]. As the physicochemical conditions in the laboratory samples were different in terms of elemental composition, temperature, light/dark cycles, microbial community composition; this could have driven changes in the supersaturation, pH, DIC conditions leading to the formation of variable polymorphs compared to the natural conditions. Controlled bioreactors with higher control over such factors should be designed in future to investigate the natural cementation processes although the aim of this study was just a preliminary investigation to compare the properties of natural and synthesised minerals. Nanomechanical properties of these crystals also confirmed their potential for use as biocement as they were comparable with the previous reports. No mineral precipitation was recorded in the sterile control sets without microbes proving the effect of indigenous microbial community's metabolic activities to drive mineralisation reactions under low nutrient seawater media conditions. This data confirms that the precipitation of minerals is dependent upon the kinetics, which is affected by the microbial activities. The living bacterial cells demonstrate the capability of overcoming kinetic barriers by reducing the activation energy barriers leading to precipitation of minerals.

The results of microbial diversity changes under native and in vitro conditions also demonstrated interesting results (Fig 3.8). There was significant community shift from dominant phyla *Proteobacteria, Actinobacteria* and *Euryarchaeota* in the native state to *Proteobacteria* under in vitro conditions. The dominant phyla in this study have been reported to play an important role in iron oxidation and carbonate mineralisation. Previous studies have reported the link of *Gammaproteobacteria* seen in this study in iron oxidation processes and precipitation of iron hydroxides including microaerophilic isolates of *Galionella, Sideroxydans, Mariprofundus* [61-63] which produce twisted iron oxyhydroxide stalks. A number of species of *Gammaproteobacteria* have also been reported to play a significant role in calcium carbonate mineralisation processes in natural formations although *Marinomonas* has not been reported earlier for its direct role in carbonate biomineralisation [22, 64, 65]. Iron oxidising bacterial communities (FeOB) have been found to be prevalent wherever anoxic ferrous-rich subsurface waters mingle with oxygenated surface waters. Zeng and Tice [47] found that actively iron-reducing cells induced increased carbonate mineral saturation and nucleated precipitation on their poles. However, precipitation only occurred when calcium was

present in solution, suggesting that cell surfaces lowered local ferrous iron concentrations by adsorption or intracellular iron oxide precipitation even as they locally raised pH. In the studies of Yoshida, Yamamoto [66] they found that microbial consortium of iron-reducing and oxidizing bacteria contributes to the accumulation of iron oxyhydroxide with a banded zonal structure. A similar hypothesis of both iron reduction and oxidation processes might hold true for the native beachrocks of current study along with an association of carbonate precipitation. While in the case of laboratory conditions, iron oxidation and carbonate mineralisation through EPS might be responsible for ferruginous and carbonate minerals.

Reports on potential of several pure microbial cultures for biocalcification have been published in the earlier studies wherein augmented bacterial cultures were grown utilising high-grade laboratory nutrients [22, 40, 47, 67]. But very few attempts have been made on utilising the indigenous microbes for mineral precipitation of calcium and iron-based biocements under simulated seawater conditions. In our previous studies, we also recorded successful biocalcification potential via biostimulation of ureolytic communities in soils under high nutrient conditions [28], but not much has been explored for ferruginous and carbonate cementation together. As per the hypothesis of Chan, De Stasio [68] at neutral and alkaline pH, the polymers produced by oxidising iron bacteria can localize the precipitation of Fe minerals. This leads to the generation of protons and an increase of the pH gradient between outside and inside of the cells further leading to increase of the energy-generating potential. Similar processes seem to be governed in the current study as pH rise was recorded under all biogenic conditions. Under laboratory conditions of the current study, iron oxidation appears to be a prevalent process due to high oxygen and neutral pH conditions. The outcome of this study is also indicative of the role of iron oxidisers and nitrogen metabolites in cement formation.

The formation of beachrock biocement via utilising indigenous microbial communities under low nutrient seawater conditions improves the fundamental understanding of ferruginous and carbonate cementation processes and hints the possibility of utilising these microbes for applications in cementation of different sands in marine environments. This pathway can provide an alternative solution for the easier and eco-friendly application of biocementation on field sites, including coastal environments wherein conventionally foreign bacterial cultures grown under high nutrient conditions in labs are proposed to be transported. The acclimatisation and potential of indigenous

communities and consortia to tolerate natural environments comprising high salts, varying temperatures, pH, and other physical conditions might be better compared to the utilisation of pure augmented strains. This signifies that biostimulation of cementing microbes under seawater media conditions can be explored for cementation of loose sands without much expense of growing laboratory cultures.

3.8 Conclusions

In brief, the salient findings in this study are:

1. Confirmation of ongoing precipitation of ferruginous and calcium-based cements in beachrock sediments at Lucky Bay, Esperance. These cements displayed conjunction of carbonate and iron-rich composites, and the carbonaceous cements were dominating in samples collected near shore compared to ferruginous ones. The predominant minerals were quartz, hematite/magnetite, kaolinite, schorl, orthoclase and tschermakite.

2. Active microbial roles found in precipitation and dissociation processes of cementation in natural structures. Native microbial communities with a dominance of genus Halococcus and Marinobacter were recorded.

3. Mineralogical imprints affect nanomechanical behaviour of natural beachrock cements. The nanoindentation modulus and hardness for terminal ferruginous cemented BR-2 sample were 74.7 ± 7.8 with a hardness of 2.7 ± 0.38 GPa while in case of carbonate-ferruginous cement BR-4, it was 93.7 ± 6.27 GPa with a hardness of 4.6 ± 0.31 GPa.

4. Microbial signatures change tremendously from native states under varying physiochemical conditions. There was significant community shift from dominant phyla *Proteobacteria*, *Actinobacteria* and *Euryarchaeota* in the native state to *Proteobacteria* under in vitro conditions.

5. Biostimulation of indigenous iron-oxidizing and carbonate precipitating communities under seawater media is a novel tool to produce biocement in coastal environments

6. Nanomechanical properties of natural and lab synthesized biocements display variation but show promise. Nanoindentation analysis carried out on the precipitated crystals and revealed that the modulus varied from 31 ± 8.4 to 57 ± 6.4 GPa while the hardness of the crystals varied from 1.9 ± 0.18 to 3.32 ± 0.27 GPa.

Although the route of biostimulation seems promising for the creation of biocement with a scope for a few engineering applications, further studies are imperative for better understanding and optimisation of the protocols for large scale applications. More

studies should be carried out at real field sites to monitor the biogeochemical processes with low supplementation of nutrient sources for microbial enrichment over a period to investigate for any signs of aggregation. This can open more doors for creating sustainable biocement with potential for erosion mitigation in a sustainable and environmentally friendly way.

3.9 Acknowledgements

The authors acknowledge the use of Curtin University's Microscopy, Microanalysis and Chemical analysis Facility at John de Laeter Research Centre whose instrumentation has been partially funded by the University, State and Commonwealth Governments. The authors also thank TSW Analytical (Perth, Australia) for their help with ICP-MS testing. The authors thank Dr Anna Heitz from the department of Civil Engineering at Curtin University for her help with sampling and fieldwork. The authors thank Ms Sakshi Tiwari from the department of Civil Engineering at Curtin University for her help with bacterial sequencing analysis.

3.10 References

1. Zhu, T. and M. Dittrich, *Carbonate precipitation through microbial activities in natural environment, and their potential in biotechnology: a review*. Front Bioeng Biotechnol, 2016. 4: p. 4.
2. Dhami, N.K., M.S. Reddy, and A. Mukherjee, *Biomineralization of calcium carbonates and their engineered applications: a review.* Front Microbiol, 2013. 4: p. 314.
3. Castro-Alonso, M.J., et al., *Microbially induced calcium carbonate precipitation (MICP) and Its potential in bioconcrete: microbiological and molecular concepts.* Front Mater, 2019. 6(126).
4. Dejong, J.T., et al., *Biogeochemical processes and geotechnical applications: progress, opportunities and challenges.* Géotechnique, 2013. 63(4): p. 287-301.
5. Anbu, P., et al., *Formations of calcium carbonate minerals by bacteria and its multiple applications.* Springerplus, 2016. 5: p. 250.
6. Hamdan, N., et al., *Carbonate mineral precipitation for soil improvement through microbial denitrification.* Geomicrobiol J, 2016. 34(2): p. 139-146.

7. DeJong, J.T. and E. Kavazanjian, *Bio-mediated and bio-inspired geotechnics,* in *Geotechnical Fundamentals for Addressing New World Challenges*. 2019. p. 193-207.
8. Easton, W.H., *An unusual inclusion in beach rock.* J Sediment Petrol, 1974. 44: p. 693-694.
9. Chivas, A., Chappell, J., Polach, H., Pillans, B., Flood, P., *Radiocarbon evidence for the timing and rate of island development, beach rock formation and phosphatization at Lady Elliot Island, Queensland, Australia.* . Mar Geol, 1986. 69: p. 273-287.
10. McCutcheon, J., et al., *Beachrock formation via microbial dissolution and re-precipitation of carbonate minerals.* Mar Geol, 2016. 382: p. 122-135.
11. Iturregui, A., et al., *The relevance of the analytical methodology in the geochemical study of beachrock outcrops: Arrigunaga Beach inside the Nerbioi-Ibaizabal estuary (Getxo, Basque Country).* Anal Methods, 2014. 6: p. 329-336.
12. Arrieta, N., et al., *Characterization of ferruginous cements related with weathering of slag in a temperate anthropogenic beachrock.* Sci Total Environ, 2017. 581-582: p. 49-65.
13. Chandrasekaran, A., et al., *Analysis of beach rock samples of Andaman Island, India by spectroscopic techniques.* J Basic Appl Zool, 2015. 2(1): p. 55-64.
14. Rusell, R.J. and W.G. McIntire, *Southern hemisphere beach rock* Geography Reviews, 1965. 55: p. 17-45.
15. Alexandersson, T., *Recent littoral and sublittoral high-Mg calcite lithification in the mediterranean.* Sedimentology, 1969. 12: p. 47-61.
16. Moore, C.H., *Intertidal carbonate cementation, Grand Cayman, West Indies.* J Sediment Petrol, 1973. 43: p. 591-602.
17. Meyers, J.H., *Marine vadose beach rock cementation by cryptocrystalline magnesian calcite - Maui, Hawaii* J Sediment Petrol, 1987. 57: p. 558-570.
18. Dickinson, W.R., *Holocene sea level record on Funafuti and potential impact of global warming on Central Pacific atolls.* Quat Res, 1999. 51(181-189).
19. Khan, M., T. Danjo, and S. Kawasaki, *Artificial beach rock formation through sand solidification towards inhibition of coastal erosion in Bangladesh.* International Journal of Geomaterials, 2015. 9: p. 1528-1533.

20. Vousdoukas, M.I., A.F. Velegrakis, and T.A. Plomaritis, *Beachrock occurrence, characteristics, formation mechanisms and impacts.* Earth-Science Reviews, 2007. 85(1): p. 23-46.
21. Fortin, D. and S. Langley, *Formation and occurrence of biogenic iron-rich minerals.* Earth Sci Rev, 2005. 72(1): p. 1-19.
22. Dhami, N.K., A. Mukherjee, and E.L.J. Watkin, *Microbial diversity and mineralogical-mechanical properties of calcitic cave speleothems in natural and in vitro biomineralization conditions.* Front Microbiol, 2018. 9.
23. Shannon Stocks-Fischer, Johnna K. Galinat, and S.S. Bang, *Microbiological precipitation of CaCO3.* Soil Biology and Biochemistry, 1999. 31: p. 1563-1571.
24. Dhami, N.K., M.S. Reddy, and A. Mukherjee, *Biomineralization of calcium carbonate polymorphs by the bacterial strains isolated from calcareous sites.* J Microbiol Biotechnol, 2013. 23(5): p. 707-714.
25. Scoffin, T.P. and D.R. Stoddart, *Beachrock and intertidal cements.* Chemical sediments and geomorphology, 1983: p. 401-425.
26. Banerjee, S. and S.R. Joshi, *Ultrastructural analysis of calcite crystal patterns formed by biofilm bacteria associated with cave speleothems.* J Microsc Ultrastruct, 2014. 2(4): p. 217-223.
27. Adetutu, E., et al., *Bacterial community survey of sediments at Naracoorte Caves, Australia.* Int J Speleol, 2012. 41(2): p. 137-147.
28. Dhami, N.K., et al., *Bacterial community dynamics and biocement formation during stimulation and augmentation: implications for soil consolidation.* Front Microbiol, 2017. 8: p. 1267.
29. Williams, A.T., et al., *The management of coastal erosion.* Ocean & Coastal Management, 2018. 156: p. 4-20.
30. Dhami, N.K., A. Mukherjee, and M.S. Reddy, *Micrographical, minerological and nano-mechanical characterisation of microbial carbonates from urease and carbonic anhydrase producing bacteria.* Ecol Eng, 2016. 94: p. 443-454.
31. Porter, H., N.K. Dhami, and A. Mukherjee, *Synergistic chemical and microbial cementation for stabilization of aggregates.* Cem Concr Compos, 2017. 83: p. 160-170.

32. Presser, V., et al., *Determination of the elastic modulus of highly porous samples by nanoindentation: a case study on sea urchin spines.* J Mater Sci, 2010. 45(9): p. 2408-2418.
33. Zamiri, A. and S. De, *Mechanical properties of hydroxyapatite single crystals from nanoindentation data.* Journal of the Mechanical Behavior of Biomedical Materials, 2011. 4(2): p. 146-152.
34. Calvaresi, M., et al., *Morphological and mechanical characterization of composite calcite/SWCNT-COOH single crystals.* Nanoscale, 2013. 5(15): p. 6944-6949.
35. Ren, D., et al., *Comparative study of carp otolith hardness: Lapillus and asteriscus.* Mater Sci Eng C Mater Biol Appl, 2013. 33(4): p. 1876-1881.
36. Zhu, W., et al., *Nanoindentation mapping of mechanical properties of cement paste and natural rocks.* Materials Characterization, 2007. 58(11-12): p. 1189-1198.
37. Porter, H., N.K. Dhami, and A. Mukherjee, *Sustainable road bases with microbial precipitation.* Proceedings of the Institution of Civil Engineers - Construction Materials, 2018. 171(3): p. 95-108.
38. Rusznyak, A., et al., *Calcite biomineralization by bacterial isolates from the recently discovered pristine karstic herrenberg cave.* Appl Environ Microbiol, 2012. 78(4): p. 1157-67.
39. Berges, J.A., D.J. Franklin, and P.J. Harrison, *Evolution of an artificial sea water medium: Improvements in enriched seawater, artificial water over the last two decades.* J Phycol, 2001. 37(6): p. 1138-1145.
40. Zamarreno, D.V., R. Inkpen, and E. May, *Carbonate crystals precipitated by freshwater bacteria and their use as a limestone consolidant.* Appl Environ Microbiol, 2009. 75(18): p. 5981-90.
41. Raybaud, V., et al., *Computing the carbonate chemistry of the coral calcifying medium and its response to ocean acidification.* J Theor Biol, 2017. 424: p. 26-36.
42. Takeshita, Y., et al., *Coral reef carbonate chemistry variability at different functional scales.* Frontiers in Marine Science, 2018. 5(175).

43. Albright, R., C. Langdon, and K.R.N. Anthony, *Dynamics of seawater carbonate chemistry, production, and calcification of a coral reef flat, central Great Barrier Reef.* Biogeosciences, 2013. 10: p. 6747–6758.
44. Kooli, W.M., et al., *Bacterial iron reduction and biogenic mineral formation for the stabilisation of corroded iron objects.* Sci Rep, 2018. 8(1): p. 764.
45. Honeyands, T., et al., *Comparison of the mineralogy of iron ore sinters using a range of techniques.* Minerals, 2019. 9(6).
46. Jubb, A.M. and H.C. Allen, *Vibrational spectroscopic characterization of hematite, maghemite, and magnetite thin films produced by vapor deposition.* ACS Appl Mater Interfaces, 2010. 2(10): p. 2804-2812.
47. Zeng, Z. and M.M. Tice, *Promotion and nucleation of carbonate precipitation during microbial iron reduction.* Geobiology, 2014. 12(4): p. 362-71.
48. Müller, W.E.G., et al., *The sponge silicatein-interacting protein silintaphin-2 blocks calcite formation of calcareous sponge spicules at the vaterite stage. .* RSC Adv, 2014. 4: p. 2577-2585.
49. Chicot, D., et al., *Mechanical properties of magnetite (Fe3O4), hematite (α-Fe2O3) and goethite (α-FeO·OH) by instrumented indentation and molecular dynamics analysis.* Mater Chem Phys, 2011. 129(3): p. 862-870.
50. Aramendia, J., et al., *Multianalytical approach to study the dissolution process of weathering steel: The role of urban pollution.* Corros Sci, 2013. 76: p. 154-162.
51. Dhami, N.K., *Biomineralization of Calcium Carbonate Polymorphs by the Bacterial Strains Isolated from Calcareous Sites.* Journal of Microbiology and Biotechnology, 2013. 23(5): p. 707-714.
52. Strasser, A. and P. Bernier, *Early diagenetic ferruginous cementation in the intertidal zone: example from Noirmoutier Island, France.* Oceanologica Acta, 1988. 11: p. 353-357.
53. Strobel, R. and S.E. Pratsinis, *Direct synthesis of maghemite, magnetite and wustite nanoparticles by flame spray pyrolysis.* Advanced Powder Technology, 2009. 20(2): p. 190-194.
54. de Faria, D.L.A. and F.N. Lopes, *Heated goethite and natural hematite: can Raman spectroscopy be used to differentiate them?* Vib Spectrosc, 2007. 45(2): p. 117-121.

55. Shen, J.-W., et al., *Holocene coquina beachrock from Haishan Island, east coast of Guangdong Province, China.* Quaternary International, 2013. 310: p. 199-212.
56. Rodriguez-Navarro, C., et al., *Influence of substrate mineralogy on bacterial mineralization of calcium carbonate: implications for stone conservation.* Appl Environ Microbiol, 2012. 78(11): p. 4017-29.
57. Cook, D.C., *Spectroscopic identification of protective and non-protective corrosion coatings on steel structures in marine environments.* Corros Sci, 2005. 47: p. 2550-2570.
58. Jianwei, W. and B. Udo, *Structure and carbonate orientation of vaterite ($CaCO_3$).* Am Mineral, 2009. 94: p. 380–386.
59. Ercole, E.C., et al., *Calcium carbonate mineralization: involvement of extracellular polymeric materials isolated from calcifying bacteria.* . Microsc Microanal, 2012. 18: p. 829-39.
60. Sanchez-Roman, M., et al., *Nucleation of Fe-rich phosphates and carbonates on microbial cells and exopolymeric substances.* Front Microbiol, 2015. 6: p. 1024.
61. Hedrich, S., M. Schlömann, and D.B. Johnson, *The iron-oxidizing proteobacteria.* Microbiology, 2011. 157(6): p. 1551-1564.
62. Kato, S., et al., *Functional gene analysis of freshwater iron-rich flocs at circumneutral pH and isolation of a stalk-forming microaerophilic iron-oxidizing bacterium.* Appl Environ Microbiol, 2013. 79(17): p. 5283-90.
63. Emerson, D., Fleming EJ, and M. JM, *Iron-oxidizing bacteria: an environmental and genomic perspective.* Annu Rev Microbiol, 2010. 64: p. 561-583.
64. García G, M., M.A. Márquez G, and C.X. Moreno H, *Characterization of bacterial diversity associated with calcareous deposits and drip-waters, and isolation of calcifying bacteria from two Colombian mines.* Microbiol Res, 2016. 182: p. 21-30.
65. Glaring, M.A., et al., *Microbial diversity in a permanently cold and alkaline environment in Greenland.* PLoS One, 2015. 10(4): p. e0124863.

Chapter 4: Multi-Scale Study of Soil Stabilization Using Bacterial Biopolymers

4.1 Abstract

Conventional methods of soil stabilization employing materials such as lime or cement have considerable environmental penalty due to their high embodied energy. Alternatives such as biopolymers can alleviate this problem significantly. This paper is the first attempt to reveal the basic mechanism of stabilizing sand using bacterial biopolymer by conducting investigations spanning from microscopic to macroscopic scales. Xanthan gum, a bacterial biopolymer, has been microscopically characterised both as a stand-alone binder and with varying proportions of clay reinforcement. Sand columns have been produced using Xanthan gum as the binder with varying quantities of clay. The biopolymer stabilized samples were characterised for strength and water absorption. Although Xanthan gum was able to bind the sand, exposure to moisture considerably affected its strength. Addition of clay significantly improved the performance by reinforcing the polymer. The mechanism of stabilization has been revealed through advanced microscopic investigations using scanning electron microscopy, nanoindentation and atomic force microscopy. The study reveals the potential of bacterial polymerisation as a means of sustainable soil stabilization.

Keywords: Soil stabilization, biopolymers, mechanical properties, water absorption, and clay reinforced biopolymer.

4.2 Introduction

As the footprint of built facilities spreads, building on soil that requires treatment for improvement of its properties has become more commonplace. Mechanical modification of soil, including soil replacement [1], compaction [2], vacuum preloading [3] and piling [4] are constrained by factors such as availability and cost. As a result, chemical soil stabilizers such as cement [5-7], lime [8, 9] have become popular. However, such stabilisation is unsustainable because of high greenhouse gas emission, leaching of chemicals into the groundwater and affecting natural lifeforms. In Australia, typical energy consumption rates for cement stabilised materials have been estimated to be approximately 5,000 mJ/tonne while the actual placement and construction of the stabilised road base is estimated to consume only 50 mJ/tonne [10]. Industrial by-products such as fly ash [11, 12], cement kiln dust [13], blast furnace slag [14], red mud and silica fumes [11] have been mixed to improve the soil properties

[15]. However, shortcomings such as brittle behaviour [16], leaching out of toxic trace elements [17, 18] and above all, lack of availability have limited their use. A sustainable soil stabilizer is essential for a country like Australia that has the highest length of roads per capita.

Inspired by natural formations such as beach rocks [19, 20], stromatolites [21] and formation of corals [22], researchers have attempted to devise sustainable soil improvement from bio-based stabilizers. In beach rocks, microbes influence the cementation of sand in a two-stage process: 1) formation of biofilms covering grain surface, and 2) precipitation of metallic carbonates [23, 24]. This process is witnessed in a wide range of soil stabilization experiments [25]. In nature, it is observed that biopolymers play a crucial role in trapping and stabilizing sediments, thereby increasing the resistance to erosion [26, 27]. However, it has been reported that the hydrated nature of the biopolymers results in the collapse of the structure upon dehydration [24, 28] limiting their applications in fluctuating moisture conditions. The collapse in structure is because the biopolymer adopts a 'closed' structure in order to prevent further moisture loss [29].

Soil stabilization with carbonate precipitation is a well-researched area [25, 30-32]. It can improve soil properties such as stiffness, resistance to water absorption and strength [10, 33, 34]. However, the role of biopolymers has remained relatively unexplored. Biopolymers have the potential to overcome certain limitations of this technology, including the lack of resilience of the cement and harmful by-products. The biopolymer can be deposited within the soil through bacterial metabolism, or manufactured biopolymers can be mixed with soil. Both methods have been explored by researchers in laboratory-scale studies [35, 36]. The Potential of Gellan gum for temporary or medium-term soil stabilization applications has been investigated [37, 38]. Biopolymers such as Guar gum [39-41], Agar gum [42, 43], β-1,3/1,6-glucan [44], Chitosan [45], Casein and sodium caseinate [46], Alginate [47] and Lignosulfonate (LS) have been reported to be promising in improving the mechanical properties of soil. Xanthan gum has been found to be effective for the stabilization of soils varying from sand to clay in several studies [36, 40-42, 48]. A low percentage of Xanthan gum biopolymer (1-3%) was adopted to improve the properties of deficient plasticity clays which were otherwise considered unsuitable for subbase and subgrade construction [49]. Xanthan gum also proved to be effective in the stabilization of mine tailings by

displaying an increase in liquid limit and undrained shear strength making it suitable for stabilization as well as dust suppression applications [35, 50]. Although there is anecdotal evidence of its efficacy, a deeper understanding of the mechanism of soil stabilization with biopolymers is elusive.

Soil with traditional stabilizers has been widely tested for Unconfined Compressive Strength (UCS) [51], resistance to water absorption [52] and some extent, microscopic analysis [53]. Nanoindentation technique has been attempted to reveal mechanical properties at the microscopic scale [54, 55]. More recently, Peak Force Quantitative Nanomechanical Mapping (PeakForce-QNM) in AFM, has been used to obtain the local nanomechanical properties of soft materials such as polymers [56, 57]. This technique can be immensely useful in unravelling the basic mechanisms of biopolymeric cementation with clay reinforcements. Spatial variations due to the heterogeneity induced in the microstructure by the clay particles could be observed [58].

The objective of the study was to reveal the basic mechanism behind the stabilization of sand-clay mixtures using bacterial biopolymer (xanthan gum) by conducting investigations spanning from microscopic to macroscopic scales. The efficacy of bacterial biopolymer, Xanthan gum was explored both as a stand-alone binder for sandy soils and with varying proportions of clay reinforcement. This paper investigates the properties of Xanthan gum stabilized sand and clay mixtures and explains the mechanism of stabilization using a range of microscopic studies that are hitherto unreported. Along with macroscopic tests such as UCS and water absorption, microscopic investigations have been performed. A rigorous microstructural investigation has been performed in this paper for the first time. Scanning electron microscopy has been undertaken to understand the attachment of the polymer to the sand visually. Then nanomechanical properties have been determined at two scales: nanoindentation and atomic force microscopy. In nanoindentation, the hardness and modulus of the clay reinforced biopolymer at 100 μm scale have been determined. The paper demonstrates the seminal effect of clay in reinforcing the biopolymer. Through AFM, we were able to observe the interaction of clay particles with biopolymer 1μm scale. Our investigation also elucidates the effect of moisture absorption on clay particles in the biopolymer. Through modulus mapping at 1μm scale, it was possible

to understand the weakening of the bond between slay and biopolymer due to moisture attack.

4.3 Experimental investigation

Sand with varying clay content (0-10%) was stabilized by commercially available biopolymer Xanthan gum. The biopolymer stabilized samples were subjected to macro and micro-scale testing by Unconfined Compressive Strength (UCS) testing, Digital Image Correlation (DIC), water absorption, and micrographic analysis using Scanning Electron Microscopy (SEM), nanoindentation and PeakForce-QNM. The schematic of the experimental workflow is shown in Fig 4.1.

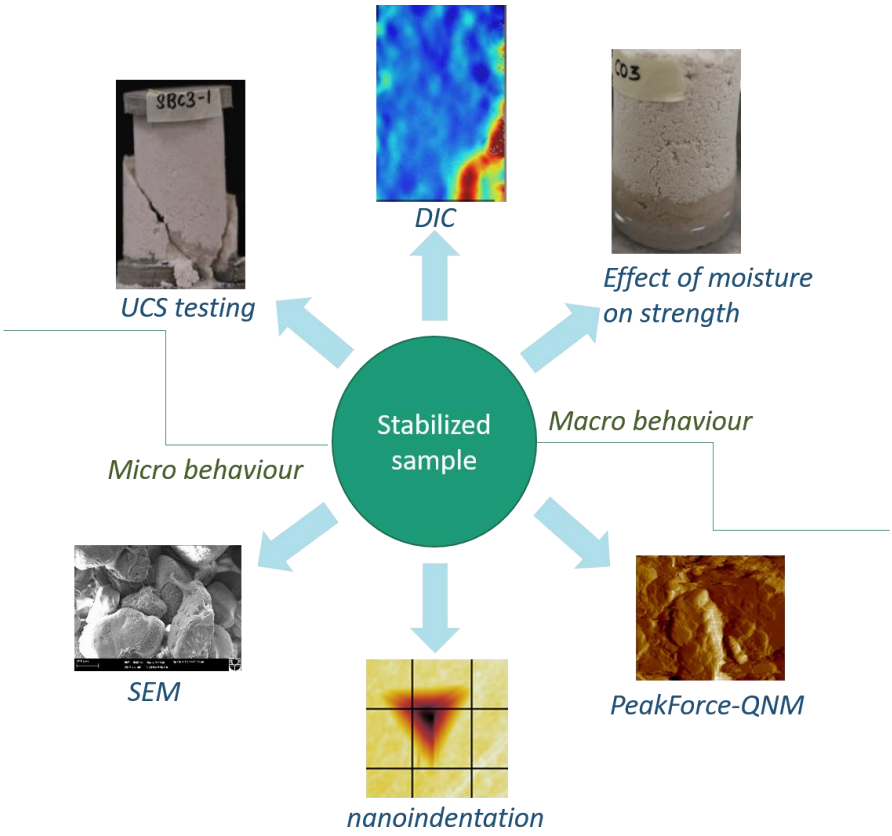

Fig 4. 1 Schematic of the present experimental investigation

4.4 Materials and methods

4.4.1 Materials

The manufactured sand used for the present study was supplied by Cook Industrial Minerals, Western Australia. The sieve analysis of the sand revealed that its particle size varied between 0.45 mm and 0.075 mm (Fig 4.2). Kaolin clay was chosen since positively charged edges of kaolinite plates was known to attach to the straight chains

of Xanthan gum, leading to the layered platy fabric. The particle size distribution (Fig 4.2) as well as the chemical composition of the clay supplied by Sibelco, Australia, are listed in Table 4.1. High tensile strength Xanthan gum biopolymer formed via the fermentation of glucose or sucrose using the bacterium *Xanthomonas campestri* [59] was used as the commercial biopolymer for the study. It was sourced from Sigma Aldrich, NSW, Australia.

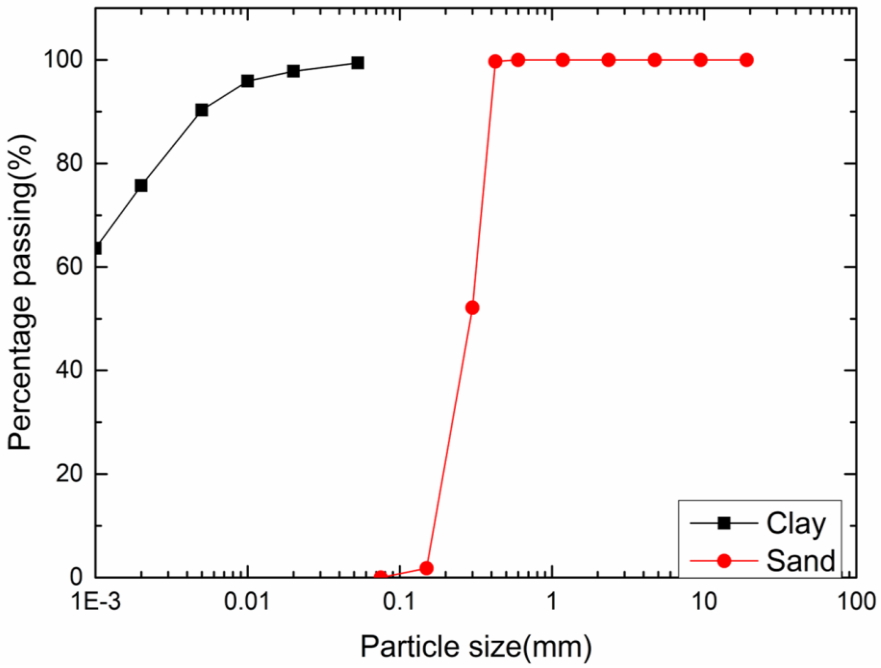

Fig 4. 2 Particle size distribution of the manufactured sand

Table 4. 1 Particle size distribution and chemical composition of clay

Particle size (µm)	**Percentage passing (% weight)**
53	99.4
20	97.8
10	95.9
5	90.3
2	75.7
1	63.6
Chemical analysis	**Composition (% Weight) ***
SiO_2	46.7
Al_2O_3	36.1

TiO_2	0.8	2694
Fe_2O_3	0.9	2695
CaO	0.7	2696
MgO	0.4	
K_2O	0.4	2697
Na_2O	0.1	2698

2699 *****(as provided by the supplier)

2700 **4.4.2 Preparation of cylinder specimens**

2701 The compaction characteristics of the Xanthan gum soil mixture with varying clay
2702 content (0%, 3%, 5%, 7% and 10%) were obtained using modified Proctor density
2703 testing according to Australian Standards [60]. Previous research has demonstrated
2704 that biopolymers can achieve up to 1.5 MPa strength at significantly lower
2705 concentrations, such as 0.5% dry weight of clayey soil [38, 61]. In order to study the
2706 effect of biopolymer content on strength, biopolymer dosage of 0.5%, 1% and 1.5%
2707 (dry weight of soil) specimens were also prepared. The biopolymer content was varied
2708 for sand samples containing 10% clay since an initial set of experiments revealed
2709 maximum performance. However, the general trend reveals that the effectiveness of
2710 stabilization is proportional to biopolymer dosage [61]. Thus, 0.5% of Xanthan gum
2711 was used. It was mixed with water as required for optimum moisture content. To
2712 prevent agglomeration, the mixing was done on a hot plate at 80^{o}C with continuous
2713 stirring as in [62]. The sand was thoroughly mixed with the prescribed percentage of
2714 clay using a spatula. The prescribed quantity of Xanthan gum solution was added and
2715 hand-mixed in a dough. Since the volume of soil used for testing was relatively small,
2716 uniform sand-clay mixtures could be obtained by hand mixing. The dough was placed
2717 in a cylindrical mould of 50 mm diameter and 100 mm height. The mould was filled
2718 in three layers and compacted to achieve the desired maximum dry density. Each layer
2719 was scarified before the addition of the next layer to ensure good bonding between the
2720 layers. Both ends of the samples were levelled to create an even surface. Furthermore,
2721 the ends were capped with cement to minimise uneven loading at the time of strength
2722 tests. A previous study has revealed that strength improvement was maximum under a
2723 curing temperature of 60^{o}C [44]. In comparison, another has used ambient conditions
2724 [35, 40]. In the present case, the samples were cured for a period of 7 days in an

incubator maintained at 60°C to allow hardening of Xanthan gum as in [46]. In order to investigate the effect of ambient curing on strength, samples containing 10% clay and varying biopolymer content (0.5%, 1% and 1.5%) were also cured at an ambient temperature of 30°C. Seven days of curing was maintained for all the samples for ease of comparison. Table 4.2 and 4.3 describes the mix proportion, nomenclature and corresponding properties of the samples. Control samples with just sand and sand mixed with 10% clay were prepared. The biopolymer concentration was kept fixed at 0.5% of the dry weight of soil, as mentioned previously. To investigate the effect of adding clay to the sand matrix, samples with varying clay content (0%, 3%, 5%, 7% and 10%) have been prepared. All samples required for macro-scale testing were prepared in triplicate to assess variation in results.

Table 4. 2 Designation for samples stabilized with commercial biopolymer

Name	**Biopolymer (%)**	**Clay (%)**	**MDD(g/cc)**	**OMC (%)**
S	0	0	1.60	9.6
SBC0	0.5	0	1.67	14.0
SBC3	0.5	3	1.69	13.9
SBC5	0.5	5	1.74	11.6
SBC7	0.5	7	1.75	11.4
SBC10	0.5	10	1.80	11.4
SC10	0	10	1.80	10.4

Table 4. 3 Designation for samples stabilized with varying biopolymer content and cured at varying temperatures.

Name	Biopolymer (%)	Clay (%)	Curing temperature (°C)
$SB_{0.5}C_{10}T_{am}$	0.5	10	Ambient temperature of 30°C
$SB_{0.5}C_{10}T_{60}$	0.5	10	60°C
$SB_{1}C_{10}T_{am}$	1.0	10	Ambient temperature of 30°C
$SB_{1}C_{10}T_{60}$	1.0	10	60°C
$SB_{1.5}C_{10}T_{am}$	1.5	10	Ambient temperature of 30°C
$SB_{1.5}C_{10}T_{60}$	1.5	10	60°C

4.5 Testing methods

4.5.1 Unconfined compressive strength (UCS)

After the curing period, the samples were subjected to UCS testing according to Australian Standards on a universal testing machine (Shimadzu AGS-X) of 10kN capacity [63]. The specimen was compressed at a constant displacement of 1mm/min until failure. The corresponding stress-strain graphs were plotted for each sample. From the graphs, secant modulus of elasticity (E_{50}) and unconfined compressive strength was obtained.

4.5.2 Digital Image correlation

Optical characterization of surface deformation of the stabilized samples was conducted using Digital Image Correlation (DIC). DIC was used to track patterns on the deforming sample surface and correlate them to strain measurements [10, 64]. At the time of UCS, a digital camera was placed securely in front of the samples to record a video of the sample during loading. Open source DIC Matlab software (NCorr) was used to obtain displacement and strain at a regular interval.

4.5.3 Water absorption test

Resistance to water absorption was determined according to Australian Standards [65]. The dry mass of the sample was recorded, and then the sample was immersed in standing water of 1 cm height. The intake of water by the specimen was monitored continuously for a period of 24 hours.

4.5.4 Scanning Electron Microscopy (SEM)

A small portion of the specimen was taken for microstructural analysis by employing SEM (Scanning Electron Microscopy). The samples were mounted on aluminium stubs and sputtered with 10 nm thick platinum coating to provide conductivity through the sample. A Zeiss Neon 40 EsB dual beam FESEM (Field Emission Scanning Electron Microscope) was employed for imaging at 15 kV and aperture size of 60µm. For imaging, the wet samples, Tescan Mira3 VP-FESEM with Oxford Instruments X-Max 150 SDD X-ray detector, NordlysNano EBSD detector and AZtec software (Tescan, Czech Republic) was used to minimize sample disturbance.

4.5.5 Nanoindentation and PeakForce-QNM

4.5.5.1 Sample preparation for micro testing

The interaction of clay with the biopolymer was investigated microscopically. For this purpose, samples were prepared with the same ratio of biopolymer and clay as in sample SBC10. The sand was not added to the sample, as the objective was to study the micro and nano-scale properties of the stabilizer alone, which was the clay-reinforced biopolymer. The biopolymer and clay solution were mixed thoroughly using a magnetic stirrer and left to harden in a drying oven maintained at 60^{o}C for a period of 7 days. A portion of the dried sample was taken for sample preparation for nanoindentation and PeakForce-QNM testing.

For preparing the samples, the hardened clay-reinforced biopolymer was placed in moulds, and epoxy resin (Epofix) was poured under vacuum (Struers Cito Vac) in order to impregnate the resin into the sample. The samples were impregnated into epoxy resin to ensure the stability of the samples during nano-indentation testing. The use of glue was eliminated completely by this method of sample preparation. The thickness of the sample measured approximately 5 mm. The final dimensions of the resin were 25 mm in diameter and 8 mm thickness. The samples were polished by using Stuers Tegramin-30 in steps as depicted in Table 4.4. Further, the sample surface was prepared by FIB milling using Technoorg Linda SEMPrep 2 to produce a sample with minimum surface roughness.

Table 4. 4 Details of sample polishing for the nanoindentation test.

Polishing step	Polishing cloth used	Lubricant	Time (min)
Step 1	Piano 220	Water	1
Step 2	Piano 1200	Water	2
Step 3	MD Chem	Colloidal silica (coarseness 0.04 micron)	2

4.5.5.2 Nanoindentation testing

Nanoindentation was carried out using a G200 nanoindenter (Agilent Technologies) fitted with a Berkovich shaped diamond tip (TB22130 XP CSM 23032018). The optical microscope attached to the nanoindenter was used at 40× magnification to choose the points of indentation. The tests were performed under the continuous

stiffness measurement (CSM) model with Testworks 4 version 4.10 (MTS System Corporation). While the traditional Oliver-Pharr [66] methodology measures the contact stiffness only at the point of unloading, the CSM technique allows measurement of contact stiffness at any point of the loading curve corresponding to any depth of penetration [67]. The maximum displacement was limited to 2000 nm and 25 indents were chosen on the sample with a spacing of 20 µm. All the indentation locations were carefully selected prior to testing to ensure that large pores or cavities were not encountered in the process. Poisson's ratio of the clay-biopolymer was taken as 0.49 [68, 69]. The calculations were performed with the aid of the software nanoTest Platform Four V.40.08 (Micro Materials Ltd).

4.5.5.3 PeakForce-QNM testing

PeakForce-QNM was employed to study the nanomechanical properties of the biopolymer at a high resolution. The instrument facilitated the mapping of elastic properties of the sample with a lateral resolution at a nanometer scale [70]. The indentation force applied to the sample is in the range of 5nN, and the depth of indentation is around 1nm, which is significantly lower as compared to the nanoindentation technique. Hence, PeakForce-QNM is suitable to determine the nanomechanical properties of soft materials as they operate at low forces and consequently, smaller deformations. This technique enabled us to understand the degradation mechanism of the clay-reinforced biopolymer on exposure to moisture. In PeakForce-QNM, the force curves were analysed at each pixel of the topographic image and the local elastic modulus was determined at each contact point using the Derjaguin-Muller-Toporov (DMT) model [71]. AFM imaging was performed using Bruker Dimension Icon AFM system with PeakForce-QNM mode under ambient conditions. MPP13120-10 probes were employed for the experiment (MPP13120-10 with spring constant 200 N/m). The imaging scan rate was maintained at 1Hz at a resolution of 256x256 pixels. The raw AFM topography images were further processed by using Bruker Nanoscope Analysis 1.9.

4.6 Results and discussion

4.6.1 Compaction characteristics

Fig 4.3 presents the compaction characteristics of sand at varying clay dosage, and the results were summarized in Fig 4.4. The Optimum Moisture Content (OMC) decreased

monotonically with an increase in clay content from 0 to 10%. At 10% clay, the OMC had reduced by 20% from the initial value at 0% clay. The Maximum Dry Density (γ_d) increased with the increase in clay dosage in a range of nearly 20%. The high OMC and low γ_d without the addition of clay are attributed to the highly viscous biopolymer with high swelling properties on exposure to water. Increase in clay content leads to two benefits: 1) more pores are filled with clay, and 2) formation of a clay-biopolymer composite. Evidently, although biopolymer content remained constant, the higher dosage of clay led to a higher γ_d. Hence, the superior performance was due to the combined pore filling as well as reinforcing effect with increased dosage of clay.

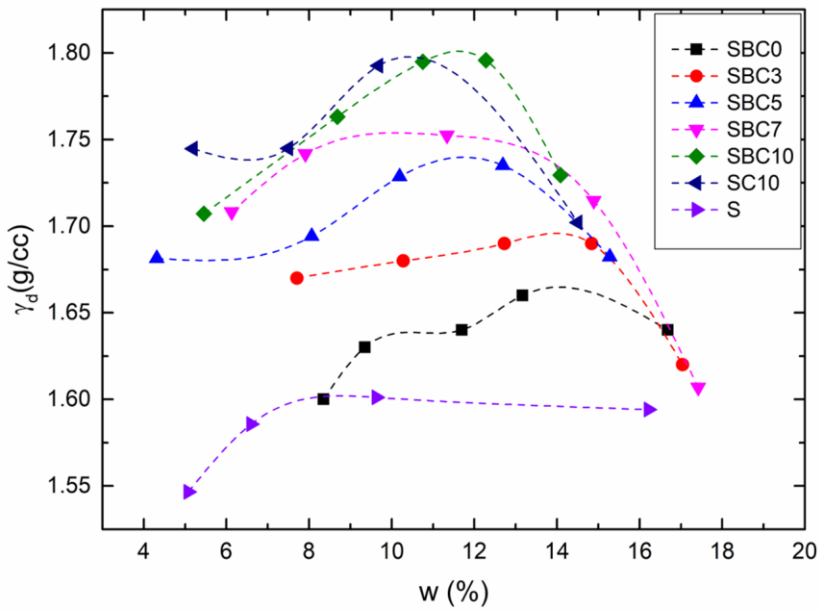

Fig 4. 3 Compaction curves of the samples

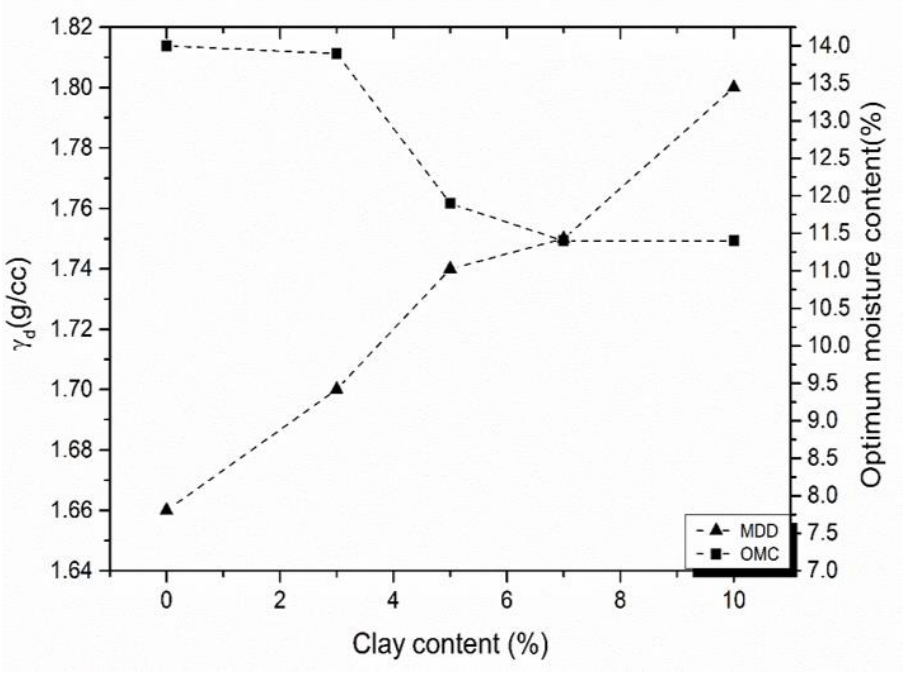

Fig 4. 4 The variation of γd and OMC with varying clay content

4.6.2 Performance of commercial biopolymer stabilized samples at macro-scale

4.6.2.1 Unconfined compressive strength (UCS) test

The average axial stress-strain plots recorded during the UCS test conducted on the stabilized columns until failure are plotted in Fig 4.5. The control sample, SC10, had the lowest strength of around 0.25 MPa. Clearly, clay alone is unable to stabilize the sand. SBC0 depicts that addition of biopolymer alone has caused a dramatic improvement in the strength, stiffness, and strain at failure of the material. Most remarkably, the strain at failure increased by 50%, showing that the biopolymer has developed cohesive bonds between sand particles. This demonstrates the ability of the biopolymer in stabilizing sand. Addition of clay particles further improved the strength and stiffness of the composite. Addition of clay was a key factor for the increase in performance of the biopolymer stabilized samples. The UCS and Secant moduli are shown in Fig 4.6. The un-stabilized sample (SC10) displayed the lowest UCS value of 0.17 MPa. The highest UCS value of 2.3 MPa was observed for the biopolymer stabilized sample (SBC10) with the highest clay content. In related research with gellan gum stabilized soil, [62] observe biopolymeric stabilisation is more effective in well-graded soil with a combination of coarse and fine particles as compared to pure sand. The strength of the biopolymer stabilized sand-clay mixture is a combination of two mechanisms viz. increase in cohesion due to the formation of clay reinforced

biopolymer (clay-biopolymer matrix) and increase in the friction angle of the soil due to higher particle contact area.

Strain at failure, on the other hand, remained around 1.5% with no appreciable change due to the addition of clay particles. This observation confirms the typical particulate-matrix composite behaviour; the high strength clay particle inclusions in the biopolymer matrix improve the stiffness and strength of the composite, but the strain capacity is governed by the polymer matrix. Although an increasing percentage of clay increasingly enhanced the strength of biopolymer stabilized granular soil, an anomaly was noticed in SBC3. It displayed a higher strength as compared to SBC5 and SBC7. The possible reason for this behaviour is discussed later in conjunction with the observed failure modes.

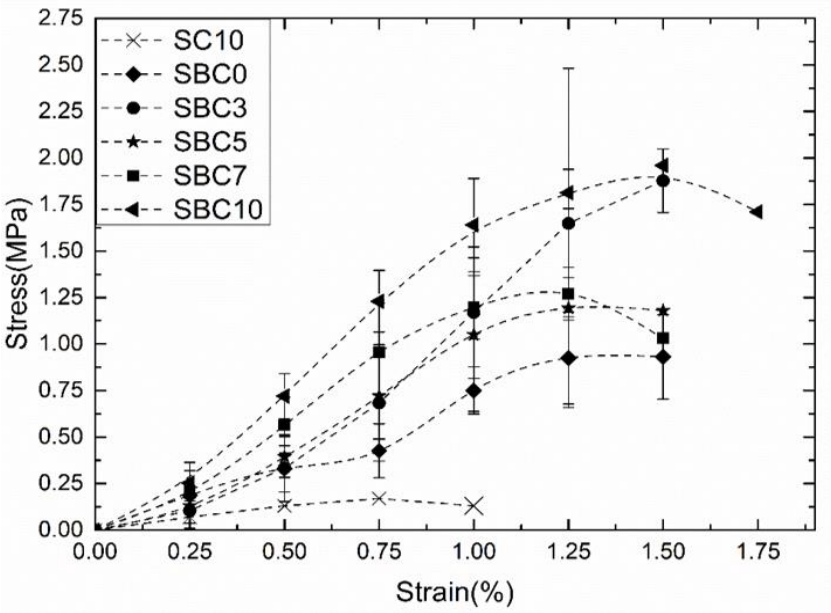

Fig 4. 5 Stress-strain behaviour of biopolymer stabilized samples with varying clay content

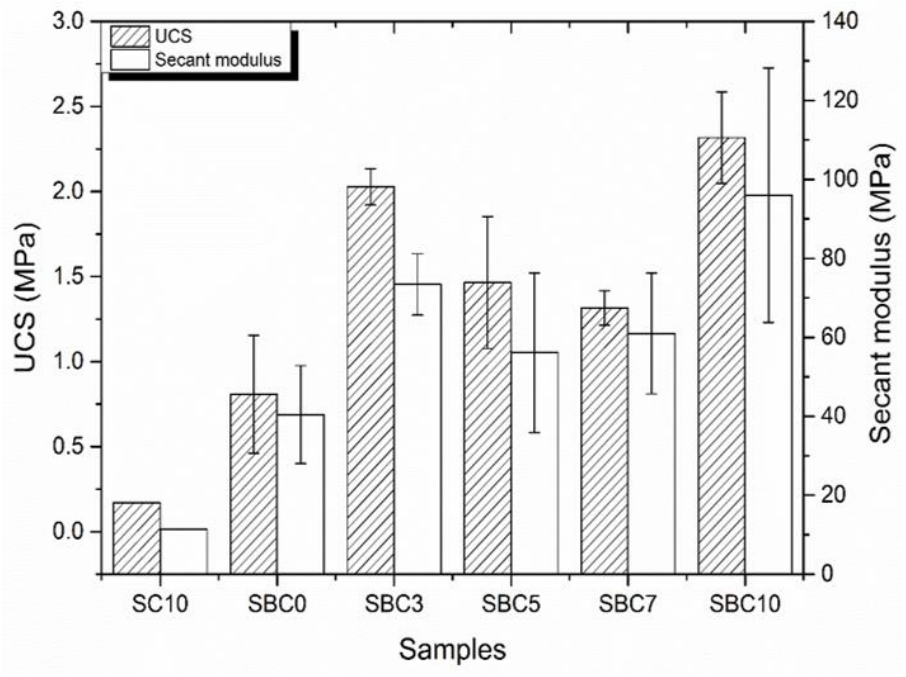

Fig 4. 6 UCS and secant modulus of the biopolymer stabilized samples with varying clay content

Fig 4.7 shows the stress-strain characteristics of the stabilized samples with varying biopolymer concentration and cured at 60^{o}C. They displayed similar behaviour. The samples with 1% biopolymer were marginally better in withstanding both stress and post-peak strain. As the dosage of biopolymer increases, workability of the mix is reduced, leaving internal voids in the sample. The UCS and Secant Moduli of the samples are shown in Fig 4.8. Sample $SB_1C_{10}T_{60}$ displayed the maximum UCS value, about 10% higher than that of $SB_{0.5}C_{10}T_{60.}$ The highest Secant modulus was achieved for sample $SB_{0.5}C_{10}T_{60}$. Thus, doubling the dosage of biopolymer from 0.5% did not result in a proportional gain in either strength or modulus.

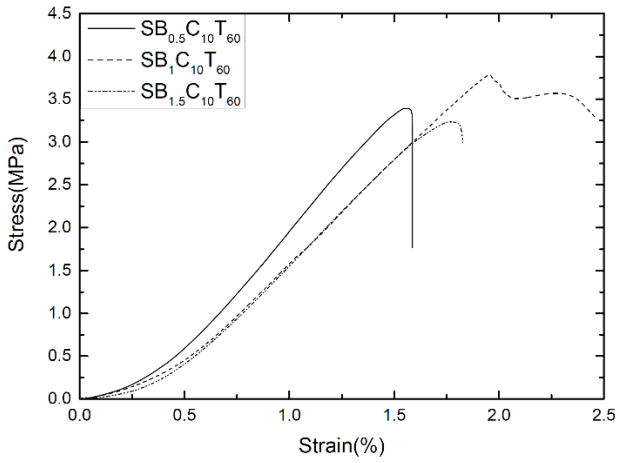

Fig 4. 7 Stress-strain characteristics of samples with varying biopolymer dosage cured at 60°C

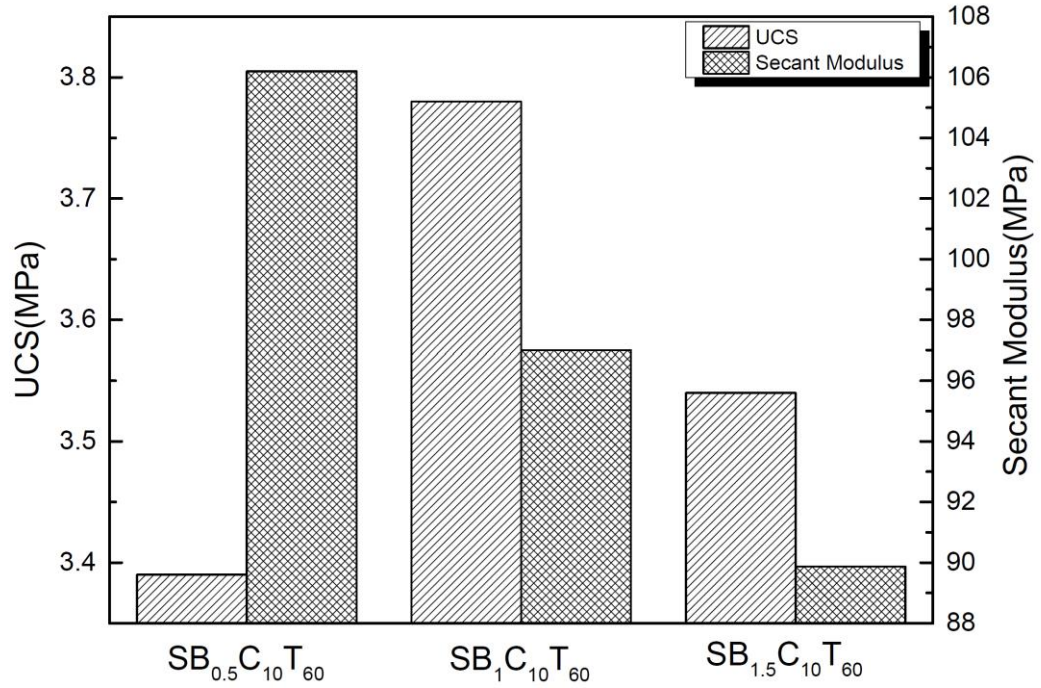

Fig 4. 8 UCS and secant moduli samples with varying biopolymer dosage cured at 60°C

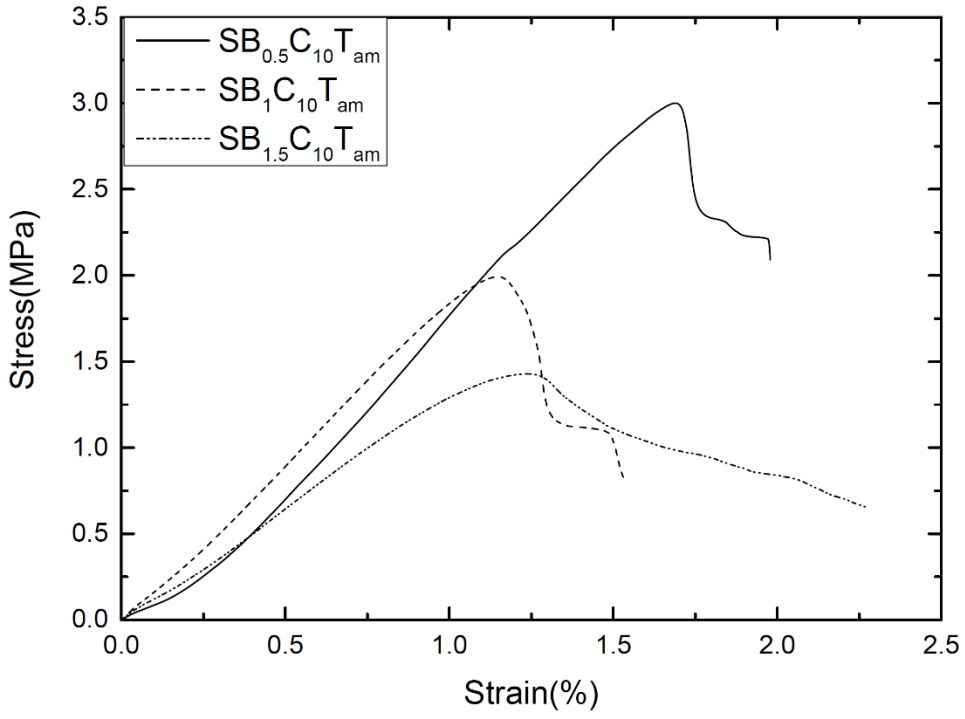

Fig 4. 9 Stress-strain characteristics of samples with varying biopolymer dosage cured at ambient temperature

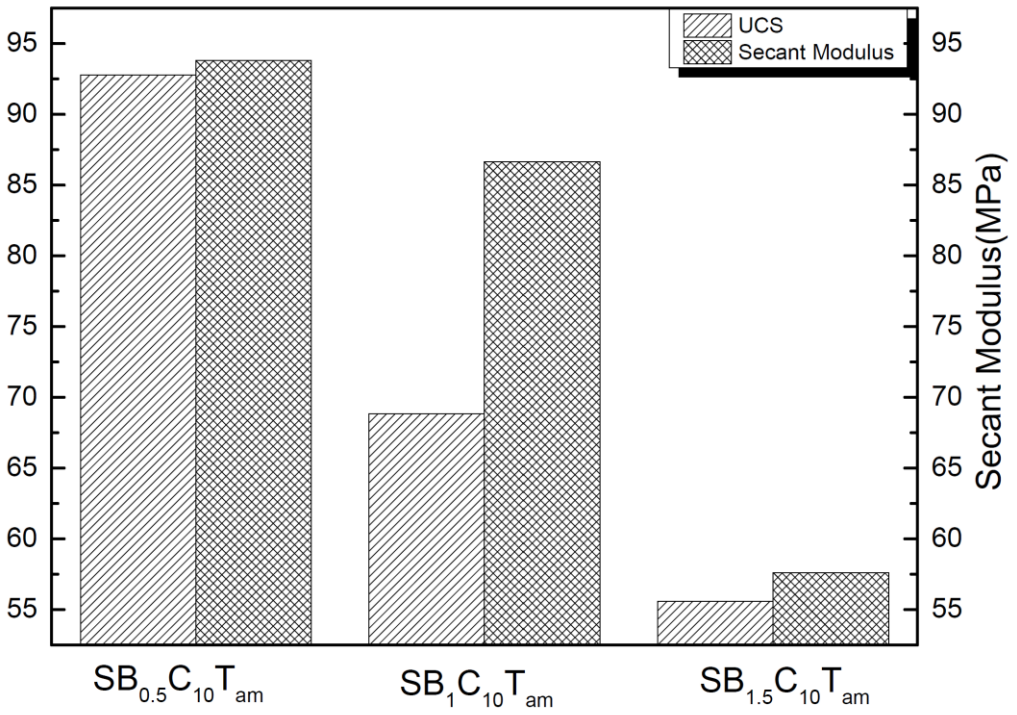

Fig 4. 10 UCS and secant moduli samples with varying biopolymer dosage cured at ambient temperature

Fig 4.10 shows the stress-strain characteristics of samples with varying biopolymer content cured at ambient temperature. $SB_{0.5}C_{10}T_{am}$ displayed the highest strength. With an increase in dosages, instead of an increase, a gradual reduction in strength was observed. Fig 4.11 shows the UCS and Secant moduli of the samples. Clearly, the samples have displayed gradually lower moduli as the dosage of biopolymer went up. The strength of a biopolymer-stabilized sample is highly dependent on its moisture content [62]. It may be noted that the rate of curing of biopolymer is slower at ambient temperature than at 60 ^{o}C. Moreover, the OMC was went up with biopolymer dosage. Thus, the initial moisture content of the samples grew with the increase in biopolymer dosage. Hence, the residual moisture content after the curing period is likely to be higher in the samples with higher biopolymer content, resulting in reduced strength. To sum up, at ambient temperature, curing of seven days may not be enough, especially when the dosage goes up. In case of samples cured at 60^{o}C, the higher temperature ensured lower residual moisture content and higher strength.

We compare the performance of $SB_{0.5}C_{10}T_{60}$ with that of $SB_{0.5}C_{10}T_{am}$ to get an idea of whether $SB_{0.5}C_{10}T_{am}$ had cured adequately. It can be seen that the UCS and moduli of the samples are comparable. Thus, it can be concluded that the samples with 0.5% biopolymer have cured in seven days. An opposite trend was observed for the samples with a higher biopolymer dosage. At 60^{o}C, both UCS and modulus went up with dosage, but at ambient temperature, they went down. This highlights the importance of taking the relationship between dosage, curing temperature and temperature into account. If a rapid strength gain at ambient temperature is desired, then the dosage of biopolymer must be kept as low as possible. For the rest of the investigation, the dosage of the biopolymer was fixed at 0.5%.

4.6.2.2 Damage progression and failure modes

During the UCS testing, the columns were observed for progression of damage and failure mode. They were monitored visually as well as through digital image correlation. Stabilized soil samples are known to have considerable variations in the mode of failure due to several factors:

1. As the material is very lightly cemented due to the low dosage of the biopolymer, it is susceptible to local defects.
2. They are susceptible to damage due to the time of handling and transportation.
3. The heads of the cylinders can be uneven, leading to local failure.

Local failure tends to under-predict the strain at failure and strength of the material. Notwithstanding all these factors, a general trend in the failure mode could be observed. Fig 4.11 shows the samples after failure. SBC0, SBC7 and SBC10 have had a part of the sample dislodged from the base. In case of SBC5, a chip off at the mid-height is noticed. All these failures have happened due to local damage while the rest of the column has remained largely intact. In the case of SBC3, on the other hand, a vertical split through the centre of the column is noticed. Clearly, this failure is global in nature. Thus, the sample exhibits higher strength than SBC 5 and SBC 7.

DIC analysis was performed to observe the strain build-up in local stress concentrations on the samples due to compressive loading. The vertical stresses occurring in the samples prior to failure are shown in Fig 4.12. The areas of higher stress concentration were clearly visible in the vertical strain images obtained by DIC.

These regions coincide with the development of cracks leading to the ultimate failure of the samples. Hence, DIC is a useful tool to gain insights into local stress concentrations during UCS testing.

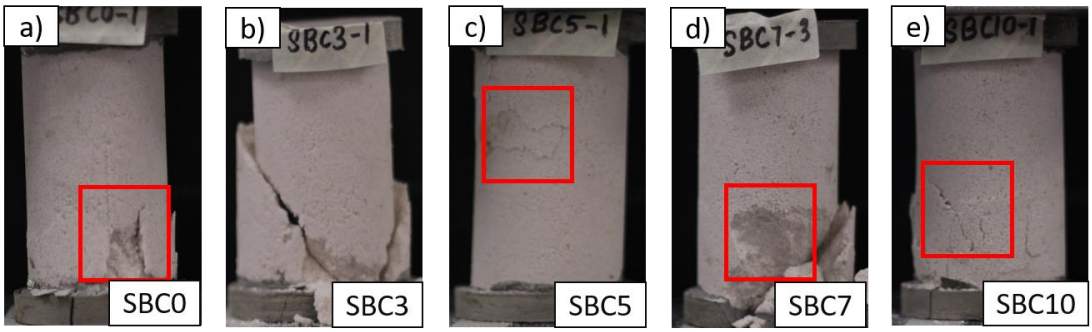

Fig 4. 11 Failure modes of the biopolymer stabilized samples

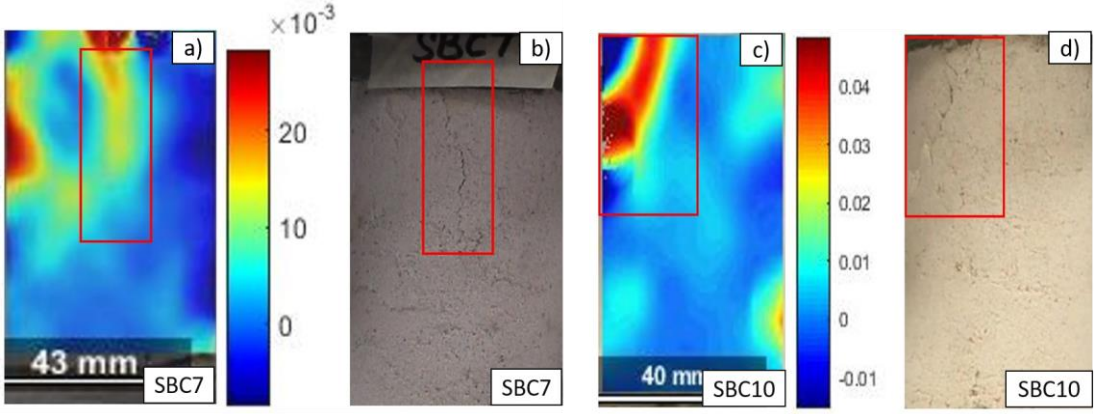

Fig 4. 12 Vertical strain in the samples prior to failure obtained by DIC analysis

4.6.2.3 Water absorption test

Moisture ingress is one of the major reasons for the reduction in strength of stabilized soils [32, 72]. Even though the swelling nature of biopolymer is well known, there have been limited attempts to quantify water absorption of the biopolymer stabilized soils. The rates of absorption of water by the columns as a percentage of their weight is shown in Fig 4.13. During the testing, sample SC10 failed immediately upon exposure to water. Thus, the plot for SC10 was not obtained. Sample SBC0 displayed swelling at the bottom of the column. The excess water led to the softening of the polymer. As a result, the bottom portion of the column was unable to withstand the weight of its top portion leading to collapse as observed in Fig 4.14. It is known that Xanthan gum has some degree of solubility in water [29, 73]. Thus, the polymer degrades considerably due to exposure to water.

Addition of clay considerably improved the water absorption tolerance of the columns due to the reinforcing effect on the biopolymer. In Fig 4.15, the columns with clay absorbed more water than samples without clay. The rate of absorption was also much faster. However, the absorption reached a steady state within a few minutes. All samples had a similar quantity of absorption. Among them, SBC10 displayed the lowest water absorption. The addition of clay has clearly altered the absorption characteristics of the composite. In the case of SBC0 sample, the rate of water absorption was the least. However, the sample failed at a lower absorption level as compared to the rest of the samples due to local swelling. In the remaining samples, we can see that the addition of clay does result in higher water absorption rate but helps in more uniform distribution of water within the sample. To sum up, even though the addition of clay does increase water absorption of the samples, it played a vital role in uniform moisture distribution within the sample, leading to structural integrity.

Fig 4.14 shows the samples after the water absorption test. Unlike SC10, all the columns could withstand the exposure to water. Thus, the addition of clay in biopolymer has a stabilizing effect against exposure to moisture when used in conjunction with biopolymer. This is not achieved by the clay alone, but due to the synergistic influence of adding clay to the biopolymer. Kaolinite clay is known to reinforce Xanthan gum due to the sorption occurring along its edges and surfaces, leading to a stronger structural composition [62]. The chemical bonding between the carboxylic acid (-COOH) of Xanthan gum and hydroxyl (-OH) of kaolinite via cation bridging and hydrogen bonding result in a highly stable structure [62]. Due to the addition of clay, the degradation of the polymer could be avoided, and the capillary action helped in evenly distributing the moisture leading to homogeneous water absorption of the sample and avoiding excessive softening (Fig 4.15). The capillary rise in the biopolymer stabilized samples with varying clay content can be visually observed from Fig 4.15. It is evident from the figure that the capillary rise for sample SBC0 is restricted within the bottom half of the sample. However, for samples SBC5, SBC7 and SBC10, the entire sample is saturated with water. To sum up, either clay or biopolymer alone is susceptible to excessive softening due to water absorption. Combination of clay and biopolymer, resulting in a more stable structure is highly effective in avoiding softening and collapse.

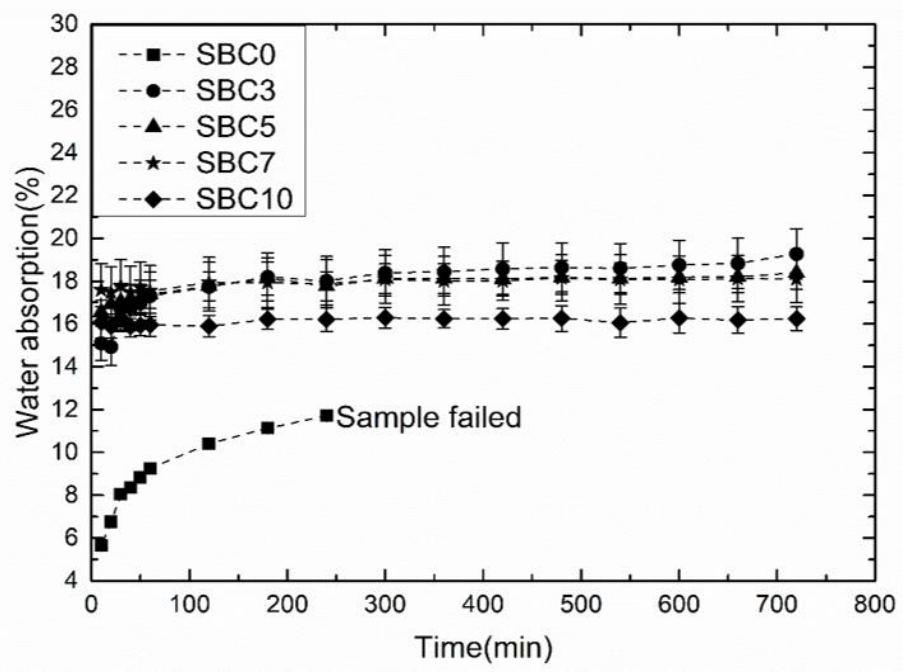

2995

2996 *Fig 4. 13 Water absorption of the stabilized samples with time*

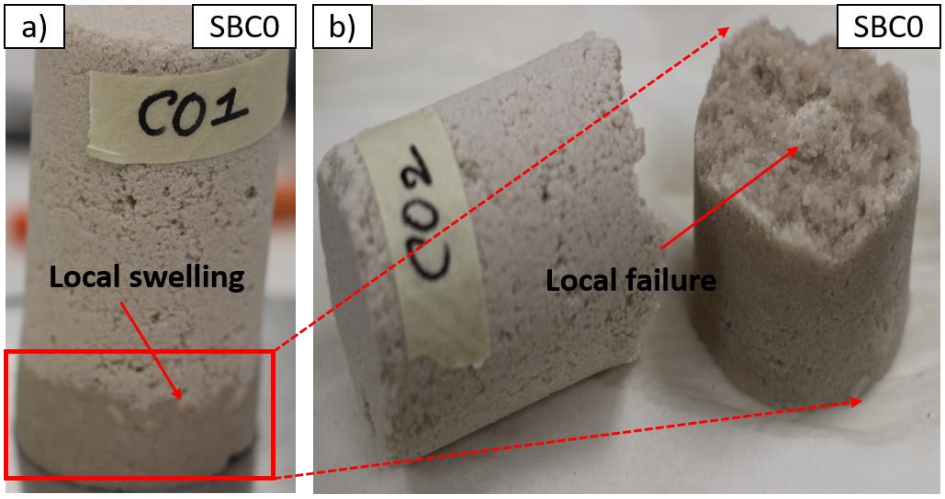

2997

2998 *Fig 4. 14 SBC0 sample failure due to local absorption of water*

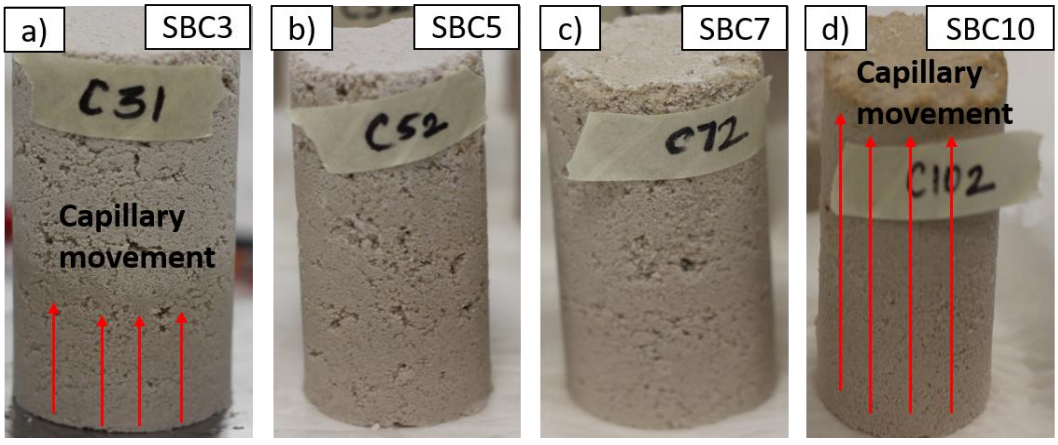

2999

Fig 4. 15 Samples with clay-reinforced biopolymer after water absorption test

4.6.2.4 Effect of moisture on strength

The degradation of strength of the columns due to exposure to water is measured. After the water absorption test, the columns were dried and subjected to the UCS test. The stress-strain graph (Fig 4.16) after exposure to moisture shows the reduction in stiffness and UCS values. The UCS and secant modulus of all samples reduced by more than 50% after a single cycle of wetting and drying (Fig 4.17 and 4.18). Similar observations were recorded during the cyclic wetting and drying of Gellan gum treated sand [37]. This study shows that the strength of biopolymer treated samples reduced significantly after being in contact with water which limits the application of biopolymers in water-saturated environments. Even though the UCS values reduced after the exposure to moisture, they were still substantially higher than the unstabilized sample SC10. Even though the UCS values decreased after the exposure to moisture, they were still significantly higher than the unstabilized sample SC10. The samples were able to regain 50% of the lost strength within 24 hours of drying, which was a promising aspect for practical implications.

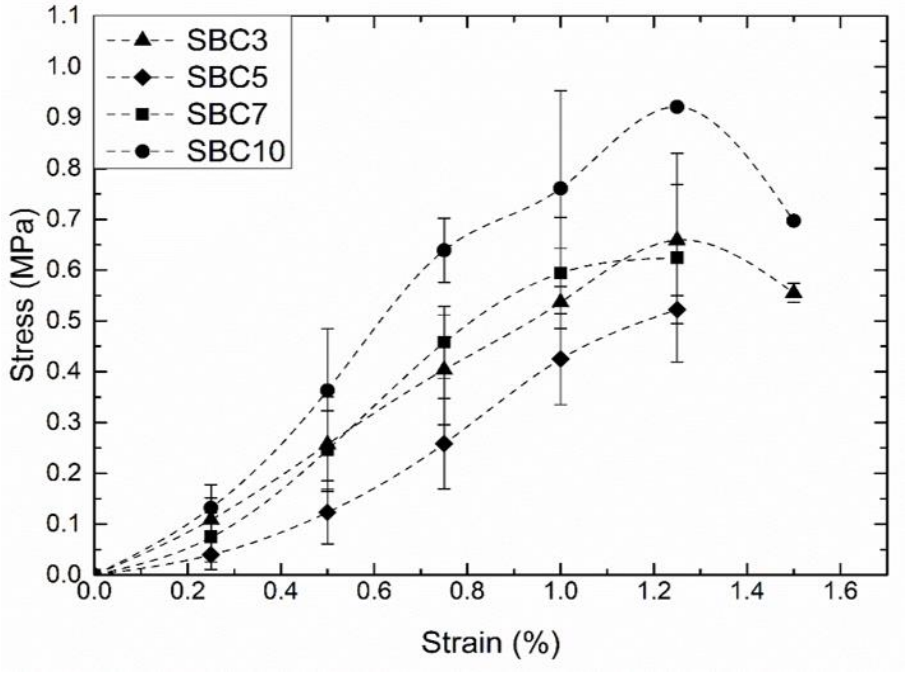

Fig 4. 16 Stress-strain behaviour of the biopolymer stabilized sample after exposure to moisture

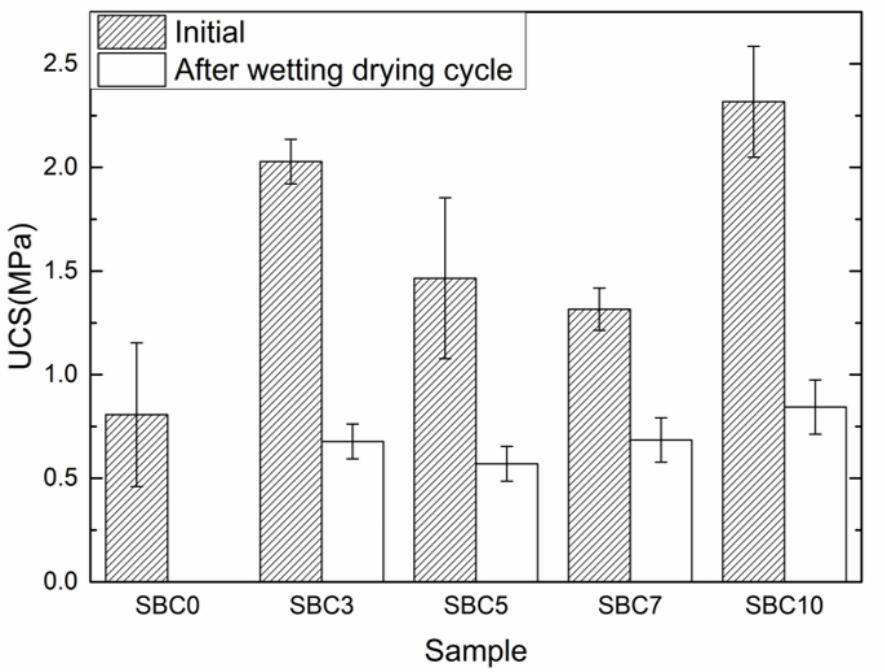

Fig 4. 17 UCS of the stabilized sample after exposure to moisture

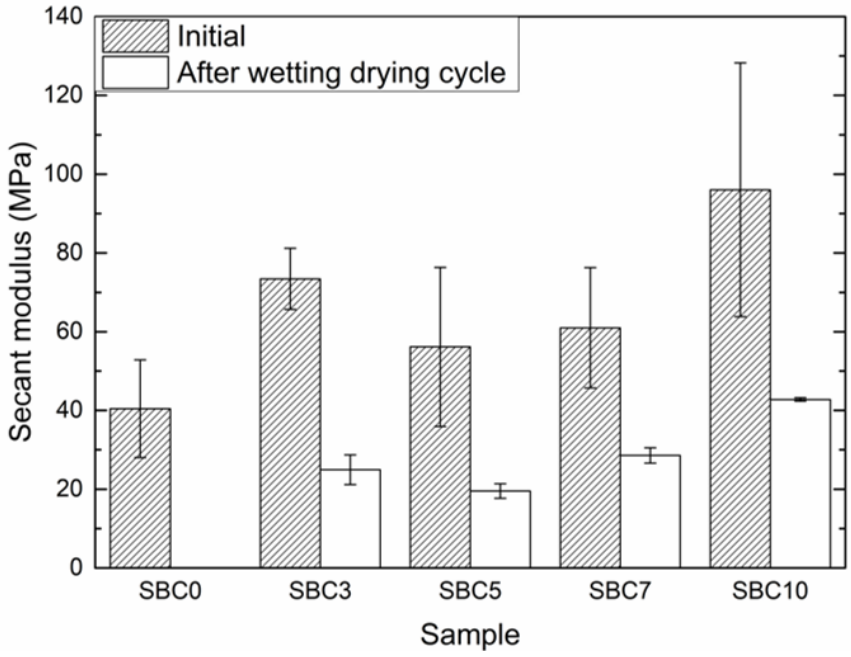

Fig 4. 18 Secant modulus of the stabilized samples after exposure to moisture

4.6.3 Micrographic analysis

The micrographic analysis was undertaken on the stabilized samples by SEM. The micrographs reveal the underlying mechanism of biopolymer stabilization at a micro-scale. Two different forms of biopolymer attachment were observed. Fig 4.19 a) shows a case where biopolymer fills the pore as a bulk. This can lead to non-uniform distribution of the biopolymer with some pores getting filled while others were not

having the polymer at all. Fig 4.19 b) shows a case where the biopolymer forms a thin sheet. In this case, the same amount of biopolymer is likely to bond a larger number of grains. Fig 4.19 c) illustrates the bridging of the grains by biopolymer. During loading, the biopolymer sheets between sand grains get stretched [Fig 4.19 d)] thereby providing cohesion among the grains. Hence, the biopolymer stabilized sand can withstand considerably higher strain at failure. It can be concluded that a highly stretchable biopolymer would be very well suited for soil stabilisation.

Next, we observe the microstructural changes due to the addition of clay by zooming in to the inner structure of the biopolymer. Fig 4.20 a) shows the clay particles embedded in the polymer. The embedment of clay particles reinforces the biopolymer both in fresh and cured phases. In the fresh phase, the clay reinforced biopolymer attains improved flow behaviour leading to the formation of sheets. Thus, a relatively more uniform distribution of the polymer is achieved. Fig 4.20 b) shows that in its cured phase, the biopolymer anchors down the clay particles, thereby arresting their movement and improving the reinforcement effect.

Fig 4.21 summarizes the mechanism of stabilisation. In the absence of clay particles, the biopolymer tends to form lumps within the pores of sand [Fig 4.21a)]. With the addition of clay particles, the biopolymer attains an improved flow behaviour resulting in sheet formation [Fig 4.21 b)]. The sheets attach with the sand grains and withstand higher strains before snapping improving the stabilisation effect. The clay particles reinforce the cured polymer leading to higher cohesion strength.

The SEM imaging on hydrated samples revealed the different structure of the biopolymer as observed in Fig 4.22. The hydrated biopolymer is more branched and open as compared to the dry state. The loss in strength of the samples after hydration could be explained with the help of Fig 4.22 a). The image reveals numerous broken biopolymer bonds leading to a loss in bridging between particles. Analysis of wet and dry biopolymer structure shows significant structural differences [Fig 4.22 b)]. It has been reported earlier than the hydrated nature of the biopolymers results in the collapse of the structure upon dehydration, leading to completely different mechanical properties in dry and hydrated states.

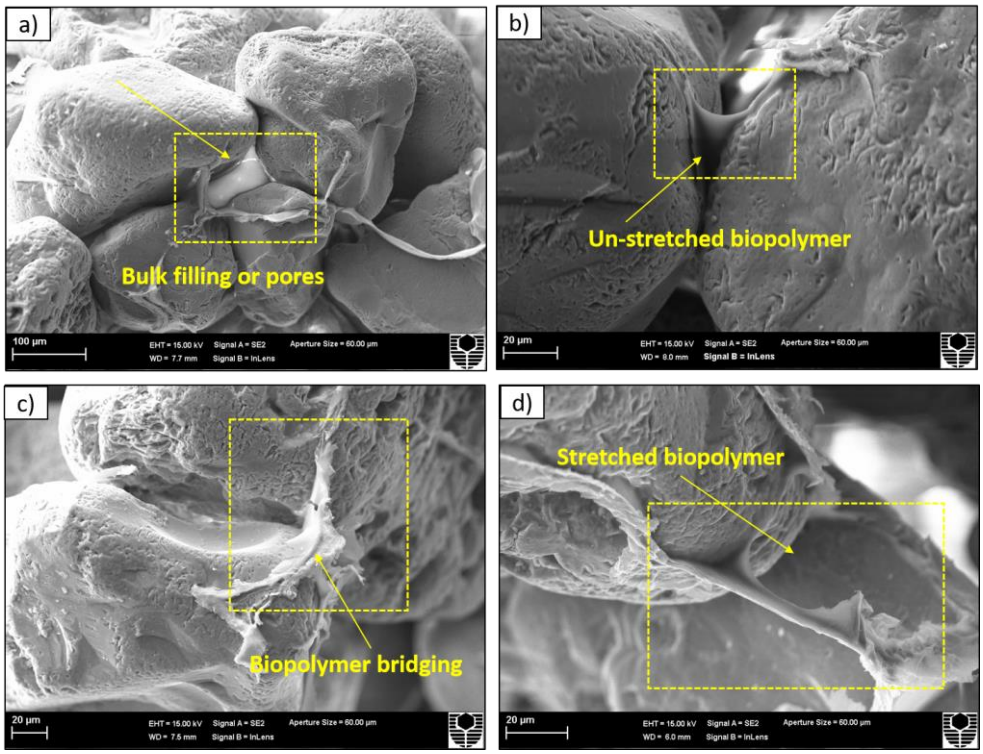

3059

3060 *Fig 4. 19 SEM micrographs of biopolymer stabilized sand samples (SBC0)*

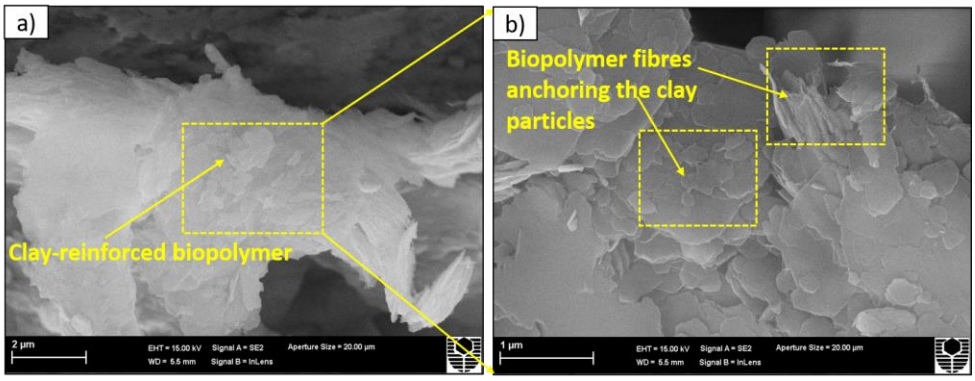

3061

3062 *Fig 4. 20 SEM micrographs of clay reinforced biopolymer sheets*

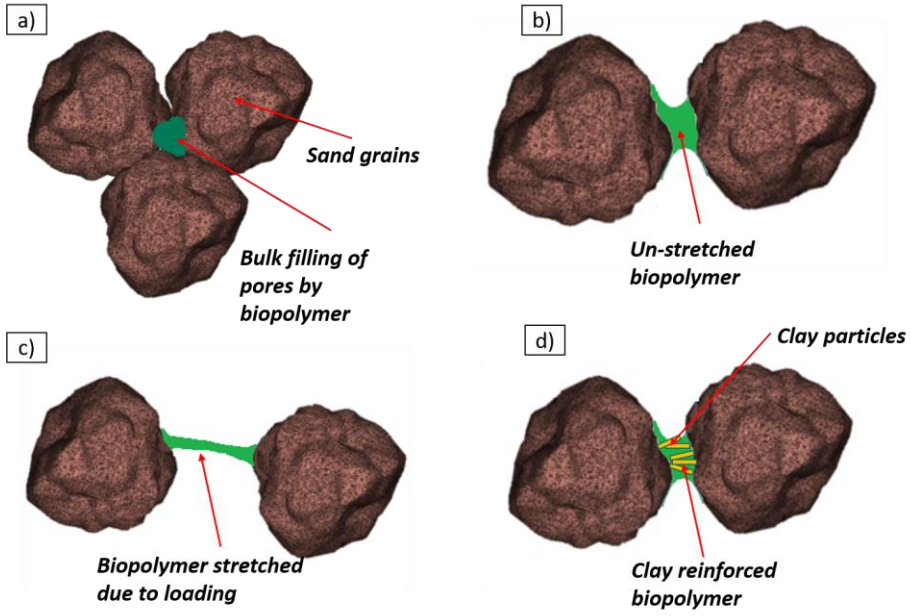

Fig 4. 21 Schematic representation of mechanism of stabilization by biopolymers

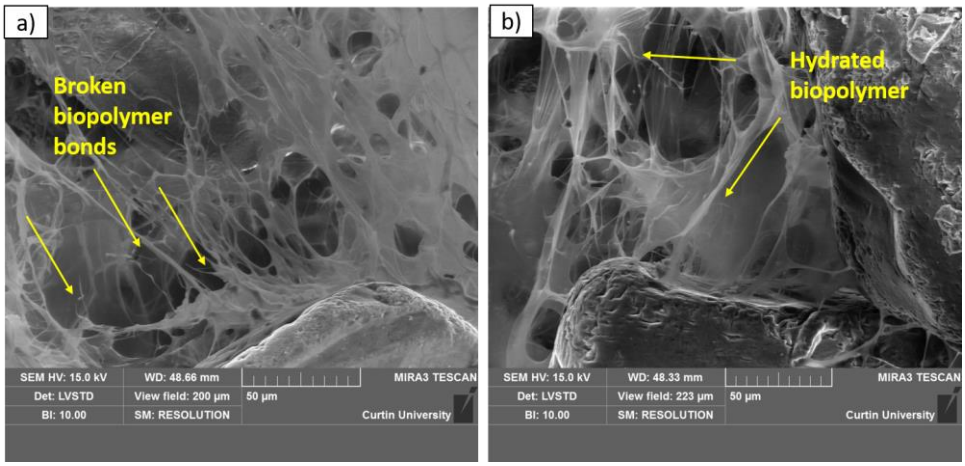

Fig 4. 22 SEM micrographs of the hydrated samples

4.6.4 Micro-mechanical properties of clay-reinforced biopolymer

4.6.4.1 Nanoindentation

The mechanical properties of the clay reinforced biopolymer are investigated using a nanoindenter. The load-displacement response of the sample during nanoindentation is displayed in Fig 4.23. Fig 4.24 shows a typical modulus-depth graph obtained from carrying out nano-indentation using CSM method. Therefore, continuous derivation of modulus and hardness data with indentation depth is obtained in this method. Further, the CSM technique has additional benefits, namely, identification of precise initial contact, fast and reliable calibration of testing procedures [74]. It is observed that the resistance peaks within 100 nm, followed by a gradual stabilisation. The uneven

measurements at a depth less than 500 nm are attributed to the indentation size effect [75]. The elastic modulus and hardness measured at depths of 1000-2000 nm yield a steady response. The elastic modulus and hardness values between the depths of 1000-2000 nm were averaged out. The average Young's elastic modulus and hardness of the sample across 25 indentation points on the sample are 5.02 ±1.3GPa and 0.078 ±0.03GPa, respectively. The Young's elastic modulus of the sample was calculated from reduced elastic modulus, Poisson's ratio of the sample and Young's modulus of the indenter [76].

The regions of low elastic modulus were grouped as pore spaces/voids in the sample [Fig 4.25)]. Nanoindentation performed by previous researchers on kaolin powder composed of 97% kaolinite gave an indentation modulus of 40.3±8.8 GPa [77]. Moreover, the literature report that the elastic modulus range of pure clay lies within 10-30GPa [80]. Hence, this range of modulus was observed when the indenter hit the clay particle. This value ranged between 6-8GPa in the present study [Fig 4.25)]. The results of our yet unpublished study on dry biopolymer revealed that its average modulus was 3.14GPa, which is in the range of the lowest values observed here. The region on intermediate modulus values ranging between 4-6GPa was classified as clay-biopolymer [Fig 4.25)]. Thus, with no clay particle, the modulus of the biopolymer is expected to be close to 4GPa. As the clay fraction increases, it will move up with a ceiling at 8GPa. The hypothesis was confirmed by a similar study, which reports that kaolin clay was effective in toughening epoxy polymer even at small dosages [78]. The microscopic increase in mechanical properties was responsible for the macroscopic increase in compressive strength, as observed by several researchers. The reinforcement of clay particles by biopolymer observed by nanoindentation was responsible for the increase in UCS by the addition of biopolymer. These findings are expected to be useful for further research in characterization and computer modelling clay-biopolymer for soil stabilization.

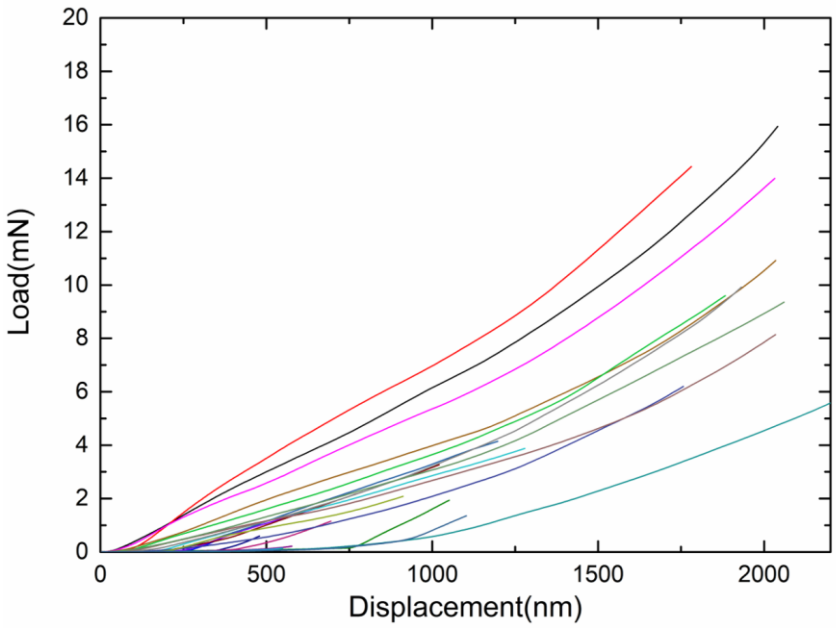

3104

3105 *Fig 4. 23 Load-displacement response of the sample during nanoindentation*

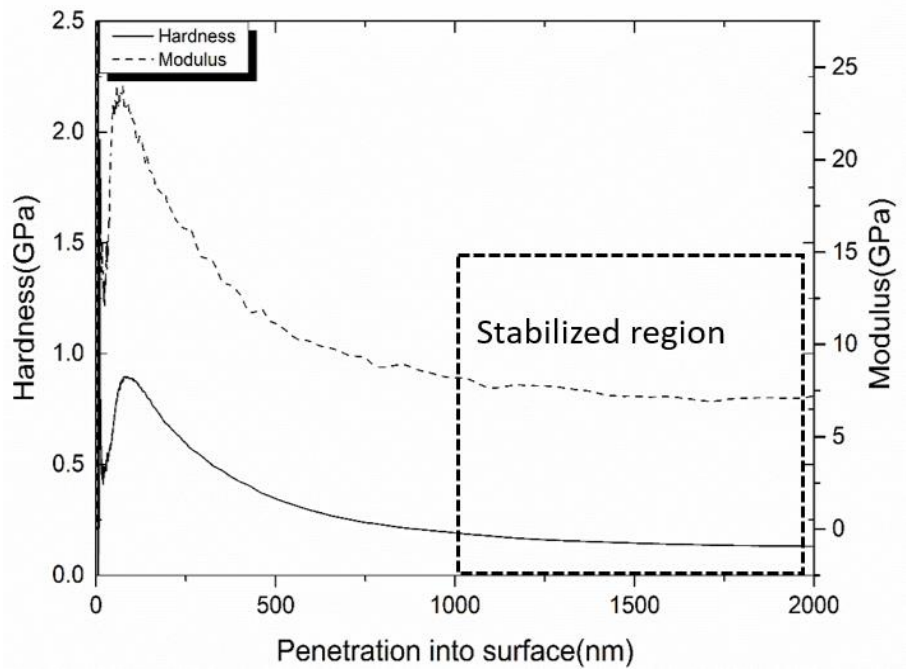

3106

3107 *Fig 4. 24 Elastic modulus and hardness as a function of the penetration depth*

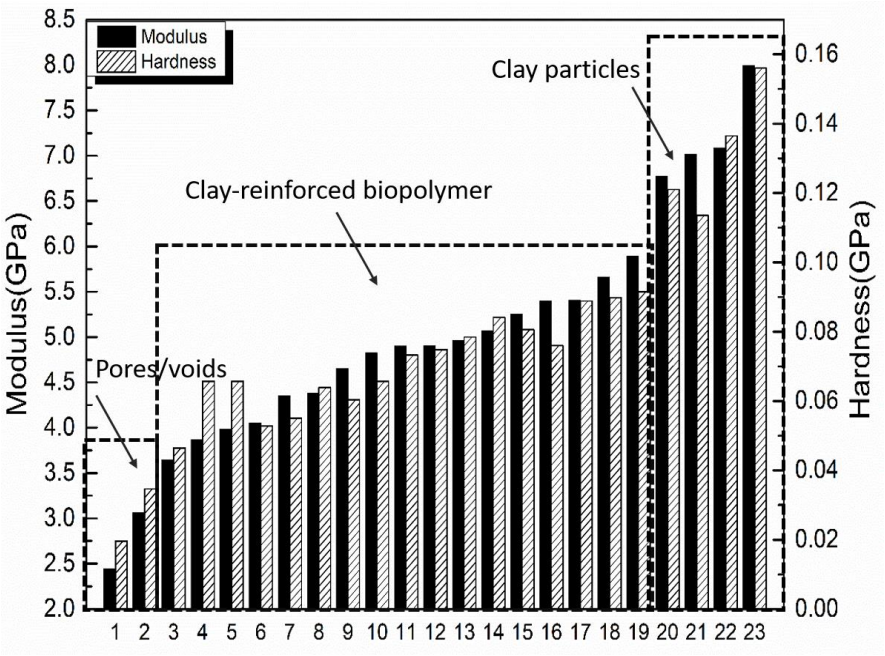

Fig 4. 25 Variation in modulus and hardness of the clay reinforced biopolymer sample

4.6.4.2 PeakForce QNM

AFM scanning was performed on 10 µm square areas to develop 256×256-pixel topography images. Fig 4.26 shows the AFM tip penetrating the sample. The clay particles are clearly visible inside the sample. The image of the clay biopolymer obtained through PeakForce QNM is shown in Fig 4.27. The average modulus of pure biopolymer obtained from PeakForce QNM was 3.6 GPa (unpublished data). The predicted modulus of clay from previous PeakForce QNM studies lies within the rage of 21-55GPa [79]. Keeping these values in mind, the surface scanning on the clay-biopolymer samples was carried out initially [Fig 4.27 a)] after exposing the sample to moisture [Fig 4.27 b)]. The flaky clay particles embedded in the biopolymer are visible in the images. However, no distinctive feature of moisture exposure is revealed. Modulus mapping is used to examine the effect of moisture on the bond between clay and biopolymer. Fig 4.27 b) and d) show the result of modulus mapping conducted on the sample surface of the initial state and after exposure to moisture, respectively. It can be observed that the modulus across the sample surface has reduced after exposure to moisture. The average modulus along the horizontal sections is 12.31±3.19 GPa, and that along the vertical sections is 11.86±2.25 GPa. After subjecting the sample to a wet-dry cycle, the average modulus across horizontal and vertical section got reduced to 9.99±0.94 GPa and 9.79±1.35 GPa respectively. Changes in elastic modulus were more prominent in the areas where clay particles were present in the sample. Due to

the fine resolution of AFM, even the clay particles of size less than 2µm could be discerned. In Fig 4.27 a) the flaky clay particles are seen. Fig 4.27 c) shows the corresponding area with a higher modulus indicating the presence of clay particles. In the case of Fig 4.27 b), after moisture exposure, the clay particles could be seen. However, the corresponding areas in Fig 4.27 d) do not show higher modulus. This indicates that the bond between the polymer and the clay particle has weakened. Therefore, it does not provide the same resistance to the AFM tip as before the exposure to moisture. This clearly demonstrates the effect of moisture on the biopolymer. It has been previously observed in the SEM micrographs that the clay particles are held fixed by the biopolymer. The disturbance of the biopolymer gel via hydrophilic water absorption leads to the network of biopolymer breaking off from the particle due to swelling. Drying results in reattachment to the particles, but the original structure is not recovered. The clay particle 1 in Fig 4.27 c) is completely free as the corresponding region in the modulus map shows a lower region of modulus. The clay particle 2 in Fig 4.27 c) might be partially free since the modulus value in the mid-region. Hence, wetting and drying have an impact on clay reinforced biopolymer at the micro-level, which significantly impacts the bulk mechanical properties as observed in UCS testing.

Compared to nano-indentation, the elastic modulus obtained from PeakForce-QNM is higher. This is because, through PeakForce-QNM, we have probed in the close vicinity of the clay particle. However, nano-indentation provides an overall estimate of the properties of the clay reinforced biopolymer. While the values obtained from nano-indentation are useful in estimating the property of the composite, the PeakForce-QNM reveals the variation in properties at a much finer scale, enabling study of microscopic changes in the composite. To sum up, AFM has been used to microscopically investigate the fundamental behaviour of clay stabilized biopolymer. The results of AFM experiments confirm the role of clay in reinforcing the biopolymer, leading to superior mechanical performance. Further, the loss in strength of the samples when exposed to moisture was visualized using AFM. The study validated the results of macroscopic testing of the samples as described in the previous sections. Therefore, the high-resolution microscopy, combined with the ability to map nanomechanical properties make AFM a very useful tool in geotechnical engineering

applications. It can be used to estimate the bond between the stabilizer and soil particles, which is otherwise difficult to visualize.

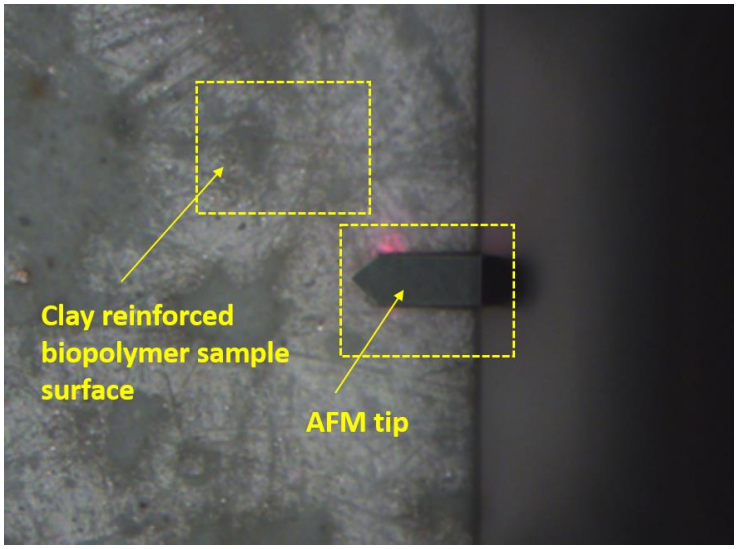

Fig 4. 26 The AFM tip scanning the sample surface

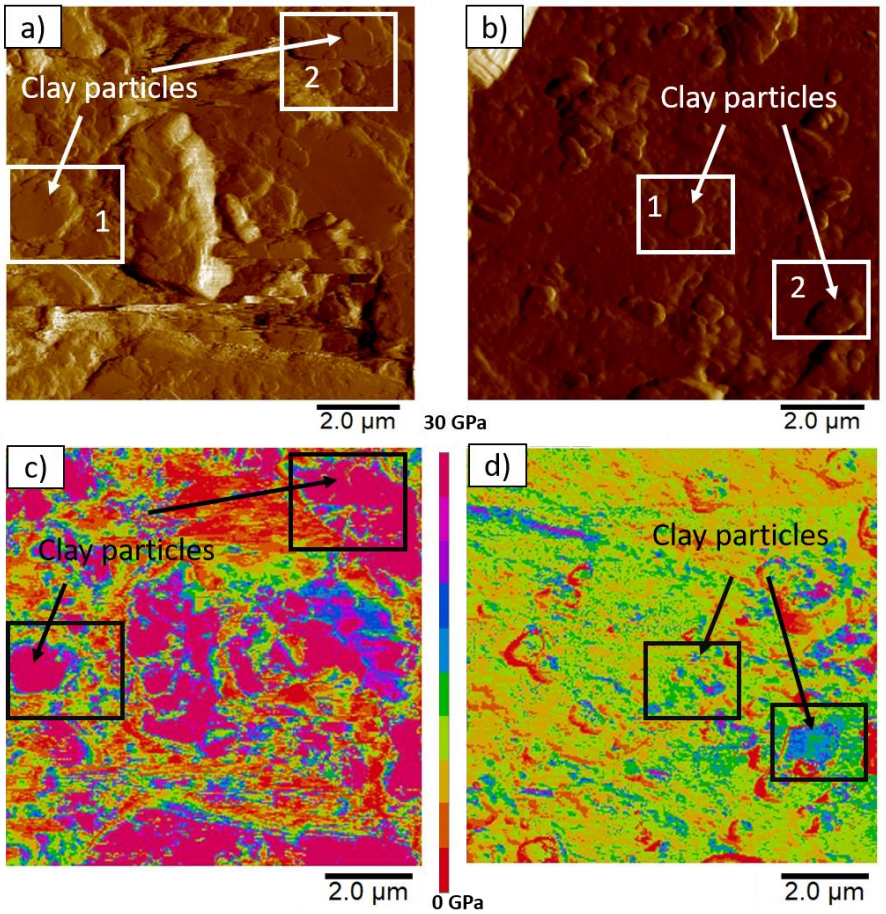

Fig 4. 27 Surface topography and modulus mapping of the clay reinforced biopolymer sample surface a) and b) prior to moisture exposure; c) and d) after exposure to moisture.

4.7 Conclusions and Recommendations

The study investigates Xanthan gum biopolymer with regard to stabilization of soil composed of sand and clay. The results provide useful insight into the underlying mechanisms of stabilization between Xanthan gum and soil. Advanced microscopic investigations using scanning electron microscopy, nanoindentation and atomic force microscopy were carried out to reveal the underlying mechanism of stabilization. The study reveals the potential of bacterial polymerisation as a means of sustainable soil stabilization. The following conclusions can be drawn from the results of the study:

1. The addition of clay leads to significant improvement in the compressive strength of biopolymer stabilized sands as observed from the mechanical properties obtained from UCS testing.

2. Investigation of modes of failure of the sample is essential for the proper interpretation of UCS values of the stabilized samples.

3. DIC proved to be a useful tool to map displacement fields from which stress fields are calculated.

4. The water absorption test revealed that the biopolymer stabilized sand samples resulted in local failure due to pore-clogging mechanism. The addition of clay helped in the uniform distribution of moisture by capillary action leading to low overall moisture absorption and avoiding sample failure.

5. Microstructural analysis on the stabilized samples using SEM revealed the mechanism of stabilization due to biopolymer alone as well as clay reinforced biopolymer. The clay particles were held in place by the biopolymer leading to higher stiffness.

6. Nanoindentation testing was carried out on dry clay reinforced biopolymer sample in order to quantify the micromechanical properties of the stabilizer. The average hardness and elastic modulus of the clay reinforced biopolymer sample obtained from nanoindentation testing are 0.078 ±0.03 GPa and 5.02 ±1.3 GPa, respectively.

7. PeakForce-QNM revealed the map of elastic modulus of the composite at 1μm resolution. It let us understand the micro-mechanism behind the reduction in strength of the clay reinforced biopolymer after exposure to moisture. The clay particles which were held fixed by the biopolymer became loose owing to the weakening of the biopolymer network on exposure to moisture. This micromechanical phenomenon resulted in the reduction in strength of the stabilized samples at a macro scale as reflected by the UCS testing.

This paper investigates the properties of Xanthan gum stabilized sand and clay mixtures and explains the mechanism of stabilization using a range of microscopic studies that are hitherto unreported. The outcome of the study reveals the potential of bacterial polymerisation as a means of sustainable soil stabilization. However, further research must be carried out, keeping in mind the limitations of the present study. The authors suggest that compressive testing on wet specimens should be carried out in the future. The dissolution of the biopolymer during water absorption testing should also be quantified. Further, to evaluate the cohesion and friction angles of the stabilized samples, a set of triaxial tests are also recommended.

4.8 Data availability statement

Some or all data, models or code generated or used during the study are available from the corresponding author by request.

4.9 Acknowledgements

The authors would like to acknowledge the contribution of Curtin International Postgraduate Research Scholarship (CIPRS) in supporting this research. Part of this research was undertaken using the instrumentation FESEM (Field Emission Scanning Electron Microscope) and Tescan Mira3 VP-FESEM at the John de Laeter Centre, Curtin University. We also acknowledge the use of equipment, scientific and technical assistance of the Curtin University Electron Microscope Facility, which has been partially funded by the University, State and Commonwealth Governments.

4.10 References

1. Murthy, G.V.L.N., A.V. Krishna, and V.V.N.P. Rao. *An Experimental Study on Partial Replacement of Clayey Soil with an Industrial Effluent: Stabilization of Soil Subgrade*. 2018. Cham: Springer International Publishing.

2. Baumann, V. and G.E.A. Bauer, *The Performance of Foundations on Various Soils Stabilized by the Vibro-compaction Method.* Canadian Geotechnical Journal, 1974. 11(4): p. 509-530.
3. Mohamedelhassan, E. and J.Q. Shang, *Vacuum and surcharge combined one-dimensional consolidation of clay soils.* Canadian Geotechnical Journal, 2002. 39(5): p. 1126-1138.
4. Madhav, M.R. and P.P. Vitkar, *Strip footing on weak clay stabilized with a granular trench or pile.* Canadian Geotechnical Journal, 1978. 15(4): p. 605-609.
5. Osula, D.O.A., *Laboratory Trial of Soil-Sodium Chloride-Cement Stabilization for Problem Laterite.* Journal of Transportation Engineering, 1993. 119(1): p. 149-158.
6. Tremblay, H., et al., *Influence of the nature of organic compounds on fine soil stabilization with cement.* Canadian Geotechnical Journal, 2002. 39(3): p. 535-546.
7. Consoli, N.C., P.D.M. Prietto, and L.A. Ulbrich, *Influence of Fiber and Cement Addition on Behavior of Sandy Soil.* Journal of Geotechnical and Geoenvironmental Engineering, 1998. 124(12): p. 1211-1214.
8. Bell, F.G., *Lime stabilization of clay minerals and soils.* Engineering Geology, 1996. 42(4): p. 223-237.
9. Al-Mukhtar, M., A. Lasledj, and J.-F. Alcover, *Behaviour and mineralogy changes in lime-treated expansive soil at 20°C.* Applied Clay Science, 2010. 50(2): p. 191-198.
10. Porter, H., N.K. Dhami, and A. Mukherjee, *Sustainable road bases with microbial precipitation.* Proceedings of the Institution of Civil Engineers - Construction Materials, 2018. 171(3): p. 95-108.
11. Yarbaşı, N., E. Kalkan, and S. Akbulut, *Modification of the geotechnical properties, as influenced by freeze–thaw, of granular soils with waste additives.* Cold Regions Science and Technology, 2007. 48(1): p. 44-54.
12. Koshy, N., et al., *Synthesis and characterization of geopolymers derived from coal gangue, fly ash and red mud.* Construction and Building Materials, 2019. 206: p. 287-296.

13. Solanki, P., N. Khoury, and M. Zaman, *A Comparative Evaluation of Various Additives Used in the Stabilization of Sulfate Bearing Lean Clay.* Journal of ASTM International, 2009. 6(8): p. 1-18.
14. Obuzor, G.N., J.M. Kinuthia, and R.B. Robinson, *Soil stabilisation with lime-activated-GGBS—A mitigation to flooding effects on road structural layers/embankments constructed on floodplains.* Engineering Geology, 2012. 151: p. 112-119.
15. Al-Rawas, A., et al., *A Comparative Evaluation of Various Additives Used in the Stabilization of Expansive Soils.* Geotechnical Testing Journal, 2002. 25(2): p. 199-209.
16. Kaniraj, S.R. and V.G. Havanagi, *Behavior of Cement-Stabilized Fiber-Reinforced Fly Ash-Soil Mixtures.* Journal of Geotechnical and Geoenvironmental Engineering, 2001. 127(7): p. 574-584.
17. Komonweeraket, K., et al., *Leaching characteristics of toxic constituents from coal fly ash mixed soils under the influence of pH.* Waste Management, 2015. 38: p. 174-184.
18. Koshy, N. and D.N. Singh, *Fly ash zeolites for water treatment applications.* Journal of Environmental Chemical Engineering, 2016. 4(2): p. 1460-1472.
19. Azulay, D.N., et al., *Biopolymers from a Bacterial Extracellular Matrix Affect the Morphology and Structure of Calcium Carbonate Crystals.* Crystal Growth & Design, 2018. 18(9): p. 5582-5591.
20. Ramachandran, A.L., et al., *Understanding and creating biocementing beachrocks via biostimulation of indigenous microbial communities.* Applied Microbiology and Biotechnology, 2020: p. 1-19.
21. Reid, R.P., et al., *The role of microbes in accretion, lamination and early lithification of modern marine stromatolites.* Nature, 2000. 406(6799): p. 989-992.
22. Chen, P.-Y., J. McKittrick, and M.A. Meyers, *Biological materials: Functional adaptations and bioinspired designs.* Progress in Materials Science, 2012. 57(8): p. 1492-1704.
23. Neumeier, U., *Experimental modelling of beachrock cementation under microbial influence.* Sedimentary Geology, 1999. 126(1): p. 35-46.

24. McCutcheon, J., et al., *Beachrock formation via microbial dissolution and re-precipitation of carbonate minerals.* Marine Geology, 2016. 382: p. 122-135.
25. Dejong, J.T., et al., *Biogeochemical processes and geotechnical applications: progress, opportunities and challenges.* Géotechnique, 2013. 63(4): p. 287-301.
26. Stal, L.J., *Microphytobenthos as a biogeomorphological force in intertidal sediment stabilization.* Ecological Engineering, 2010. 36(2): p. 236-245.
27. Szcześ, A., M. Czemierska, and A. Jarosz-Wilkołazka, *Calcium carbonate formation on mica supported extracellular polymeric substance produced by Rhodococcus opacus.* Journal of Solid State Chemistry, 2016. 242: p. 212-221.
28. Flemming, H.-C., T.R. Neu, and D.J. Wozniak, *The EPS Matrix: The "House of Biofilm Cells".* Journal of Bacteriology, 2007. 189(22): p. 7945-7947.
29. Chen, C., L. Wu, and M. Harbottle, *Exploring the effect of biopolymers in near-surface soils using xanthan gum-modified sand under shear.* Canadian Geotechnical Journal, 2019.
30. Achal, V. and A. Mukherjee, *A review of microbial precipitation for sustainable construction.* Construction and Building Materials, 2015. 93: p. 1224-1235.
31. Achal, V., et al., *Biomineralization for sustainable construction – A review of processes and applications.* Earth-Science Reviews, 2015. 148: p. 1-17.
32. Porter, H., N.K. Dhami, and A. Mukherjee, *Synergistic chemical and microbial cementation for stabilization of aggregates.* Cement and Concrete Composites, 2017. 83: p. 160-170.
33. DeJong, J.T., et al., *Bio-mediated soil improvement.* Ecological Engineering, 2010. 36(2): p. 197-210.
34. DeJong, J.T., M.B. Fritzges, and K. Nüsslein, *Microbially Induced Cementation to Control Sand Response to Undrained Shear.* Journal of Geotechnical and Geoenvironmental Engineering, 2006. 132(11): p. 1381-1392.
35. Chen, R., I. Lee, and L. Zhang, *Biopolymer Stabilization of Mine Tailings for Dust Control.* Journal of Geotechnical and Geoenvironmental Engineering, 2015. 141(2): p. 04014100.

36. Chang, I., et al., *Soil consistency and inter-particle characteristics of xanthan gum biopolymer containing soils with pore-fluid variation.* Canadian Geotechnical Journal, 2018.
37. Chang, I., et al., *Strength durability of gellan gum biopolymer-treated Korean sand with cyclic wetting and drying.* Construction and Building Materials, 2017. 143: p. 210-221.
38. Chang, I., J. Im, and G.-C. Cho, *Geotechnical engineering behaviors of gellan gum biopolymer treated sand.* Canadian Geotechnical Journal, 2016. 53(10): p. 1658-1670.
39. Reddy, N.G., B.H. Rao, and K.R. Reddy, *Biopolymer amendment for mitigating dispersive characteristics of red mud waste.* Géotechnique Letters, 2018. 8(3): p. 201-207.
40. Ayeldeen, M., et al., *Enhancing mechanical behaviors of collapsible soil using two biopolymers.* Journal of Rock Mechanics and Geotechnical Engineering, 2017. 9(2): p. 329-339.
41. Muguda, S., et al., *Mechanical properties of biopolymer-stabilised soil-based construction materials.* Géotechnique Letters, 2017. 7(4): p. 309-314.
42. Chang, I., et al., *Soil strengthening using thermo-gelation biopolymers.* Construction and Building Materials, 2015. 77: p. 430-438.
43. Khatami, H.R. and B.C. O'Kelly, *Improving Mechanical Properties of Sand Using Biopolymers.* Journal of Geotechnical and Geoenvironmental Engineering, 2013. 139(8): p. 1402-1406.
44. Chang, I. and G.-C. Cho, *Strengthening of Korean residual soil with β-1,3/1,6-glucan biopolymer.* Construction and Building Materials, 2012. 30: p. 30-35.
45. Hataf, N., P. Ghadir, and N. Ranjbar, *Investigation of soil stabilization using chitosan biopolymer.* Journal of Cleaner Production, 2018. 170: p. 1493-1500.
46. Fatehi, H., et al., *A novel study on using protein based biopolymers in soil strengthening.* Construction and Building Materials, 2018. 167: p. 813-821.
47. Galán-Marín, C., C. Rivera-Gómez, and J. Petric, *Clay-based composite stabilized with natural polymer and fibre.* Construction and Building Materials, 2010. 24(8): p. 1462-1468.

48. Latifi, N., et al., *Xanthan gum biopolymer: an eco-friendly additive for stabilization of tropical organic peat.* Environmental Earth Sciences, 2016. 75(9): p. 825.
49. Cabalar, A.F., M.H. Awraheem, and M.M. Khalaf, *Geotechnical Properties of a Low-Plasticity Clay with Biopolymer.* Journal of Materials in Civil Engineering, 2018. 30(8): p. 04018170.
50. Chen, R., L. Zhang, and M. Budhu, *Biopolymer Stabilization of Mine Tailings.* Journal of Geotechnical and Geoenvironmental Engineering, 2013. 139(10): p. 1802-1807.
51. Joel, M. and I.O. Agbede, *Mechanical-Cement Stabilization of Laterite for Use as Flexible Pavement Material.* Journal of Materials in Civil Engineering, 2011. 23(2): p. 146-152.
52. Zhang, Z. and M. Tao, *Durability of Cement Stabilized Low Plasticity Soils.* Journal of Geotechnical and Geoenvironmental Engineering, 2008. 134(2): p. 203-213.
53. Dash, S.K. and M. Hussain, *Lime Stabilization of Soils: Reappraisal.* Journal of Materials in Civil Engineering, 2012. 24(6): p. 707-714.
54. Zhu, W., et al., *Nanoindentation mapping of mechanical properties of cement paste and natural rocks.* Materials Characterization, 2007. 58(11): p. 1189-1198.
55. Li, W., et al., *Experimental investigation on quantitative nanomechanical properties of cement paste.* ACI Materials Journal, 2015. 112(2).
56. Young, T.J., et al., *The use of the PeakForceTMquantitative nanomechanical mapping AFM-based method for high-resolution Young's modulus measurement of polymers.* Measurement Science and Technology, 2011. 22(12): p. 125703.
57. Olsson, A.L.J., et al., *The influence of ionic strength on the adhesive bond stiffness of oral streptococci possessing different surface appendages as probed using AFM and QCM-D.* Soft Matter, 2012. 8(38): p. 9870-9876.
58. Dokukin, M.E. and I. Sokolov, *Quantitative Mapping of the Elastic Modulus of Soft Materials with HarmoniX and PeakForce QNM AFM Modes.* Langmuir, 2012. 28(46): p. 16060-16071.

59. Palaniraj, A. and V. Jayaraman, *Production, recovery and applications of xanthan gum by Xanthomonas campestris.* Journal of Food Engineering, 2011. 106(1): p. 1-12.
60. Australia, S., *1289.5.1.1:2017 : Methods of testing soils for engineering purposes - Soil compaction and density tests - Determination of the dry density/moisture content relation of a soil using standard compactive effort.* 2017, Standards Australia: Sydney.
61. Latifi, N., et al., *Improvement of Problematic Soils with Biopolymer An Environmentally Friendly Soil Stabilizer.* Journal of Materials in Civil Engineering, 2017. 29(2): p. 04016204.
62. Chang, I., et al., *Effects of Xanthan gum biopolymer on soil strengthening.* Construction and Building Materials, 2015. 74: p. 65-72.
63. Australia, S., *AS 5101.4-2008 : Methods for preparation and testing of stabilized materials - Unconfined compressive strength of compacted materials.* 2008, Standards Australia: Sydney.
64. Deniz Akin, I. and W. Likos, *Brazilian Tensile Strength Testing of Compacted Clay.* Geotechnical Testing Journal, 2017. 40(4): p. 608-617.
65. Australia, S., *AS 5101.5-2008 (R2017) : Methods for preparation and testing of stabilized materials - Absorption, swell and capillary rise of compacted materials.* 2008, Standards Australia: Sydney.
66. Oliver, W.C. and G.M. Pharr, *An improved technique for determining hardness and elastic modulus using load and displacement sensing indentation experiments.* Journal of Materials Research, 1992. 7(6): p. 1564-1583.
67. Huen, W.Y., et al., *Nanomechanical properties of thermal arc sprayed coating using continuous stiffness measurement and artificial neural network.* Surface and Coatings Technology, 2019. 366: p. 266-276.
68. Tranchida, D., et al., *Mechanical Characterization of Polymers on a Nanometer Scale through Nanoindentation. A Study on Pile-up and Viscoelasticity.* Macromolecules, 2007. 40(4): p. 1259-1267.
69. Baniasadi, M., et al., *Nanoindentation ofPseudomonas aeruginosabacterial biofilm using atomic force microscopy.* Materials Research Express, 2014. 1(4): p. 045411.

70. Nair, S.S., C. Wang, and K.J. Wynne, *AFM Peakforce QNM mode for measurement of nanosurface mechanical properties of Pt-cured silicones.* Progress in Organic Coatings, 2019. 126: p. 119-128.
71. Derjaguin, B.V., V.M. Muller, and Y.P. Toporov, *Effect of contact deformations on the adhesion of particles.* Journal of Colloid and Interface Science, 1975. 53(2): p. 314-326.
72. Porter, H., et al., *Rammed earth blocks with improved multifunctional performance.* Cement and Concrete Composites, 2018. 92: p. 36-46.
73. Sworn, G., *Xanthan gum*, in *Handbook of hydrocolloids*. 2009, Elsevier. p. 186-203.
74. Oliver, W.C. and G.M. Pharr, *Measurement of hardness and elastic modulus by instrumented indentation: Advances in understanding and refinements to methodology.* Journal of materials research, 2004. 19(1): p. 3-20.
75. Nix, W.D. and H. Gao, *Indentation size effects in crystalline materials: A law for strain gradient plasticity.* Journal of the Mechanics and Physics of Solids, 1998. 46(3): p. 411-425.
76. Pharr, G.M., W.C. Oliver, and F.R. Brotzen, *On the generality of the relationship among contact stiffness, contact area, and elastic modulus during indentation.* Journal of Materials Research, 1992. 7(3): p. 613-617.
77. Ulm, F.-J. and Y. Abousleiman, *The nanogranular nature of shale.* Acta Geotechnica, 2006. 1(2): p. 77-88.
78. Castrillo, P.D., et al., *Mechanical characterization and fractographic study of epoxy–kaolin polymer nanocomposites.* Composite Structures, 2015. 133: p. 70-76.
79. Eliyahu, M., et al., *Mechanical properties of organic matter in shales mapped at the nanometer scale.* Marine and Petroleum Geology, 2015. 59: p. 294-304.
80. Zhang, Guoping, Zhongxin Wei, and Ray E. Ferrell. 2009. "*Elastic Modulus and Hardness of Muscovite and Rectorite Determined by Nanoindentation."* Applied Clay Science 43(2): 271–81.

Chapter 5: Multi-functional Performance of Biopolymers and Biocement in Aggregation of Sandy Soil and Road Bases

5.1 Abstract

To achieve the sustainability goals, bio-based binders for soil stabilization are gaining attention. Biocementation through Microbially Induced Calcite Precipitation (MICP) is well researched. Some research on biopolymeric stabilization is also available. This paper explores the synergistic effect of combined biopolymer and biocement for the stabilization of sand-clay mixture. The study was further extended to road base material to observe the effect at site. The soil of varying grain size distribution spanning from sand to clay mixtures and road base material has been aggregated using both the biopolymer xanthan gum and MICP. A portion of the samples has been further treated with MICP. For the sand clay mixtures, the amount of biopolymer is kept constant and the MICP is varied. While, for the road base material, the amount of MICP is kept constant and biopolymer content is varied. The unconfined compressive strength tests and micrographic analysis through scanning electron microscope and energy dispersive X-ray spectroscopy results revealed that synergistic effect of biopolymer and MICP resulted in superior performance. Water absorption test indicated that xanthan gum was susceptible to water attack and incorporation of MICP helped in addressing the concern. In general, xanthan gum treated road base exhibited significant improvement in compressive strength, stiffness, and ultimate strain with increasing biopolymer dosage from 0.5%-1.5%. However, the use of biopolymer as a stand-alone stabilizer for road base materials is not advisable as they are prone to moisture degradation. The study proved that MICP surface coating is a sustainable solution to overcome this limitation of biopolymer. Likewise, the addition of biopolymers reduces the release of ammonia into the atmosphere. The present study was successful in overcoming the individual limitations of biopolymer and MICP by combining the two techniques.

Keywords: Soil stabilization; biopolymer, microbially induced calcite precipitation; mechanical properties; water absorption; scanning electron microscopy

5.2 Introduction

Growing demands for urbanization and infrastructure development has made it imperative to build on the soil of deficient quality. Soil stabilization is resorted to altering the native soil resulting in improved bearing capacity, shear strength or

durability against moisture and stress [1, 2, 4]. Stabilization helps in addressing several concerns such as the differential settlement of foundations and buildings [1], cracking of pavement under loading [2, 3], slope failures [4], the collapse of mine tailings [5] and soil liquefaction [6]. In Australia, consumption of Portland cement in the stabilization of road bases and mine tailings is close to its use in concrete. As a measure of reducing emission from construction activities, it is essential to explore technologies that are carbon neutral or carbon negative.

Current practices of soil stabilization involve either mechanical modification or chemical treatment of the soil. These mechanical techniques are highly energy-intensive in terms of their production or installation [7]. The chemical stabilizers commonly used for soil include cement [8], lime [9], bituminous materials [10], industrial by-products such as fly ash [11] and Ground Granulated Blast Furnace Slag (GGBFS) [12]. Though chemical stabilizers are cost-effective and durable, several underlying issues such as high alkalinity [9], the presence of leachable heavy metals [13] are concerns for their usage. It has been reported that the typical energy consumption rates for cement-stabilised materials are approximately 5000 MJ/t [2]. In addition to this, low efficiency of cement with a certain type of soils (organic soils and soils rich in sulphates and chlorides) along with issues such as low temperature cracking and brittle failures are some of the problems associated with cement and lime stabilisation of soils [14]. To sum up, conventional soil improvement techniques have both technical and environmental lacunae.

The key to the solution of this problem may lie in nature, especially in natural formations such as beach rocks [15, 16], corals [17] and stromatolites [18, 19] that bind loose granular material in a technologically sound and environmentally benign way [2]. Inspired from natural formations, bio-geotechnology is an emerging area which facilitates cement formation in a sustainable manner [7, 20-22]. It focuses primarily on MICP, the process by which microorganisms produce carbonate minerals. The process of MICP has been explored in various geotechnical engineering applications [2, 7]. However, limitations of this technology include brittle nature of calcite crystals; the necessity of time-consuming repeated applications and release of harmful by-products such as ammonia.

Detailed examination of the natural formations such as beach rocks and stromatolites revealed that biomineralization is strongly associated with biopolymer formation. In

an investigation on the formation of beach rocks is the Western Australian coast, the authors noticed a distinct biopolymeric phase that holds the grains together and facilitates the growth of the slower mineral phase [23]. Thus, a synergy between the polymeric and mineral cementation is noticed. In comparison to MICP, less attention has been focussed on the ability of biopolymer to stabilize the soil. Commonly used biopolymers for soil stabilization include xanthan gum [24-26], guar gum [27, 28], gellan gum [29, 30] and chitosan [31]. The ductile behaviour of the stabilized soils, as well as higher toughness, are advantages of using biopolymer as a stabilizer [32]. However, their susceptibility to moisture is a concern.

Australia needs sustainable technologies for mass cementation applications such as stabilization of road bases and mine tailings. For a smooth transition to new technologies, it is important to find synergies between the existing and new systems. Synergistic effect of industrial and biological cement has been explored previously by researchers [33, 34]. Surface treatment using MICP on traditional rammed earth blocks was found to reduce water absorption dramatically [34]. Thus, the use of biocement in a minute quantity but using the right method has proven to be extremely beneficial.

The objective of the study is to explore the synergistic role of biopolymer and biocement under laboratory conditions. The efficacy of biopolymer Xanthan gum and MICP in aggregating soils of varying grain size distribution spanning from sand to clay mixtures are to be tested in the study. The hypothesis to be tested is that if synergising the two techniques will lead to overcoming the individual limitations of biopolymer and MICP. This paper explores the synergy between biopolymer and biocement stabilizers. Biopolymeric stabilisation is a rapid, single-step process. Moreover, in this process release of toxic ammonia of MICP is avoided. However, biopolymers are susceptible to moisture to the extent that quite a few of them are soluble in water. This paper explores a synergy between biopolymer and biocement for the first time. The aim is to achieve all the superior properties of biopolymer stabilizers while improving its water resistance through MICP. An experimental investigation has been performed by stabilizing sand using the biopolymer, xanthan gum (control). The sand is mixed with variable fractions of clay to investigate the interaction of clay with biopolymer. Finally, a set of samples has been surface treated with MICP at varying degrees to assess the improvement in water absorption and post absorption strength.

5.3 Experimental investigation

The schematic of the experimental investigation is shown in Fig 5.1. Columns of sand and sand-clay mixtures were stabilized via biopolymer, xanthan gum (0.5% dry weight of soil). The samples were cured at 60^{o}C for a period of 7 days. The cured samples were subjected to further surface stabilization using MICP. MICP was performed by spraying the bacterial and cementation media (Table 5.2) and continued for varying cycles. For the sand clay mixtures, the amount of biopolymer is kept constant and the MICP is varied. While, for the road base material, the amount of MICP is kept constant and biopolymer content is varied. After MICP treatment, the samples were cured and subjected to unconfined compression strength tests (UCS), water absorption tests as well as microscopic observation via scanning electron microscopy.

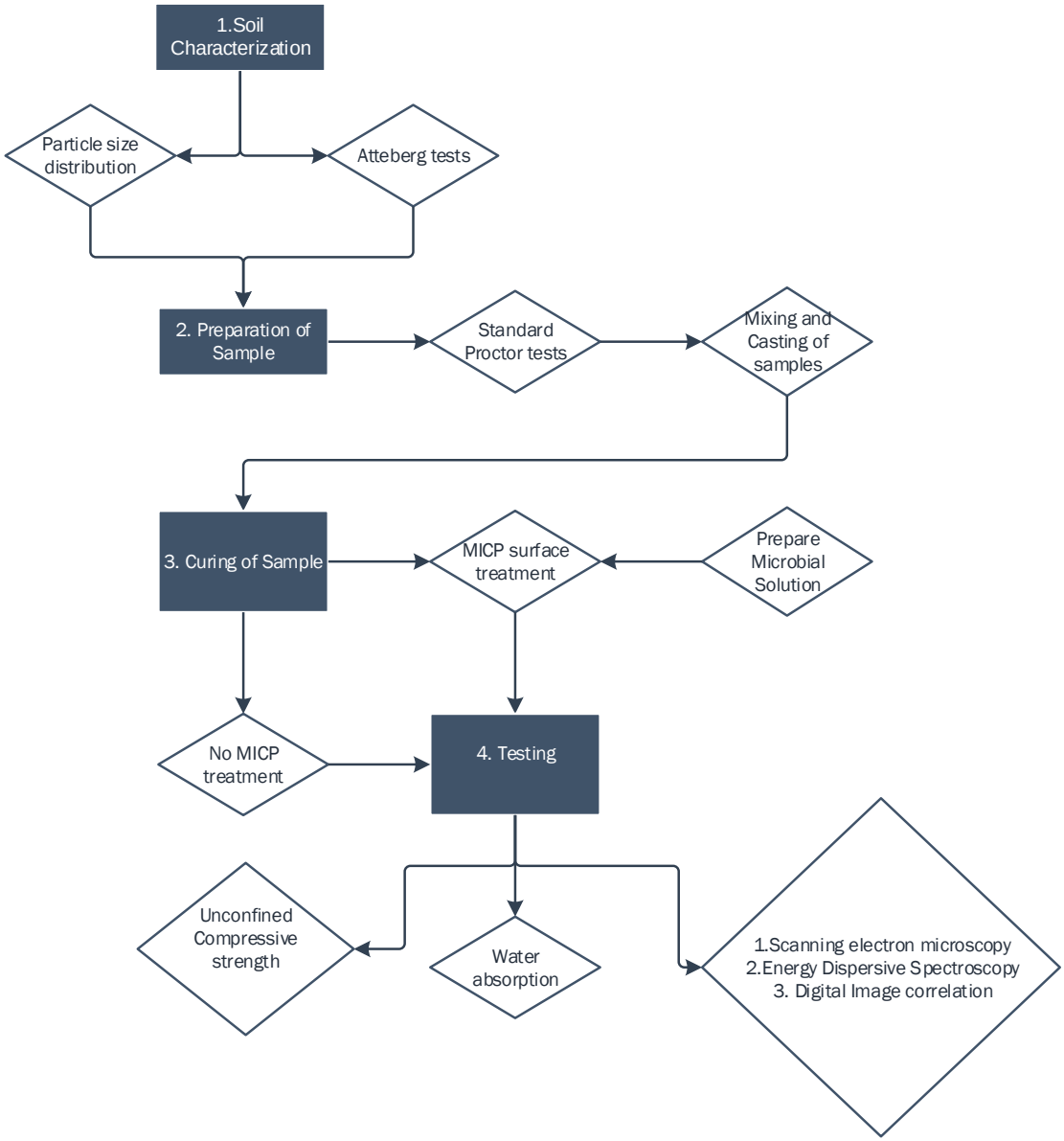

Fig 5. 1 Schematic of experimental investigation and test matrix

5.4 Materials and methods

5.4.1 Materials

The materials consisted of sand, clay, and the stabilisers. Manufactured sand used for the present study was sourced from Cook Industrial Minerals, Western Australia. The particle size of the sand varied between 0.45 mm and 0.075 mm (Fig 5.2). Sibelco, Australia provided the low shrinkage kaolin clay used for this study. The particle size distribution and chemical composition of the clay are listed in Table 5.1. The road base used in this study was sourced Department of Transport and Main Roads, WA. Sieve analysis was carried in accordance to AS1289.3.6.1:2009. Atterberg's limit were determined as per AS 1289.3.2.1:2009 and AS 1289.3.9.1:2015. The Atterberg's limit of the road base material is given in Table 5.2.

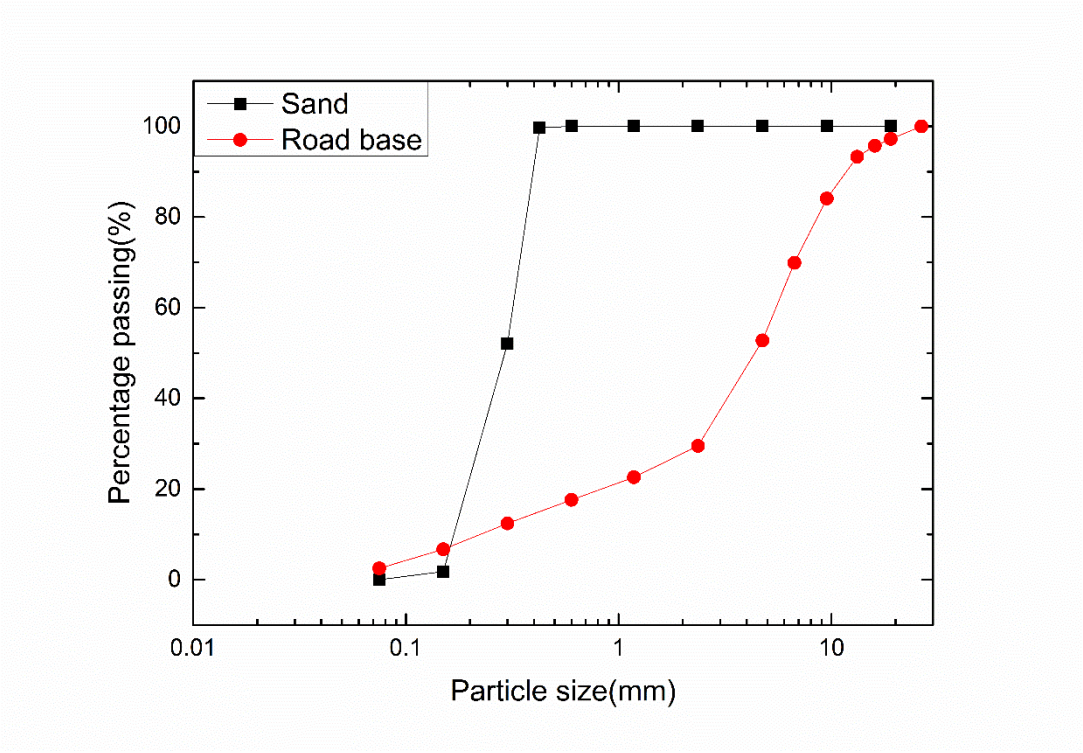

Fig 5. 2 Particle size distribution of manufactured sand and road base material

Table 5. 1 Particle size distribution and chemical composition of clay

Particle size (μm)	Percentage passing (% weight)
53	99.4
20	97.8

10	95.9	
5	90.3	
2	75.7	
1	63.6	

Chemical analysis	Composition (% Weight) *
SiO_2	46.7
Al_2O_3	36.1
TiO_2	0.8
Fe_2O_3	0.9
CaO	0.7
MgO	0.4
K_2O	0.4
Na_2O	0.1

Table 5. 2 Atterberg's limit for the road base material

Atterberg's limit	
Plastic Limit (PL)	22 %
Liquid Limit (LL)	34 %
Plasticity Index (PI)	12 %

Commercial biopolymer, xanthan gum, produced by the fermentation of *Xanthomonas campestri* was supplied by Sigma Aldrich, NSW, Australia. Xanthan gum is a polysaccharide composed of glucose, mannose, and glucuronic acid and highly hydrophilic in nature [35]. The growth media for bacteria consisted of yeast extract Ammonium sulphate, and Tris base (Sigma Aldrich, NSW). Urea and calcium chloride used for the cementation media was supplied by Perth Scientific Pty Ltd, Western Australia. The composition of the media is given in Table 5.3.

Table 5. 3 Details of bacterial media and cementation media used for MICP

Media	Composition	Concentration
Bacterial media	*Sporosarcina pasteurii*(ATCC 11859)	$0.8 < OD_{600} < 1.5$
	Yeast extract	20 g/L
	Ammonium sulphate	10 g/L

	Tris base (pH 9)	0.13 M
Cementation media	Calcium chloride	0.5 M
	Urea	0.5 M
	Yeast extract	1 g/L

5.4.2 Sample preparation

Sand clay mixture

Xanthan gum of 0.5% dry weight of soil (w_b/w_s: 0.5%) was mixed with water on a hot plate at 80^{o}C with continuous stirring to prevent agglomeration [35]. The amount of water used for mixing was calculated from the modified proctor density testing, according to AS 1289.5.1.1[36]. Sand and clay (10% dry weight) were mixed in the desired proportion, and the xanthan gum solution was added to it and thoroughly mixed. It was compacted into moulds of 50 mm diameter and 100 mm height to achieve maximum dry density. The sample could cure for a period of 7 days in an incubator maintained at 60^{o}C prior to the commencement of MICP spraying. After ensuring that the samples were completely cured allowing the hardening of xanthan gum, the MICP treatment was commenced. Urease producing bacteria *Sporosarcina pasteurii* was grown in an ammonium-yeast extract media (Table 5.3) maintained at 37^{o}C and 180 rpm to reach an optical density of 1.0 [37]. Subsequently, approximately 10mL of the bacterial solution was sprayed on the outer surface of the cylindrical specimens using a spray bottle, in a biosafety cabinet to maintain sterile conditions. Utmost care was taken to prevent any loss of bacterial solution while spraying. The sample was incubated at 37^{o}C for 6 hours to promote bacterial growth. This was followed by the spraying of approximately 10mL of cementation media (Table 5.3) twice a day for a period of 4 days. During spraying, some loss of the material is expected, and 10% extra solution was sprayed each time to account for the loss. This entire process was marked as one cycle of MICP, and treatment was repeated for various cycles of MICP. After the desired number of cycles, the samples were cured, capped, and tested further. Table 5.4 contains the description and designation for the samples.

Road base material

Xanthan gum powder was poured in to heated (80 ^{o}C) water while being continuously stirred using a magnetic stirrer. A Hobart mixer was then used to mix viscous Xanthan gum solution and road base in order to allow for a uniform Xanthan gum-soil matrix. Varying ratios of Xanthan gum to dry soil mass (w_b/w_s: 0.5%, 1% and 1.5%) was used in this study.

5.4.3 Sample designation and description

The sand columns were given designation based on their composition as Ca Bb Mc where C, B and M designate clay, biopolymer and MICP, respectively. The suffixes a, b and c are the corresponding weight percentages of sand (see Table 5.4). The maximum percentage weight of clay used is 10%, and the biopolymer concentration is maintained at 0.5% dry weight of sand. The road base samples are designated by R B_b M_c (since the amount of clay is constant in the samples). The percentage of MICP, however, cannot be measured directly. It has been derived from the total amount of calcium ions present in the cementation solution converted to the equivalent weight of calcium carbonate. The underlying assumption is that all the calcium gets converted to carbonate. The MICP percentage varies from 2.4-14.3% depending on the number of MICP cycles.

Table 5. 4 Description and designation of the samples

Sample designation (general)	a (%) Wt. of clay/ wt. of sand	b (%) Wt. of Biopolymer/Wt. of sand	c (%) Wt. of MICP/Wt. of sand
C_a B_b M_c	0%, 10%	0.5% (Constant)	2.4-14.3% (varied)
R B_b M_c	X%	0.5%, 1.0%, 1,5%(varied)	3.3%

5.5 Testing methods

5.5.1 Unconfined compressive strength (UCS)

The samples were dried after the end of MICP treatment and subjected to UCS testing in accordance with Australian Standards [38] on a universal testing machine (Shimadzu AGS-X) of 10kN capacity. A constant displacement of 1 mm/min was used during the compression testing, and corresponding stress-strain graphs were plotted for each sample. Secant modulus of elasticity (E_{50}) and unconfined compressive strength (q_u) was calculated from the stress-strain graphs [39].

5.5.2 Digital Image correlation

During the compressive testing, the stabilized samples were subjected to optical characterization of surface deformation using Digital Image Correlation (DIC). The patterns on the deforming sample surface were tracked using DIC and correlated to the strain measurements [2]. During UCS testing, a digital camera was placed securely in front of the samples to record a video of the sample during loading. Open source DIC Matlab software (NCorr) was used to obtain displacement and strain at a regular interval.

5.5.3 Water absorption test

The ability of the sample to absorb water was monitored by water absorption testing, according to AS 5101.5 [40]. The dry mass of the sample was recorded, followed by immersing it in standing water of 1 cm height for a period of 24 hours. The intake of water by the specimen was monitored continuously throughout the duration of testing.

5.5.4 Scanning Electron Microscopy (SEM)

A small portion of the specimen subjected to UCS testing was taken for microstructural analysis by employing SEM (Scanning Electron Microscopy). The samples were mounted on aluminium stubs and sputtered with 10 nm thick platinum coating to provide conductivity through the sample. The platinum coating was chosen since biopolymer is composed of carbon. A Zeiss Neon 40 EsB dual beam FESEM (Field Emission Scanning Electron Microscope) was employed for imaging at 15 kV and aperture size of 60µm.

5.5.5 Quantitative EDS mapping

Epoxy resin (Epofix) was poured under vacuum (Struers Cito Vac) on the samples placed in moulds and to mount them. The samples were polished by using Stuers Tegramin-30 in steps as depicted in Table 5.5. The exposed sample surface was coated with 10 nm thick platinum coating and EDS mapping was carried out using Zeiss Neon 40 EsB dual beam FESEM (Field Emission Scanning Electron Microscope) was employed for imaging at 15 kV and aperture size of 60µm using Aztech software.

Table 5. 5 Details of sample polishing for quantitative EDS mapping

Polishing step	Polishing cloth used	Lubricant	Time (min)
Step 1	Piano 220	Water	1

Step 2	Piano 1200	Water	2
Step 3	MD Chem	Colloidal silica (coarseness 0.04 micron)	2

5.5.6 Ammonia generation of samples with MICP

In MICP, the overall equilibrium equation is given (Eq.1). The high pH environment provided by the decomposition of urea triggers Eq.2 (DeJong et al., 2006). Each mole of carbonate generated by MICP also releases 2 moles Ammonia as a by-product (Eq. 4).

$$Ca^{2+} + CO_3^{2-} \overset{yields}{\longleftrightarrow} CaCO_3 \qquad (1)$$

$$Ca^{2+} + HCO_3^- + OH^- \overset{yields}{\longrightarrow} CaCO_3 + H_2O \qquad (2)$$

$$Ca^{2+} + 2HCO_3^- \overset{yields}{\longleftrightarrow} CaCO_3 + CO_2 + H_2O \qquad (3)$$

$$NH_2 - CO - NH_2 + 3H_2O \overset{yields}{\longrightarrow} 2NH_4^+ + 2OH^- + CO_2 \qquad (4)$$

$$Ca^{2+} + cell \overset{yields}{\longrightarrow} cell - Ca^{2+} \qquad (5)$$

$$Cell - Ca^{2+} + CO_3^{2-} \overset{yields}{\longrightarrow} cell - CaCO_3 \qquad (6)$$

The ammonia generated was calculated from chemical mass balancing using the equations mentioned previously (Equations 1-6). Since, the amount of calcium ions provided is known (from the molarity and amount of cementation media sprayed on the sample), the ammonia released during spraying on each sample can be calculated.

5.6 Results and discussion

5.6.1 Compaction characteristics

Table 5.6 presents the results of compaction on the biopolymer stabilized samples. It is observed that at 10% clay content the OMC has reduced by 20% in comparison to sample with 0% clay content. The Maximum Dry Density (γ_d) increased with the increase in clay dosage in a range of nearly 20%. The high OMC and low γ_d without the addition of clay are attributed to the viscous nature of biopolymer on exposure to water. Increase in clay content leads to two benefits: 1) more pores are filled with clay, and 2) formation of a clay-biopolymer composite with superior mechanical

performance. Evidently, although biopolymer content remained constant, the higher dosage of clay led to a higher γ_d. Hence, the superior performance was due to the combined pore filling as well as reinforcing effect with increased dosage of clay. For the road base samples, $\boldsymbol{\gamma_d}$ decreased with increasing biopolymer dosage as the clay content was constant in all the samples. The OMC increased with higher biopolymer content due to the hydrophilic nature of Xanthan gum biopolymer. As the road base material composed of a well graded system, the γd was higher than the sand-clay mixture. When stabilized with 0.5% xanthan gum, the road base material displayed lower OMC and higher γd than sand-clay mixtures.

Table 5. 6 Results of compacted samples

	Biopolymer	Clay	MDD (γ_d)	OMC
Sand	0	0	1.6	9.6
$C_0\,B_{0.5}\,M_0$	0.5	0	1.67	14.0
$C_{10}\,B_{0.5}\,M_0$	0.5	10	1.8	11.4
$C_{10}B_0\,M_0$	0	10	1.8	10.4
RB_0M_0	0	2.5	1.83	12.44
$RB_{0.5}M_0$	0.5	2.5	1.77	12.93
$RB1M_0$	1	2.5	1.76	13.10
$RB1.5M_0$	1.5	2.5	1.72	14

5.6.2 Stress-strain behaviour

Sand clay samples

The stress-strain behaviour of the stabilised columns is discussed by introducing the stabilisers sequentially. First, sand columns stabilised with clay alone with a surface treatment of MICP is investigated. MICP surface treatment has been performed on samples with 10% clay but no biopolymer. It is known that while the clay can stabilise sand to form free-standing columns, its strength is marginal. Fig 5.3 shows the stress-strain plots of the samples with varying MICP surface treatment. Clearly, MICP surface treatment resulted in a significant increase in strength (Fig 5.4). The strength went up with increasing MICP. It was 0.79 MPa at an M (mass of calcium carbonate by the mass of sand) of 2.4% but went up to 3.6 MPa when M was 12%. The failure strain also increased significantly with an increase in M.

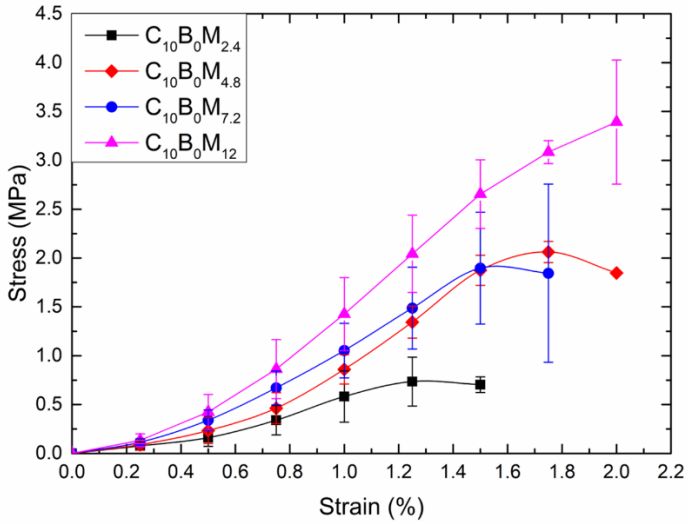

Fig 5. 3 Stress-strain behaviour of samples with MICP treatment cycles

Next, we observe the behaviour of columns with biopolymer added. The stress-strain behaviour of the samples is presented in Fig 5.4. When the sand is stabilised with 0.5% biopolymer alone ($C_0B_{0.5}M_0$) the strength is around 1MPa. Addition of 10% clay to the mix ($C_{10}B_{0.5}M_0$) increased both strength and stiffness of the columns. The effect of reinforcing biopolymer with varying clay content has been already reported by us (unpublished data). It is noticed that the clay particles reinforce the biopolymer and pack the voids in the sand. Thus, they have two beneficial effects. In this paper, we investigate the effect of MICP surface treatment on biopolymer stabilized samples. Samples stabilized with biopolymer and surface treated with 7.6% MICP ($C_0B_{0.5}M_{7.6}$) showed a substantial reduction in strength. It is noticed that xanthan gum softens with exposure to water. As MICP solutions are sprayed on the surface, the loss is strength due to the softening on the biopolymer outweighs the gain in strength due to MICP. It exhibits vulnerability of the biopolymer to moisture. It is noted earlier that clay can reduce the susceptibility of xanthan gum to moisture. The sample ($C_{10}B_{0.5}M_{14.3}$) demonstrates the synergy of clay, biopolymer and MICP. In this case, the strength of the column has increased by more than 100%, and the strain at failure has also risen by 60%. It is postulated that although initially, MICP on biopolymer degrades strength, after a few cycles of MICP, the degradation of a biopolymer is overridden by the increase in strength due to MICP. Beyond a threshold, MICP dramatically increases the strength of biopolymer stabilised columns. Comparing samples $C_{10}B_0M_{12}$ and $C_{10}B_{0.5}M_{14.3}$, even though the same strength was achieved, the synergistic effect can be observed during water absorption testing in section 5.6.5.

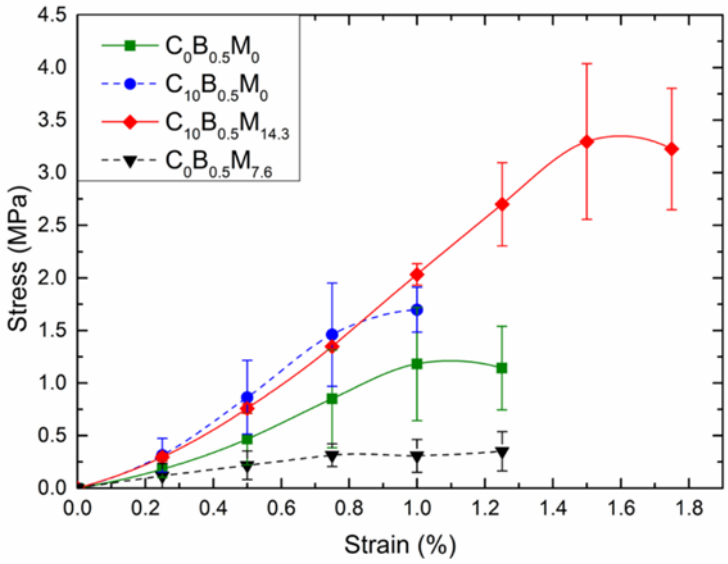

Fig 5. 4 Stress-strain behaviour of samples with various treatments

The effect of varying MICP on columns stabilised with clay and biopolymer is presented next. The average stress-strain plots for varying MICP with 0.5% biopolymer is presented in Fig 5.5. Both strength and maximum strain went up with the increase in MICP. The strength of the samples increased from 0.86 to 3.2 MPa, with an increase in M from 2.4 to 14.3%. The failure strain also went up by 100%. It should be noted that the degradation of the biopolymer happened only in the first cycles of MICP. From the next cycle, MICP resulted in monotonic improvement of performance. Thus, enough calcium carbonate was deposited to overcome the softening effect of biopolymer due to the water present in the MICP solution. This result clearly demonstrates the synergy between clay, biopolymer and MICP.

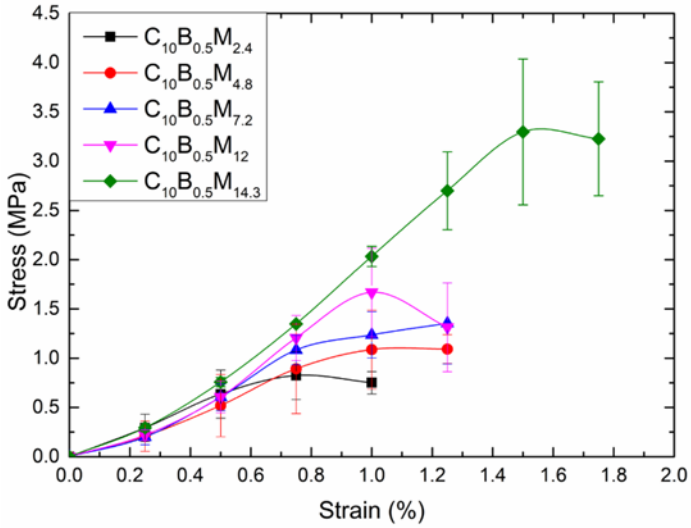

Fig 5. 5 Stress-strain behaviour of clay-biopolymer samples with MICP treatment cycles

Road base samples

For road base material treated with MICP, the ultimate strain improved by more than 70% indicating a higher ductility when compared to untreated road base (Fig 5.6). The unstabilised road base recorded a compressive strength of 1.07 MPa while MICP treated road base recorded a value of 3.5 MPa (Fig 5.6). This dramatic improvement is most likely due to high porosity of evenly distributed coarse and fine particles in the surface, allowing a uniform layer of calcium carbonate precipitates to be formed. It can be noticed that the MICP treated sample achieved a higher stiffness indicating substantial degree of cementation. Thus, MICP surface treatment was effective in improving the strength, stiffness, and ultimate strain of road base. The strength increase can be attributed to the formation of MICP crust which increased the confinement of the unstabilsed samples. Similar results have been reported in rammed earth blocks stabilised with MICP surface treatment (Porter et al., 2018a).

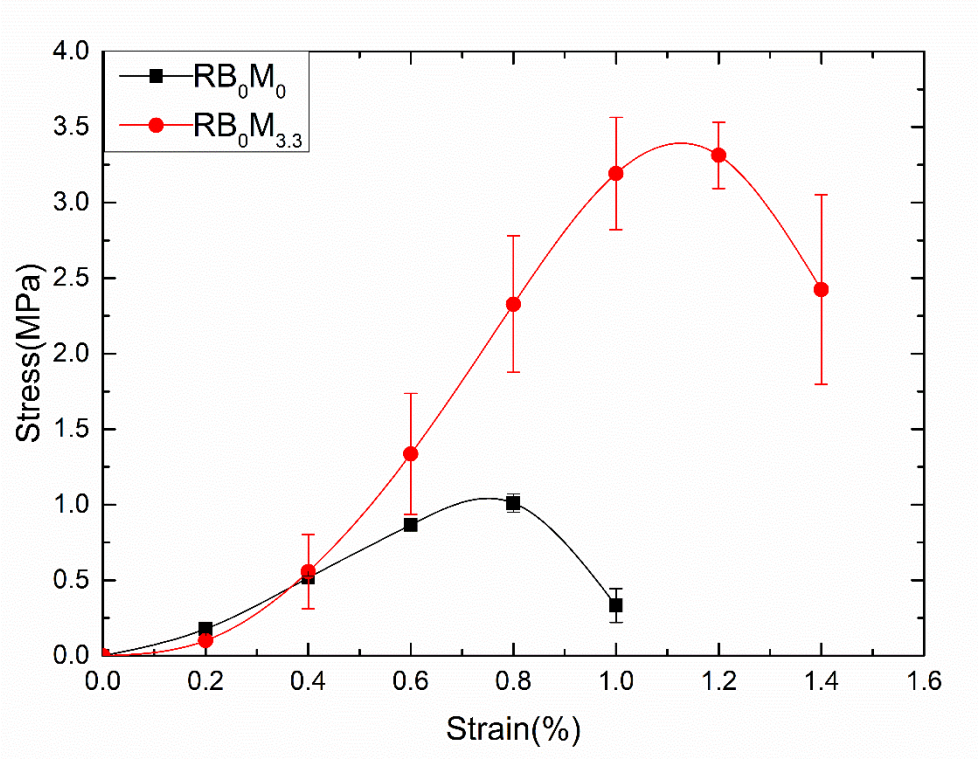

Fig 5. 6 Stress-strain behaviour and of road base material

Road base material stabilized with biopolymer

In general, xanthan gum treated road base exhibited significant improvement in compressive strength, ultimate strain with an increase of xanthan gum content (Fig 5.7). Sample $RB_{1.5}M0$ can withstand 60% higher ultimate strain in comparison to $RB_{0.5}M_0$ samples. The ultimate strain increases with Xanthan gum content indicating that biopolymer has developed bonds of cohesive nature between the soil particles. This depicts that strain capacity is governed by the polymer-particle matrix.

Road base with constant MICP and varying biopolymer concentration

In the case of Xanthan gum stabilised samples, a significant improvement in compressive strength, stiffness and ultimate strain was observed after MICP surface treatment (Fig 5.7). When the xanthan gum stabilised road base samples were further treated with MICP, UCS increased by more than 100%. Samples $RB_{0.5}M_{3.3}$ and $RB_{1.5}M_{3.3}$ samples were able to take nearly 1.5% ultimate strain. Additionally, stiffness of the MICP treated samples improved by more than 50% when compared to corresponding samples treated with biopolymer only. Ostensibly, MICP treatment reinforces the stabilization by Xanthan gum in a very effective manner. The mechanical properties of stabilized road base samples are shown in Fig 5.8. The UCS of samples increased with biopolymer content as well as MICP surface treatment. The trend is secant modulus was less obvious for the samples treated with varying biopolymer content.

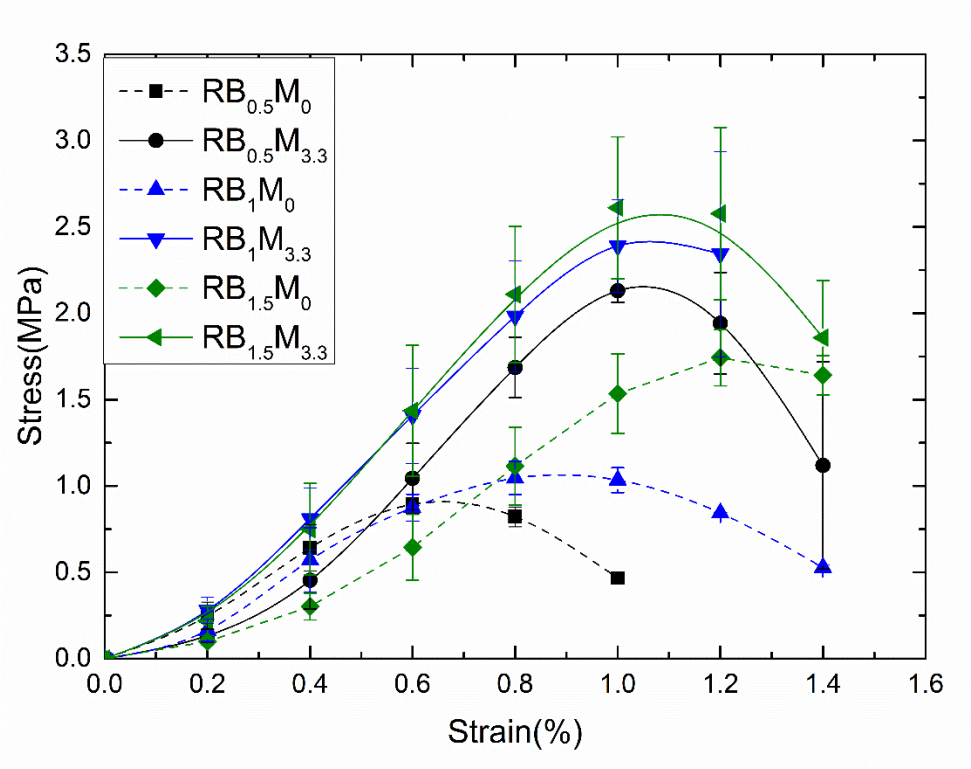

3805

3806 *Fig 5. 7 Stress-strain of biopolymer stabilized samples with MICP treatment*

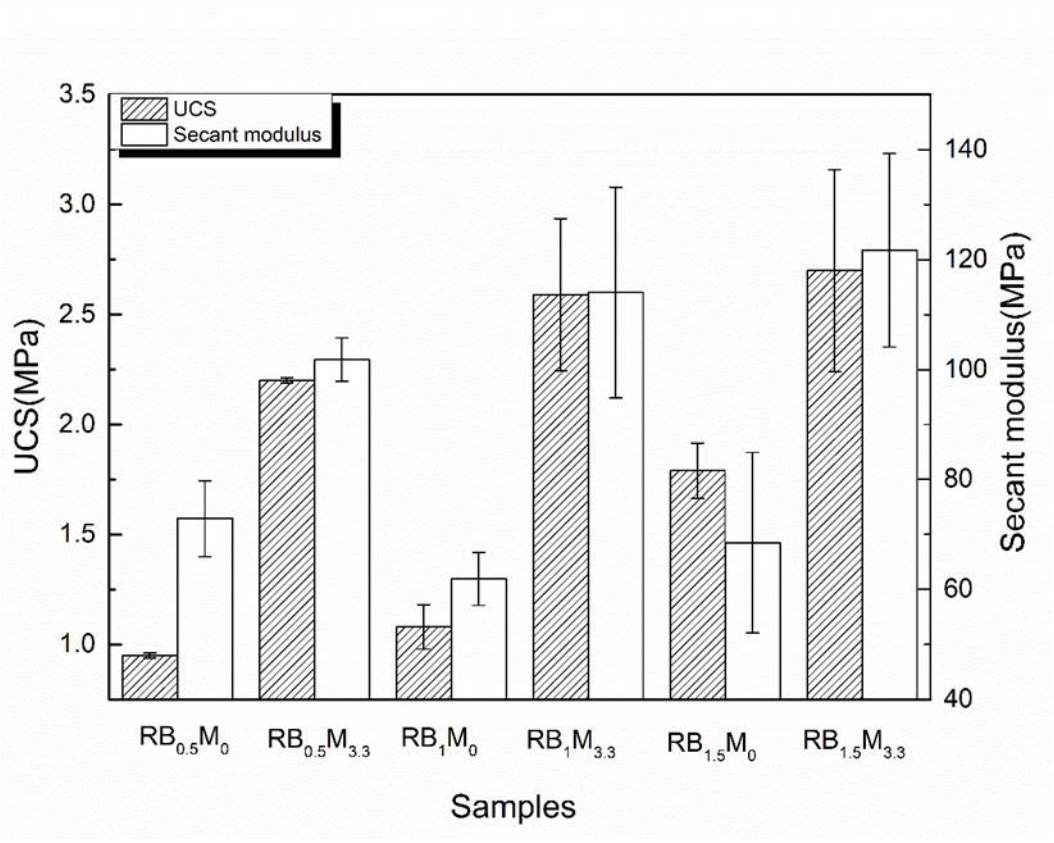

3807

3808 *Fig 5. 8 Mechanical properties of the stabilized road base material*

5.6.2 Mechanical properties with varying MICP

The previous Section has established that MICP improves the performance of both clay and clay-biopolymer columns. A relationship between the mechanical performance parameters and M% is attempted here. These relationships would be useful in designing the stabilisation systems with a combination of biopolymers.

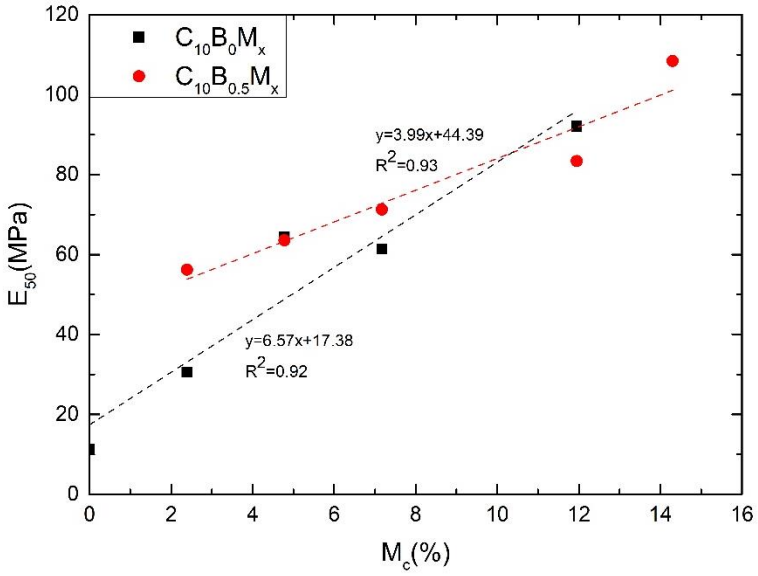

Fig 5. 9 E_{50} of $C_{10}B_0M_x$ and $C_{10}B_{0.5}M_x$ samples with varying M_c

Fig 5.9 shows the modulus at 50% strain (E_{50}) of $C_{10}B_0M_c$ samples with an increasing c. A linear fit between M_c and E_{50} is performed, and an R^2 value of 0.93 was obtained. The slope of the line is the rate of increase in E_{50} with M%. E50 increases at a rate of 6.6 MPa/M%. The E_{50} of samples $C_{10}B_{0.5}M_c$ with varying c is shown in Fig 5.9. A linear fit between $E_{50}$and M_c gave an R^2 value of 0.93. The rate of change of E_{50} is around 10 MPa/M%. This rate is higher than that obtained in case of the samples without clay—the addition of clay results in better mechanical performance than the sand alone.

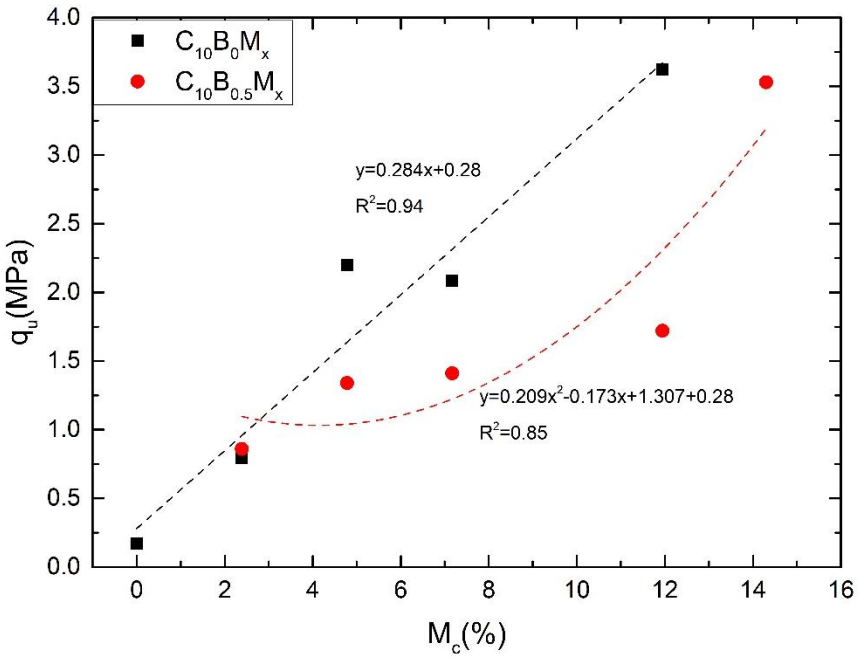

Fig 5. 10 q_u of $C_{10}B_0M_x$ and $C_{10}B_{0.5}M_x$ samples with varying M_c

Fig 5.10 shows the variation of compressive strength (q_u) with M%. In this case, too, a linear fit resulted in an R^2 0.94. The rate of increase in q_u is predicted to be 0.28 MPa/M%. These values are useful in designing stabilization systems for target performance. However, it may be noted that these values are valid within the range of MICP used in this investigation, and their accuracy is uncertain when extrapolated beyond that range. The variation of q_u with M% can be observed in Fig 5.1. In this case, an even higher rate of increase of q_u with M% is observed. The rate is increase increases with M%. Thus, a quadratic fit between q_u and M% is attempted, and an R^2 of 0.85 was obtained. The relatively lower R^2 value is due to a drastic increase in the q_u values at a higher percentage of MICP.

5.6.3 Damage progression and failure modes

Sand clay samples

The samples were observed for progression of damage and failure modes during UCS testing. Fig 5.11 shows the samples with no biopolymer with increasing level of MICP. It is noted that initially local of the samples was the cause of failure. This is due to uneven distribution of cementation over the samples. As the M% increased, more uniform distribution of cementation led to the global failure of the samples. A dramatic increase in the failure stress was also observed for these samples. Fig 5.11 shows the failed samples with biopolymer with increasing MICP, $C_{10}B_{0.5}M_c$. At lower levels of

MICP surface spalling leads to failure of the sample. It may be recalled that water in the MICP solution causes degradation of the biopolymer at the surface of the samples. Thus, these samples exhibit spalling. However, as the M% crosses a threshold, the degradation of a biopolymer is compensated by the cementation due to MICP. Thus, surface spalling is arrested, and a global failure is obtained.

Fig 5. 11 Failure patterns of the samples

DIC analysis was performed on all the samples after UCS testing to observe the strain distribution in the sample with advancing loads. The areas of high-stress concentration in sample $C_{10}B_{0.5}M_{12}$ (shown as an example) are visible in the vertical strain images obtained using DIC (Fig 5.12). Ultimately, they coincide with the development of cracks leading to failure of the samples. Therefore, DIC is a useful tool to gain insights into local stress concentrations during loading.

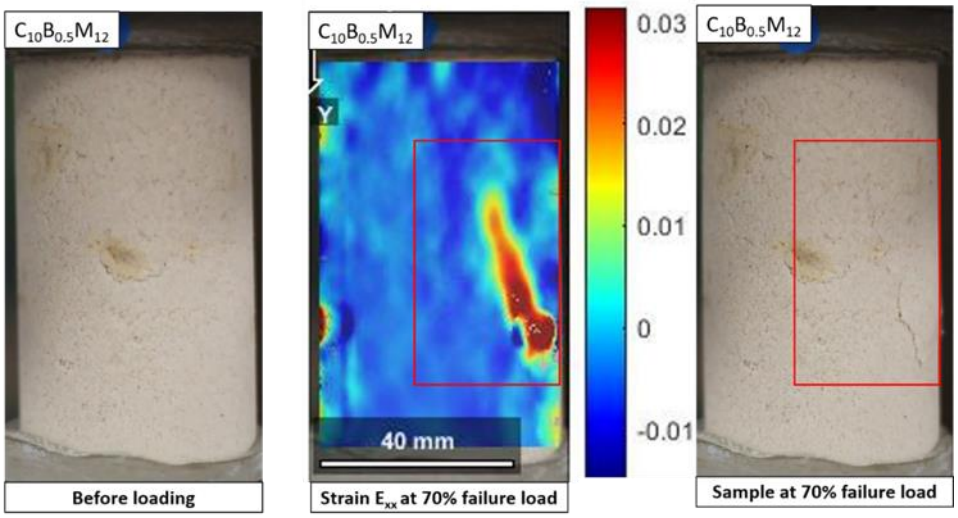

Fig 5. 12 DIC analysis on $C_{10}B_{0.5}M_{12}$ samples

Road base samples

Sample	Sample image	Strain at 70% of failure load (Exx)	Failure image	Strain at failure (Exx)
RB_0M_0		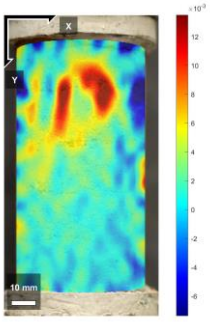		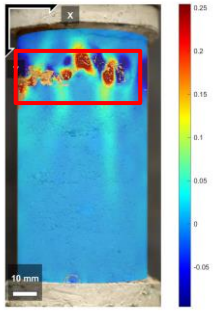
$RB_0M_{3.3}$		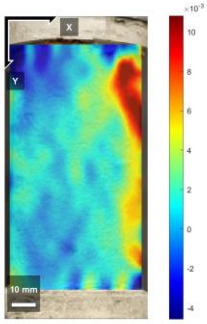		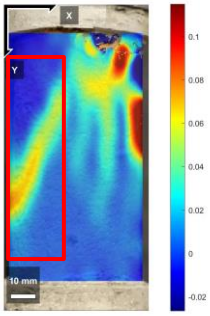

$RB_{0.5}M_0$		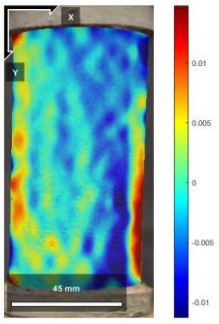		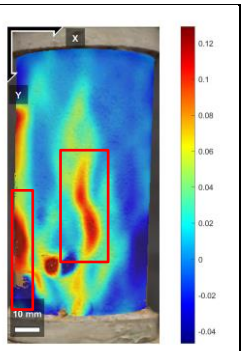
$RB_{0.5}M_{3.3}$		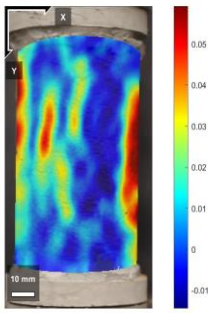		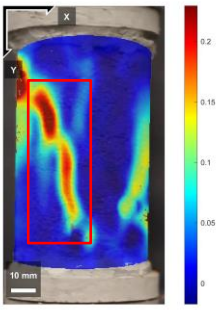
RB_1M_0		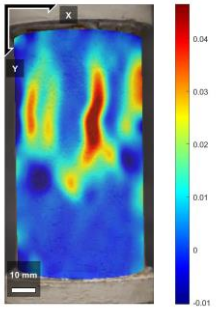		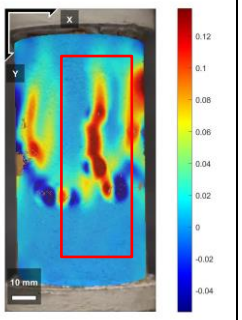
$RB_1M_{3.3}$		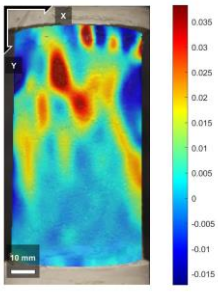		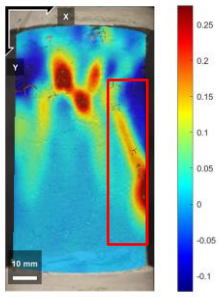
$RB_{1.5}M_0$		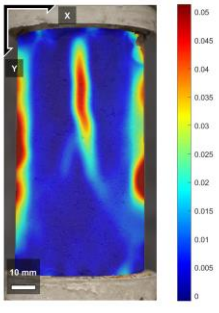		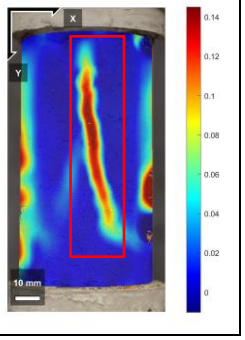

$RB_{1.5}M_{3.3}$		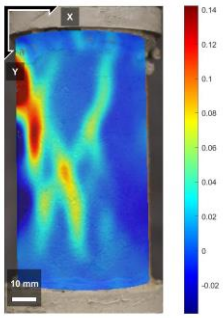		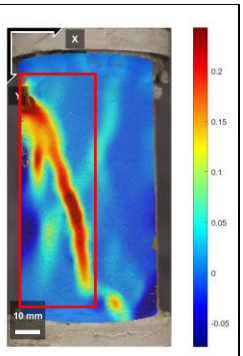

Fig 5. 13 DIC analysis on road base samples

The failure modes of the samples were recorded to assess any correlation between the sample type and failure modes. Two modes of failure were noted: (1) Vertical splitting and (2) Diagonal cracking (Fig 5.13). In vertical splitting, crack started from either top or bottom of the sample and developed through middle, ultimately splitting in to two or more pieces. In Diagonal cracking, crack started from one side of the samples, ultimately developing a slip plan of failure. No correlation was found between the failure mode and the type of samples.

Strain build up occurring in regions of local stress concentrations on surface of the samples are shown in Fig 5.13. At around 70% of the total load, these regions of strain build were clearly plotted in the DIC images which is before the cracks were visible from the samples. These regions are where crack starts propagating leading to ultimate failure of the sample.

Relative performance of the soils: Strength

The maximum strength of MICP treated sand-clay mixture was 3.6 MPa when M was 12%. The failure strain also increased significantly with an increase in M. However, the road base recorded a compressive strength of 3.5 MPa when M was 3.3%. The significant strength is attributed to the well-graded road base samples which displayed an unstabilzied compressive strength of 1MPa.For the sand-clay samples stabilized with xanthan gum, the strength of the samples increased from 0.86 to 3.2 MPa, with an increase in M from 2.4 to 14.3%. For road base samples treated with xanthan gum and MICP, the UCS of samples increased with biopolymer content at an M of 3.3%. During DIC, two modes of failure were common for the road base samples: (1) Vertical splitting and (2) Diagonal cracking. However, in sand-clay mixtures, surface spalling leads to failure of the sample at lower levels of MICP.

5.6.4 Water absorption

Sand clay samples

The stabilized columns were tested for water absorption. Samples with just clay ($C_{10}B_0M_0$) collapsed immediately upon exposure to water during the absorption testing. This demonstrates that clay alone cannot prevent collapse due to water absorption. Even MICP surface treatment ($C_{10}B_0M_c$) was unable to arrest the collapse of these samples. This may be due to the non-uniform distribution of MICP within the sample due to spraying. This illustrates the necessity of a primary stabilizer to hold the particles together throughout the sample to avoid collapse due to excessive water absorption.

In samples $C_{10}B_{0.5}M_c$, stabilized by mixing the biopolymer, the water absorption was significantly reduced as the samples were able to avoid collapse during testing. Our previous investigation with biopolymer alone as the stabilizer revealed that the hydrophilic nature of xanthan gum leads to excessive water absorption that makes it susceptible to moisture ingress hindering its successful application in saturated ground conditions (unpublished data). Sand samples without clay collapsed immediately upon exposure to water. Clay reinforced biopolymer samples were more resistant to water ingress (unpublished data). It was also observed that exposure to water leads to swelling and subsequent strength reduction in the samples. In this investigation, we observe the effect of MICP surface treatment on clay reinforced biopolymer samples. Fig 5.10 shows that MICP surface treatment significantly reduces the damage caused to the biopolymer due to water absorption. It is noticed that samples initially absorbed water at a significantly higher rate in the initial minutes of exposure. However, the peak absorption was reached swiftly, and no more water was absorbed even after 24 hours of exposure. The water absorption value decreased monotonically with increasing M%. The sample $C_{10}B_{0.5}M_{14.3}$ displayed the lowest water absorption of 8%, which is 50% lower than that with no MICP treatment. The effect of the surface treatment can be clearly visualised in Fig 5.11. The sample without surface treatment has a uniformly soft cross-section. MICP surface treatment has created an annular layer that prevents water absorption. Previous studies have also reported a reduction in water absorption due to MICP surface treatment on rammed earth blocks [34]. However, this study demonstrates the formation of the annular layer that protects the inner core. Numerous studies have reported that the main factor limiting the

application of biopolymer for soil stabilization is its susceptibility to moisture attack. This investigation successfully addresses the problem by combining MICP surface treatment with biopolymer core.

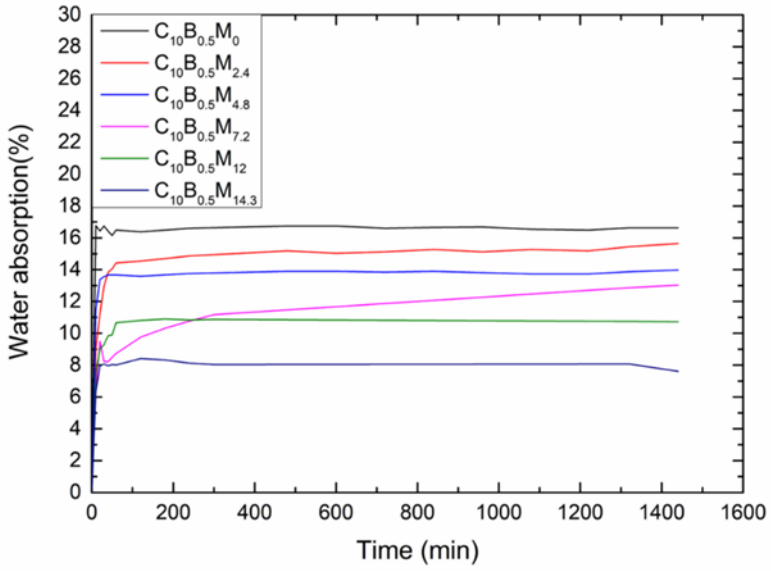

Fig 5. 14 Water absorption of $C_{10}B_{0.5}M_c$ samples

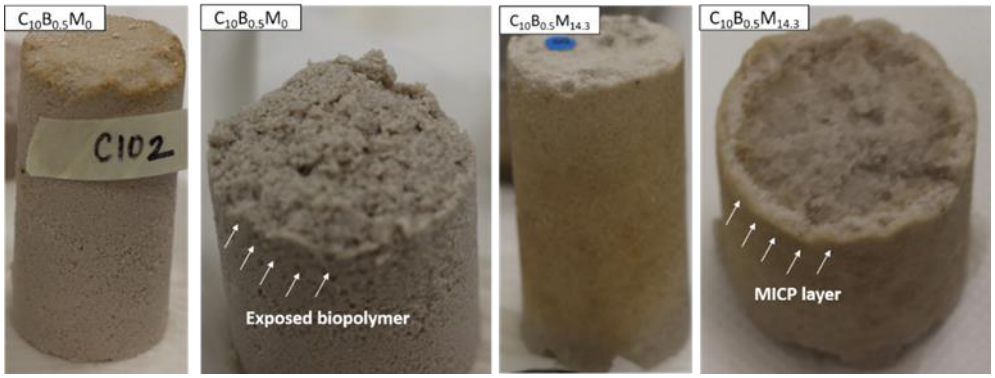

Fig 5. 15 Condition of samples with and without MICP layer after water absorption

The effect of M% on water absorption is calibrated in Fig 5.12. The resistance to water absorption is plotted with M%. The relationship is linear with an R^2 value of 0.92. The rate of reduction in water abortion is around 1%/M%. The previous Section has demonstrated that the strength of samples is highest when clay, biopolymer and MICP are combined. This Section notes that the resistance to water too goes up substantially with the combined action of clay, biopolymer and MICP. Hence, their synergistic effect is evidenced.

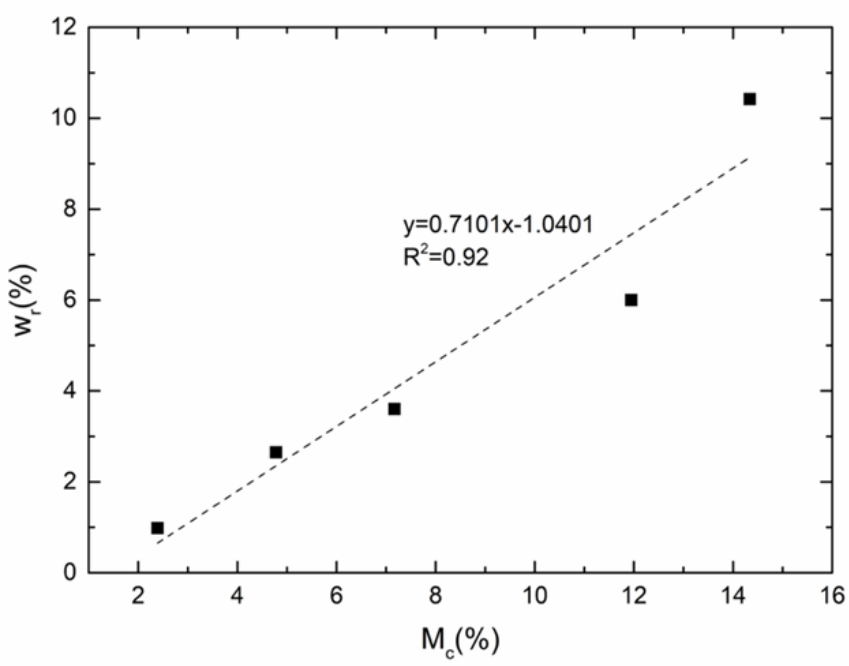

Fig 5. 16 w_r of $C_{10}B_{0.5}M_c$ samples with varying M_c

Road base samples

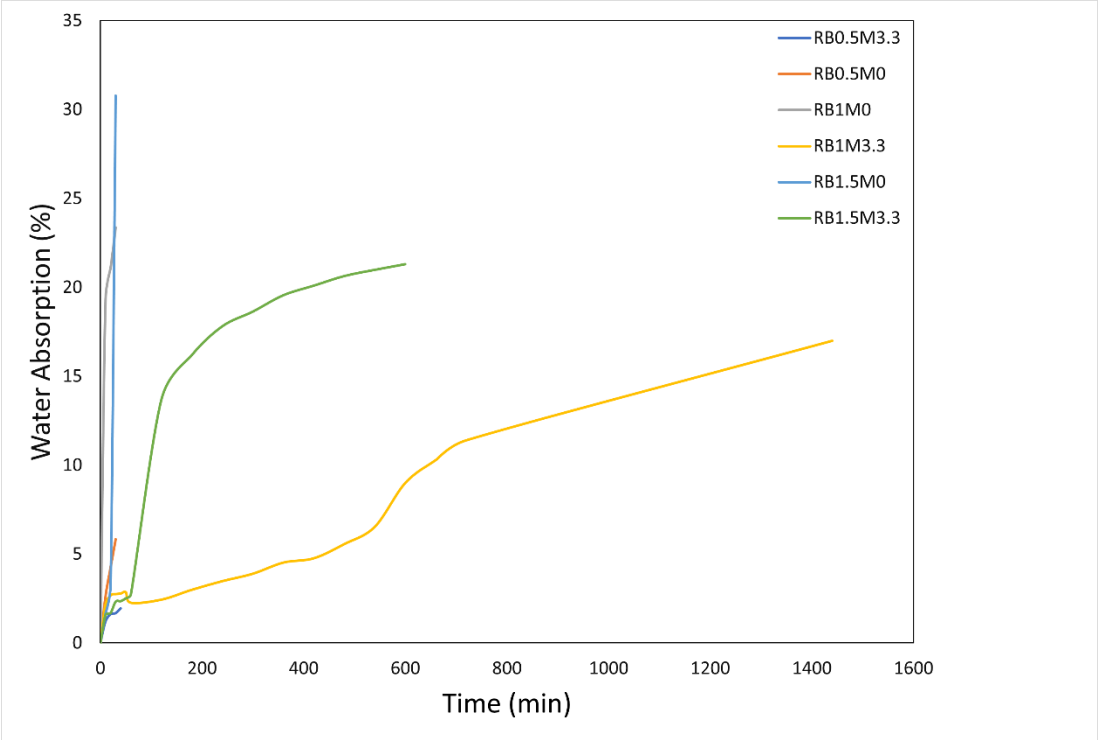

Fig 5. 17 Water absorption of road base samples

During testing, sample RB_0M_0 collapsed immediately upon exposure to water. The lack of stabilizer is responsible for this behaviour. However, as anticipated, the biopolymer stabilized samples treated with MICP demonstrated a considerable

resistance to water absorption (Fig. 17). In general with varying content of biopolymer, the percentage of water absorbed increases for higher dosage of biopolymer. This results which are not reported hitherto demonstrates the hydrophilic nature of Xanthan gum biopolymer. Additionally, at 30 minutes, the water absorbed by MICP treated samples is considerably less when compared XG samples without MICP. The treatment of MICP clearly has a stabilizing effect against the exposure to moisture. The reason behind this resistance to water absorption is likely to be due to calcium carbonate precipitation in the pore spaces of surface layers of the sample. These results concur with previous studies which has used MICP surface treatment to reduce water absorption (Porter and Dhami 2018; Porter et al. 2018). To sum up, increase of XG content increases the water absorption while MICP treatment is effective in reducing the water absorption and collapse. The use of biopolymer as a stand-alone stabilizer for road base materials is not advisable as they are prone to moisture degradation. Hence, MICP surface coating is a sustainable solution to overcome the limitations of biopolymer stabilizer.

Relative performance of the soils: Durability/Water absorption

During water absorption testing, in samples C10B0.5Mc, the water absorption was significantly reduced as the samples were able to avoid collapse during testing. For sand-clay mixtures, the water absorption value decreased monotonically with increasing M%. The sample C10B0.5M14.3 displayed the lowest water absorption of 8%, which is 50% lower than that with no MICP treatment. For the road base samples in general, the percentage of water absorbed increases for higher dosage of biopolymer. To sum up, increase of xanthan gum content increases the water absorption while MICP treatment is effective in reducing the water absorption and collapse. The use of biopolymer as a stand-alone stabilizer for road base materials is not advisable as they are prone to moisture degradation. Therefore, MICP surface coating is a sustainable solution to overcome this limitation.

5.6.5 Micrographic analysis

Fig 5.13 shows the micrographs of $C_{10}B_{0.5}M_0$ samples. These samples contain sand, clay, and biopolymer. They reveal that biopolymer xanthan gum formed a coating over the sand particles and bonded them together when the biopolymer film connected the particles together. Considerable void spaces have been observed between the grains

that have contributed to the high-water permeability of the material. It may be noted that these samples did not get any MICP treatment.

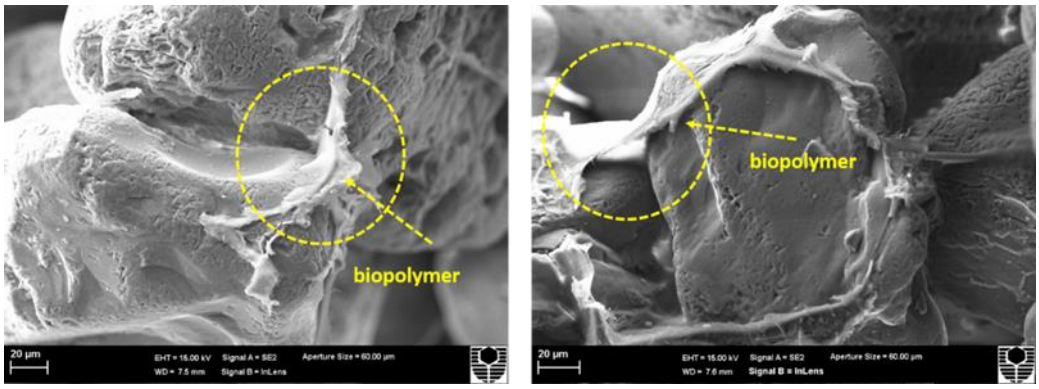

Fig 5. 18 SEM micrographs of $C_{10}B_{0.5}M_0$ sample

Fig 5.14 shows the surface of $C_{10}B_{0.5}M_c$ samples that received MICP surface treatment in addition to the biopolymer and clay stabilization. Clear evidence of rhombohedral calcite crystal formation is obtained. The MICP surface treatment filled the inter-granular voids and protected the biopolymer stabilized core. Thus, the degradation of biopolymer due to exposure to water could be avoided.

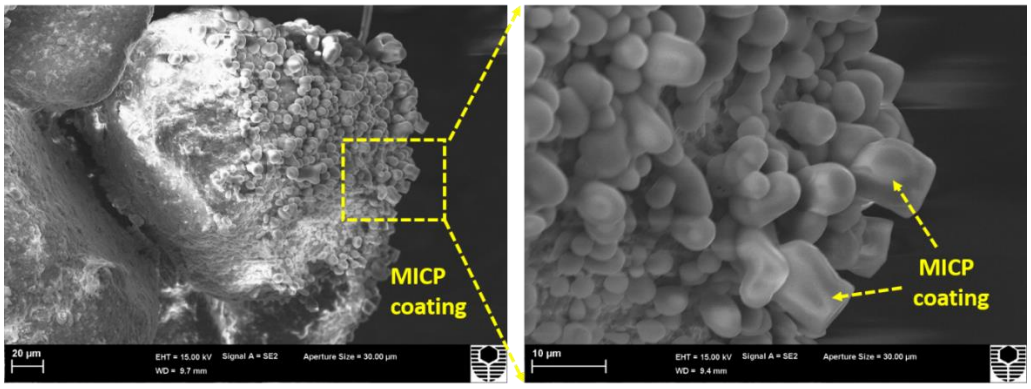

Fig 5. 19 SEM micrographs showing the surface layer of calcite

Quantitative EDS was performed on polished samples to gain further insights into the elemental composition of the constituents. The elemental maps of each sample were generated by assigning a specific colour to each element. Fig 5.15 a-c are the maps for sample $C_{10}B_{0.5}M_0$ Fig 5.15a presents the greyscale map of the specimen. The particles of sand and the cementing material can be clearly identified. In Fig 5.15b the coloured map is presented. The dominant colour is cyan that signifies silicon present in the sand. Thus, sand particles are shown in cyan. The clay particles are much smaller in size, and they contain aluminium in addition to silicon. Aluminium is presented in purple. Thus, the areas in purple signify the abundance of clay—the contours of the purple

match with that of the cementing material in Fig 5.15a. Clearly, the clay particles are embedded in the biopolymer. Clay (composed of alumina-silicates) played the role of a filler closing in the pore spaces as well as coating the sand grains as observed in Fig 5.15a-c. It is expected that the biopolymer will follow the same distribution as it forms a matrix with clay particles due to its chemical compatibility with clay. The microscopic maps of sample $C_{10}B_{0.5}M_{14.3}$ are in Fig 5.15d-f. In this case. Calcium is mapped in maroon colour. Thus, maroon signifies the presence of calcium carbonate. Clearly, calcite has formed on top of the clay-reinforced biopolymer matrix, thereby strengthening the bonds further as well as preventing water penetration. Noticeably, calcite was formed around the grain surface and bridged the individual sand grains as expected.

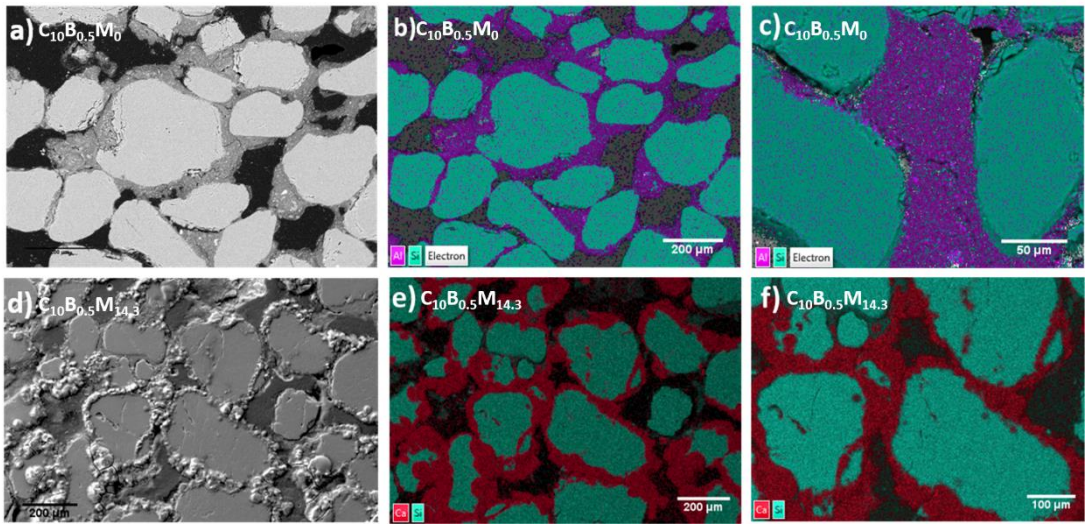

Fig 5. 20 EDS mapping of sample a), b) and c) sample $C_{10}B_{0.5}M_0$ and d), e) and f) sample $C_{10}B_{0.5}M_{14.3}$

5.6.6 Ammonia generation

In MICP, the overall equilibrium equation is given (Eq.1). The high pH environment provided by the decomposition of urea triggers Eq.2 [41]. Each mole of carbonate generated by MICP also releases 2 moles Ammonia as a by-product (Eq. 4).

$$Ca^{2+} + CO_3^{2-} \overset{yields}{\longleftrightarrow} CaCO_3 \qquad (1)$$

$$Ca^{2+} + HCO_3^- + OH^- \overset{yields}{\longrightarrow} CaCO_3 + H_2O \qquad (2)$$

$$Ca^{2+} + 2HCO_3^- \overset{yields}{\longleftrightarrow} CaCO_3 + CO_2 + H_2O \qquad (3)$$

$$NH_2 - CO - NH_2 + 3H_2O \overset{yields}{\longrightarrow} 2NH_4^+ + 2OH^- + CO_2 \qquad (4)$$

$$Ca^{2+} + cell \overset{yields}{\longrightarrow} cell - Ca^{2+} \qquad (5)$$

$$Cell - Ca^{2+} + CO_3^{2-} \xrightarrow{yields} cell - CaCO_3 \quad (6)$$

Ammonia is a harmful gas that restricts the applicability of MICP. This Section compares the techniques where MICP alone is used for cementation vis-à-vis biopolymer-MICP combination. The amount of ammonia released (a_r) in the process of cementation for achieving similar unconfined compression strength is presented in Fig 5.16. The results of cementing sand columns with MICP alone, as obtained by us in Kashizadeh, Mukherjee at al. (unpublished data) is utilised. The graph reveals that to achieve the same targeted strength for sand columns of the same volume (196.25 cc), the generation of ammonia is significantly higher for the sand samples treated with MICP alone. The addition of an alternate stabilizer such as biopolymer-reinforced clay, significantly helped in reducing the ammonia release as a lower amount of MICP was required to achieve a similar strength. This was a significant advantage of using a synergistic system consisting of biopolymer and MICP. This study is the first attempt to address the issue of ammonia release in MICP by synergising it with another bio-based stabilizer without compromising on its mechanical performance. However, a more comprehensive estimate of the biopolymer manufacturing would be necessary to have a thorough understanding of the benefits of the combined process.

Table 5. 7 Estimate of ammonia generation

Sample	Days of MICP treatment	Mass of $CaCO_3$/ Mass of sand (%)	UCS (MPa)	Ammonia generated a_r (g)	Ammonia generated/ MPa
MICP Sand (SM)	12	13.38	1.03	14.6	0.02
	21	23.41	1.84	29.2	0.02
	33	36.78	2.22	43.8	0.03
	42	46.82	2.59	51.1	0.03
	53	59.08	3.44	65.7	0.03
MICP Clay Biopolymer Sand (SBCM)	8	2.4	0.86	0	0
	16	4.8	1.34	7.3	0.01
	24	7.2	1.41	7.3	0.01
	40	12.0	1.72	14.6	0.01
	48	14.3	3.53	14.6	0.01
Road base MICP Biopolymer	14	3.3	2.20	7.3	0.005
	14	3.3	2.59	7.3	0.004
	14	3.3	2.70	7.3	0.004

(RBM)

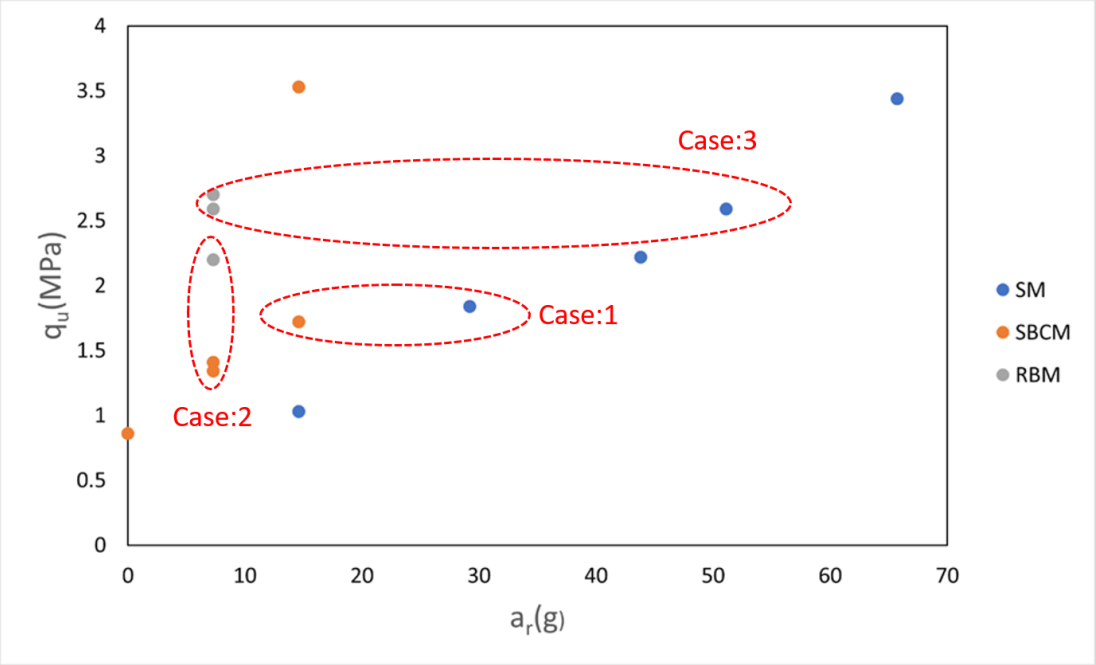

Fig 5. 21 Relation between q_u and a_r of the stabilized samples

Relative performance of soils: ammonia generation

As observed from Fig. 21, comparisons can be made between ammonia generation and q_u of samples. For samples SBCM and SM (Fig 21. Case 1), for a target compressive strength of ~1.5-2 MPa, the ammonia generated was twice for the latter in comparison to the former. For samples SBCM and RBM (Fig 21. Case 2), if the amount of ammonia generated was 5g, the q_u of former was ~1.5 MPa while that of latter was v2.25 MPa. The most significant impact was observed in samples SM and RBM (Fig 21. Case 3), where for a target q_u of ~2.5 MPa, the ammonia generated by the former was 5 times as that of the latter. Therefore, the addition of biopolymer was able to significantly lower the ammonia generated due to MICP process, in order to achieve a target compressive strength. It was observed that the road base samples stabilized with biopolymer resulted in significant ammonia reduction without compromising on the compressive strength.

5.7 Conclusions

This study was the first attempt to synergise biopolymer and MICP technology to overcome their individual limitations. Previous research has revealed that biopolymers are capable of stabilising soil, but they are prone to degradation on exposure to water.

MICP too can stabilise the soil. They can resist degradation due to water, but they release a considerable amount of harmful ammonia gas. Combining the technologies helped in reducing the water susceptibility of the biopolymer samples in addition to a significant reduction in ammonia generation without compromising on the mechanical performance of the stabilized samples. The results of this study will encourage the application of bio-based stabilisers for soil stabilisation applications. Some significant contributions of the research are:

- In general, xanthan gum treated road base exhibited significant improvement in compressive strength, stiffness, and ultimate strain with increasing biopolymer dosage from 0.5%-1.5%.
- For samples $C_{10}B_0M_c$, the secant modulus increased from 30.5 MPa to 92 MPa with an increase in M_c from 2-12% and the nature of variation is linear.
- The increase in unconfined compressive strength of samples $C_{10}B_0M_c$ ranged from 0.79 MPa to 3.6 MPa with an increase in M_c from 2-12%; the nature of variation is linear.
- The increase in unconfined compressive strength of samples $C_{10}B_{0.5}M_c$ varied from 0.86 MPa to 3.6 MPa with an increase in M_c from 2 to 14%, and the nature of variation is quadratic.
- The use of biopolymer as a stand-alone stabilizer for road base materials is not advisable as they are prone to moisture degradation. Hence, MICP surface coating is a sustainable solution to overcome this limitation of biopolymer.
- The reduction in water absorption of samples $C_{10}B_{0.5}M_c$ ranged between 1-10% with an increase in M_c from 2 to 14% with a linear relationship.
- Microscopic investigations revealed the synergistic nature of biopolymer and MICP in the stabilisation of samples which provided superior mechanical and durability performance.
- Synergising biopolymer with MICP surface treatment helped in significantly lowering the amount of ammonia released during the MICP process, to achieve a target strength.

The assumption that UCS samples are homogeneous and representation should be taken into consideration during the interpretation of the results. In order to gain further insights into MICP mechanism on the performance of the stabilized samples, samples

with varying levels of MICP outer core should be tested. Further, in addition to water absorption testing, permeability tests are also recommended for future work. Ultimately, permeating bacterial solutions into the sample, which is capable of producing both bacterial biopolymer and MICP would be the ideal way to achieve a synergistic system

5.8 Data availability statement

All data, models, and code generated or used during the study appear in the submitted article.

5.9 Acknowledgements

The authors would like to acknowledge the contribution of Curtin International Postgraduate Research Scholarship (CIPRS) in supporting this research. Part of this research was undertaken using the instrumentation FESEM (Field Emission Scanning Electron Microscope) and Tescan Mira3 VP-FESEM at the John de Laeter Centre, Curtin University. We also acknowledge the use of equipment, scientific and technical assistance of the Curtin University Electron Microscope Facility, which has been partially funded by the University, State and Commonwealth Governments.

5.10 References

1. Garbin, J., Edward J, et al., *Mass Stabilization for Settlement Control of Shallow Foundations on Soft Organic Clayey Soils*, in *Geo-Frontiers 2011: Advances in Geotechnical Engineering*. 2011. p. 758-767.
2. Porter, H., N.K. Dhami, and A. Mukherjee, *Sustainable road bases with microbial precipitation.* Proceedings of the Institution of Civil Engineers-Construction Materials, 2018. 171(3): p. 95-108.
3. Gnanendran, C. and D.K. Paul, *Fatigue characterization of lightly cementitiously stabilized granular base materials using flexural testing.* Journal of Materials in Civil Engineering, 2016. 28(9): p. 04016086.
4. Fatehi, H., et al., *A novel study on using protein based biopolymers in soil strengthening.* Construction and Building Materials, 2018. 167: p. 813-821.
5. Gorakhki, M.H. and C.A. Bareither, *Unconfined compressive strength of synthetic and natural mine tailings amended with fly ash and cement.* Journal of Geotechnical and Geoenvironmental Engineering, 2017. 143(7): p. 04017017.

6. Bo, M.W., et al., *Densification of land reclamation sands by deep vibratory compaction techniques.* Journal of Materials in Civil Engineering, 2014. 26(8): p. 06014016.
7. Mujah, D., M.A. Shahin, and L. Cheng, *State-of-the-Art Review of Biocementation by Microbially Induced Calcite Precipitation (MICP) for Soil Stabilization.* Geomicrobiology Journal, 2017. 34(6): p. 524-537.
8. Tennant, A.G., C.D. Foster, and B.V. Reddy, *Detailed experimental review of flexural behavior of cement stabilized soil block masonry.* Journal of Materials in Civil Engineering, 2016. 28(6): p. 06016004
9. Chittoori, B.C., A.J. Puppala, and A. Pedarla, *Addressing clay mineralogy effects on performance of chemically stabilized expansive soils subjected to seasonal wetting and drying.* Journal of Geotechnical and Geoenvironmental Engineering, 2018. 144(1): p. 04017097.
10. Asi, I.M., *Stabilization of sebkha soil using foamed asphalt.* Journal of materials in civil engineering, 2001. 13(5): p. 325-331.
11. Soleimanbeigi, A., T. Edil, and C. Benson, *Evaluation of fly ash stabilization of recycled asphalt shingles for use in structural fills.* Journal of materials in civil engineering, 2013. 25(1): p. 94-104.
12. He, J., et al., *Shear strength of stabilized clay treated with soda residue and ground granulated blast furnace slag.* Journal of Materials in Civil Engineering, 2019. 31(3): p. 06018029.
13. Kuntikana, G. and D. Singh, *Contemporary Issues Related to Utilization of Industrial Byproducts.* Advances in Civil Engineering Materials, 2017. 6(1): p. 444-479.
14. Puppala, A.J., et al., *Studies on sulfate-resistant cement stabilization methods to address sulfate-induced soil heave.* Journal of geotechnical and geoenvironmental engineering, 2004. 130(4): p. 391-402.
15. McCutcheon, J., et al., *Beachrock formation via microbial dissolution and re-precipitation of carbonate minerals.* Marine Geology, 2016. 382: p. 122-135.
16. McCutcheon, J., et al., *Building biogenic beachrock: Visualizing microbially-mediated carbonate cement precipitation using XFM and a strontium tracer.* Chemical Geology, 2017. 465: p. 21-34.

17. Dunphy, C.M., et al., *Structure and stability of the coral microbiome in space and time.* Scientific Reports, 2019. 9(1): p. 6785.
18. Proemse, B.C., et al., *Stromatolites on the rise in peat-bound karstic wetlands.* Scientific Reports, 2017. 7(1): p. 15384.
19. Suosaari, E.P., et al., *New multi-scale perspectives on the stromatolites of Shark Bay, Western Australia.* Scientific Reports, 2016. 6: p. 20557.
20. DeJong, J.T., et al., *Bio-mediated soil improvement.* Ecological Engineering, 2010. 36(2): p. 197-210.
21. Achal, V. and A. Mukherjee, *A review of microbial precipitation for sustainable construction.* Construction and Building Materials, 2015. 93: p. 1224-1235.
22. Achal, V., et al., *Biomineralization for sustainable construction – A review of processes and applications.* Earth-Science Reviews, 2015. 148: p. 1-17.
23. Ramachandran, A.L., et al., *Understanding and creating biocementing beachrocks via biostimulation of indigenous microbial communities.* Applied Microbiology and Biotechnology, 2020: p. 1-19.
24. Lee, S., et al., *Xanthan Gum Biopolymer as Soil-Stabilization Binder for Road Construction Using Local Soil in Sri Lanka.* Journal of Materials in Civil Engineering, 2019. 31(11): p. 06019012.
25. Chen, R., I. Lee, and L. Zhang, *Biopolymer stabilization of mine tailings for dust control.* Journal of Geotechnical and Geoenvironmental Engineering, 2015. 141(2): p. 04014100.
26. Chang, I., et al., *Soil consistency and interparticle characteristics of xanthan gum biopolymer–containing soils with pore-fluid variation.* Canadian Geotechnical Journal, 2018. 56(8): p. 1206-1213.
27. Hussaini, S.M.S. and V. Toufigh, *Strength and Fracture Behavior of Rammed-Earth Materials*. Journal of Materials in Civil Engineering, 2019. 31(10): p. 04019228.
28. Hamdan, N., et al., *Hydrogel-assisted enzyme-induced carbonate mineral precipitation.* Journal of Materials in Civil Engineering, 2016. 28(10): p. 04016089.

29. Chang, I., J. Im, and G.-C. Cho, *Geotechnical engineering behaviors of gellan gum biopolymer treated sand.* Canadian Geotechnical Journal, 2016. 53(10): p. 1658-1670.
30. Chang, I. and G.-C. Cho, *Shear strength behavior and parameters of microbial gellan gum-treated soils: from sand to clay.* Acta Geotechnica, 2019. 14(2): p. 361-375.
31. Hataf, N., P. Ghadir, and N. Ranjbar, *Investigation of soil stabilization using chitosan biopolymer.* Journal of Cleaner Production, 2018. 170: p. 1493-1500.
32. Iyengar, S.R., et al., *Pavement subgrade stabilization using polymers: Characterization and performance.* Journal of Materials in Civil Engineering, 2013. 25(4): p. 472-483.
33. Porter, H., N.K. Dhami, and A. Mukherjee, *Synergistic chemical and microbial cementation for stabilization of aggregates.* Cement and Concrete Composites, 2017. 83: p. 160-170.
34. Porter, H., et al., *Rammed earth blocks with improved multifunctional performance.* Cement and Concrete Composites, 2018. 92: p. 36-46.
35. Chang, I., et al., *Soil strengthening using thermo-gelation biopolymers.* Construction and Building Materials, 2015. 77: p. 430-438.
36. Australia, S., *1289.5.1.1:2017 : Methods of testing soils for engineering purposes - Soil compaction and density tests - Determination of the dry density/moisture content relation of a soil using standard compactive effort.* 2017, Standards Australia: Sydney.
37. Bernardi, D., et al., *Bio-bricks: Biologically cemented sandstone bricks.* Construction and Building Materials, 2014. 55: p. 462-469.
38. Australia, S., *AS 5101.4-2008 : Methods for preparation and testing of stabilized materials - Unconfined compressive strength of compacted materials.* 2008, Standards Australia: Sydney.
39. Xiao, Y., et al., *Effect of Particle Shape on Strength and Stiffness of Biocemented Glass Beads.* Journal of Geotechnical and Geoenvironmental Engineering, 2019. 145(11): p. 06019016.
40. Australia, S., *AS 5101.5-2008 (R2017) : Methods for preparation and testing of stabilized materials - Absorption, swell and capillary rise of compacted materials.* 2008, Standards Australia: Sydney.

41. DeJong, J.T., M.B. Fritzges, and K. Nüsslein, *Microbially induced cementation to control sand response to undrained shear*. Journal of Geotechnical and Geoenvironmental Engineering, 2006. 132(11): p. 1381-1392.

Chapter 6: Nanoscale to macroscale characterization of in – situ bacterial biopolymers for applications in soil stabilization

6.1 Abstract

Bacterial biopolymers produced extracellularly due to microbial metabolic activities have gained considerable interest in various engineering applications. The major advantages of bacterial biopolymers is their *in-situ* production and low water solubility, eliminating the requirement for mixing in granular substrates such as soils. These properties make them highly desirable and preferable than manufactured biopolymers. But for any engineering applications, it is crucial to understand the mechanical properties of these materials which have been less explored. This investigation is the first attempt to quantify the nano and macro mechanical properties of in-situ bacterial biopolymer dextran produced by bacterial culture *Leuconostoc mesenteroids*. The fundamental mechanism of bacterial biopolymer-based cementation has been revealed through their morphographic and nanomechanical testing via atomic force microscopy, nanoindentation and scanning electron micrographs. Effect of bacterially produced biopolymers and commercial biopolymers on macro-mechanical properties of soils was then investigated via needle penetration tests. In-situ biopolymers were found to be highly effective in stabilizing soils with comparable mechanical properties as commercial biopolymers. This study has demonstrated novel methods for testing in situ polymers and opened up the channels for their applications in numerous subsurface as well as surface applications.

Keywords: Biopolymers, bacterial dextran, nanoindentation, AFM, needle penetration

6.2 Introduction

The role of microbial metabolic activities in the creation of several naturally cementing structures as beach rocks, microbialites, cave speleothems has been widely accepted [1-3]. In particular, bacterial extracellular biopolymers have been found to significantly influence soil properties in natural systems as around 10^{12} microorganisms per kilogram of soils have been recorded [4]. This ability of microbes to create Extracellular polymeric substances (EPS) and biopolymers leading to the cementation of granular materials in natural environments s now being harnessed for several engineering applications including stabilization of soils, improvement of

concrete and immobilization of heavy metals [5, 6]. These bacterially produced biopolymers offer immense benefits, including their eco-friendly nature, recyclability and low water solubility, making them desirable for achieving sustainability goals in the construction industry.

Commercially available biopolymers and biologically induced polymers offer the advantages of ease of use and sustainability compared to conventional chemical stabilizers [7]. A range of biopolymers from microbially sources have been utilized for soil stabilization applications including xanthan, guar gum, gellan gum, chitosan, sodium alginate [7, 8]. Commercial biopolymers are first mixed with water creating viscous gels and then supplemented into the soil for applications into soils. Two of the most widely used commercially available biopolymers xanthan gum and guar gum have been used extensively in soil stabilization, and their positive impact on soil engineering properties has been recorded in several previous studies [9, 10]. The properties of the soils improved include strength [11, 12], stiffness [13], hydraulic conductivity [14, 15] and dust resistance [16, 17]. Although these commercial biopolymers have several benefits but their high water solubility and high viscosity often limits their ability to penetrate through the soils restricting their usage for several applications.

Emulating the natural process through in-situ production of biopolymers within the soils can overcome the workability issues associated with commercial biopolymers. Stimulation of bacteria present in the soil and subsequent injection of the chemicals required for fermentation can also produce in-situ biopolymers [18]. This process would obviate the challenges posed by commercial biopolymers with minimum disturbance to the treated soil. Not much information is available on the enrichment and application of native biopolymer producing communities for the creation of in situ polymers, especially for soil applications. A variety of bacterial strains such as *Alcaligenes faecalis, Alcaligenes eutrophus* and *Alcaligenes viscolactis, Microbacterium arborescens* [19], *Rhizobium tropici* [20, 21], *Enterobacter aerogenes* and *Pseudomonas fluorescens* [22] and *Leuconostoc mesenteroids* [23] have been studied for their ability to produce biopolymers. Amongst these cultures, *Leuconostoc mesenteroids* (ATCC 14935) has been of keen interest for several engineering applications [24]. It is a facultative microbe which grows well in both

aerobic and anaerobic conditions. When supplied with sucrose, it can produce insoluble biopolymer dextran [25]. The reactions are as:

$$\text{sucrose} + 0.2\text{NH}_4 + +0.341\text{HCO}_3 - \rightarrow 0.20\text{C}_5\text{H}_7\text{O}_2\text{N}_{(\text{w})} + 0.141\text{Fructose} + 0.071\ \text{lactate} + 0.071\ \text{acetate} + 0.014\ \text{Mannitol} + 0.071\ \text{Ethanol} + 0.418\text{CO}_2 + 0.71\text{H}_2\text{O} + \text{Dextransucrase} \quad (1)$$

$$5.3\ Sucrose + Dextransucrase \rightarrow 2.0\ Dextran(w) + 4.5\ Fructose + Dextransucrase \quad (2)$$

$$\text{C}_5\text{H}_7\text{O}_2\text{N}_{(\text{w})} \rightarrow \text{C}_5\text{H}_7\text{O}_2\text{N(s)} \quad (3)$$

$\text{Dextran}_{(\text{w})} \rightarrow \text{Dextran}_{(\text{s})}$ (4)Dextran is poorly soluble in water and therefore, it is of prime interest.

However, practical applications require the examination of their suitability as a stabilizer with desired mechanical properties. Very little information is available about the mechanical properties and behaviour of these in situ polymers, especially at the nanoscale. Till date, most of the studies have been limited to macroscale tests as strength and stiffness [20, 21], ductility [24], hydraulic conductivity [26] and cohesion [23]. A thorough understanding of the biopolymer behaviour at the microscale is crucial before the design and development of its applications at a larger scale.

The engineering properties and durability performance of construction materials at the macroscale are significantly affected by their structural features and properties at the micro and nanoscale where the deterioration and failure process initiates [27, 28]. In soils, the nanoindentation technique was exploited in various fields of material characterization such as determination of elastic modulus and hardness [29] and mechanical properties of shale [30]. However, the mechanical properties of biopolymer stabilized soils are yet to be quantified using the nanoindentation technique.

The objective of the present study was, therefore, to fill in the gaps of previous research in the characterization of commercial as well as in situ biopolymers at different scales. In order to achieve desired amounts of in situ biopolymers, optimization of media components in order to enhance the production of biopolymer was also carried out. Quantification of nano and micromechanical properties of the biopolymer was

conducted. The ultimate objective was to introduce bacterial cells into soils samples in Petri dishes to investigate its effect on surface strength. For this purpose, needle-penetration testing was conducted on the soil samples surface stabilized with in-situ biopolymer. This paper explores the micromechanical and macro mechanical properties of soil stabilized with in-situ deposition of the bacterial polymer. The present study is focussed on the advanced nanomechanical characterization of biopolymer dextran leading to application in sand-clay mixtures. Atomic Force Microscopy (AFM) and nanoindentation techniques were used to probe the mechanical properties of the biopolymers at nanoscale and microscale, respectively. Further, penetration tests were carried out in soil samples stabilized with in-situ biopolymer. The mechanism of stabilization has been revealed through advanced microscopic investigations using scanning electron microscopy, nanoindentation and atomic force microscopy.

6.3 Materials and methods

6.3.1 Microorganism and growth medium

The bacterial strain *Leuconostoc mesenteroids* (ATCC 14935) was selected as a model bacterium for biopolymer production. *Leuconostoc mesenteroids* is a facultative microbe and grows in both aerobic and anaerobic conditions. Since *Leuconostoc mesenteroids* was previously known to plug porous media by producing insoluble biopolymer, it was chosen for the study [31]. In addition to this, the bacterial cells have a coccoid morphology with an average diameter of 600nm, which facilitates microbial transport within the soil matrix. The bacteria produce biopolymer known as dextran while metabolizing sucrose [32]. Dextran has a branched structure with α-1 and α-2 glycosidic linkages and is insoluble in water [32]. Table 1 describes the chemical composition of the growth medium used for growing the bacteria and stimulating Dextran production.

6.3.2 Soil specimen preparation

Manufactured sand with particle size varying from 0.45 mm and 0.075 mm (Fig 1) used for the present study was sourced from Cook Industrial Minerals, Western Australia. Kaolin clay with low swelling and shrinkage properties supplied by Sibelco, Australia was chosen for the study. The particle size distribution and chemical

composition of the clay are listed in Table 2. Commercially available biopolymer, Xanthan gum was sourced from Sigma Aldrich, NSW, Australia.

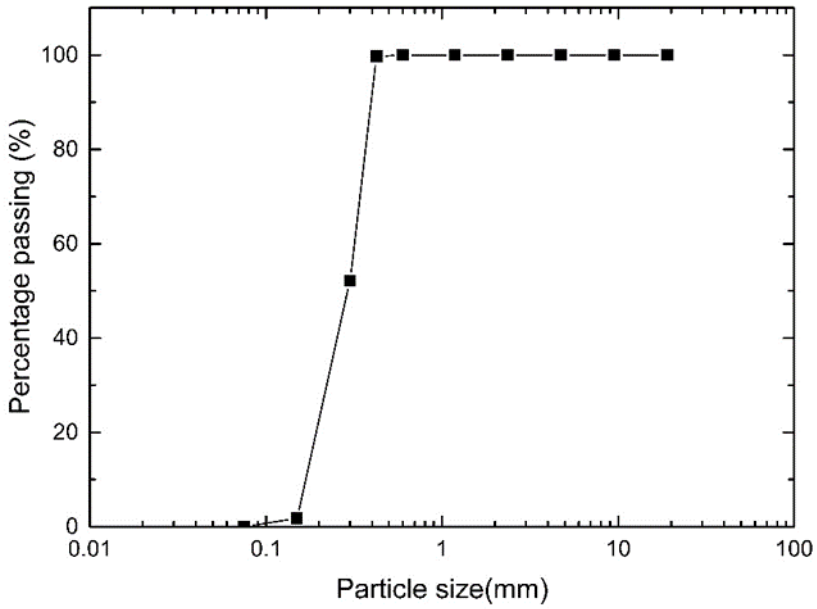

Fig 6. 1 Particle size distribution of the manufactured sand

Table 6. 1 Particle size distribution and chemical composition of the clay

Particle size (µm)	**Percentage passing (% weight)**
53	99.4
20	97.8
10	95.9
5	90.3
2	75.7
1	63.6
Chemical analysis	**Composition (% Weight) ***
SiO_2	46.7
Al_2O_3	36.1
TiO_2	0.8
Fe_2O_3	0.9
CaO	0.7
MgO	0.4
K_2O	0.4

	Na_2O	0.1	4350

6.3.3 Dextran production

Sucrose concentration in the biopolymer media (Table 1) was varied between 15-500 g/L to study the effect of sucrose concentration on Dextran production. For biopolymer production, the bacteria were grown in MRS media until it reached an OD_{600} of 1. The bacterial strains were further inoculated in biopolymer media (Table 1) containing varying concentrations of sucrose (15-500 g/L). The flasks containing bacteria in biopolymer media was maintained at 37^{o}C and 50 rpm for 72 hours to monitor biopolymer production. The pH was monitored continuously during the process. The contents of the flasks were filtered through Whatman^{TM} filter paper 1(150 mm diameter) and dried in the oven at 60^{o}C to estimate the weight of biopolymer produced.

Table 6. 2 Media for the growth of bacteria and biopolymer production

Media description	**Composition**	**Concentration**
Bacterial growth media	*Leuconostoc mesenteroids* (ATCC 14935)	0.8 <OD_{600}<1.5
	De Man, Rogosa and Sharpe (MRS) broth	52 g/L
Biopolymer media	Sucrose	15-500 g/L
	Yeast extract	10 g/L
	1M Monobasic KH_2PO_4	41 mL/L
	1M Dibasic K_2HPO_4	59 mL/L

6.3.4 Dextran purification

Biopolymer extraction was carried out using the modified protocol [33]. To sum up, the media containing bacteria was centrifuged at 6000 rpm for 20 min at 4^{o}C to remove bacterial cells. The supernatant was precipitated with 2.2 volume of absolute chilled ethanol by incubating the mixture at -20^{o}C for one hour. The precipitated EPS was collected by centrifugation at 6000 rpm for 20 min at 4^{o}C. The supernatant was decanted, and the pellet containing EPS was dried at room temperature in the laminar hood for 6 hours. The dry weight of the EPS was estimated.

6.3.5 Scanning Electron Microscopy (SEM)

Bacterial biopolymer imaging on glass coverslip substrate was carried out on Tescan Mira3 VP-FESEM with Oxford Instruments X-Max 150 SDD X-ray detector, NordlysNano EBSD detector and AZtec software (Tescan, Czech Republic). The glass coverslips were first rinsed with ethanol followed by deionized water. Further, it is coated with poly-L-lysine 0.01% (Sigma Aldrich, Australia) and left under a sterile environment for 2h. Then 20µL of the bacterial grown in sucrose media was added to the coverslips and left overnight. Prior to the test, the 10 µL of 4% glutaraldehyde (Ajan Finechem) was added to fix the cells and left for a period of 10min. The sample was finally washed with 0.1M phosphate-buffered saline (PBS) buffer at pH 7.2 and taken for SEM imaging.

6.3.6 Nanoindentation

6.3.6.1 Sample preparation

Leuconostoc mesenteroids were cultured in MRS medium initially until a desirable OD was reached. Further, 1% of the inoculum was transferred to a media containing sucrose (Table 6.2) to induce the production of biopolymer at 37^{o} for 48 h at 100 rpm. The polymer produced was filtered into Whatman^{TM} filter paper no 1 and dried to remove the moisture. The samples were placed in plastic moulds, and epoxy resin (Epofix epoxy) was poured under vacuum (Struers Cito Vac) in order to impregnate resin into the sample. The samples were polished by using Stuers Tegramin-30 in steps as depicted in Table 4. Further, the sample surface was prepared by FIB milling using Technoorg Linda SEMPrep 2 to produce a sample with minimum surface roughness.

Table 6. 3 Steps involved in polishing for nanoindentation

Polishing	Cloth used	Lubricant	Time (min)
Step 1	Piano 220	Water	1
Step 2	Piano 1200	Water	2
Step 3	MD Chem	Colloidal silica (coarseness 0.04 micron)	2

6.3.6.2 Testing methodology

Nanoindentation was carried out using a G200 nanoindenter (Agilent Technologies) fitted with a Berkovich shaped diamond tip (TB22130 XP CSM 23032018). The optical microscope attached to the nanoindenter was used at 40X magnification to

choose the points of indentation. The tests were performed under the continuous stiffness measurement (CSM) model with Testworks 4 version 4.10 (MTS System Corporation). While the traditional Oliver-Pharr methodology measures the contact stiffness only at the point of unloading, the CSM technique allows measurement of contact stiffness at any point of the loading curve corresponding to any depth of penetration. The maximum displacement was limited to 2000 nm and 100 indents were chosen on the sample with a spacing of 20 µm. All the indentation locations were carefully selected prior to testing to ensure that the pores or cavities are not encountered in the process. Poisson's ratio of the biofilm was taken as 0.45 (unpublished study). The calculations were performed with the aid of the software nanoTest Platform Four V.40.08 (Micro Materials Ltd). To obtain the properties of hydrated biopolymers, the sample cast in resin was immersed in deionised water for 24 hours and allowed to saturate before carrying out the test.

6.3.7 Peakforce QNM

PeakForce quantitative nanomechanical imaging (PeakForce QNM) was employed to study the nanomechanical properties of biopolymer at high resolution. The instrument facilitated the mapping of elastic properties of the sample with a lateral resolution at the nanometre scale. The force curves were analyzed at each pixel of the topographic image, and the local elastic modulus was calculated at each surface contact with the sample using the Derjaguin-Muller-Toporov (DMT) model [34]. The forces during tip-surface interaction can be described elsewhere [34]. The above calculations were carried in real-time for each force-distance curve obtained at every pixel leading to the simultaneous mapping of the nanomechanical properties and topography of the sample. AFM imaging was performed using Bruker Dimension Icon AFM system with PF QNM mode under ambient conditions. SCANASYST-FLUID probes were employed for the experiment (SCANASYST-FLUID with spring constant 0.7 N/m, Bruker, US). The imaging scan rate was maintained at 1Hz at a resolution of 256x256 pixels. The raw AFM topography images were further processed by using Bruker Nanoscope Analysis 1.9.

6.3.8 Needle penetration

Petri dishes (85 mm diameter and 10 mm height) were filled with 100 g of soil each and tapped for compaction (Fig 6.2). The soil was a well-graded system with sand and varying percentage of kaolin clay (0, 3, 5, 7 and 10%). The initial weights of the

samples were measured. During the treatment process, MRS media (10 mL) containing *Leuconostoc mesenteroids* was sprayed on the soil surface under sterile conditions. The samples were transferred to an incubator maintained at 37^{o}C to promote the growth of the bacteria. After 6 hours, the sample was taken out, and 10 mL of biopolymer media containing sucrose was sprayed on the sample to initiate biopolymer production. Weights of the samples were continuously taken prior to and after each spraying to estimate the amount of media absorbed by the sample accurately. After four days of spraying the samples with biopolymer media, fresh bacteria were resprayed. The cycle was repeated for 21 days of treatment. The amount of polymer deposited was estimated by chemical mass balancing. While the needle penetration test is not a standardized test, it has been used by researchers in order to achieve an indirect measure of the strength of stabilized soil [35-37]. A penetration test set up was developed in house with Chenille 22 needle of diameter 0.94 mm and length. The needle inserted into a stainless-steel holder, and the set up was clamped to the jaws of universal testing machine (Shimadzu AGS-X). The loading was carried at a rate of 0.5 mm/min to a maximum penetration of 5 mm. For each sample, the penetration was carried out at 25 points spaced 10 mm apart to obtain average Needle Penetration Resistance (NPR) values.

To compare the performance of in-situ biopolymer with commercial biopolymer Xanthan gum, a set of needle penetration and UCS tests were conducted on soil samples (sand with 0%, 3%, 5%, 7% and 10% kaolin clay) stabilized with Xanthan gum. The percentage of Xanthan gum used was kept constant at 0.5% dry weight of the soil. The results of needle penetration and UCS were compared to achieve a correlation. After the curing period, the samples were subjected to UCS testing according to Australian Standards on a universal testing machine (Shimadzu AGS-X) of 10kN capacity. The specimen was compressed at a constant displacement of 0.5 mm/min. This correlation can be useful in predicting the UCS of in-situ samples whose needle penetration results are known. The designations of the samples are listed in Table 4.

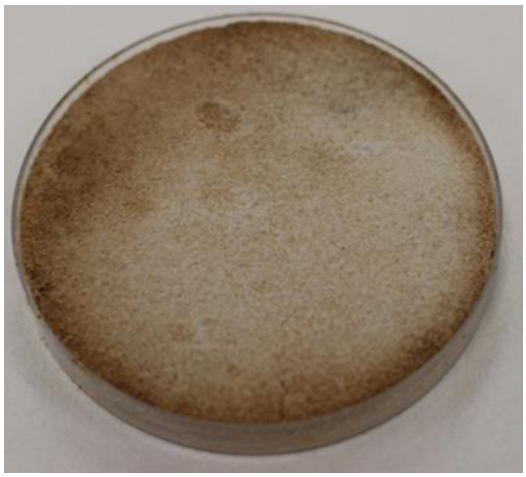

Fig 6. 2 Petri dish sample prepared for needle penetration testing after completion of in-situ biopolymer treatment (Sample SBC10).

Table 6. 4 Sample designation for Needle penetration testing

Designation	Biopolymer	Clay (%)
SB_dC0	Dextran (In-situ)	0
SB_dC3		3
SB_dC5		5
SB_dC7		7
SB_dC10		10
SB_xC0	Xanthan gum (Commercial)	0
SB_xC3		3
SB_xC_5		5
SB_xC7		7
SB_xC10		10

6.4 Results and discussion

6.4.1 Bacterial growth and biopolymer production

Fig. 3 presents the growth curves with varying sucrose concentrations. The highest rate of bacterial growth was observed with sucrose concentration of 100 and 250 g/L with bacterial OD_{600nm} greater than one. The lowest growth rate of the bacteria occurred in media with the highest sucrose concentration of 500g/L. The ATCC suggested media (MRS media) for the growth of the bacteria displayed an OD_{600nm} of 0.6. Hence, a sucrose concentration of the media was maintained at 15 g/L and100g/L of sucrose for needle penetration experiments. The initial pH of the media was adjusted to 7 by the addition of phosphate buffers. With the growth of bacteria, the pH of the media dropped due to the production of carbon dioxide and other by-products of fermentation reaction (Fig.4). The pH drop is drastic between 5-12 hours from the

period of inoculation. The value of the pH attains a stable value after the end of 24 hours, indicating the end of the fermentation reaction. Fig 6.5 shows the weight of biopolymer production with an increase in sucrose concentration in the media from 15-500 g/L. The biopolymer formation increased with an increase in sucrose concentration as observed from Fig.5. It has been reported that the bacterial activity leading to dextran production can be divided into three stages, namely, bacterial growth, dextran production and dextran precipitation [43]. When *Leuconostoc mesenteroids* are grown in sucrose rich conditions, the bacteria produce an enzyme known as dextransucrase leading to the precipitation of biopolymer dextran $(C_6H_{10}O_5)_n$ [50]. The reaction for cell growth and enzyme production are as follows:

$$\text{sucrose} + 0.2NH_4 + +0.341HCO_3 - \rightarrow 0.20C_5H_7O_2N_{(w)} + 0.141\text{Fructose} + 0.071\text{ lactate} + 0.071\text{ acetate} + 0.014\text{ Mannitol} + 0.071\text{ Ethanol} + 0.418CO_2 + 0.71H_2O + \text{Dextransucrase} \quad (1)$$

$$5.3\ Sucrose + Dextransucrase \rightarrow 2.0\ Dextran(w) + 4.5\ Fructose + Dextransucrase \quad (2)$$

$$C_5H_7O_2N_{(w)} \rightarrow C_5H_7O_2N(s) \quad (3)$$

$$\text{Dextran}_{(w)} \rightarrow \text{Dextran}_{(s)} \quad (4)$$

The subscript w represents biomass species that are present in water but not dissolved in it and the subscript S represents species that are attached to the solid. Where n was assumed to be 6.2 due to the molecular weight of generated dextran being approximately 10,000 g $mol^{-1.}$ The dextran produced is said to have very low solubility in water and contribute to permeability reduction.

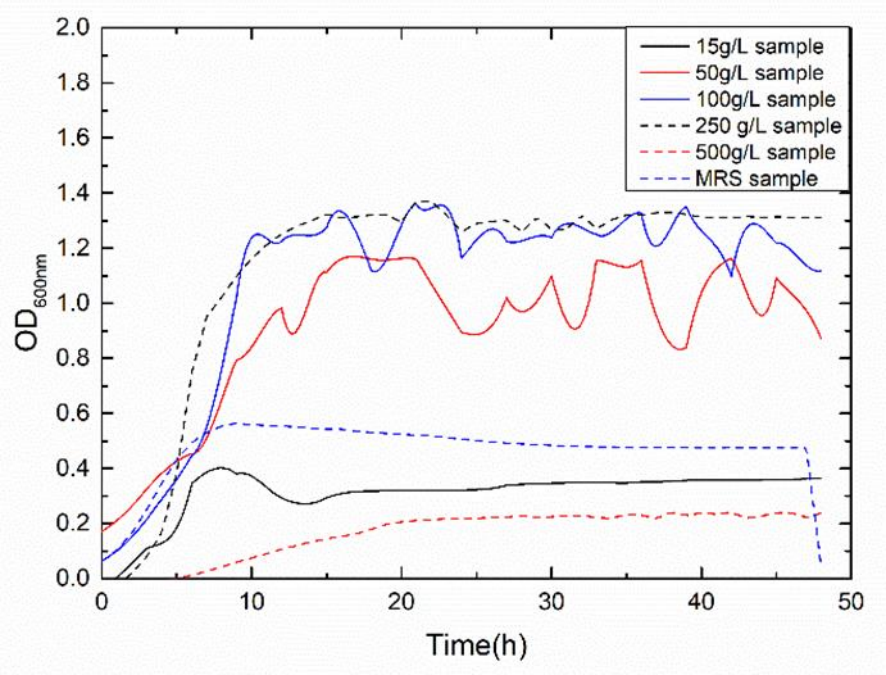

4501

4502 *Fig 6. 3 Bacterial growth in media with different sucrose concentrations*

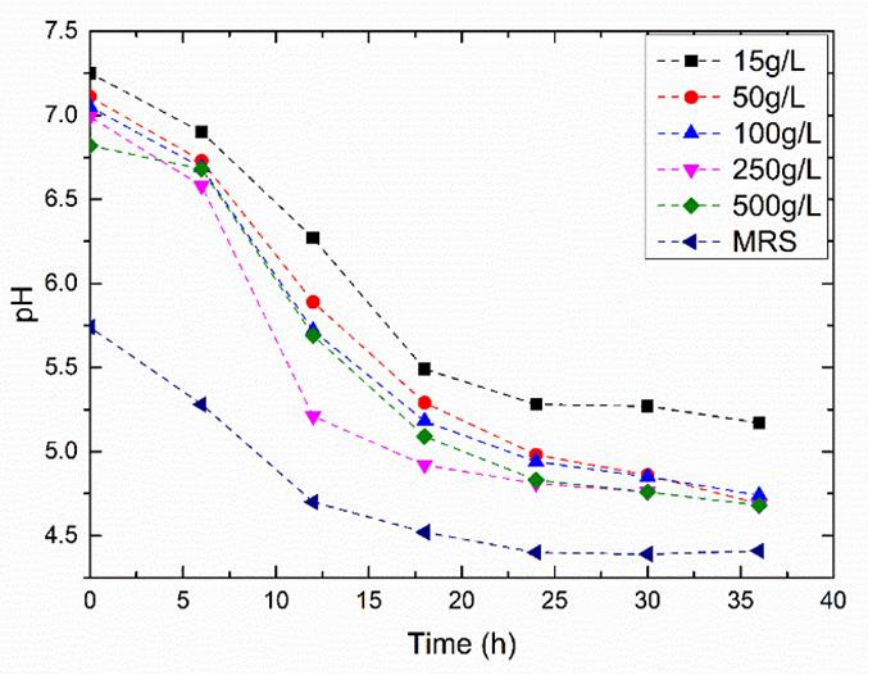

4503

4504 *Fig 6. 4 Variation of pH with sucrose concentration*

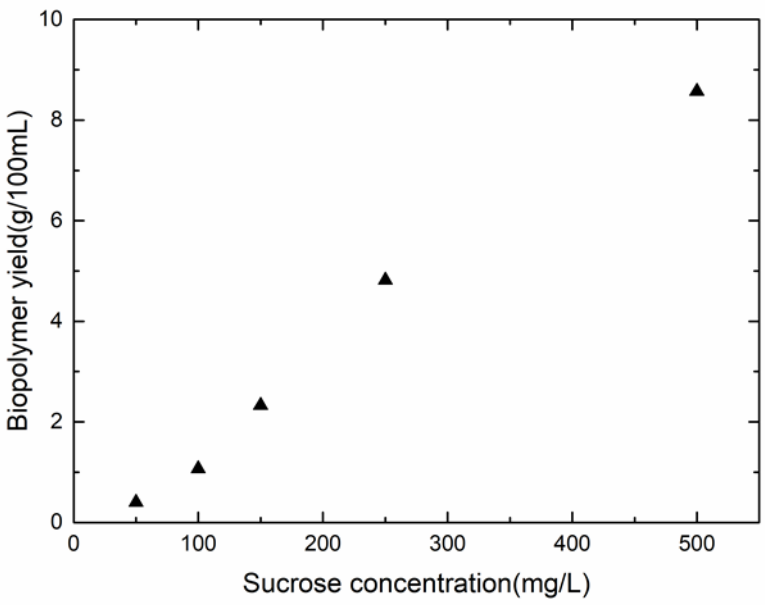

Fig 6. 5 Biopolymer yield with varying sucrose concentration

6.4.2 Scanning Electron Microscopy (SEM)

Fig 6.6 shows the typical morphology of microbial biopolymers along with the bacterial cells. They are viscous and stretch to thin threads when pulled. The length of a single biopolymer thread is around 10 µ as seen in Fig 6.6a. Fig 6.6b shows several such threads. The micrographs clearly show that bacteria use the biopolymers as anchors to attach themselves to a substrate. Thus, the bacteria attach on to soil grains, and the threads bridge the grains. The stiffness of the bacterial biopolymers is significantly different in the dry and hydrated states leading to the difference in their mechanical properties as well. When wet, the threads can elongate considerably to attach to several grains. When the polymer dries, the threads develop cohesive strength among the grains.

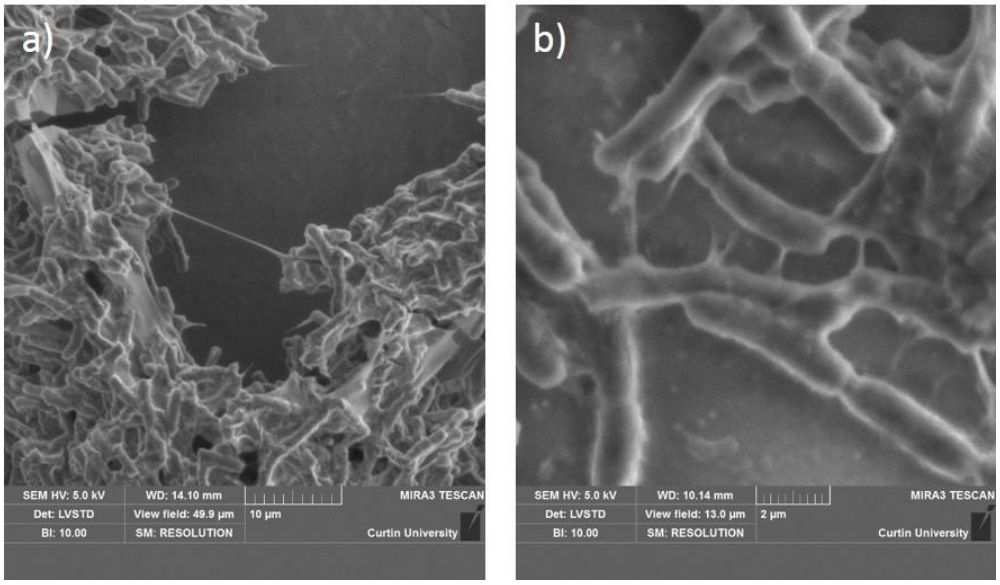

Fig 6. 6 SEM micrographs of bacterial biopolymer on glass-slides

6.4.3 Nano-indentation

Fig 6.7a shows the biopolymer sample prepared for nanoindentation. It is embedded in a resin and polished using the ion milling technique. Fig 6. 7b shows the indentation marks left on the samples after the indentation test. Nano-indentation was performed by constantly penetrating the indenter into the polymer and measuring the force of resistance.

Fig 6.8a shows a typical variation of the elastic modulus and hardness with the depth of penetration. It is observed that for the initial 250 nm of penetration, the indenter moves freely, and the force of resistance has a downward trend with penetration. This is possibly due to the surface unevenness of the sample. From 260 nm to 500 nm, the indenter experiences increased resistance—the force of resistance peaks at around 55 nm penetration. Thereafter, there is a gradual reduction in resistance. The force of resistance stabilizes at around 1000 nm. The force of resistance stabilizes at around 1000 nm. From 1000 nm to 2000 nm depth, there is little change in the force of resistance. Similar observations have been made in [38]. The average elastic modulus measured at depths of 1000-2000 nm is considered to be representative. It was observed that the average elastic modulus of the dry biopolymer is 3.14 GPa ± 0.035. The hardness of the biopolymer is derived from the measured elastic modulus. The average hardness is observed to be 0.2 GPa.

The elastic modulus of the biopolymer lies within the modulus range of 0.1 to 5 GPa [39, 40]. The possible reason for such a large variation is the extreme moisture sensitivity of the biopolymer. The authors have reported that the strength of biopolymer stabilized soil columns degrades rapidly with moisture ingress (unpublished data). The authors demonstrated that the bond strength of the polymer degraded with moisture ingress. Nano-indentation allows us to measure the properties of biopolymer in both dry and hydrated condition. Fig 6.8b compares the elastic moduli of a dry and a wet biopolymer subjected to a cycle of saturated wetting. The average modulus of the wet samples was 1.47 GPa, with a standard deviation of 0.057. Thus, wetting was responsible for a reduction of modulus by more than 50%. This study documents the powerful effect of hydration on biopolymer soil stabilizers. Water sorption partially plasticizes the polymers resulting in lowering of their stiffness and elastic modulus [41]. The disturbance of the biopolymer gel via hydrophilic water absorption leads to the biopolymer particles closer to the water breaking off from the main structure due to swelling. The detached particles have no interaction with the remaining structure leading to a loss in strength. The drying process leads to reattachment of the particles, but the original structure is not fully recovered, resulting in loss of strength in each cycle. The penetration was performed in a matrix of x-y positions. Fig 6.9 presents the results as colour contours. The 3-D image in Fig 6.9b shows the depth of a typical indent on the sample.

The modulus mapping results in Fig 6.10 a show that the elastic modulus of the biopolymer sample mainly varied between 2.9-3.8 GPa. The variation of modulus across the horizontal scan distance is shown in Fig. 10 b). The high standard deviation of the modulus at X= 80 µm and between X=120 µm and 140 µm (Fig.10 b) may be due to the presence of surface defects or pores observed in the surface scanning. The elastic modulus of dried and well as hydrated biopolymer dextran has been reported for the first time in the paper. This will be useful data for future modelling work on biopolymer stabilized soils.

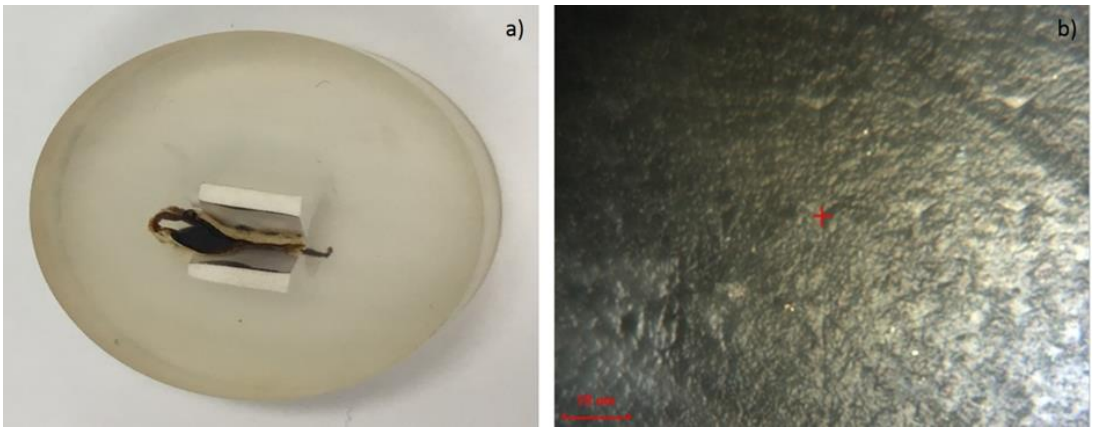

Fig 6. 7 Biopolymer sample embedded in resin for nanoindentation testing b) image of a typical indent on the sample

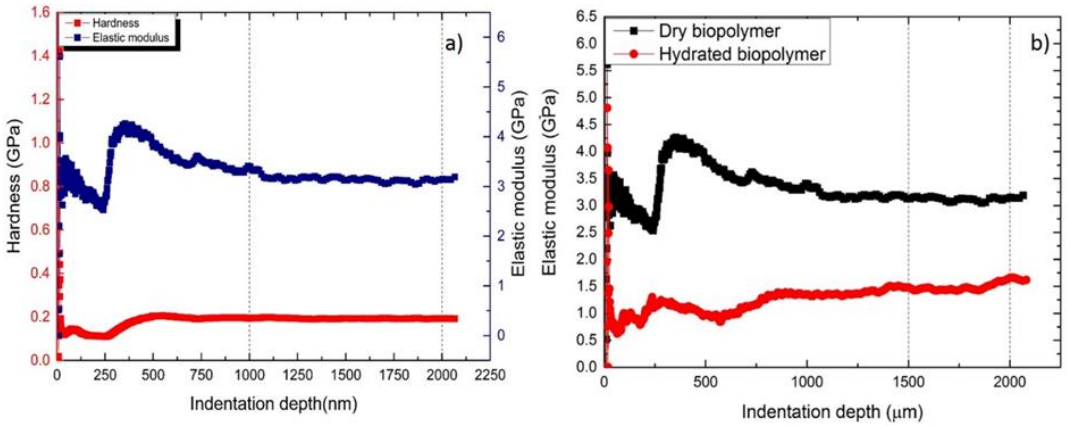

Fig 6. 8 a) Elastic modulus and hardness as a function of the penetration depth b) Variation in modulus of dry and hydrated biopolymer sample

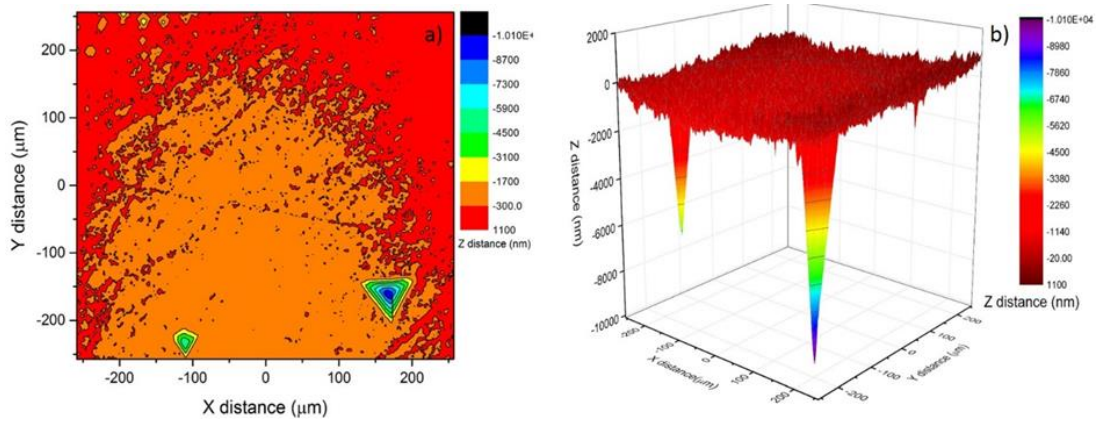

Fig 6. 9 Survey scanning results on the polished sample after indentation

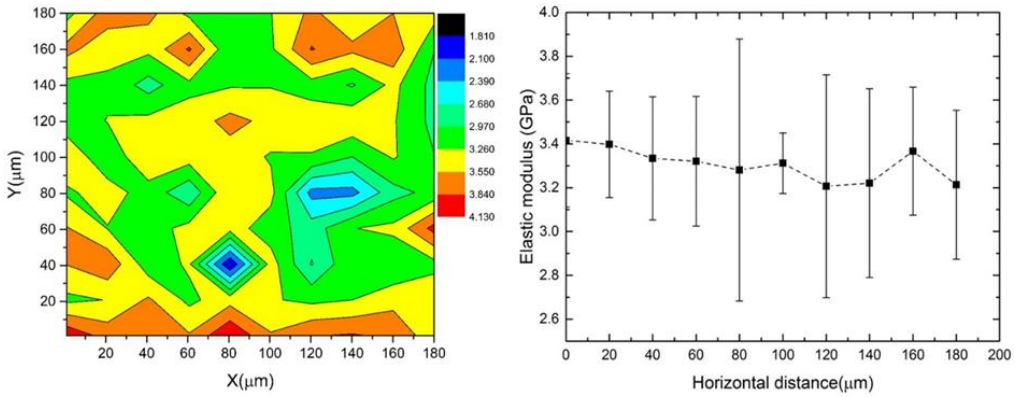

Fig 6. 10 a) Modulus mapping on 180x180 micro m^2 area using nanoindentation b) variation in modulus across horizontal direction

6.4.4 Peakforce QNM

Fig. 11 shows the comparison between surface scanning results obtained on 550X500 μm^2 area using nanoindentation. The 256X256 pixel topography images of the scan area of size 20x20 μm^2 of the biopolymer sample obtained through PeakForce QNM are shown in Fig.11. The image clearly shows the significant difference between resolutions of surface scanning image obtained using nanoindenter and AFM. The image reveals that even after polishing, the surface topography of the biopolymer sample has a wide variation. The dark areas in the image depict porous areas with low elastic modulus. The high standard deviation observed in the nanoindentation test at X=80 μm might be due to the indent being placed on such an area which may not be visible due to the low resolution of the nanoindentation microscope objective. Even though the sample preparation should result in low roughness, the root means square roughness of the sample is 558 nm. The surface profile of the in-situ biopolymer after drying is scanned using an AFM. Fig.11 b reveals that the resolution of the AFM image is much higher than that of nanoindenter. The surface scanning results show the unevenness on the sample surface even after rigorous polishing. It helps to better understand the variation in nanomechanical properties of the sample.

The modulus contour map in Fig. 12 a shows micro-level pores with low elastic modulus. Changes in elastic modulus were more prominent between the interface of the micropores and the sample. When pores or local depressions are encountered in the sample during scanning, the subsequent areas will display a lower modulus. In the modulus mapping image in Fig.12 a, one can clearly see that the depressions have a lower modulus as compared to the other relatively smooth regions in the sample. The

variation in modulus across a horizontal and vertical section can also be clearly seen in Fig.12 b. The modulus obtained from PeakForce QNM was lower than that obtained from nanoindentation using CSM method. This is generally attributed to the confinement effect and plastic deformation in nanoindentation testing [28]. However, compared to nanoindentation PeakForce QNM allows for evaluation of local mechanical properties within smaller measuring areas at the nanoscale. It can provide modulus maps with a higher spatial resolution which is very highly critical in a heterogeneous sample. Significantly lower elastic modulus is measured in areas with surface defects. Therefore, PeakForce QNM was successful in mapping the elastic modulus of the sample at higher resolutions as compared to nanoindentation, where indent spacing of 20 µm was essential to avoid interference from subsequent indents. The average modulus of across the vertical section was 2.09 ±0.48 GPa and horizontal section 1.89 ± 0.19 GPa. The reduction in modulus across the horizontals section is because the section passes through surface irregularities and pores as clearly seen in Fig12 a.

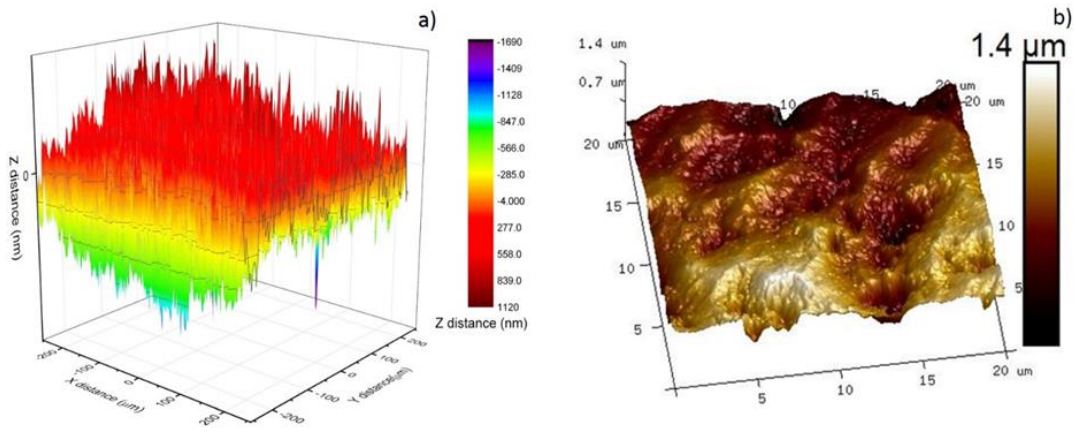

Fig 6. 11 Surface topography obtained from a) nanoindentation 500x500 µm^{2}b) PF-QNM on 20x20 µm^2

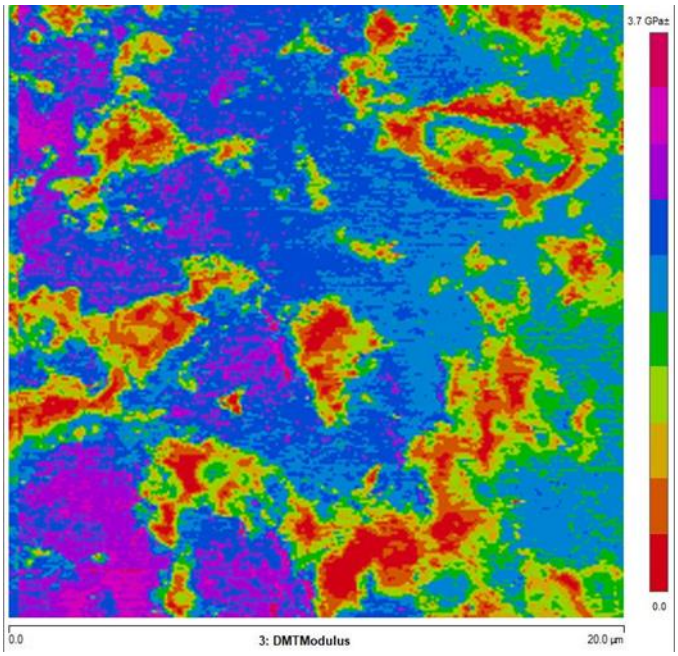

Fig 6. 12 AFM modulus mapping results

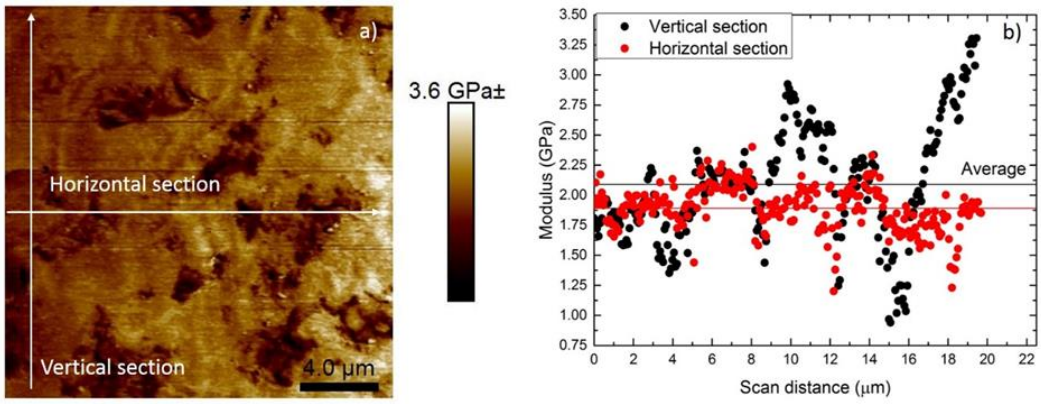

Fig 6. 13 a) Modulus contour map and b) modulus distribution across the horizontal and vertical section

6.4.5 Needle penetration

Soft insoluble biopolymers produced by in situ bacterial activities are explored to improve the surface properties of treated sand and sand-clay mixtures. The bacteria, *Leuconostoc mesenteroids* was stimulated to produce insoluble biopolymer known as dextran, in the soil. Though it is a promising technology, the quantity of biopolymer produced is relatively small compared to the pore spaces in soil [23]. Fig 6.14 shows the force-penetration graphs of samples treated with in-situ biopolymer. Firstly, the addition of in-situ biopolymer enhanced the surface strength of the treated samples. Even in the needle penetration test, the clay inclusion of clay enhanced the mechanical performance of biopolymer treated sand.

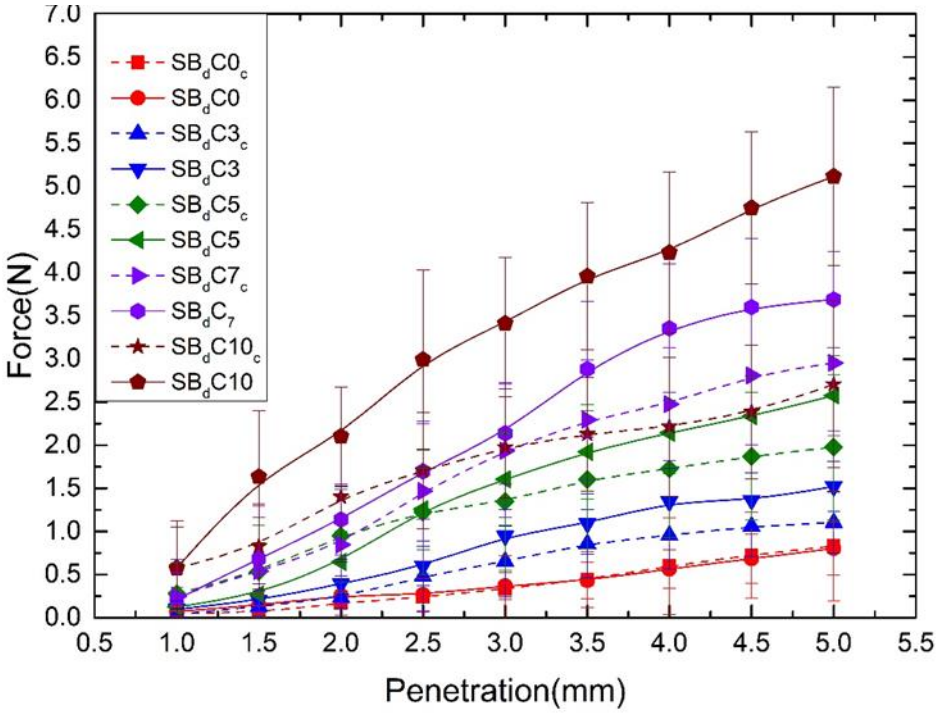

Fig 6. 14 Needle penetration of in-situ biopolymer

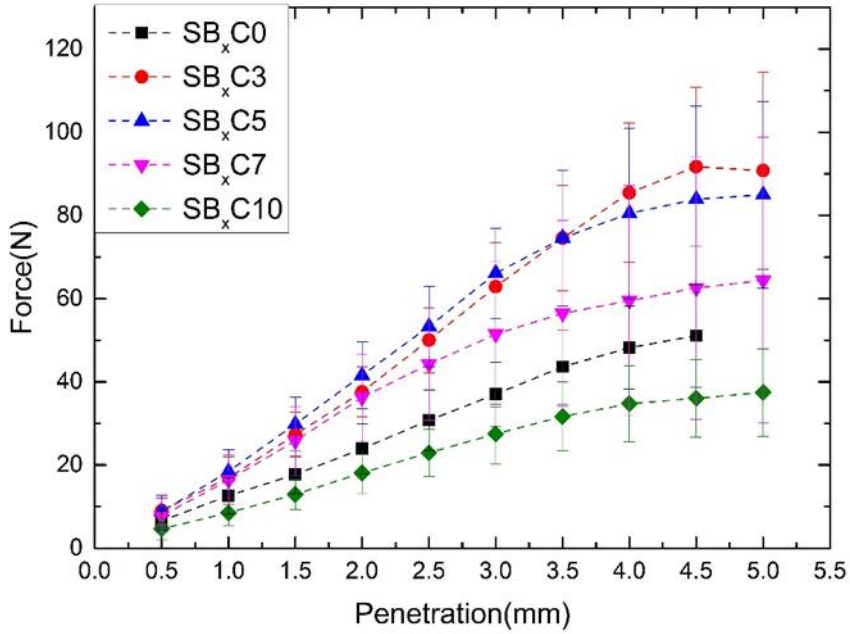

Fig 6. 15 Needle penetration results on petri dish samples treated with Xanthan gum

The load-penetration graphs of the samples treated with Xanthan gum are shown in Fig 6.15. The corresponding slopes for each graph were extracted. Sample with 3% clay displayed a maximum slope as observed in Fig 6.15.

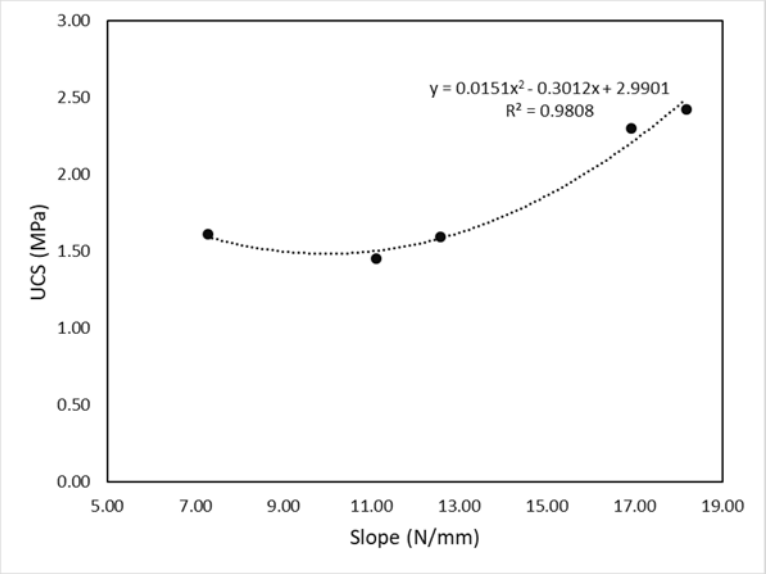

Fig 6. 16 Correlation between the slope of the needle penetration curve and UCS of Xanthan gum treated samples

The correlation between the slope of needle penetration curves is plotted with corresponding UCS in Fig 6.16. The relationship was quadratic with an R^2 value of 0.98. It can be observed that the needle penetration test can be used to predict approximate UCS values of the stabilized samples.

6.4.6 Microscopic investigation of stabilised soils

The SEM micrographs of uncoated samples after the needle penetration test are shown below. It is evident that the amount of in situ biopolymer produces is less to fill all the pore spaces in the soil matrix. However, we can notice that the in-situ polymer production is more in the grain contact areas as compared to the pores. This is due to the bacteria, who prefer to settle down in the grooves in the sand grains and secrete biopolymers thereafter. Similar results are seen from the study where bacteria are used to produce calcite to bridge the sand particles through the process of bio-mineralization. Hence, it is more advantageous to produce in-situ biopolymers than mixing it with soil are there is a more targeted production of the biopolymers in the former as compared to the latter. The SEM micrographs of biopolymer treated samples after the needle penetration test are shown in Fig. 16 a to b. It is evident that the amount of in situ biopolymers produced is less to fill all the pore spaces in the soil matrix. However, it is observed that the in-situ polymer production is more targeted towards grain contact areas as compared to the pores Fig. 16. This is due to the nature of the bacteria, which prefers to settle down in the grooves in the sand grains and secrete

biopolymers/biominerals thereafter through their metabolic activities [42]. Hence, it is more advantageous to produce in situ biopolymers than mixing it with soil since there is a more targeted production of the biopolymers in the former as compared to the latter. Fig. 17 a and b shows the formation of clay biopolymer matrix within the soil, which helps in filling the pores as well as creating grain contacts leading to higher penetration resistance.

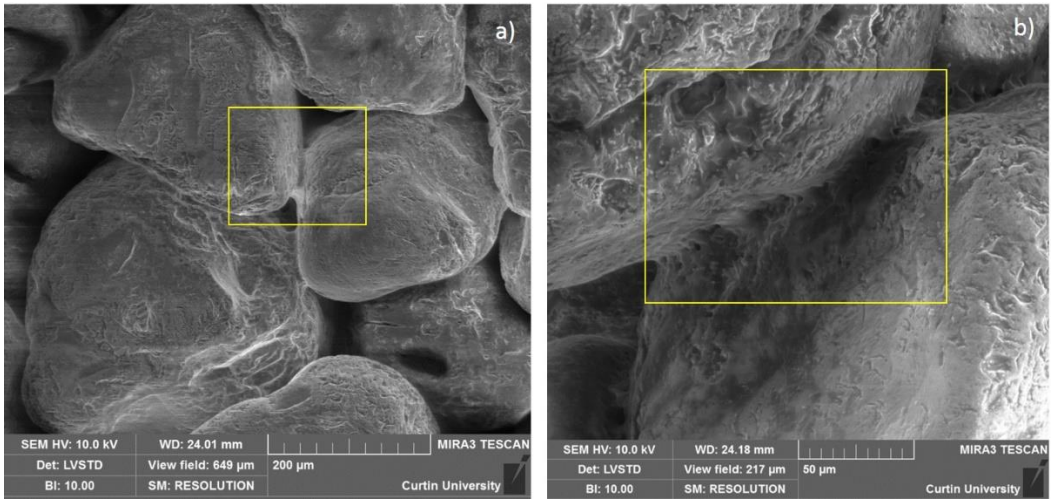

Fig 6. 17 SEM of in-situ biopolymers between sand grains

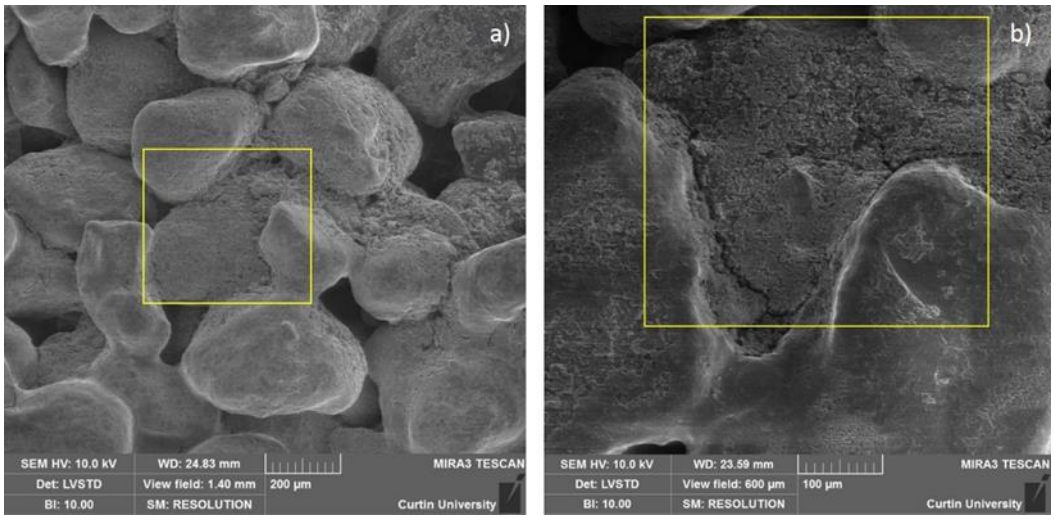

Fig 6. 18 SEM of in-situ biopolymer-clay matrix

6.4.7 Discussion

6.4.7.1 Bacterial growth and dextran production

The fundamental mechanism of bacterial biopolymer production was revealed using a model bacterium *Leuconostoc mesenteroids*. Exopolysaccharides produced from lactic acid bacteria (LAB) such as *Leuconostoc mesenteroids* is generally regarded as

safe since they are widely used in the food industry [43]. Among the several exopolysaccharides available today, dextran has gained recognition since *Leuconostoc mesenteroids* is capable of producing both soluble as well as insoluble dextran [43]. Dextran is a homopolymer of glucose synthesized by dextransucrase in the presence of sucrose, and dextran produced by various strains differ in their type of branching, mass, glucosidic linkages, physical and chemical characteristics [43]. Dextran is composed of α-1,6 linkages (65%) and combination of α-1,2 linkages (27-30%) and α-1,3 linkages [44]. The production of both dextransucrase and dextran is highly depended on various physicochemical factors. Sucrose concentration, neutral pH of 6.7 and high temperature (40^{o}C) were reported to be favourable for dextran production [44]. Our study reports that at a maximum concentration of sucrose (500 g/L), the dextran production was maximum (Fig5). The data is consistent with literature which reports that dextran production increased with sucrose concentration up to 20% [45, 46]. The reduction in pH with the production of dextran via fermentation, as seen in Fig 4 is also consistent with the literature [47]. The dextransucrase production is optimal at pH values between 7–8, but the enzyme denatured irreversibly when maintained at that pH range for an extended period of time [46]. The pH had much less effect on the molecular weight s of the synthesized dextrans than the sucrose concentration or the temperature [45]. The literature reports that the optimum conditions for the synthesis of very high molecular weight dextran are relatively low sucrose concentrations (0.1–0.3 M), high pH values of 5.5–6.0, and high temperature of 37–45 °C [45]. However, the optimum conditions for the synthesis of low molecular weight dextran would be high sucrose concentrations of 3.0–4.0 M, low pH (4.5), and intermediate temperatures of 23–28 °C [45]. It was observed that the dextran production was at higher sucrose concentration even though the OD was low (Fig 3 and 5). This confirms that bound enzyme polymerizes the substrate sucrose to dextran without the need for additional cell growth [46].

6.4.7.2 Nano and micro-mechanical properties of dextran

Measuring the mechanical properties of biopolymers remains a challenge due to their multi-component nature and fragile structure [48]. Investigation of mechanical properties of biopolymers and biopolymer stabilized soils is often limited to the macroscopic scale which does not provide information on interfacial properties and microstructure. In the present study, we employed a combination of atomic force

microscopy (AFM) and instrumented nanoindentation to study the nanomechanical properties. Nanoindentation is a versatile technique reserved for the characterization of materials at the scale of heterogeneities or composite phases [49]. However, Nanoindentation testing requires an adequate sample preparation because accurate results are obtained only if the depth of indentation is larger than the specimen's surface topography [49]. A meticulous preparation was carried out to significantly reduce the uncertainty in determining the surface properly before testing. The nanomechanical properties of bacterial dextran were unreported in literature hitherto. The modulus mapping results in Fig. 10 a show that the elastic modulus of dextran mainly varied between 2.9-3.8 GPa. The average elastic modulus of the dry biopolymer is 3.14 ± 0.035 GPa at micro scale. The study also revealed that exposure to moisture was a major reason for the varying mechanical properties of the biopolymer.

AFM has been widely used to measure the nanomechanical properties of biological systems such as the cell wall elasticity, cell surface polymers, and cell adhesion [50]. Besides probing cell surface morphology and surface forces, AFM allows the characterization of the local mechanical properties of biological samples [51]. In the present study, the average modulus of across the vertical section was 2.09 ± 0.48 GPa and horizontal section 1.89 ± 0.19 GPa at the nanoscale. The higher variation may be due to the presence of local irregularities on the sample surface due to polishing. Further, study reports the presence of small nanoscale pores in dextran, which may also contribute to the variation in elastic modulus [52]. The radius of pores in dextran ranged from 1 to 100 μm and ~95% of the radius was less than 20 μm [52].

Previous studies reported that the biofilms formed under high nutrient conditions (4.98 ± 0.02 kPa) compared to that of biofilms formed under low nutrient of the biofilm of *C. neoformans* ranged from 0.1 to 6 GPa [48]. However, it is to be noted that the properties are measured under hydrated conditions [53]. Moreover, the storage moduli of the biofilm of *C. albicans* varied from 0.1 to 4 GPa, while that conditions by *Pseudomonas fluorescens* were less stiff, as shown by their Young's modulus values (2.35 ± 0.08 kPa) [53]. Unlike alginate biopolymers, the dextrans are neutrally charged. This means that even in the absence of any salt ions, attractive interactions will be present in dextran solutions leading to increased gelation [54]. This makes dextran an ideal candidate for soil stabilization applications.

6.4.7.3 Implications on soil stabilization

When *Leuconostoc mesenteroids* is grown within the soil, the accumulation of dextran can clog the pore spaces within the soil, leading to changes in soil properties. The effectiveness of biopolymers in aggregating soil relies on various factors. They include the amount of biopolymer production and survival of the bacteria in various soil conditions. It was observed that type of soil and sucrose concentration had a direct effect on the effectiveness of stabilization. The biopolymer stabilized samples had a higher surface strength when the soil has higher clay content (Fig 13). The scanning electron microscopy images of the tested sand revealed Dextran production within the pore spaces and coating the soil particles (Fig 16 and 17). The mechanism of stabilization includes increasing the cohesion of soils and reducing the void ratio. However, the quantity of dextran produced by the bacteria was quite low under in-situ conditions. Increasing the sucrose concentration and providing periodic injections can be used to overcome this limitation. Spraying method can be used for surface applications while injection method can be used for subsoil applications. The application of this technology includes permeability reduction in cohesionless soils. Other applications include reducing seepage through dams, biobarriers for contaminant remediation, prevention of soil liquefaction.

6.4.7.4 Summary and Future recommendations

The use of bacterial biopolymers or biofilms has garnered significant interest as a promising means to cause bioclogging, reducing permeability, increasing strength, and eventually to seal cracks or leakage in various geotechnical engineering applications. With increasing focus on using bacterial biopolymers in geotechnical practices, quantification of mechanical properties of biopolymers is important in predicting their efficacy in soil stabilization applications. These micro and nanomechanical properties are quintessential in predicting the behaviour of biopolymer-modified soils. Yet, the till date these properties remain poorly identified. In the present study, biopolymer dextran produced by *Leuconostoc mesenteroides* was found to be a promising candidate in soil stabilization application. The model bacteria utilize sucrose as working material and synthesize biopolymer dextran, which forms a complex and inhomogeneous polymer network within the pore spaces of soil [52]. In the present study, the biopolymer yield was quantified, and its mechanical properties were measured at varying length scales. The study reports the first attempt to quantify the

elastic modulus of dextran biopolymer using nanoindentation technique. Further, the elastic modulus was measured at higher resolution using AFM. Therefore, we demonstrate for the first time that the morphology and nanomechanical properties of dextran using various techniques such as nanoindentation, AFM and SEM. The obtained microscale properties are expected to be implemented for modelling of soil particle-soft biopolymer interactions at the particle scale.

Tailoring the morphology and material properties of biopolymers could confer new functionalities to sustainable stabilizers and would make possible novel advanced engineering applications. Achieving these targets would require the precipitation of stable biopolymers with tailored moduli and high hardness. The current study demonstrated that insoluble biopolymer dextran could be produced and used for soil stabilization applications. To the authors' knowledge, this is the first report of the direct measurement of the spatial variation in nanomechanical properties of dextran at various length scales. Further, in-situ dextran production was carried out on soil samples, and its efficacy was tested at macro-scale using in custom made needle penetration apparatus.

6.5 Conclusion

1. Successful optimization of biopolymer producing media and culture conditions was achieved in this study. We recorded linear increase in bacterial dextran production with the substrate concentration of sucrose between 15-500 g/L.
2. The micromechanical properties of in-situ biopolymer Dextran were quantified for the first time using nanoindentation technique. The average elastic modulus of the dry biopolymer is 3.14 ± 0.035 GPa. The average hardness of the sample was 0.2 GPa.
3. The average modulus of the wet samples was 1.4 ± 0.057 GPa. Hydration of the sample was responsible for a reduction of modulus by more than 50%.
4. The average modulus of across the vertical section was 2.09 ± 0.48 GPa and horizontal section 1.89 ± 0.19 GPa.
5. Needle penetration test results revealed that addition of in-situ biopolymer enhanced the surface strength of the treated samples. For samples stabilized with commercial biopolymer Xanthan gum, the correlation between the slope of needle penetration curves and UCS was quadratic with an R^2 value of 0.98.

A needle penetration test can be used to predict approximate UCS values of the stabilized samples.

6. The variation in local micro and nanomechanical properties od dextran biopolymer produced in-situ by *Leuconostoc mesenteroides* was mapped for the first time using nanoindentation nd AFM techniques, respectively.

With increasing focus on using bacterial biopolymers in soil stabilization applications, quantification of mechanical properties of biopolymers become essential. However, to date, these properties remain poorly understood. This investigation is the first attempt to quantify the nano and macro mechanical properties of in-situ bacterial biopolymer dextran produced by bacterial culture *Leuconostoc mesenteroids*. The fundamental mechanism of bacterial biopolymer-based cementation was revealed through their morphographic and nanomechanical testing via AFM, nanoindentation and scanning electron micrography. Finally, its extended application on soil stabilization was investigated via needle penetration tests. Further, biopolymer dextran was found to be highly effective in stabilizing soils varying from sand to clay. This study has demonstrated novel methods for testing in situ polymers and opened up the channels for their applications in numerous subsurface as well as surface applications. However, the present work can be extended to include mechanical modelling of bacterial biopolymer stabilized soils. The petri-dish samples should also be upscaled to carry out triaxial testing to obtain the cohesion and friction angle of the stabilized soils. A detailed geotechnical investigation of the stabilized soils will help in providing more confidence in biopolymer modified soil applications.

6.6. Reference

1. Couradeau, E., et al., *Prokaryotic and eukaryotic community structure in field and cultured microbialites from the alkaline Lake Alchichica (Mexico).* PloS one, 2011. **6**(12): p. e28767.

2. Dhami, N.K., A. Mukherjee, and E.L. Watkin, *Microbial diversity and mineralogical-mechanical properties of calcitic cave speleothems in natural and in vitro biomineralization conditions.* Frontiers in microbiology, 2018. **9**: p. 40.

3. Ramachandran, A.L., et al., *Understanding and creating biocementing beachrocks via biostimulation of indigenous microbial communities.* Applied Microbiology and Biotechnology, 2020. **104**(8): p. 3655-3673.

4. DeJong, J., et al. *Biogeochemical processes and geotechnical applications: progress, opportunities and challenges*. in *Bio-and Chemo-Mechanical Processes in Geotechnical Engineering: Géotechnique Symposium in Print 2013*. 2014. Ice Publishing.

5. Terzis, D. and L. Laloui, *A decade of progress and turning points in the understanding of bio-improved soils: A review.* Geomechanics for Energy and the Environment, 2019. **19**: p. 100116.

6. Dhami, N.K., M.S. Reddy, and A. Mukherjee, *Biomineralization of calcium carbonate polymorphs by the bacterial strains isolated from calcareous sites.* Journal of microbiology and biotechnology, 2013. **23**(5): p. 707-714.

7. Choi, S.-G., et al., *Review on geotechnical engineering properties of sands treated by microbially induced calcium carbonate precipitation (MICP) and biopolymers.* Construction and Building Materials, 2020. **246**: p. 118415.

8. Chang, I., et al., *Review on biopolymer-based soil treatment (BPST) technology in geotechnical engineering practices.* Transportation Geotechnics, 2020. **24**: p. 100385.

9. Dehghan, H., et al., *Use of xanthan and guar gums in soil strengthening.* Clean Technologies and Environmental Policy, 2019. **21**(1): p. 155-165.

10. Lee, S., et al., *Xanthan Gum Biopolymer as Soil-Stabilization Binder for Road Construction Using Local Soil in Sri Lanka.* Journal of Materials in Civil Engineering, 2019. **31**(11): p. 06019012.

11. Arab, M.G., et al., *Resilient Behavior of Sodium Alginate–Treated Cohesive Soils for Pavement Applications.* Journal of Materials in Civil Engineering, 2019. **31**(1): p. 04018361.

12. Fatehi, H., et al., *A novel study on using protein based biopolymers in soil strengthening.* Construction and Building Materials, 2018. **167**: p. 813-821.

13. Ayeldeen, M., et al., *Enhancing mechanical behaviors of collapsible soil using two biopolymers.* Journal of Rock Mechanics and Geotechnical Engineering, 2017. **9**(2): p. 329-339.

14. Bouazza, A., W.P. Gates, and P.G. Ranjith, *Hydraulic conductivity of biopolymer-treated silty sand.* Géotechnique, 2009. **59**(1): p. 71-72.

15. Cabalar, A., M. Wiszniewski, and Z. Skutnik, *Effects of xanthan gum biopolymer on the permeability, odometer, unconfined compressive and triaxial shear behavior of a sand.* Soil Mechanics and Foundation Engineering, 2017. **54**(5): p. 356-361.

16. Chen, R., I. Lee, and L. Zhang, *Biopolymer stabilization of mine tailings for dust control.* Journal of Geotechnical and Geoenvironmental Engineering, 2015. **141**(2): p. 04014100.

17. Chen, R., et al., *Improving dust resistance of mine tailings using green biopolymer.* Environmental Geotechnics, 2019: p. 1-10.

18. Kim, Y.-M., T. Park, and T.-H. Kwon, *Engineered bioclogging in coarse sands by using fermentation-based bacterial biopolymer formation.* Geomech. Engng, 2019. **17**.

19. Godinho, A.L. and S. Bhosle, *Sand Aggregation by Exopolysaccharide-Producing Microbacterium arborescens—AGSB.* Current microbiology, 2009. **58**(6): p. 616-621.

20. Cole, D.M., D.B. Ringelberg, and C.M. Reynolds, *Small-scale mechanical properties of biopolymers.* Journal of Geotechnical and Geoenvironmental engineering, 2012. **138**(9): p. 1063-1074.

21. Ringelberg, D., et al., *Compressive strength of soils amended with a bacterial succinoglycan: effects of soluble salts and organic matter.* Canadian geotechnical journal, 2014. **51**(7): p. 747-757.

22. Proto, C., J. DeJong, and D. Nelson, *Biomediated permeability reduction of saturated sands.* Journal of Geotechnical and Geoenvironmental Engineering, 2016. **142**(12): p. 04016073.

23. Ham, S.-M., et al., *Improvement of Surface Erosion Resistance of Sand by Microbial Biopolymer Formation.* Journal of Geotechnical and Geoenvironmental Engineering, 2018. **144**(7): p. 06018004.

24. Ta, H.X., et al., *Effects of bacterial dextran on soil geophysical properties.* Environmental Geotechnics, 2017. **5**(2): p. 114-122.

25. Abbasi, B., et al., *Modeling of permeability reduction in bioclogged porous sediments.* Journal of Geotechnical and Geoenvironmental Engineering, 2018. **144**(4): p. 04018016.

26. Martin, G., T. Yen, and S. Karimi. *Application of biopolymer technology in silty soil matrices to form impervious barriers*. in *7th Australia New Zealand conference on geomechanics: geomechanics in a changing world: conference proceedings*. 1996. Institution of Engineers, Australia.

27. Zhu, W., et al., *Nanoindentation mapping of mechanical properties of cement paste and natural rocks.* Materials characterization, 2007. **58**(11-12): p. 1189-1198.

28. Li, W., et al., *Experimental investigation on quantitative nanomechanical properties of cement paste.* 2015.

29. Oliver, W.C. and G.M. Pharr, *An improved technique for determining hardness and elastic modulus using load and displacement sensing indentation experiments.* Journal of materials research, 1992. **7**(6): p. 1564-1583.

30. Li, C., et al., *Multi-scale assessment of mechanical properties of organic-rich shales: A coupled nanoindentation, deconvolution analysis, and homogenization method.* Journal of Petroleum Science and Engineering, 2019. **174**: p. 80-91.

31. Jeong, M.S., et al., *Systematic modeling approach to selective plugging using in situ bacterial biopolymer production and its potential for microbial-enhanced oil recovery.* Geomicrobiology Journal, 2019. **36**(5): p. 468-481.

32. Noh, D.H., et al., *P and S wave responses of bacterial biopolymer formation in unconsolidated porous media.* Journal of Geophysical Research: Biogeosciences, 2016. **121**(4): p. 1158-1177.

33. Sarwat, F., et al., *Production & characterization of a unique dextran from an indigenous Leuconostoc mesenteroides CMG713.* International Journal of Biological Sciences, 2008. **4**(6): p. 379.

34. Smolyakov, G., et al., *AFM PeakForce QNM mode: Evidencing nanometre-scale mechanical properties of chitin-silica hybrid nanocomposites.* Carbohydrate polymers, 2016. **151**: p. 373-380.

35. Ulusay, R., et al., *ISRM suggested method for the needle penetration test.* Rock mechanics and rock engineering, 2014. **47**(3): p. 1073-1085.

36. Callebaut, F., et al., *Determination of soil surface strength with a needle-type penetrometer.* Soil and Tillage Research, 1985. **5**(3): p. 227-245.

37. Gowthaman, S., et al., *Feasibility study for slope soil stabilization by microbial induced carbonate precipitation (MICP) using indigenous bacteria isolated from cold subarctic region.* SN Applied Sciences, 2019. **1**(11): p. 1480.

38. Nix, W.D. and H. Gao, *Indentation size effects in crystalline materials: A law for strain gradient plasticity.* Journal of the Mechanics and Physics of Solids, 1998. **46**(3): p. 411-425.

39. Jee, A.-Y. and M. Lee, *Comparative analysis on the nanoindentation of polymers using atomic force microscopy.* Polymer Testing, 2010. **29**(1): p. 95-99.

40. Wang, S.F., et al., *Biopolymer chitosan/montmorillonite nanocomposites: Preparation and characterization.* Polymer Degradation and Stability, 2005. **90**(1): p. 123-131.

41. Hosaka, K., et al., *Effect of wet vs. dry testing on the mechanical properties of hydrophilic self-etching primer polymers.* Eur J Oral Sci, 2007. **115**(3): p. 239-45.

42. Porter, H., N.K. Dhami, and A. Mukherjee, *Synergistic chemical and microbial cementation for stabilization of aggregates.* Cement and Concrete Composites, 2017. **83**: p. 160-170.

43. Aman, A., N.N. Siddiqui, and S.A.U. Qader, *Characterization and potential applications of high molecular weight dextran produced by Leuconostoc mesenteroides AA1.* Carbohydrate Polymers, 2012. **87**(1): p. 910-915.

44. Dols-Lafargue, M., et al., *Factors affecting alpha,-1,2 glucooligosaccharide synthesis by Leuconostoc mesenteroides NRRL B-1299 dextransucrase.* Biotechnol Bioeng, 2001. **74**(6): p. 498-504.

45. Kim, D., et al., *Dextran molecular size and degree of branching as a function of sucrose concentration, pH, and temperature of reaction of Leuconostoc mesenteroides B-512FMCM dextransucrase.* Carbohydrate Research, 2003. **338**(11): p. 1183-1189.

46. Santos, M., J. Teixeira, and A.r. Rodrigues, *Production of dextransucrase, dextran and fructose from sucrose using Leuconostoc mesenteroides NRRL B512(f).* Biochemical Engineering Journal, 2000. **4**(3): p. 177-188.

47. Siddiqui, N.N., et al., *Structural analysis and characterization of dextran produced by wild and mutant strains of Leuconostoc mesenteroides.* Carbohydrate Polymers, 2014. **99**: p. 331-338.

48. Pham, D.Q., et al., *Micro-to nano-scale chemical and mechanical mapping of antimicrobial-resistant fungal biofilms.* Nanoscale, 2020. **12**(38): p. 19888-19904.

49. Guessasma, S., et al., *Viscoelasticity properties of biopolymer composite materials determined using finite element calculation and nanoindentation.* Computational Materials Science, 2008. **44**(2): p. 371-377.

50. Wang, H., et al., *Role of Capsular Polysaccharides in Biofilm Formation: An AFM Nanomechanics Study.* ACS Applied Materials & Interfaces, 2015. **7**(23): p. 13007-13013.

51. Dorobantu, L.S. and M.R. Gray, *Application of atomic force microscopy in bacterial research.* Scanning, 2010. **32**(2): p. 74-96.

52. Jeon, M.-K., et al., *In situ viscoelastic properties of insoluble and porous polysaccharide biopolymer dextran produced by Leuconostoc mesenteroides using particle-tracking microrheology.* Geomechanics and Engineering, 2017. **12**(5): p. 849-862.

53. Allen, A., O. Habimana, and E. Casey, *The effects of extrinsic factors on the structural and mechanical properties of Pseudomonas fluorescens biofilms: A*

combined study of nutrient concentrations and shear conditions. Colloids and Surfaces B: Biointerfaces, 2018. **165**: p. 127-134.

54. Padmanabhan, P.A., et al., *Rheology and gelation of water-insoluble dextran from Leuconostoc mesenteroides NRRL B-523.* Carbohydrate Polymers, 2003. **53**(4): p. 459-468.

Chapter 7: Conclusions

7.1 Introduction

Soil stabilization is a necessity for present-day infrastructure projects due to the lack of availability of good soil for construction. In Australia, chemical stabilisation using materials such as lime, cement, gypsum and fly ash is commonly employed for the stabilisation of soil against erosion, liquefaction and for the construction of road base [1, 2]. However, the heavy reliance of the construction industry on chemical stabilizers have raised concerns owing to its high embodied energy and environmental impact [1, 3]. However, current socio-economic developments demand environmentally friendly stabilizer, which meets the requirement for adequate engineering performance. With bio-geotechnology emerging as a sub-discipline of geotechnical engineering, numerous laboratory and field-scale experiments has been already conducted on bio-based stabilizers [4-6]. However, the potential of biopolymer for soil stabilization application has received less notice in comparison to MICP. The thesis is an investigation on bio-based stabilizers with a prime focus on biopolymer and MICP on the stabilization of soil. The key objective of the thesis is as follows:

- To investigate the formation mechanism and characterization of the beach rocks sediments from Lucky Bay, Esperance, Western Australia.
- To investigate the potential of bacterial biopolymer (xanthan gum) in the stabilization of soil.
- To investigate the potential synergistic effects of biopolymer and MICP in the aggregation of soil.
- To investigate in-situ bacterial biopolymer production and characterisation for potential soil stabilization applications.

In chapter 2, an extensive review of the literature was carried out on bio-based stabilizers. On-going research in this area was critically synthesized and summarised in the chapter. This comprehensive review addresses the limitations of traditional stabilizers leading to the development of sustainable alternatives with a prime focus on biopolymers. The evolution of biopolymers and advanced characterising tools used for studying the interactions between biopolymers and soils were also discussed in detail. Finally, the existing challenges in their large-scale implementation, as well as the direction of future research, were also presented.

In chapter 3, the ongoing precipitation of ferruginous and calcium-based cements in beachrock sediments at Lucky Bay, Esperance, Western Australia, was investigated. The role of active microbes responsible for the precipitation and dissociation processes of cementation was confirmed in the study. In addition to this, the mineralogical, morphological and nanomechanical characterization of the beach rock was carried out. Biostimulation of indigenous iron oxidising and carbonate precipitating communities under seawater media was identified as a novel tool for the production of biocement in coastal environments. Nanomechanical properties of natural and lab synthesised biocements were also quantified. The role of biopolymers in the aggregation of natural sediments were also identified.

Chapter 4 reports the stabilization of sand-clay mixtures with bacterial biopolymer xanthan gum. Experimental investigation of the stabilized samples were carried out in varying length scales. The study reports significant enhancement in compressive strength of biopolymer stabilized soils with increasing clay dosage. Also, DIC proved to be a useful tool to understand the local stress concentrations in the samples subjected to compressive loading. The study also reports that the biopolymer stabilized sand samples resulted in local failure due to the pore-clogging mechanism, and the addition of clay helped in the uniform distribution of moisture by capillary action leading to low overall moisture absorption and avoiding sample failure. Microstructural analysis on the stabilized samples using SEM revealed the mechanism of stabilization due to biopolymer alone as well as clay reinforced biopolymer. This study also reports the nanomechanical properties of the stabilized composite for the first time. The average hardness and elastic modulus of the clay reinforced biopolymer sample obtained from nanoindentation testing carried out on the clay reinforced biopolymer are 0.078 ±0.03 GPa 5.02 ±1.3 GPa and respectively. AFM was very useful in understanding the underlying mechanism behind the strength loss of the samples due to exposure to moisture. The μm resolution of the instrument revealed that the clay particle's, which were held fixed by the biopolymer, became loose owing to the weakening of the biopolymer network on exposure to moisture. This micromechanical phenomenon resulted in the reduction in strength of the stabilized samples at a macro scale as reflected by the UCS testing.

Chapter 5 reports the first attempt to synergise biopolymer and MICP technology to overcome their individual limitations, thus emulating cementation occurring in nature.

Previous research has revealed that biopolymers are capable of stabilising soil, but they are prone to degradation on exposure to water. It has been reported that MICP treatment can resist degradation due to water, but they release a considerable amount of harmful ammonia gas. Combining the technologies helped in reducing the water susceptibility of the biopolymer samples in addition to a significant reduction in ammonia generation without compromising on the mechanical performance of the stabilized samples. The results of this study will encourage the application of bio-based stabilisers for soil stabilisation applications. The mechanical performance of the samples improved due to synergy. The key highlight of the study was the reduction in water abortion of the biopolymer stabilized samples due to MICP treatment. Thus, a major drawback of biopolymer technology was addressed by synergising MICP with biopolymer. Microscopic investigations reinforced the synergistic nature of biopolymer and MICP in the stabilization process, which provided superior mechanical and durability performance. Synergising biopolymer with MICP surface treatment helped in significantly lowering the amount of ammonia released during the MICP process to achieve a target strength.

Chapter 6 was a novel attempt at a synthesis of in-situ bacterial biopolymer, its characterisation and investigation on its potential for soil stabilization applications. The mechanical properties and effect of in-situ bacterial biopolymers have been relatively unexplored by previous researchers. This chapter reports the first attempt to quantify the nano and macro mechanical properties of in-situ bacterial biopolymer dextran produced by the bacteria *Leuconostoc mesenteroids*. The study also reveals that a well-graded soil is an ideal candidate to be used for biopolymer stabilization. As anticipated, the properties of biopolymer in the hydrated and dry state can be significantly different, which limit its application in saturated conditions. AFM and nano-indentation techniques proved to be useful in investigating the nanomechanical properties of the deposited biopolymer.

The results presented in this dissertation provide new insights towards a better understanding of the fundamentals of bio-based stabilizers with a prime focus on biopolymer soil stabilization.

7.2 Recommendation for future research

- The study should be conducted on a variety of biopolymers available in the market to identify the ones which are more resistant to moisture to increase the overall efficiency of treatment.
- The stabilization should be carried out on a large variety of soils to generate a database for engineers.
- The use of bio-based stabilizers in practical applications, such as in the stabilization of road base materials and mine tailings, are also recommended.
- The area of in-situ biopolymer treatment should be explored further as it is a promising technique for in-situ stabilization under existing structures.
- The ultimate goal will be to synergise in-situ biopolymer production with MICP so that it can eliminate the need to mix the materials with soil ex-situ.
- The sustainability aspect, including life cycle analysis of the bio-based stabilizers, should be carried out.

7.3 References

1. Vinod, J.S., B. Indraratna, and M.A. Mahamud, *Stabilisation of an erodible soil using a chemical admixture.* Proceedings of the Institution of Civil Engineers-Ground Improvement, 2010. 163(1): p. 43-51.
2. Indraratna, B., et al., *Predicting the erosion rate of chemically treated soil using a process simulation apparatus for internal crack erosion.* Journal of Geotechnical and Geoenvironmental Engineering, 2008. 134(6): p. 837-844.
3. Porter, H., N.K. Dhami, and A. Mukherjee, *Sustainable road bases with microbial precipitation.* Proceedings of the Institution of Civil Engineers-Construction Materials, 2018. 171(3): p. 95-108.
4. Dejong, J.T., et al., *Biogeochemical processes and geotechnical applications: progress, opportunities and challenges.* Géotechnique, 2013. 63(4): p. 287-301.
5. DeJong, J.T., M.B. Fritzges, and K. Nüsslein, *Microbially induced cementation to control sand response to undrained shear*. Journal of Geotechnical and Geoenvironmental Engineering, 2006. 132(11): p. 1381-1392.
6. DeJong, J.T., et al., *Bio-mediated soil improvement.* Ecological Engineering, 2010. 36(2): p. 197-210.

“Every reasonable effort has been made to acknowledge the owners of copyright material. I would be pleased to hear from any copyright owner who has been omitted or incorrectly acknowledged.”